NEUROANATOMICAL CORRELATES OF A BIFACTOR MODEL OF INTERNALIZING PSYCHOPATHOLOGY ACROSS THE LIFESPAN

by

HARRY R. SMOLKER

B.A., Vassar College, 2009
M.A., University of Colorado-Boulder, 2018

A thesis submitted to the
Faculty of the Graduate School of the
University of Colorado in partial fulfillment
of the requirement for the degree of
Doctor of Philosophy
Department of Psychology
2020

Committee Members:

Dr. Marie T. Banich

Dr. Naomi P. Friedman

Dr. Roselinde H. Kaiser

Dr. Soo H. Ree

Dr. Monique K. LeBourgeois

ABSTRACT

Smolker, Harry R. (Ph.D., Department of Psychology and Neuroscience)
Neuroanatomical Correlates of a Bifactor Model of Internalizing Psychopathology Across the Lifespan
Thesis directed by Professor Marie Banich

High rates of comorbidity between internalizing disorders and heterogeneity in the behavioral manifestations of a single disorder have made it challenging to identify biological signatures of specific mental illnesses. This may in part be due to the case-control frameworks which dominate psychopathology research, frameworks which draw stark distinctions between patients and healthy individuals despite evidence that such distinctions may not reflect the distribution of behavior across the population. To address these issues, there has been a recent emphasis on employing dimensional models of psychopathology which characterize psychopathology as arising through the interaction of behaviors that are continuously distributed throughout the general population. In the current dissertation project, we first propose a novel six-factor dimensional model of internalizing psychopathology and demonstrate that dimensions in this model show preferential associations with specific internalizing disorders. We then employ gray matter morphometry analyses to identify the degree to which individual differences in internalizing dimensions are associated with structural properties of gray matter across the brain. Finally, we evaluate which dimensions are driven by genes or the environment, as well as the degree to which relationships between these dimensions and gray matter structure result from overlapping genetic or environmental influences. Our findings suggest 1) previous dimensional models of internalizing psychopathology may be improved by including cognitive dimensions of behavior, including rumination and repetitive negative thought, 2) the brain regions associated with internalizing dimensions are more distributed than the regions identified in case-control studies while also changing with age and differing by sex, and 3) behaviors that are common

across internalizing disorders are largely genetic in nature, whereas behaviors that are specific to anxiety may be influenced by shared environmental factors.

ACKNOWLEDGEMENTS

I would like to acknowledge the following people and agencies who made this research possible. First, thank you to my mentors, Marie Banich and Naomi Friedman, whose support and opinions were essential in formulating and executing this research. Thank you to Kathy Pearson for her assistance in data management and analyses. Thank you to Teryn Wilkes, Nicole Speer, and the rest of the staff at the Intermountain Neuroimaging Consortium for their essential roles in data collection. Thank you to all of those involved in the Colorado Cognitive Neuroimaging Family Emotion Research Study and the Longitudinal Twin Study who made data collection possible. Thank you to the Institute for Behavioral Genetics and the National Institute of Mental Health for their financial support through the T32 training grant program. Thank you to my dissertation committee, whose thoughtful comments and suggestions helped to refine this project. Finally, thank you to my wife, Roxana Astemborski, whose patience, love, and support kept me grounded as I toiled through the many stages of this project.

TABLE OF CONTENTS

LIST OF TABLES

LIST OF FIGURES

CHAPTER 1

INTRODUCTION

1.1. Overview

Psychopathology is one of the most burdensome health-related issues in the world today and internalizing disorders accounting for the majority of this burden (Roehrig, 2016). Internalizing disorders are psychiatric conditions in which an individual has severe and frequent negative thoughts and behaviors that are focused on the self as opposed to the outside world, and include conditions like major depression (MDD) and anxiety disorders. Despite decades of research into the etiology of internalizing disorders, our understanding of the biological causes and consequences of specific behaviors that make up internalizing psychopathology remains quite limited. A better understanding of the neurobiological underpinnings of these behaviors may not only provide insight into the etiology of psychopathology, but may also aid in the development of new diagnostic tools and treatment targets. Complicating this endeavor, however, is that current diagnostic schema do not capture the behavioral complexities within internalizing psychopathology, often failing to account for strong associations between disorders, heterogeneity within disorders, and subclinical levels of symptomology. Furthermore, there is evidence that the etiologies and manifestations of psychopathology may change with age (Lahey et al., 2017; Schmaal et al., 2017), and differ between the sexes (Hankin et al., 2008); Zahn-Waxler et al., 2006), calling into question the generalizability of preexisting research into the brain systems associated with internalizing psychopathology. These issues present major challenges to effectively translating neuroimaging methodologies into clinical practice, while

emphasizing the need to seriously consider multiple sources of heterogeneity in both psychopathological behaviors and the neural pathways associated with these behaviors.

In the current dissertation project, we attempt to shed light on these issues through a series of three studies. First, utilizing structural equation modeling, we introduce a novel dimensional model of internalizing psychopathology and show that this model maps on to preexisting diagnostic schema (see Chapter 3). Then, employing neuroimaging methodologies, we evaluate the degree to which each of these dimensions are associated with variability in regional brain anatomy, and how these associations may change according to age and sex (see Chapter 4). Finally, through twin analyses, we test for genetic and environmental contributions to the internalizing dimensions while also evaluating the degree to which relationships between neuroanatomical structure and internalizing psychopathology are driven by overlapping or distinct genetic and environmental influences (see Chapter 5).

1.2. Limitations of Case-Control Studies of Psychopathology

Under the classic diagnostic schema for mental illness, individuals must meet a specific set of criteria to be considered as being affected by a disorder. This schema inevitably leads to the dichotomization of mental illness into cases (i.e., individuals who meet some diagnostic criteria) and controls (i.e., all individuals who do not meet this criteria). As such, “case-control” designs have dominated psychopathology research, in which group differences on some characteristic are compared between cases and controls. Not surprisingly, this case-control framework has dominated neuroimaging studies of psychopathology as well, with such studies pointing to a collection of brain systems as being atypical in cases as compared to control.

However, this literature fails to provide a mapping of specific behaviors that make up internalizing psychopathology to specific neural systems. This is particularly problematic in light of major inconsistencies across case-control studies as to methodologies employed to account for cross-disorder comorbidity, within-disorder heterogeneity, and subclinical symptomology. More specifically, the use of categorical nosologies of psychopathology in case-control designs are limited in three important ways: 1) they often do not delineate neural properties driving comorbidity and shared symptomology between internalizing disorders; 2) they generally do not identify brain systems associated with specific, distinct clusters of internalizing behaviors; and 3) they frequently ignore that internalizing behaviors are distributed across the general population, even in individuals who do not meet diagnostic criteria for a disorder. Indeed, the need to rethink our conceptualizations of psychopathology has become a prominent issue, with major funding agencies promoting initiatives to move research beyond case-control designs (Cuthbert & Insel, 2013; Insel 2014; Insel et al., 2010) as researchers suggest new, dimensional approaches for characterizing psychopathology (Kotov et al., 2017, 2018).

First, case-control designs struggle to account for cross-disorder comorbidity. Research into the neuroanatomical correlates of internalizing psychopathology has been dominated by case-control studies which categorize individuals as either healthy controls or disordered and test for groups differences. The resulting body of literature has often implicated similar brain regions across disorders, suggesting that a common set of brain systems are associated with most mental health disorders (Goodkind et al., 2015). These results align with behavioral observations of high degrees of comorbidity between disorders (Essau et al., 2018; Kessler et al., 2005a,b; Merikangas et al., 2010), as well as overlapping symptomologies (Clark & Watson, 1991a,b; Zbozinek et al., 2012), likely emerging due to shared neural mechanisms (Menon, 2011). For

example, major depressive disorder (MDD) and generalized anxiety disorder (GAD), two of the most frequently comorbid internalizing disorders (Kessler et al., 1996), both include concentration difficulties, psychomotor issues, and sleep disturbance as criterial symptoms (American Psychiatric Association, 2013), and are both associated with volumetric properties of the amygdala, anterior cingulate, and middle frontal gyrus (MDD: Bora et al., 2012; GAD: Hilbert et al., 2014). The high degree of comorbidity and similar symptom presentation across disorders makes accurate diagnoses difficult while also suggesting that many disorders may have similar etiological influences, blurring the distinctions between disorders that are imposed under a case-control framework. One potential way to begin to address this issue within the case-control framework is to compare patients with a single diagnosis to patients with different patterns of comorbidity, yet such studies are relatively few and far between and are generally underpowered due to the explosion in the number of groups needed to properly compare individuals with different patterns of comorbidity. Instead, most case-control studies either ignore comorbidity all together or exclude individuals with comorbid disorders, effectively limiting the inferences that can be made within a single study despite comorbidity being the norm.

A second major shortcoming of case-control designs is they often ignore the considerable diagnostic heterogeneity that can occur within a given disorder. For example, looking across over 850 patients with MDD, Park and colleagues (2017) identified 119 distinct symptom profiles that all met criteria for an MDD diagnosis (Park et al., 2017). In related work, Chen and colleagues (2000) found multiple subtypes within MDD through latent class analyses, with each subtype not only driven by distinct symptom profiles, but also showing dissociations in terms of age of onset, number of lifetime episodes, and relationships with distinct risk factors including

family history, exposure to stressful life events, and gender. These results suggest that individual differences in symptom profiles may in fact reflect distinct etiological pathways with important ramifications for lifetime trajectories of psychopathology. As such, the value of treating internalizing disorders as unitary constructs is open to debate. What is clear, however, is that by treating a given disorder as a unitary construct in spite of evidence suggesting considerable heterogeneity within that disorder, researchers only gain insight into broad commonalities shared by individuals meeting criteria for that disorder, while losing the ability to detect more nuanced information that may be highly relevant to understanding the causes and consequences of psychopathology

Finally, case-control designs, by definition, treat psychopathology as dichotomous, categorical constructs when, in fact, behaviors at the core of internalizing psychopathology are distributed continuously throughout the population (Henry & Crawford 2005; Watson et al. 1995b). Individuals who do not meet clinical criteria for a diagnosis may still exhibit behaviors generally associated with a disorder with varying levels of accompanied impairment. Such subclinical presentations of symptomology, though not reaching the level indicative of a disorder, may still provide important information regarding the nature of psychopathology, particularly in an individual differences context. By lumping individuals who do not meet clinical criteria for diagnoses into a single control group, case-control designs impose an artificial distinction between healthy and disordered and ignore the full breadth of relevant behavior. Instead, individual differences techniques allow for a more nuanced understanding of the covariance between continuous behaviors and some other characteristic of interest, like brain structure.

The three aforementioned issues with case-control designs make it difficult to identify disorder-specific neural correlates, calling into question the degree to which case-control designs are capturing disorder-specific neural markers or identifying brain regions that are associated with psychopathology more broadly. One way to begin to address this issue it to employ dimensional models of psychopathology, which characterize psychopathology as emerging through the interaction of multiple, continuously distributed behavioral dimensions.

1.3. Dimensional Models of Internalizing Psychopathology

The strong behavioral and neural overlap between internalizing disorders have led some researchers to rethink classic characterizations of psychopathology as falling into discrete categories and to instead focus on dimensional models (Kotov et al., 2017). Such models identify latent behavioral constructs at the core of psychopathology, including behaviors common across disorders, and quantify these constructs as continuous individual differences (Caspi et al., 2014; Kotov et al., 2017). In quantifying psychopathology as individual differences, dimensional models depart from making artificial distinctions between non-affected and clinical groups, instead treating psychopathology as emerging through interactions of continuous spectra of behaviors that manifest across the general population in varying degrees (Kotov et al., 2017). Such approaches may have particular relevance in helping to understanding the neural basis of internalizing psychopathology, a class of behaviors with high rates of comorbidity (Cummings et al., 2014; Garber & Weersing, 2010; Spinhoven et al., 2011), symptom overlap (Zbozinek et al., 2012), and shared neural correlates (Goodkind et al., 2015; Menon, 2011).

One powerful approach to develop dimensional models of psychopathology is to employ structural equation modeling to identify latent behavioral constructs underlying a given class or classes of disorders (Chen et al., 2012; Kim & Eaton, 2015). Specifically, bifactor models are able to capture constructs associated with commonalities across disorders, while simultaneously modeling both within- and across- disorder heterogeneity (Reise, 2012). They do so by identifying general latent factors that capture covariation across all relevant behaviors, as well as specific latent factors that capture additional behavioral dimensions that may be specific to certain disorders. For example, looking across symptoms from all major disorders, Caspi and colleagues (2014) identified three dimensions underlying psychopathology symptomology that act in a hierarchical manner. At the top of the hierarchy is a general psychopathology factor (i.e., "p-factor") associated with co-occurrence of symptoms spanning all disorders. Beneath this are two factors, one specific to internalizing disorders and the other specific to externalizing disorders, a class of disorders in which negative thoughts and behaviors are directed outwards towards things in the environment. Whereas Caspi et al. (2014) demonstrated this bifactor structure across psychopathology in general, bifactor models can be extended to internalizing disorders specifically. To do so, it is important to first identify empirically grounded constructs that can be measured in a reliable fashion and that form a theoretically coherent model.

1.4. Novel Bifactor Model of Internalizing Psychopathology

In now classic work, Watson and Clark proposed the tripartite model of anxiety and depression, which differentiated behaviors associated with internalizing disorders into three factors: a common factor termed negative affect, as well as two specific factors, namely anxious

arousal and low positive affect (Clark & Watson, 1991a,b). Though Watson and Clark did not explicitly employ bifactor modeling, in their model, negative affect is theoretically similar to a common factor, capturing general affective distress, a criterial symptom of both MDD and anxiety disorders (Clark & Watson 1991a,b). On the other hand, anxious arousal is an anxiety-specific factor, capturing somatic behaviors grounded in unpleasant bodily states and sensations (Clark & Watson, 1991a,b; Sharp et al., 2015), whereas low positive affect is depression-specific, capturing a loss of pleasure and flattened affect (Clark & Watson, 1991a,b), likely emerging due to aberrant reward processing (Gorwood, 2008; Keedwell et al., 2005).

Though the tripartite model is well validated and provides a useful multidimensional characterization of a portion of internalizing behaviors, it does not fully address aberrant patterns of cognition central to internalizing disorders. Behavioral and neural evidence suggests anxiety-specific behaviors can be better accounted for under a two factor of model of anxiety which includes anxious arousal but also adds anxious apprehension (i.e., worry), a cognitive dimension characterized by repetitive negative thoughts about the potential impact of future events and external stressors (Andrews & Borkovec 1988; Zinbarg et al. 1994; Nitschke et al. 2001). In a confirmatory factor analysis, Nitschke and colleagues (2001) demonstrated that a four factor expanded model including anxious apprehension is a better fit than the classic three-factor tripartite model. In related work, anxious arousal and anxious apprehension were shown to have distinct neural substrates, with anxious arousal associated with atypical functioning in brain regions supporting threat detection, while anxious apprehension was associated with brain systems supporting language and working memory (Sharp et al., 2015). When framed under the prevailing cognitive models of internalizing disorders that posit interactions between bottom-up affect and top-down control processes (Disner et al., 2011), anxious arousal captures more

bottom-up, sensory and bodily awareness processes, while anxious apprehension captures more top-down, cognitive control and linguistic processes (Engels et al. 2007; Sharp et al. 2015).

We propose that this four factor model of internalizing psychopathology can be expanded into a six factor model including rumination and repetitive negative thought, a dimension capturing commonalities between rumination and anxious apprehension (for conceptual model, see figure 1).

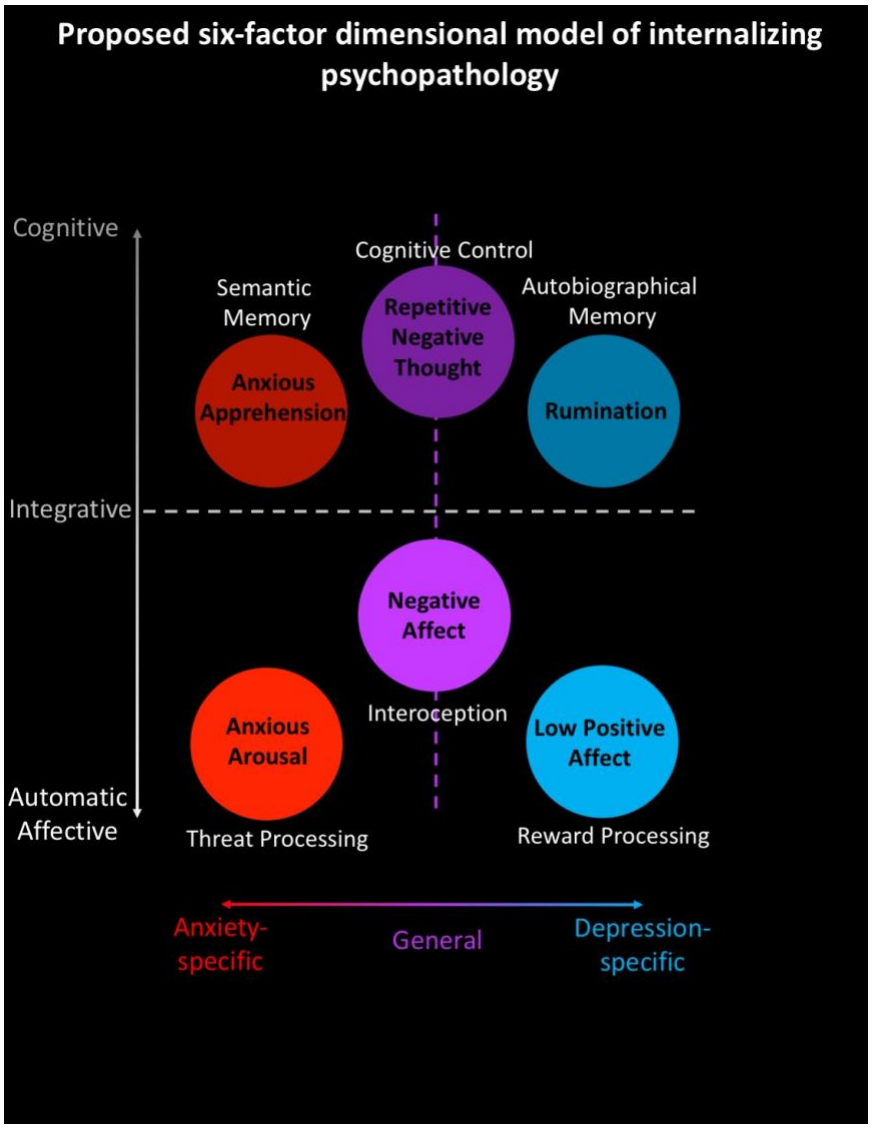

Figure 1. Conceptual description of six-factor internalizing model. The six dimensions can be conceptualized as following along two general axes: automatic affective to cognitive, with dimensions relying on the integration of these systems lying in the middle, as well as anxiety-specific to depression-specific, with non-specific, general dimensions falling in the middle. Proposed domains of processing are shown in white by each dimension.

Whereas anxious apprehension represents a cognitive dimensions of anxiety, rumination has been put forth as a cognitive dimension of depression. Behaviorally, rumination is defined as repetitive negative thoughts about past events and the self (Goring & Papageorgiou 2008; Nolen-Hoeksema 1991,2000). While it shares much in common with anxious apprehension, including associations with gray matter morphometry in dorsolateral prefrontal regions supporting cognitive control regions (anxious apprehension: Castagna et al., 2018; rumination: Wang et al. 2015), the two constructs have consistently proved dissociable (Fresco et al. 2002; Goring & Papageorgiou 2008; Gustavson et al., 2019; Hong, 2007; Hughes et al. 2008; Watkins et al., 2005). For example, in an attempt to identify what is common and unique to anxious apprehension and rumination, respectively, Watkins and colleagues (2005) found that the two dimensions differ in their temporal orientation, with rumination associated with past-oriented thoughts and anxious apprehension associated with future-oriented thoughts. This suggests that the two may emerge from similar processes, but differ in the representations that these processes act on (Hughes et al. 2008; Watkins et al. 2005). Additionally, Gustavson and colleagues (2019) found that individual differences in repetitive negative thought were largely explained by covariation between rumination and anxious apprehension, but even after taking into account this covariation, rumination-specific and anxious apprehension-specific residuals remained. Similar results have been note employing bifactor modeling, with evidence suggesting that rumination and anxious apprehension are best explained by three factors: a repetitive negative thought factor that is shared across the two dimensions, as well as rumination- and anxious apprehension-specific residuals (Hur et al., 2016).

1.5. Structural Magnetic Resonance Imaging

Magnetic resonance imaging (MRI) is an essential tool for non-invasively mapping neural properties associated with mental illness. Falling into two general methodologies, namely structural MRI (sMRI) and functional MRI (fMRI), MRI research can provide insight into the specific brain systems associated with, and potentially contributing to, internalizing psychopathology. While invaluable insights into internalizing psychopathology can be gleaned using fMRI (Haldane & Frangou, 2006; Sheline, 2003), the signals tracked via fMRI are fleeting and susceptible to confounding factors such as fatigue, stimulus exposure (Grill-Spector et al., 2006), and mood (Posse et al., 2003). Furthermore, fMRI protocols often varying across studies sites in consequential ways, making it difficult to aggregate across the now thousands of fMRI studies of internalizing disorders. sMRI, on the other hand, provides relatively stable metrics of brain organization that may change with development, but do not fluctuate on a day-to-day or moment-to-moment basis, as is the case with fMRI. Additionally, the protocols used to collect sMRI data are largely consistent across studies, particularly protocols relevant for gray matter morphometry, allowing for the creation of large-scale standardized data sets, the type of data sets that will be necessary to move MRI methodologies from the lab into the clinic. In the current project we utilize sMRI methodologies, namely surface-based gray matter morphometry (SBM) (Fischl, 2012), in hopes that the insights gleaned have the greatest potential to inform the development of neural biomarkers of psychopathology for clinical practice.

SBM is a methodology by which research can quantify the structural properties of the brain in vivo a relatively fine-grained spatial resolution. Importantly, SBM allows for the

decomposition of neuroanatomy into a number of geometric properties, with the most popular being volume, surface area, and cortical thickness of gray matter. While the precise causes and consequences of variability in gray matter structure remain unclear, it is widely believed that this variability reflects properties of neural organization that may impact behavior. From an evolutionary standpoint, changes in the structure of gray matter are considered central to the ascent of man. As compared to our primate ancestors, humans show a rapid expansion in surface area of the brain with a comparatively small increase in cortical thickness and head size (Rakic, 1995). It is thought that this increase in surface area, which was made possible by an increase in folding within the neocortex, allowed for additional neuronal complexity that ultimately allowed for the development of the cognitive prowess that has come to define our species. Yet even within the lifespan of a single individual, changes in the structure of gray matter appear to have profound relationships with behavior. For instance, during adolescence the brain undergoes a rapid, widespread reduction in cortical thickness with more regionally specific increases in surface area. It is thought these changes in gray matter structure reflect neuronal pruning process through which the brains of adolescents become more efficient and their behavior becomes more adult-like in proficiency. Thus, despite a lack of clarity as to the specific functional consequences of variability in gray matter structure, this variability appears to have important consequences on behavior.

Over the past three decades there has been a rapid proliferation of peer-reviewed studies utilizing SBM measures of gray matter structure in patient populations, providing a robust literature regarding alterations in brain structure in individuals meeting diagnostic criteria for internalizing disorders (for a review see Chapter 2). However, despite some commonalities in results across studies, this literature is rife with inconsistencies in terms of the brain regions

associated with psychopathological status, the specific neuroanatomical properties implicated, and the direction of effects. As such, our ability to glean generalizable inferences that may have positive impacts on clinical practice has been somewhat stymied. To resolve these inconsistencies, it is important to consider two important factors: the framework with which we characterize and measure psychopathology as well as the potential moderating effects of age and sex on both the brain and behavior.

1.6. Utility of Twin Designs

Twins provide an opportunity for researchers to parse the contributions of genetic and environmental influences on individual differences in a range of phenotypes relevant to psychopathology. Though molecular genetic studies have recently taken the human genetics field by storm, twin studies still provide important information that may guide molecular genetic work. This includes highlighting traits that are heritable and worthy of molecular follow up (Wood & Neale, 2010), while also setting the benchmark for understanding the total heritability of a specific trait. Indeed, molecular studies have thus far only been able to explain a fraction of the twin estimates of heritability of complex traits, highlighting the possibility that, in the absence of twin studies, molecular work alone may have led us to the incorrectly conclude that most traits are only minimally heritable.

The value of twin research goes beyond merely estimating the contributions of genes and the environment to a single trait. Some of the most impactful inferences that can be gleaned from twin studies are through bi- or multivariate twin modeling, in which the interrelationship between two or more traits is parsed into the relative influence of overlapping genetic or

environmental factors. In the field of behavioral genetics, such analyses are generally utilized to provide insight into two theoretical issues. First, if two behavioral traits of interest are correlated, twin studies can provide insight into whether or not the covariation between these traits is driven by overlapping genetic or environmental influences. For example, in now seminal work trying to understand the factors driving comorbidity between MDD and generalized anxiety (GAD), Kendler and colleagues (1992) found that the genetic influences on both disorders were completely overlapping while the environmental influences were largely distinct. Second, twin studies allow researchers to identify target biological endophenotypes that may play important intermediary roles between molecular genetic processes and complex behavioral traits. Though the methodologies are the same as the scenario outlined above, the interpretation is different. For example, brain volume has been associated with general intelligence (Thompson et al., 2001) and this relationship appears to be driven solely by genes, not the environment (Posthuma et al., 2002). As such, brain volume is a neural endophenotype, bridging genetic action to behavior, in this case intelligence, suggesting that further insight into the genetic mechanisms driving intelligence may be gleaned by investigating the genetic mechanisms driving brain volume. While similar questions can be asked in the context of molecular genetic studies, the enormous sample sizes required to be powered to test shared genetic markers between traits often make such studies untenable, particularly for more nuanced phenotypes that are not commonly collected as a matter of course in most studies.

1.7. Current Project

1.7.1. Analysis Plan

In the current dissertation project, we put forth a novel six-factor dimensional model of internalizing psychopathology and evaluate the associations of each dimension with multiple measures of gray matter morphometry. This six-factor model builds off of the four factors put forth by Nitschke and colleagues (2001) in three important ways. First, we employ bifactor modeling to produce a single latent factor capturing covariation across all internalizing behaviors measured, termed "negative affect". This factor is analogous to the negative affect dimension proposed by Watson and Clark but instead of treating it as a factor correlated with all other factors in the model, we explicitly partition covariation between behaviors into the single negative affect factor. This technique allows us to precisely identify the neuroanatomical correlates that are shared across internalizing behaviors in a way that is not possible through the correlated factors model presented by Nitschke and colleagues. The use of bifactor modeling additionally affords us the ability to partition variance associated with dimension-specific residuals over and above the common factor, improving the precision and purity of our dimensional measures. Second, much like Nitschke and colleagues (2001) amended the tripartite model to include anxious apprehension, we amend their model to include rumination as an additional dimension, given strong evidence that rumination is not only central to MDD, but dissociable from worry. Finally, we include a second common factor capturing covariation between rumination and anxious apprehension that is not accounted for by the negative affect

factor. This additional dimension, termed “repetitive negative thought”, is grounded in strong evidence linking rumination and anxious apprehension to similar, if not overlapping, cognitive processes.

Employing this six-factor model, we first set out to evaluate a number of questions regarding the neuroanatomical correlates of internalizing psychopathology. This includes identifying the neuroanatomical correlates of internalizing psychopathology that are consistent regardless of age. Because of the relatively early development of subcortical reward and threat processing systems and previous research implicating these structures in internalizing disorders, we hypothesize that amygdala, hippocampus, and portions of the ventral striatum will be associated with distinct dimensions of internalizing psychopathology regardless of age. Second, we test for differences between in the neuroanatomical correlates of internalizing psychopathology between two distinct age groups: adolescence (ages 14 to 22) and young adults (ages 27 to 29). Third, within adolescence and young adulthood, we evaluate the degree to which the neuroanatomical correlates of internalizing psychopathology differ in accordance with sex. Finally, within the young adult sample, we employ twin modeling to evaluate the degree to which individual differences in internalizing psychopathology, associated neuroanatomical properties, and their relationships are driven by genetic and/or environmental influences.

1.7.2. Hypotheses

1.7.2.1. Factor Structure of Internalizing Psychopathology

We hypothesize that a six factor dimensional model of internalizing psychopathology will provide a better fit than nested four and five factor models. Of particular interest is determining the relationship between anxious apprehension and rumination after taking into account negative affect. We specifically test whether they represent a single unitary construct, two completely distinct constructs, or a conjunction of three constructs, including a repetitive negative thought construct that is common between them. In line with previous research (e.g., Hur et al., 2016), we predict that a six factor model in which anxious apprehension, rumination, and repetitive negative thought are treated as distinct constructs will provide the best fit. We also test the degree to which each of the six dimensions show associations with diagnostic status for three disorders: MDD, GAD, and antisocial personality disorder (ASPD). We predict that negative affect will be associated with diagnostic status for all three disorders, repetitive negative thought will be associated with MDD and GAD, but not ASPD, anxious arousal-specific and anxious apprehension-specific will be preferentially associated with GAD but not MDD, and low positive affect-specific and rumination-specific will be preferentially associated with MDD but not GAD.

1.7.2.2. Brain Regions Associated with Internalizing Dimensions

To our knowledge no study has evaluated the neuroanatomical correlates of the current six-factor bifactor model of internalizing psychopathology. However, our specific hypotheses are informed by related findings and theory. While we expect there to be considerable differences in the results across age groups, in general, we hypothesize that all six dimensions will show

dissociable regional topographies across the brain that reflect the neural underpinnings of distinct modes of behaviors at the core of each dimension.

It is particularly important is understanding the brain systems associated with negative affect and repetitive negative thought, two dimensions we propose as being central to the comorbidity between internalizing disorders. Comorbidity between internalizing disorders is associated with worse prognoses in clinical groups, including treatment resistance and high rates of suicidality (Aina & Susman, 2006), making it an important topic for further investigation. Because we did not explicitly model behaviors outside of internalizing psychopathology (e.g., p-factor), we believe that the negative affect dimension is likely not entirely specific to internalizing disorders, instead capturing some behaviors that are common across all of psychopathology. As such, our hypotheses for the brain regions associated with this dimensions are informed by findings from Goodkind and colleagues (2015), who found that caudal portions of anterior cingulate and anterior insula show altered gray matter volume across all major Axis 1 disorders. In light of these findings, we hypothesize that negative affect will be associated with caudal anterior cingulate and the insula.

Repetitive negative thought, on the other hand, is considered to emerge from higher-level cognitive control mechanisms (Beckwe et al., 2014; Zetsche et al., 2018), mechanisms which are thought to be largely instantiated by anterior portions of middle frontal gyrus. Previous research suggests that anxious apprehension and rumination, two dimensions we believe to be both driven by repetitive negative thought, are associated with gray matter in the middle frontal gyrus (worry: Castagna et al., 2018; rumination: Wang et al. 2015), and fMRI research suggests that the frontal pole is involved in temporally oriented thoughts (Addis et al., 2007; Underwood et al., 2015), a key aspect of repetitive negative thought. Taken together, this conjunction of theory and

previous research lead us to predict that repetitive negative thought will be associated with gray matter in the middle frontal gyrus and frontal pole.

Due to associations with threat processing (Sharp et al., 2015) and motoric symptomology (Clark & Watson, 1991a,b), we predict that ROI analyses will reveal associations between anxious arousal-specific and the amygdala, the purported core of automatic threat detection (Ohman, 2005) whereas exploratory whole brain analyses will reveal associations with gray matter in regions supporting sensorimotor functions, including the pre- and postcentral gyri.

Because of preexisting links between low positive affect and atypical reward processing (Nikolova et al., 2012), we predict that individual differences in low positive affect will be associated with gray matter morphometry in brain regions responsible for reward processing, rostral anterior cingulate) reward-processing systems.

In line with findings implicating linguistic and semantic processes in anxious apprehension (Engels et al., 2007, 2010; Nitschke et al., 2001; Sharp et al., 2015), we predict anxious apprehension-specific will be associated with brain regions supporting language (i.e. inferior frontal gyrus) and amodal semantic processes (i.e., temporal lobe) as well as the default mode network involved with internally directed thought (Andrews-Hanna, 2012; Servaas et al., 2014).

Finally, because rumination is often about past events, we predict that rumination will be associated with gray matter of the hippocampus due to the hippocampus's role in memory retrieval, a key process in ruminative forms of thought which has been previously shown to preferentially activate during rumination induction paradigms (Addis et al., 2007).

1.7.2.3. Age Moderation

Because of the relatively early development of subcortical and motoric brain systems (Gogtay et al., 2004), we predict that these brain regions will show consistent associations with the internalizing dimensions across all ages because they will have largely finished development even in our adolescent sample. As noted above, we expect these effects to include associations between a) anxious arousal and the precentral gyrus, postcentral gyrus, and the amygdala, b) low positive affect and the ventral striatum, and c) rumination and the hippocampus. In terms of difference between age groups, because the prefrontal cortex is the last brain region to complete neurodevelopment, we predict that we will observe age group moderation effects on the relationship between internalizing dimensions and prefrontal gray matter morphometry in the adult samples that will not be present in the adolescent sample.

1.7.2.4. Sex Moderation

We predict that we will observe sex differences in the relationships between internalizing dimensions and gray matter morphometry predominately in the adolescent sample, as adolescence marks a period of time of considerable differences between the sexes in both neuronal organization (Gennatas et al., 2017; Sussman et al., 2016) and psychopathology (Hankin, 2009; Salk et al., 2017). Specifically, we predict that these sex-related effects will occur in regions showing differential neuroanatomical trajectories between the sexes during adolescence, particularly portions of the postcentral gyrus, frontal pole, lingual gyrus, and inferior frontal gyrus (Vijayakumar et al., 2016).

1.7.2.5. Genetic and Environmental Influences

Though the twin-based heritability analyses in Chapter 5 are largely exploratory, we hypothesize that all six dimensions will show dissociable genetic and environmental influences, and that the associations between dimensions and neuroanatomy will be primarily driven by shared genetic influences. This prediction is grounded in observations of moderate degrees of additive genetic influences on both internalizing psychopathology (Scaini et al., 2014; Sullivan et al., 2000; Taylor, 2011) and gray matter morphometry (Winkler et al., 2010), with very little evidence of shared environmental effects on both domains. We additionally hypothesize that the relationships between internalizing dimensions and gray matter morphometry will refeclt overlapping genetic architecture, as opposed to overlapping environmental factors.

CHAPTER 2

REVIEW OF THE LITERATURE

In the following chapter, we provide a literature review of studies relevant to the aims of this project. This inclused a review of previous studies evaluating the gray matter morphometry of internalizing psychopathology, beginning with case-control studies of internalizing disorders and moving to more dimensional approaches. We then review research into the heritability of internalizing dimensions. Though no study has evaluated the heritability of the precise six-factor dimension model we introduce in this project, we highlight heritability studies of closely related dimensions.

2.1. Gray Matter Morphometry of Internalizing Disorders

Research into the neuroanatomical correlates of internalizing psychopathology has been dominated by case-control studies in adults. These studies have generally employed voxel-based morphometry (VBM) (Ashburner & Friston, 2000) to evaluate focal differences in gray matter volume between patient groups and healthy controls. Though surface-based morphometry (SBM) (Fischl, 2012) has been used less than VBM historically, SBM has considerable appeal over voxel-based measures of gray matter volume. SBM not only captures volumetric properties of the cortex, but also allows for the decomposition of volume into additional measures of cortical structure, including surface area and thickness. By delineating between multiple properties of neuroanatomical structure, surface-based morphometry can provide a more nuanced picture of the neural correlates of psychopathology, a picture that may be obscured by looking at volume alone.

Studies examining brain morphology using VBM and SBM in adults have found that there are high degrees of regional overlap across psychiatric disorders. These findings support a model in which a common set of brain systems are associated with most mental health disorders (e.g., Goodkind et al., 2015). These results align with behavioral observations of high degrees of comorbidity between disorders (Kessler et al., 2005a,b; Merikangas et al., 2010), as well as overlapping symptomologies (Clark & Watson, 1991a,b; Zbozinek et al., 2012), likely emerging due to neural mechanisms that confer a risk for psychopathology in general (Menon, 2011). Indeed, meta-analyses across diagnoses of predominately adult patients report that cognitive control and limbic brain regions show similar alterations in functional (Menon, 2011) and structural (Goodkind, et al., 2015) properties across a range of internalizing disorders.

Under the case-control framework, one can begin to gain insight into the neuroanatomical correlates that are shared and unique across internalizing disorders by comparing and contrasting the brain regions associated with one disorder or the other, as well as comorbid disorders. To date, this literature has been dominated by VBM studies in adults, with meta-analyses highlighting a few core regions with atypical gray matter volume in MDD and anxiety disorders, including prefrontal and subcortical regions. While SBM studies have only recently begun to proliferate, case-control SBM studies primarily identify similar regions. In the following section, we review the literature of case-control VBM and SBM studies of MDD, anxiety disorders, and comorbidity between the two, first in adults, and then in adolescence. Of particular interest is determining which brain regions appear to be associated with specific internalizing disorders as compared to internalizing disorders more broadly, or a general susceptibility to psychopathology.

2.1.1 Case-control Studies of MDD in Adults

In one of the first meta-analyses of region-of-interest VBM studies of MDD status, Koolschijn and colleagues (2009) found adults with MDD show reductions in gray matter volume in prefrontal regions, specifically in the anterior cingulate cortex and orbitofrontal cortex, as well as subcortical regions including the hippocampus and striatum. Focusing on whole-brain voxel-wise studies instead of region-of-interest studies, a meta-analysis conduct by Sacher and colleagues (2012) also identified reductions of volume in the anterior cingulate cortex and nearby dorsomedial prefrontal cortex, as well as the amygdala, a subcortical structural immediately adjacent to and highly interconnected with the hippocampus. Associations between MDD and properties of the anterior cingulate cortex and hippocampus were further reinforced in a meta-analysis of MDD patients by Du and colleagues (2012), who found reductions in gray matter volume in not just the anterior cingulate and hippocampus, but also right lateral prefrontal cortex (i.e., middle- and inferior frontal gyri) and left thalamus. That same year, another meta-analysis by Bora and colleagues (2012) reported that MDD status was associated with reductions in anterior cingulate cortex volume and lateral prefrontal cortex regions, namely the right middle frontal gyrus.

This collection of meta-analyses of VBM studies largely confirm models of internalizing psychopathology as being associated with prefrontal cognitive control and subcortical affective systems (e.g., MDD: Disner et al., 2011; anxiety disorders: Etkin, 2009), yet there remain inconsistencies in the specific regions implicated. Whereas all four meta-analyses implicate the anterior cingulate cortex, there appears to be inconsistencies as to whether MDD status is a) associated with the amygdala, hippocampus, or both, b) thalamic alterations, and c) lateral prefrontal regions. While there is substantial overlap in the studies included across all four meta-

analyses, the meta-analyses often differed on important methodological considerations. These include the method for determining significance, decisions regarding inclusion or exclusion of region-of-interest vs. whole-brain voxel-based studies, and, important to the current project, the decision to include or exclude studies involving individuals with comorbid disorders. Because of the high rates of comorbidity between MDD and anxiety disorders, by not carefully accounting for the co-occurrence of multiple disorders, it is impossible to determine whether a given region shows a unique association with one disorder over another. Indeed, in a follow-up meta-analysis conducted by Lai (2013) in which the authors explicitly controlled for comorbidity, MDD status was only associated with anterior cingulate volume after controlling for the presence of comorbid disorders. These results suggest that at least some of the brain regions showing altered gray matter volume in case-control studies may not be unique markers of MDD, but instead reflect neural properties that are associated with multiple and/or co-occurring disorders, namely anxiety disorders.

Over the past decade, research into the neuroanatomical correlates of internalizing disorders has transitioned from predominately using VBM to predominately using SBM. Though fewer studies currently exist, SBM provide a more nuanced picture of the neuroanatomical correlates of MDD and anxiety disorders, not only implicating regions identified in VBM studies, such as the anterior cingulate and orbitofrontal cortices, but also suggesting that additional regions may show altered gray matter morphometry in patients as compared to controls. As found in VBM studies, an overwhelming number of SBM studies in adults confirm that MDD status is associated with atypical neuroanatomy in the anterior cingulate (Han et al., 2014; Liu et al., 2015; Meier et al., 2016; Schmaal et al., 2017; van Eijndhoven et al., 2013; Wagner et al., 2012), orbitofrontal cortex (Han et al., 2014; Liu et al., 2015; Na et al., 2016;

Ozalay et al., 2016; Schmaal et al., 2017; Qiu et al., 2014; Tu et al., 2012; van Eijndhoven et al., 2013; Won et al., 2016; Yang et al., 2015; Zuo et al., 2018), but also the middle frontal gyrus (Han et al., 2014; Qiu et al., 2014; Tu et al., 2012; Wagner et al., 2012; Zuo et al., 2018) and, to a lesser degree, the inferior frontal gyrus (Na et al., 2016; Qiu et al., 2014) and hippocampus/parahippocampal gyrus (Han et al., 2014; Papmeyer et al., 2015; Schmaal et al., 2016; Wagner et al., 2012; Zhao et al., 2017). Across all of these studies with adult samples, the majority of these effects show that adult patients have less volume, surface area or cortical thickness as compared to healthy controls. Interestingly, SBM studies also show converging evidence that MDD patients have neuroanatomical alterations in brain regions not commonly implicated in meta-analyses of VBM studies. These regions include the insula (Liu et al., 2015; Schmaal et al., 2017; Tu et al., 2012; Wagner et al., 2012; Zuo et al., 2018), precentral gyrus (Ozalay et al., 2016; Papmeyer et al., 2015; Tu et al., 2012), lateral parietal lobe (Ozalay et al., 2016; Perlman et al., 2016; Qiu et al., 2014; Tu et al., 2012; Yang et al., 2015), occipital regions (Na et al., 2016; Tu et al., 2012; Zuo et al., 2018) and temporal regions outside of the medial temporal lobe (Ozalay et al., 2016; Perlman et al., 2017; Tu et al., 2012; van Eijndhoven et al., 2013; Wagner et al., 2012; Yang et al., 2015). Of note is the fact that, outside of the inferior- and middle frontal gyri and lateral parietal lobe, all of the aforementioned regions were implicated in two of largest MDD case-control studies ever, both from the ENIGMA consortium, evaluating cortical (Schmaal et al., 2017) and subcortical (Schmaal et al., 2016) alterations in over 2000 and 1500 MDD patients, respectively. In these studies, adults with MDD showed reduced cortical thickness in anterior and posterior cingulate, orbitofrontal cortex, insula, and lateral temporal lobes (Schmaal et al., 2017) as well as reduced volume in the hippocampus (Schmaal et al., 2016). In a recent meta-analysis of this literature, Suh and colleagues (2019) found when looking

across cortical thickness studies that MDD status was associated with reduced cortical thickness in bilateral medial orbitofrontal cortex, left inferior frontal gyrus and, surprisingly, portions of the occipital lobe, as well as increased thickness in the supramarginal gyrus.

Looking across the findings from both VBM and SBM studies, a couple of trends are apparent. First, across both methodologies, MDD status is associated with alterations in neuroanatomical characteristics in the anterior cingulate and orbitofrontal cortex and, to a lesser degree, the inferior and middle frontal gyri, as well as the hippocampus/parahippocampal gyri. Second, SBM studies further suggest widespread alterations in cortical thickness in regions not commonly implicated by VBM, including the precentral gyrus, temporal lobe, parietal lobe, and occipital lobe, suggesting that neuroanatomical alterations in MDD extend beyond the prefrontal cortex and limbic system. Third, whereas early VBM studies suggested that amygdala volume is reduced in MDD patients, more recent SBM studies have provided little evidence of amygdala alterations in MDD. However, inconsistencies across studies in how researchers treat comorbidity are common place, calling into question the degree to which the plethora of regions associated with MDD status are in fact specific to MDD, associated with comorbid anxiety disorders, or both.

2.1.2. Case-control Studies of Anxiety Disorders in Adults

Gray matter morphometry studies investigating the neuroanatomical correlates of anxiety disorders in adults show both similar and distinct brain regions as compared to studies of adult MDD patients. Because of the multiple diagnoses that fall under the umbrella of anxiety

disorders, we begin our review of this literature by highlighting studies of specific anxiety disorders, moving on to studies evaluating neuroanatomical alterations across anxiety disorders.

To our knowledge, no meta-analysis has been conducted on gray matter studies of adults with generalized anxiety disorder (GAD). Looking across studies, however, a few trends emerge. First, adults with GAD show relatively consistent gray matter alterations in the prefrontal cortex, including reductions in both volume and thickness of the anterior cingulate and nearby orbitofrontal cortex (Andreescu et al., 2017; Carnevali et al., 2019; Schienle et al, 2011), as has been observed in MDD patients and across psychopathology more broadly (Goodkind et al., 2015). SBM studies additionally show evidence of reduced lateral prefrontal cortex thickness in GAD, including the inferior frontal (Andreescu et al., 2017), middle frontal (Veronese et al., 2015; Molent et al., 2018), and superior frontal gyri (Andreescu et al., 2017; Veronese et al., 2015). Subcortically, adults with GAD show reduced volume in the hippocampus (Abdallah et al., 2013; Moon et al., 2014), but limited evidence of reduced amygdala volume (Schienle et al., 2011), and inconsistent evidence of alterations in additional subcortical structures, with one study reporting reduced thalamus volume (Moon et al., 2014) and another reporting increased thalamus and putamen volume (Hilbert et al., 2015) in patients as compared to controls. Though the specific subregions differed across studies, multiple studies have found evidence of alterations in the temporal cortex, including increased temporal pole volume (Hilbert et al., 2015), decreased superior temporal gyrus volume (Moon et al., 2014), and, in the one study evaluating gyrification, increased gyrification in the superior frontal gyrus, temporal fusiform, and inferior temporal gyrus (Molent et al., 2018). Also of note, though some models of psychopathology suggest that the insula is a key region in anxiety, only one study reviewed

showed altered gray matter morphometry in the insula in GAD patients, with Moon and colleagues (2014) reporting reduced volume in patients as compared to controls.

In a recent meta-analysis of VBM studies of social anxiety disorder, Wang and colleagues (2018) observed that adult patients showed increased gray matter volume in the precuneus, superior frontal gyrus, angular gyrus, middle temporal gyrus, occipital lobe, and supplementary motor area (Wang et al., 2018). Though this meta-analysis of VBM studies did not implicate the anterior cingulate or orbitofrontal cortex, SBM studies implicate an expanded set of regions beyond those identified by VBM including the anterior cingulate and orbitofrontal cortex (Bruhl et al., 2014; Syal et al., 2012) as well as the middle frontal gyrus (Bruhl et al., 2014; Syal et al., 2012) and the insula (Bruhl et al., 2014; Syal et al., 2012), albeit with inconsistency in terms of the direction of effects across all regions. Some evidence suggests that the inconsistency in direction of effects may reflect the inclusion or exclusion of comorbid MDD patients, with Bruhl and colleagues (2014) excluding comorbid MDD and reporting only increased thickness in social anxiety patients in the anterior cingulate, middle frontal gyrus, insula, and temporal pole, amongst other regions. In contrast, Syal and colleagues (2012) found reduced thickness in these same regions when including social anxiety patients with comorbid MDD.

Gray matter morphometry studies of panic disorder suggest a range of regional alterations in patients as compared to controls. Whereas an earlier meta-analysis of VBM studies in panic disorder patients only found reduced gray matter volume in the right caudate and right parahippocampal gyrus (Lai, 2011), a more recent meta-analysis focusing explicitly on whole-brain VBM studies found panic disorder patients to have reduced volume in the orbitofrontal cortex, frontal pole, superior frontal gyrus, insula, superior temporal gyrus and the middle

temporal gyrus. However, additional studies report reduced volume in the anterior cingulate (Asami et al., 2008), amygdala (Asami et al., 2018a; Hayano et al., 2009; Massana et al., 2003) and thalamus (Asami et al., 2018b), as well as increased volume in the insula (Uchida et al., 2008). One study reported relatively widespread gray matter alterations in panic disorder patients, with volumetric reductions in the amygdala and insula significantly greater in men as compared to women, suggesting sex effects on the neuroanatomical correlates of panic disorder (Asami et al., 2009).

A meta-analysis of VBM studies of obsessive compulsive disorder by Rotge and colleagues (2010) found patients to have reduced volume in the orbitofrontal cortex, middle and superior frontal gyri, and the supramarginal gyrus, as well as increased volume in the putamen and frontal pole. Interestingly, there is little correspondence between these VBM results and SBM studies of obsessive compulsive disorder. For example, in the largest neuroanatomical study of obessessive compulsive disorder to date with over 700 patients, Fouche et al., (2017) only found similar results to those of Rotge and colleagues (2010) in the superior frontal gyrus. Instead, Fouche and colleagues (2017) identified a number of other regions spread throughout the brain, all showing reduced cortical thickness in patients, including the inferior frontal gyrus, precentral gyrus, inferior parietal lobe, precuneus, posterior cingulate, and middle temporal gyrus. Of these findings, reduced cortical thickness in the middle temporal gyrus and precuneus have been replicated elsewhere (Kuhn et al., 2013b), whereas that same study also implicated the precentral gyrus, but found patients to have increased as opposed to decreased thickness (Kuhn et al., 2013b). Additionally, two studies report reduced insular cortical thickness in patients as compared to controls (Kuhn et al., 2013b; Nakamae et al., 2012).

In a meta-analysis of VBM studies of post-traumatic stress disorder (PTSD), Kuhn & Gallinat (2013a) found volume reductions in the anterior cingulate, middle temporal gyrus, and hippocampus. Related work found that patients with PTSD show reductions in the volume of the anterior cingulate, superior frontal gyrus, middle temporal gyrus, and hippocampus in comparison to trauma-exposed controls (Li et al., 2014). SBM studies have suggested widespread, largescale alterations in gray matter structure, particularly prefrontal alterations, with one study reporting reduced cortical thickness in the inferior, middle and superior frontal gyri (Geuze et al., 2008), and another ROI based study reporting reduced thickness in most subregions of frontal and temporal lobes, as well as vertex-wise reductions in thickness in inferior parietal lobe, superior frontal gyrus, and superior temporal gyrus, and decreased volume of the thalamus and hippocampus (Sussman et al., 2016b).

Looking across distinct anxiety disorders, there is considerable convergence in the brain regions that show altered gray matter morphometry in patients. For example, as was observed in MDD, most anxiety disorders implicate prefrontal regions, including the anterior cingulate, orbitofrontal cortex, and, to a lesser yet notable degree, lateral prefrontal regions including the inferior, middle, and superior frontal gyri. Furthermore, multiple anxiety disorders appear to be associated with atypical anatomy in the hippocampus, amygdala, and putamen, as well as alterations in the temporal cortex, albeit with different disorders showing alterations in different sets of temporal regions. In an attempt to directly test for commonalities in gray matter alterations across all anxiety disorders, a meta-analysis of VBM studies across anxiety disorders by Shang and colleagues (2014) found that anxiety diagnoses in adults are associated with reductions in volume of the right anterior cingulate, as has been consistently observed in MDD, but also reductions in left inferior frontal gyrus, right precentral gyrus, and left middle temporal

gyrus after removing studies that included anxiety patients with comorbid MDD. In a similar meta-analysis across anxiety disorders, Radua and colleagues (2010) found obsessive compulsive disorder, panic disorder and post-traumatic stress disorder in adults were all associated with reductions in gray matter volume in the anterior cingulate and orbitofrontal cortex, as well subcortical structures, including the putamen and caudate.

2.1.3. Case-control Studies of MDD and Anxiety Comorbidity in Adults

While studies comparing patient groups to healthy controls can begin to highlight specific brain regions associated with internalizing disorders, inconsistencies in methodologies in this body of literature make it unclear the degree to which a specific brain region is associated with MDD, anxiety disorders, or both. As such, comparing the neuroanatomical correlates of different diagnoses implicated by distinct studies can provide only limited, imprecise inferences into brain regions that show disorder-specific alterations, as compared to alterations that are transdiagnostic. For example, even if the anterior cingulate cortex is associated with multiple disorders, because many of these disorders co-occur it is almost impossible to know if this region is associated with all disorders, or merely associated with a disorder(s) that is often comorbid with the disorder of interest. One technique to further disentangle this issue within a case-control framework is to directly compare patients meeting criteria for only one disorder to patients with comorbid disorders. Notably, only a few such studies exist.

In adults, MDD patients with comorbid anxiety symptoms show a number of alterations in gray matter morphometry when compared to patients with MDD only. For example, in a meta-

analysis of the VBM MDD literature, Bora and colleagues (2012) found that studies including MDD patients with comorbid anxiety disorders reported additional volumetric reductions in the amygdala, extending into the parahippocampal gyrus, and putamen as compared to healthy controls. However, this meta-analysis was unable to explicitly test the contrast between patients with comorbid MDD and anxiety to patients with MDD only, instead testing for moderating effects of studies that did not explicitly exclude individuals with comorbid disorders. To gain even further insight into the brain systems associated with the co-occurrence of MDD and anxiety, it is important to evaluate studies that directly compare groups of only comorbid patients to groups of patients with only one disorder. In once such study, Qi and colleagues (2014) found that patients with comorbid MDD and anxiety had *increased* volume across much of the brain when compared to an MDD only group, including in the superior frontal gyrus, insula, inferior and middle temporal lobes, precentral gyrus, parahippocampal gyrus, lingual gyrus, angular gyrus, rectal gyrus, and supplementary motor area. In a more recent SBM study, Canu and colleagues (2015) compared MDD patients with and without comorbid generalized anxiety, finding that comorbid patients have thinner medial orbitofrontal cortex, temporal pole, lateral occipital cortex, and fusiform gyrus. In related SBM work directly comparing MDD patients with comorbid anxiety to MDD-only patients, comorbid patients showed thinner gray matter in left superior frontal gyrus, right superior temporal lobe, and lingual gyrus, as well as increased volume in the caudate, while both patient groups showed thinner temporal lobes, inferior frontal gyrus, and reduced hippocampus volume as compared to healthy controls (Zhao et al., 2017). In a similar but even more recent study, Peng and colleagues (2019) found that comorbid MDD and anxiety was associated with reduced volume in the orbitofrontal cortex and inferior frontal gyrus relative to MDD-only and healthy controls. Furthermore, comorbid patients showed increased

gray matter volume in the precentral gyrus as compared to MDD-only (Peng et al., 2019). While multiple studies have compared MDD with comorbid anxiety to MDD-only patients in adults, far fewer studies have compared adult patients with comorbid MDD and anxiety, MDD-only, and anxiety-only. In one such study, all three patient groups showed reduced volume in the anterior cingulate cortex when compared to healthy controls, whereas MDD-only was associated with reductions in right inferior frontal gyrus and anxiety disorders were associated with reduction in lateral temporal lobe volume (van Tol, et al., 2010).

Though large inconsistencies exist in this literature, these results converge on the notion that the presence of anxiety in addition to MDD is associated with atypical temporal cortex anatomy over MDD alone. Indeed, alterations in the temporal lobe in the comorbid groups were observed in multiple studies (Canu et al., 2015; Inkster et al., 2011; Qi et al., 2014; Zhao et al., 2017) with all studies but one (Qi et al., 2014) reporting decreased neuroanatomy in the comorbid group as compared to the MDD-only group. This provides compelling evidence that anxiety disorders area associated with alterations in temporal lobe structure over and above gray matter alterations observed in MDD. In addition to associations with temporal lobe anatomy, some evidence suggests that comorbid MDD and anxiety is associated with atypical morphology in the precentral gyrus (Peng et al., 2019; Qi et al., 2014), superior frontal gyrus (Qi et al., 2014; Zhao et al., 2017), lingual gyrus (Qi et al., 2014; Zhao et al., 2017), parahippocampal gyrus (Bora et al., 2012; Qi et al., 2014), and striatum (Bora et al., 2014; Zhao et al., 2017), albeit with inconsistency as to the direction of effects across all of these regions. These results suggest that the presence of comorbid MDD and anxiety is associated with widespread alteration in gray matter as compared to MDD only patients. However, these results do not mean that these regions are necessarily unique to anxiety or comorbidity between MDD and anxiety as there is

considerable evidence suggesting that comorbidity between disorders is associated with greater severity of a given disorder (Angst et al., 1999; Kaufman & Charney, 2000). Thus, comparing MDD patients with comorbid anxiety to MDD-only patients may be capturing brain regions associated with increased MDD severity, not anxiety per se. To further disentangle the brain regions that are associated with internalizing disorders broadly vs. specific to MDD or anxiety, it may be necessary to move away from the case-control context and to instead employ methodologies that directly quantify covariation in behaviors shared between disorders, as well as behaviors thought of as being more specific to one class of disorders over the other.

2.1.4. Neuroanatomical Correlates of Internalizing Disorders in Adolescence

Despite the literature on gray matter morphometry in internalizing disorder being dominated by studies with adult, it is critically important to understand the neural markers of internalizing psychopathology in adolescence, as adolescence often marks the onset of internalizing behaviors (Hankin, 2006, 2009, 2015), behaviors that can be predictive of later mental health problems (Zisook et al., 2007). One yet to be addressed question is the degree to which adolescent patients show similar or distinct patterns of gray matter morphometry as to those observed in adults. In the following, we review the case-control literature of gray matter morphometry studies in adolescents with internalizing disorders, with an eye towards similarities and differences in neuroanatomy between adolescent and adult patients.

As compared to studies investigating adults, far fewer gray matter morphometry studies have investigated the neuroanatomical correlates of internalizing disorders in adolescents. From both VBM and SBM studies, however, it can be inferred that adolescents with internalizing

disorders show alterations in gray matter structure in similar regions to those identified in adults. However, the specific patterns of results differ in important ways, with adolescents showing much more inconsistency in terms of the direction of effects and specificity of region-diagnosis relationships. Beginning with the prefrontal cortex, as frequently observed in adults, multiple studies implicate the anterior cingulate cortex and contiguous ventromedial prefrontal regions in both MDD (Koenig et al., 2018; MacMaster et al., 2014; Pannekoek et al., 2014; Reynolds et al., 2014) and anxiety disorders (Gilbert et al., 2008; Gold et al., 2017; Hoexter et al., 2011; Strawn et al., 2015; Suffren et al., 2019; Szeszko et al., 2004). However, whereas adult studies almost exclusively demonstrate decreased anterior cingulate anatomy in patient groups, adolescent studies report both decreases (MDD: Koenig et al., 2018; MacMaster et al., 2014; anxiety: Gilbert et al., 2008; Hoexter et al., 2011; Suffren et al., 2019) and increases (MDD: Reynolds et al., 2014; anxiety: Gold et al., 2017; Strawn et al., 2015; Szeszko et al., 2004) in neuroanatomical characteristics (e.g., thickness, volume) in patients as compared to healthy controls. As has been observed in adults with MDD or anxiety, studies in adolescents show that MDD or anxiety patients each show reductions in neuroanatomical characteristics in orbitofrontal cortex (MDD: Shad et al., 2012; Schmaal et al., 2017; anxiety Hoexter et al., 2012; Strawn et al., 2014). In fact, results from the largest gray matter morphometry study of MDD found that the only region commonly implicated across adolescent and adult MDD patients is the medial orbitofrontal cortex, though adolescents showed reduced cortical surface area in this region whereas adults showed reduced cortical thickness (Schmaal et al., 2017). Another notable dissociation between the adolescent and adult literature occurs in the lateral prefrontal cortex, namely the inferior and middle frontal gyri. Whereas adult patients consistently show atypical neuroanatomy in these regions, particularly MDD patients, studies implicating the lateral prefrontal cortex in adolescent

internalizing disorders are less frequent and inconsistent. Whereas Shad et al., (2012) reported reduced volume in the inferior and middle frontal gyri in MDD patients and Koenig et al., (2018) reported decreased middle frontal gyrus thickness, Reynolds et al., (2014) reported increased middle frontal gyrus volume. Across anxiety disorders, Strawn et al., (2015) found adolescent anxiety patients had reduced volume in the inferior frontal gyrus, but these results have largely not been replicated. This discrepancy between adolescents and adults is interesting developmentally, as the lateral prefrontal regions are some of the last brain regions to undergo maturation (Diamond et al., 2002; Gogtay et al., 2004; Shaw et al., 2008), with some evidence suggesting that complete maturation does not occur until young adulthood (e.g., age 25). Further research is warranted, but the lack of consistent associations between lateral prefrontal regions and internalizing disorders in adolescence may reflect developmentally driven heterogeneity in the neural substrates of internalizing disorders, with internalizing disorder becoming more frontally mediated as individuals develop out of adolescence and into adulthood. Investigating this issue further sits at the crux of the current report.

Subcortically, as in adults, adolescent patients with internalizing disorders show alterations in the hippocampus and amygdala. Specifically, hippocampal volume was found to be reduced in both MDD and anxiety patients, (MDD: Jaworska et al., 2016; MacMaster et al., 2014; anxiety: Mueller et al., 2013). Additionally, amygdala volume appears to be altered in adolescent MDD (Rosso et al., 2005) and anxiety disorders (De Bellis et al., 2000; Milham et al, 2005; Strawn et al., 2015; Suffren et al., 2019; Szesko et al., 2004). As is the case of studies with adults, results linking amygdalar and hippocampal volume to one class of disorders over the other are inconsistent, likely due to studies not considering comorbidity in their analyses.

In addition to associations with subcortical medial temporal lobe structures, adolescent internalizing disorders appears to be associated with alterations in lateral temporal lobe, albeit with inconsistent associations across disorders. Specifically, in VBM studies, De Bellis and colleagues (2002) demonstrated increased volume in the superior temporal gyrus in adolescent diagnosed with GAD, whereas Shad and colleagues (2012) found reduced superior and middle temporal gyri volume in adolescent MDD patients. In SBM studies, Strawn and colleagues (2014) found increased cortical thickness left medial and inferior temporal lobe in adolescents with GAD as compared to healthy controls, though no other adolescent SBM study implicates lateral temporal structures across MDD or anxiety disorders.

Due to inconsistencies in methods for correcting for comorbidity, it is important to consider studies that directly compare adolescents with comorbid disorders to adolescents with only one disorder. To our knowledge, only one study has evaluated differences in gray matter volume between adolescents with comorbid MDD and anxiety, MDD-only, and healthy controls. Though likely underpowered, this study found strikingly similar results to what was observed in adults by Peng and colleagues (2019), including reductions in right lateral prefrontal cortex volume in the comorbid group as compared to the MDD-only and healthy control groups, as well as increased volume in the pre- and post-central gyri in the comorbid group as compared to the MDD-only group (Wehry et al., 2015). Additionally, Wehry and colleagues (2015) identified a number of regions in which MDD-only patients had greater gray matter volume than healthy controls, including the right middle frontal gyrus, left precuneus, right thalamus and right caudate.

2.1.5 Summary

When looking across the case-control literature of morphometry studies of internalizing disorders in adults and adolescents, a number of trends emerge. First, it appears that in adult and adolescent patients, the anterior cingulate cortex and orbitofrontal cortex have reduced gray matter volume and thickness across internalizing disorders, suggesting that these regions may play transdiagnostic roles in internalizing psychopathology more broadly. In fact, research looking across all major Axis 1 disorders suggests that anterior cingulate gray matter alterations may not be unique to internalizing disorders but may instead be transdiagnostic across *all* psychopathologies, including externalizing disorders and psychoses (Goodkind et al., 2015).

Second, lateral prefrontal regions show relatively consistent reductions in cortical volume and thickness in adult patient groups across internalizing disorders, but this is not the case in adolescent patients, potentially reflecting the delayed developmental trajectory of lateral prefrontal systems commonly associated with psychopathology. Within adults, there is some evidence for a dissociation with the lateral prefrontal cortex, with MDD more frequently associated with middle frontal gyrus alterations (Han et al., 2014; Koenig et al., 2018; Qiu et al., 2014; Reynolds et al., 2014; Shad et al., 2012; Tu et al., 2012; Wagner et al., 2012; Zuo et al., 2018) than the inferior frontal gyrus (Na et al., 2016; Qiu et al., 2014; Shad et al., 2012), whereas anxiety disorders show similar frequency of studies implicating the middle frontal gyrus (Geuze et al., 2008; Hu et al., 2017; Bruhl et al., 2014; Molent et al., 2018; Rotge et al., 2010; Syal et al., 2012; Veronese et al., 2015) as the inferior frontal gyri (Andreescu et al., 2017; Fouche et al., 2010; Geuze et al., 2008; Hu et al.,, 2017; Shang et al., 2014; Strawn et al., 2015)

Third, there is some evidence of differential associations of subcortical structures with MDD and anxiety disorders. Much of theory and research into internalizing disorders has

focused on the role of subcortical structures, namely the hippocampus and amygdala and, not surprisingly, both regions have shown some evidence of alterations in gray matter across multiple internalizing disorders. However, inconsistencies in how studies account for comorbidity make it unclear as to the specificity of hippocampal and amygdalar alterations. One important question regarding the relationship between the hippocampus and amygdala and internalizing disorders is whether the two brain structures show differential associations with MDD and anxiety disorders. In terms of gray matter morphometry, meta-analyses of volumetric alterations in MDD that did not account for comorbidity separately implicated the hippocampus (Koolschijn et al., 2009) and amygdala (Sacher at al., 2012), but not both. On the other hand, in a meta-analysis directly evaluating the neuroanatomical correlates of comorbid MDD and anxiety, Bora and colleagues found volumetric reductions in both the amygdala and parahippocampal regions, suggesting that the inconsistency in findings from Koolschijn and Sacher regarding subcortical alterations in MDD may stem from not accounting for comorbidity. However, in one of the largest MDD patient groups evaluated, Schmaal and colleagues (2016) found evidence that MDD may only be associated with hippocampal volume, findings that have been noted elsewhere (Campbell et al., 2004; MacMaster et al., 2008; Videbech & Rivnkilde, 2004). Furthermore, a meta-analysis specifically focusing on amygdala volume in MDD found no significant differences between MDD patients and healthy controls. To date, case-control studies in adults suggest that the amygdala is altered anatomically in anxiety patients across a range of anxiety disorders (De Bellis et al., 2000; Milham et al, 2005; Strawn et al., 2015; Suffren et al., 2019; Szesko et al., 2004). These results suggest a potential dissociation between MDD and anxiety disorders, with hippocampal neuroanatomy preferential associating with MDD status and amygdalar volume preferentially associating with anxiety disorders. Indeed, though speculative,

this dissociation aligns with theories of the neural factors driving these disorders, with depressed behaviors stemming from self-referential, memory-centric processes supported by the hippocampus and anxious behaviors stemming from amygdala-centric threat detections systems.

Fourth, in addition to associations of internalizing disorders with the hippocampus and amygdala, the case-control literature suggests internalizing disorders may also be associated with other subcortical structures, namely the thalamus and striatum. Specifically, across both MDD and anxiety disorders in adolescents and adults, studies frequently report alterations in the thalamus (MDD: Du al., 2012; Koolschijn et al., 2009; Wehry et al., 2015; Anxiety: Hilbert et al., Liao et al., 2013, 2014; Moon et al., 2014; Shad et al., 2012; Sussman et al., 2016), the putamen (MDD: Bora et al., 2012; Anxiety: Hoexter et al., 2011; Hu et al., 2017; Zarei et al., 2011) and, to a lesser degree, the caudate (Anxiety: Hu et al., 2017; Zarei et al., 2011). Though inconsistencies across these studies regarding sample demographics and comorbidity status make it difficult to make firm inferences, it appears that these subcortical regions show robust relationships with internalizing disorders generally.

Fifth, though not frequently discussed in relation to internalizing disorders, a number of additional regions stand out in the review of the adult case-control literature. These include regions commonly implicated in movement, including the pre- and post-central gyri, as well as lateral temporal regions generally associated with semantic processes. Pre- and postcentral gyri alterations are implicated in both adults and adolescent studies, across MDD (Falluca et al., 2011; Ozalay et al., 2016; Papmeyer et al., 2015; Schmaal et al., 2017; Tu et al., 2012;) and anxiety disorders (Fouche et al., 2010; Gold et al., 2017; Kuhn et al., 2013; Shang et al., 2014; Strawn et al., 2013), as well as comorbid groups (Peng et al., 2019; Qi et al., 2014). Another general brain region not commonly discussed in terms of internalizing disorders that consistently

showed alterations across MDD and anxiety patients is the temporal cortex. Whereas medial temporal lobe structures are frequently implicated in internalizing disorders, lateral temporal cortex is rarely discussed in relation to internalizing psychopathology. After reviewing the literature, however, it is apparent that alterations in temporal cortex, including the inferior-, middle-, and superior temporal lobes, as well as the temporal pole, are common across both adolescent and adult patient groups. In particular, multiple studies suggest that comorbid MDD and anxiety are associated with altered temporal cortex anatomy when compared to MDD-alone (Canu et al., 2015; Inkster et al., 2011; Qi et al., 2014; Zhao et al., 2017).

Finally, the insula is considered a major convergence zone with strong influences on affect. As such, it has been previously associated with a broad range of psychopathologies (Goodkind et al., 2015), and is thought to contribute to general feelings of interoceptive distress that are inherent across many internalizing psychopathologies (Craig, 2009, 2011). While alterations in insula neuroanatomy were observed in a number of studies, the overwhelming majority of these studies employed SBM measures of cortical thickness (Bruhl et al., 2014; Kuhn et al., 2013; Liu et al., 2015; Nakamae et al., 2012; Schmaal et al., 2017; Syal et al., 2012; Tu et al., 2012; Wagner et al., 2012; Zuo et al., 2018), with far fewer VBM studies (Moon et al., 2014; Mueller et al., 2013) detecting insular alterations in patients as compared to controls. This highlights the utility of not just considering gray matter volume alone, but also testing for relationships between internalizing psychopathology and multiple other measures of gray matter morphometry.

2.2. Gray Matter Correlates of Internalizing Psychopathology Dimensions

2.2.1. Overall Symptom Severity

As compared to case-control studies, dimensional approaches can provide a more precise mapping of the neuroanatomical correlates of specific behaviors not just in patients, but across the general population. Such approaches characterize psychopathology in a continuous fashion, allowing for a more nuanced understanding of the relationship between degrees of behavior and neural organization. Yet even within individual differences studies, there is considerable variability in how researchers quantify behaviors central to psychopathology. The most common approach is to employ a single measure, often from self-report questionnaires, that captures general severity for a given disorder, but does not differentiate between distinct symptom dimensions within that disorder. For example, employing a multitude of measures of severity in patients, healthy control, and mixed groups, overall depression severity has been associated with variability in gray matter morphometry across much of the adult brain, including the anterior cingulate (Carlson et al., 2015; Webb et al., 2014), orbitofrontal cortex (Vasic et al., 2008; Webb et al., 2014), lateral prefrontal regions (Besteher et al., 2017; Salvadore et al., 2011; Vasic et al., 2008; Webb et al., 2014), temporal cortex (Besteher et al., 2017; Webb et al., 2014), motor regions (Besteher et al., 2017; McLaren et al., 2018; Stratmann et al., 2014), parietal lobe (Besteher et al., 2017), and occipital lobe (Besteher et al., 2017), as well as subcortical structures, including the hippocampus (Cheng et al., 2010; Vasic et al., 2008), amygdala (Zhang et al., 2016), and thalamus (Webb et al., 2014; Pillay et al., 1998). As is the case for depression severity, studies evaluating relationships between gray matter morphometry and general

measures of anxiety severity report associations across much of the brain in both patients and healthy controls. This includes associations of anxiety severity with the anterior (Donzuso et al., 2014; Frick et al., 2013; Gorka et al., 2014; Spampinato et al., 2009), mid (Besteher et al., 2017), and posterior (Carnevali et al., 2019; Spampinato et al., 2009) cingulate, orbitofrontal cortex (Blackmon et al., 2011; Carnevali et al., 2019; Kuhn et al., 2011), lateral prefrontal regions (Hu & Dolcos, 2017; Spampinato et al., 2009), temporal cortex (Besteher et al., 2017; Blackmon et al., 2011), motor regions (Besteher et al., 2017), and the parietal lobe (Besteher et al., 2017), as well as subcortical structures, including the thalamus (Modi et al., 2019), nucleus accumbens (Kuhn et al., 2011), and the amygdala (Baur et al., 2012; Blackmon et al., 2011; Spampinato et al., 2009). Though fewer studies in adolescents exist, adolescent studies of general symptom severity implicate a subset of the regions identified in adults. For example, looking across over 300 children and adolescents ages 7 to 21, Merz and colleagues (2018) found that depression severity was associated with gray matter morphometry in the orbitofrontal cortex, hippocampus, and pallidum whereas Boes and colleagues (2008) found that in healthy individuals ages 7 to 17, increased depression severity was associated with reduced anterior cingulate volume, but only in boys. In a sample of both anxiety patients and controls ages 8 to 18, Gold and colleagues (2017) found that greater anxiety severity was only associated with reduced volume in the right hippocampus in healthy controls, but not patients (Gold et al., 2017).

In general, the literature evaluating correlations between overall symptom severity and individual differences gray matter morphometry largely confirm case-control studies, suggesting that, while overall symptom severity is correlated with gray matter morphometry over much of the brain, the correlations are predominately observed in prefrontal and subcortical regions, and there is considerable overlap in the regions implicated for depression and anxiety symptom

severity, respectively. However, much like case-control designs, using overall symptom severity to identify the neuroanatomical correlates of psychopathology ignores the considerable behavioral heterogeneity that can occur within a given internalizing disorder and do not account for the fact that discrete internalizing disorders show overlapping symptomology (Chen et al., 2000; Park et al., 2017). To address this issue, researchers can parse behaviors associated with psychopathology into distinct, continuous constructs that differentiate the myriad of behaviors associated with internalizing psychopathology, including behaviors that are shared across disorders. By then testing for the neural correlates of these specific behaviors and not just overall severity, we can gain a better understanding of the specific neural systems supporting a range of behaviors at the core of psychopathology. For example, whereas McLaren and colleagues (2016) found overall depression severity to be associated with the paracentral gyrus in the elderly, when they decomposed overall severity into more precise symptom dimensions, they found additional associations between depressed mood and portions of the temporal cortex, low positive affect and the lingual gyrus, and somatic complaints with the temporal pole. Despite the appeal of evaluating the neuroanatomical correlates of specific dimensions, there exists considerable discrepancies across studies as to the specific dimensions that are deemed relevant to internalizing psychopathology. Because the current project evaluates the neuroanatomical of a specific set of internalizing dimensions, namely negative affect, repetitive negative thinking, anxious arousal, anxious apprehension, low positive affect, and rumination, the following section reviews studies evaluating the neuroanatomical correlates of these, or analogous dimensions.

2.2.2. Neuroanatomical Correlates of Negative Affect-like Dimensions

To our knowledge, very few studies has evaluated the neuroanatomical correlates of a bifactor estimate of commonalities across internalizing psychopathology as is done in the current study. In one relevant study in children and adolescents, Cardinale and colleagues (2019) employed bifactor modeling to capture covariation between anxiety and irritability, but found no significant associations between a common factor and gray matter morphometry. While the use of bifactor methodologies in the context of gray matter morphometry is uncommon, a number of preexisting studies have performed gray matter morphometry on manifest measures that are conceptually similar to common factors, including measures of shared symptoms between anxiety and depression, as well as negative affect and neuroticism, two highly related constructs that are thought to be associated with general psychological distress shared across many psychopathologies. For example, employing a negative affect dimension that was a composite of a number of internalizing behavior questionnaires, Holmes and colleagues (2012) found that, in a late adolescent to young adult sample of over 1000 participants, increased negative affect was associated with reduced volume of the anterior cingulate cortex and increased volume of the amygdala. Looking at overlapping brain regions implicated across multiple internalizing symptom dimensions, Lener and colleagues (2016) showed that in both MDD patients and subclinical individuals, irritation and fatigue were both negatively associated with anterior cingulate while worry, fatigue, and sadness were all negatively associated with volume of the inferior frontal gyrus, but in MDD patient. Because these dimensions were all correlated, the authors suggest that these overlapping associations across dimensions represent commonalities across these dimensions, and are thus capturing covariation in symptomology driven by a general negative affect dimension that is shared across anxiety and depression.

Studies investigating the neuroanatomical correlates of neuroticism in largely adult samples implicate a wide range of brain regions, with relatively little consistency. Looking across much of the lifespan in a sample ranging from 20 to 80 years old, Bjornebekk and colleagues (2013) found that neuroticism was associated with reduced surface area in prefrontal (i.e., anterior cingulate and middle frontal gyrus) and temporal regions (i.e., middle, inferior, and superior temporal gyrus and fusiform gyrus). In a similar study using data from the Human Connectome Project (van Essen et al., 2012), Riccelli and colleagues (2017) similarly found that increased neuroticism was associated with large scale reductions in area and volume, and increases in thickness, across much of the brain, but largely centered in prefrontal and temporal regions. These findings align with results from case-control studies suggesting that psychopathology in general is associated with anterior cingulate alterations (e.g., Goodkind et al., 2015) whereas comorbidity between anxiety and depression is associated with alterations in temporal lobe anatomy as compared to MDD alone (e.g., Canu et al., 2015; Inkster et al., 2011; Qi et al., 2014; Zhao et al., 2017). Interestingly, the constellation of regions observed by Bjornbekk and colleagues (2013) may be driven by older adults in the sample, as similar regions are implicated in studies focusing specifically on the elderly (Kapogiannis et al., 2013; Wright et al., 2007), but less so in younger samples. Looking at more restricted, younger age groups reveal additional associations between neuroticism and gray matter. Much of this research has focused on samples spanning late adolescence (i.e., ~18 years old) to early- (i.e., ~30 years old) or middle adulthood (i.e., ~40 years old), but show very little overlap in results, potentially due to inconsistent use of covariates across studies (for a review, see Hu et al., 2011). For example, across four studies employing general population samples of a similar age, the cerebellum stands out as the only region commonly implicated across studies, with increased neuroticism

associated with increased cerebellar volume in two studies (De Young et al., 2010; Lu et al., 2014). Beyond this, there is little agreement across the this literature, with a wide range of cortical brain regions showing associations with neuroticism, including the orbitofrontal cortex (Wright et al., 2016), mid cingulate (De Young et al., 2010), medial superior frontal gyrus (De Young et al., 2010), precentral gyrus (De Young et al., 2010), and the inferior parietal lobe in females only (Privado et al., 2017), as well as number of subcortical structures, including the hippocampus (De Young et al., 2010), amygdala (Omura et al., 2005), and basal ganglia (De Young et al., 2010).

Though only a few relevant studies exist focused specifically on childhood and adolescence, the studies that do exist suggest that dimensions capturing commonalities across internalizing psychopathology are associated with prefrontal and subcortical brain regions implicated in case-control studies, and are moderated by both age and gender. As was the case across internalizing disorder diagnoses, dimensions capturing behaviors shared across internalizing disorders are associated with the anterior cingulate cortex (Blankstein et al., 2009; Ducharme et al., 2014) and orbitofrontal cortex (Ducharme et al., 2014), as well as the hippocampus (Koolschijn et al., 2013). Of note is the diversity of relationships between common internalizing-like dimensions and neuroanatomy of the subgenual portion of the anterior cingulate. Looking across childhood and adolescence, Ducharme and colleagues found that, during childhood, when controlling for gender, increased anxiety/depression symptomology was negatively associated with cortical thickness of the subgenual cingulate from ages 5 to 8, but this relationship changed as individuals entered into adolescence, becoming non-significant from ages 9 to 17, then transitioning to a positive relationship by the time individuals reach 18 years of age (Ducharme et al., 2014). The lack of a significant effect across genders observed from ages 9

to 17 may be a result of profound gender differences. For example, Blankstein and colleagues (2009) found that in adolescents ages 16 to 17, boys and girls showed opposing relationships between neuroticism and subgenual cingulate thickness and volume, with boys showing negative associations and girls showing positive associations, associations that are not apparent when collapsing across gender. These results highlight the importance of directly testing for both age and gender effects instead of merely controlling for them, particularly in adolescent samples in which the brain is undergoing rapid neuroanatomical reorganization, reorganization that shows distinct trajectories between the genders.

2.2.3. Neuroanatomical Correlates of Anxious Arousal-like Dimensions

To date, very few studies have investigated the neuroanatomical correlates of anxious arousal or similar constructs capturing somatic behaviors of anxiety. In healthy young adults, increased scores on an anxiety measure which includes somatic symptoms similar to those inherent to anxious arousal was associated with increased volume across much of the brain, including the inferior frontal gyrus, mid cingulate, middle- and superior temporal lobe, pre- and postcentral gyri, paracentral lobule, middle and superior temporal gyri, and the occipital lobe (Besteher et al., 2017). In a late adolescent/emerging adult sample ages 17 to 27, increased somatic anxiety symptoms were associated with reduced volume in the postcentral gyrus and increased volume in the parahippocampal gyrus (Wei et al., 2015). Finally, in a child and adolescent sample ranging from ages 8 to 17, Castagna and colleagues (2018) found that a manifest measure of anxious arousal was associated with increased cortical thickness across much of the brain, including the inferior, middle, and superior frontal gyri, anterior insula, pre-

and postcentral gyri, superior and inferior parietal lobe, precuneus, inferior and superior temporal lobe, and lateral occipital lobe, as well as the hippocampus and amygdala. Though only a few studies, this body of literature suggests that, across adolescents and young adults, somatic dimensions of anxiety similar to anxious arousal are associated with regions supporting cognitive control, namely the inferior frontal gyrus, sensorimotor functions, including pre-, post- and paracentral regions, vision and visual attention, including the occipital lobe and cuneus, and, regions supporting semantic representations, namely the temporal lobes. While other brain regions have been implicated in single studies, without further replication and in the absence of methodologies that distinguish somatic anxiety behaviors from other related behaviors, it is unclear how robust these associations are. Indeed, a number of the regions observed by Castagna and colleagues (2018) overlap with regions observed as associating with anxious apprehension, highlighting the utility of methodologies that allow researchers to parse variance in behaviors into common and specific constructs, as is done in the current study, providing further clarity as to the brain regions that are associated with a specific set of behaviors as opposed to brain regions associated with other behaviors that may co-vary with the behavior of interest.

2.2.4. Neuroanatomical Correlates of Anxious Apprehension-like Dimensions

Previous research into the gray matter correlates of anxious apprehension or worry implicate a number of regions across the brain, but only show a relative degree of consistency in the orbitofrontal cortex (Carnevali et al., 2019; Castagna et al., 2018; Mohlman et al., 2009) and the cingulate gyrus (Andreescu et al., 2017; Carnevali et al., 2019; Hilbert et al., 2015; Schinele et al., 2011). In fact, the orbitofrontal cortex has been associated with anxious apprehension

across most age groups, including children and adolescents (Castagna et al., 2018), young adults (Carnevali et al., 2019), and the elderly (Mohlman et al., 2009), as well as in both healthy controls (Carnevali et al., 2019; Castagna et al., 2018) and anxiety patients (Mohlman et al., 2009), suggesting that the orbitofrontal cortex may provide a marker of anxious apprehension severity regardless of demographics and clinical status. Interestingly, while the cingulate gyrus was implicated in most reviewed studies, the specific portion of the cingulate differed between studies, with two studies that included GAD patients implicating the anterior cingulate (Andreescu et al., 2017; Schinele et al., 2011), a single study in GAD patients implicating the mid cingulate, and a single study in healthy controls implicating the posterior cingulate (Carnevali et al., 2019). However, given associations between the orbitofrontal cortex and the anterior cingulate with negative affect/neuroticism discussed previously, it is unclear if the associations between these regions and anxious apprehension are in fact specific to anxious apprehension or instead reflect a more general internalizing dimension that is highly correlated with anxious apprehension. Because none of the studies evaluating the gray matter correlates of anxious apprehension partitioned variance that is specific to anxious apprehension from other more general internalizing dimensions, the preexisting literature does not speak to this issue.

Outside of the orbitofrontal cortex and cingulate, there is very little regional correspondence between studies, with single studies reporting associations between anxious apprehension and the inferior and middle frontal gyri (Castagna et al., 2018), medial superior frontal gyrus (Schinele et al., 2011), paracentral lobule (Hilbert et al., 2015), anterior insula (Castagna et al., 2018), and the inferior parietal lobe (Hilbert et al., 2015), with only one study implicating subcortical regions, namely the basal ganglia (Hilbert et al., 2015). There is some evidence that the direction of the relationship between anxious apprehension and anatomy differs

across the age groups, with adult samples showing both positive and negative relationships, whereas samples including adolescents showing only positive associations (Castagna et al., 2018; Hilbert et al., 2015), but given the relatively few number of studies and the fact that no study directly compared age groups, more research is needed to test this possibility.

2.2.5. Neuroanatomical Correlates of Low Positive Affect-like Dimensions

Low positive affect, and the analogous dimension of anhedonia, are characterized by blunted affect and reduced reward processing common to depression (for a review, see Der-Avakian & Markou, 2012). Previous studies evaluating the gray matter correlates of low positive affect, anhedonia, or similar dimensions have frequently detected associations with the basal ganglia, yet show little consistency in terms of cortical regions. Though the specific subregions of the basal ganglia and direction of effects differ between studies, basal ganglia volume has been associated with anhedonia in distinct samples spanning the lifespan, with increased anhedonia having been associated with reduced nucleus accumbens volume in adolescents (Auerbach et al., 2017), late adolescents and emerging adults (Wacker et al., 2009), and young- to middle aged adults (Enneking et al., 2019), reduced volume of the caudate in young to middle aged adults (Enneking et al., 2019), increased volume of the pallidum in late adolescence and emerging adults (Wang et al., 2014), and decreased volume of the pallidum in emerging and middle adults (Harvey et al., 2007). In fact, some evidence suggests that basal ganglia volume can prospectively predict individual differences in anhedonia, with putamen volume in early adolescence significantly predicting anhedonia three years later even after taking baseline anhedonia levels into account (Auerbach et al., 2017). Given the role of the basal ganglia in

reward processing (for a review, see Schultz, 2016) and the fact that low positive affect/anhedonia are defined by an altered experience of reward, associations between the basal ganglia and low positive affect/anhedonia are not surprising. What is surprising, however, is the lack of an association of low positive affect/anhedonia orbitofrontal and medial frontal regions. These prefrontal cognitive control regions are thought to play critical roles in modulating reward processing via bidirectional connections with subcortical structures, including the basal ganglia, and have been implicated in reward processing in previous fMRI studies (e.g., Keedwell et al., 2005). Instead, cortically, there is very little convergence across studies, with low positive affect/anhedonia associating with a broad range of cortical regions, generally outside of classic prefrontal reward processing regions, including increased thickness of the lingual gyrus in the elderly (McLaren et al., 2016), increased volume of the precuneus and posterior cingulate in young adults (Lee et al., 2011) and decreased thickness of the superior frontal gyrus, as well as increased thickness in the inferior parietal lobe and postcentral gyrus in late adolescence (Wang et al., 2014). Though speculative, the general lack of an association between gray matter morphometry of prefrontal cognitive control regions and low positive affect/anhedonia tentatively suggests that low positive affect/anhedonia may be driven more by bottom-up reward processing mechanisms instead of aberrant top-down control over these systems.

2.2.6. Neuroanatomical Correlates of Rumination-like Dimensions

Preexisting studies evaluating the neuroanatomical correlates of rumination stand out for showing considerable regional consistency across studies. In studies of healthy controls, MDD

patients, and PTSD patients, individual differences in rumination have been consistently associated with lateral prefrontal regions, particularly the middle frontal gyrus (Qiao et al., 2013; Sin et al., 2018; Wang et al., 2015, 2018) and, to a lesser degree, the inferior frontal gyrus (Kuhn et al., 2012; Qiao et al., 2013), as well as the cingulate, including the anterior cingulate (Floyd et al., no date; Kuhn et al., 2012; Sin et al., 2018), mid cingulate (Kuhn et al., 2012), and posterior cingulate (Floyd et al., no date), with some evidence also suggesting alterations in the lateral (Machino et al., 2014) and medial (Wang et al., 2015) temporal lobe. One potential reason for the striking consistency across studies is the fact that there is relatively little variability in the age groups employed across these studies, with all reviewed studies focusing on samples including emerging, young, and/or middle adults. While some of these studies including individuals in late adolescence (i.e. ~18 years old), none of the reviewed studies focused on adolescence specifically nor on the elderly. Within this literature, a couple of findings are of note. First, Wang and colleagues (2015) found that healthy controls and MDD patients showed opposing relationships between rumination and middle frontal gyrus volume, with increased rumination correlating with increased volume in controls and decreased volume in patients, suggesting that relationship between the middle frontal gyrus and rumination may change at the extremes of internalizing psychopathology associated with MDD diagnoses. Second, distinct forms of rumination appear to show dissociations in the direction of associations with neuroanatomy, with Sin and colleagues (2018) showing that brooding, a form of rumination thought to be a risk factor for depression, and reflection, a form of rumination thought to be protective against depression, respectively showing positive and negative associations with middle frontal gyrus and anterior cingulate volume.

The current study has considerable potential to make important contributions to this literature. Not only do none of the reviewed studies evaluating the gray matter correlates of rumination in adolescence, none of the studies evaluated surface-based morphometry measures of thickness or surface area, as is done in the current study. As such, we hope to contribute to this literature by assessing whether the consistent association between middle frontal gyrus volume and rumination in adults holds in adolescence and whether such associations are specific to volume, or instead better accounted for by thickness or surface area.

2.2.7. Neuroanatomical Correlates of Repetitive Negative Thought-like Dimensions

To our knowledge, no study has evaluated the gray matter correlates of repetitive negative thinking beyond looking at anxious apprehension or rumination separately. As such, to gain insight from the preexisting literature into the gray matter correlates of repetitive negative thinking, it may be useful to compare studies evaluating anxious apprehension and rumination and to identify where in the brain there appears to be conjunction across these dimensions. Conjunction between morphometry studies of anxious apprehension and rumination show that both dimensions are associated with gray matter morphometry in prefrontal regions, including the inferior (anxious apprehension: Castagna et al., 2018; rumination: Kuhn et al., 2012; Qiao et al., 2013) and middle frontal (anxious apprehension: Castagna et al., 2018; rumination: Qiao et al., 2013; Wang et al., 2015, 2018) gyri, as well as the cingulate, including the anterior (anxious apprehension: Andreescu et al., 2017; Schinele et al., 2011; rumination: Floyd et al., no date; Kuhn et al., 2012), mid (anxious apprehension: Hilbert et al., 2015; rumination: Kuhn et al.,

2012), and posterior cingulate (anxious apprehension: Carnevali et al., 2019; rumination: Floyd et al., no date).

2.3. Heritability of Internalizing Psychopathology

To pinpoint the etiological factors driving internalizing psychopathology it is essential to determine the degree to which relevant behaviors are driven by genetic or environmental influences. Twin studies that partition variance in a given phenotype into variance that can be explained by genetic, shared, and non-shared environmental factors, play an important role in this process, highlighting potential etiological domains for further investigation while also providing a guide for molecular genetic studies. To date, a number of twin studies have investigated the relative contribution of genes and the environment to individual differences in phenotypes relevant to internalizing psychopathology, including case-control status and individual differences in internalizing behaviors. Such studies fall into two general categories: univariate models, which identify the variance in a single phenotype that is attributable to genetic and environmental factors, and bivariate or multivariate models, which partition covariation between two or more phenotypes into covariance that can be explained by genetic and environmental factors common across a set of phenotypes.

Twin studies of internalizing disorders in adults generally suggest that specific disorders are largely driven by genetic and non-shared environmental influences only, with little evidence of an influence of shared environmental factors. This pattern of results has been observed across distinct internalizing disorders, including MDD (for a review and meta-analysis, see Sullivan et

al., 2000), GAD (e.g., Kendler et al., 1992; Roy et al., 1995), SAD (for a meta-analysis, see Scaini et al., 2014), and OCD (for a review, see Taylor, 2011), with some evidence suggesting that PTSD may be influenced by shared environmental factors (for a review, see Afifi et al., 2010). However, the relative contribution of genetic and environmental influences appears to differ across the lifespan, with children and adolescents often showing higher degrees of heritability than adults (e.g., Scaini et al., 2014), with some evidence that internalizing disorders in youth may, in part, be influenced by shared environmental factors (Ehringer et al., 2006; Eley et al., 1999; Kovacs & Devlin, 1998). For example, looking across externalizing and internalizing disorders, Ehringer and colleagues (2006) found evidence that shared environmental influences account for a small but notable proportion of variance in MDD and GAD diagnostic status. As such, it remains an open question as to the degree to which shared environmental factors influence internalizing disorders.

In attempts to better understand the source of comorbidity between internalizing disorders, a number of studies have employed bivariate twin models to evaluate the degree to which genetic, shared environmental, and non-shared environmental influences overlap across disorders. In some of earliest work of this kind, Kendler and colleagues (1992) found that MDD and GAD have a genetic correlation approaching unity, suggesting that these two disorders are influenced by the same genes, but show only partially overlapping non-shared environmental influences, results that have been replicated many times since (e.g., Kendler et al., 2007; Neale & Kendler, 1995; Roy et al., 1995). Similar patterns of results have been reported across other pairs of internalizing disorders, including MDD and PTSD (Koenen et al., 2008), and GAD and PTSD (Goenjian et al., 2008), however the genetic correlation between MDD and GAD stands out for being particularly strong. Multivariate twin models looking across more than two disorders

suggest common genetic influences across all internalizing disorders accounting for a modest proportion of variance in risk for each disorder, but also disorder-specific genetic and environmental influences (Chantarujikapong et al., 2001; Kendler et al., 1995). Recently, there has been a trend to capture the relationships across internalizing disorders into a single internalizing factor capturing covariation across internalizing disorders, along with a general psychopathology factor (i.e., p-factor) associated with a risk for all psychopathology, and an externalizing-specific factor (Caspi et al., 2014). Twin studies of these factors largely confirm the observation that internalizing disorders have overlapping genetic influences, with the p-factor, internalizing factor, and externalizing factor all showing dissociable genetic influences (Rosenstrom et al., 2019).

Though much of the twin studies on internalizing psychopathology have focused on diagnostic status, there may be considerable value in evaluating the genetic and environmental contributions to continuous internalizing behaviors. While most studies of diagnostic status report robust influences of genetic and non-shared environmental factors only, specific internalizing behaviors need not follow this same pattern of results. For instance, it may be that certain symptoms of a given disorder are driving the genetic component for that disorder, whereas other symptoms are driving the environmental component. Furthermore, there may be specific internalizing symptoms or behaviors within the general population that are indeed associated with shared environmental influences, but these associations are masked because the criterial symptoms for that disorder only show genetic and non-shared environmental influences. Indeed, twin studies of continuous internalizing dimensions show far greater variability in the pattern of genetic, shared, and non-shared environmental influences. For example, looking across a range of behaviors associated with MDD, Jang and colleagues (2004) found evidence of a

number of symptom dimensions that show no significant genetic influences, as well as a number of symptoms that showed sizable contributions of shared environmental influences.

To date, some studies have investigated the heritability of internalizing dimensions analogous to the six investigated in the current report, with neuroticism, a dimension similar to negative affect, being the most frequently investigated dimension. Twin studies of neuroticism, much like twin studies of internalizing diagnoses, suggest that neuroticism is influenced by genetic and non-shared environmental factors, with little evidence of shared environmental influences (e.g., Fanous et al., 2002; Hansell et al., 2012; Mackintosh et al., 2006). However, Hansell and colleagues (2012) found evidence that a measure of combined anxiety/depression symptomology is indeed influenced by shared environmental factors, while also reporting that somatic distress, a dimension bridging negative affect and anxious arousal, is associated with genetic and non-shared environmental influences. Looking specifically at a dimension analogous to anxious arousal, Gustavsson and colleagues (1996) found that somatic anxiety was influenced by genetic, shared environmental, and non-shared environmental factors, suggesting that at least a portion of anxiety symptomology may indeed be influenced by shared environmental influences. This notion has been reinforced by findings that anxious apprehension. Specifically, looking within children, Warren and colleagues (1999) found some evidence that a model including shared and non-shared environmental influences was comparable in fit to a model including genetic and non-shared environmental influences. Studies evaluating the heritability of anhedonia or other reward-related phenotypes analogous to low positive affect, show a wide range of heritability estimates, though some of these early studies are underpowered for full biometrical modeling and often focused on individuals with schizophrenia (Berenbaum et al., 1990; Kendler et al., 1991). However, in a relatively large-scale general population sample,

social anhedonia (Hay et al., 2001; MacDonald et al., 2001), physical anhedonia (Hay et al., 2001), introvertive anhedonia (Linney et al., 2003), and reward dependence (Keller et al., 2005; Ono et al., 2002) associated with genetic and non-shared environmental influences of modest effects, with no evidence of shared environmental influences. Finally, twin studies of rumination suggest that rumination is influenced by genetic and non-shared environmental factors, with a strong genetic overlap between rumination and major depression and other related internalizing constructs (Chen & Li, 2013; du Pont et al., 2019; Johnson et al., 2014, 2016)

To summarize, twin studies evaluating the contribution of genetic and environmental influences to internalizing disorders suggest that nearly all internalizing disorders are predominately driven by genetic and non-shared environmental factors, with one possible exception being PTSD. While there are some studies that report evidence of shared environmental factors, these studies are largely far and few between, with the overwhelming majority of disorders showing minimal evidence of shared environmental influences. When employing dimensional characterizations of internalizing psychopathology, a subtler picture emerges in which common behaviors shared across internalizing disorders appear to be largely genetic in nature, whereas dimensions thought to be preferentially associated with anxiety show some evidence of shared environmental influences. However, no single study has investigated the heritability of the six internalizing dimensions utilized in the current project in the context of a bifactor model. As a result, previous research into the heritability of internalizing dimensions may employ impure measures of that dimension, something we try to address in the current project by employing orthogonal internalizing dimensions.

CHAPTER 3

A SIX FACTOR DIMENSIONAL MODEL OF INTERNALIZING PSYCHOPATHOLOGY

3.1. Introduction

Categorical nosologies of mental illness have been the dominating framework with which researchers and clinicians have conceptualized psychopathology. Under such frameworks, there are hard lines between normal functioning and mental illness, with individuals needing to meet specific criteria to be clinically diagnosed. While this conceptualization of psychopathology has enabled a degree of diagnostic reliability across clinicians, it does not capture the gradient between normality and mental illness, turning what is undoubtedly a continuous distribution of psychopathology-related behaviors across the population into an all-or-nothing characterization. Recently, however, there has been a marked shift in the focus of psychopathology research, with an emerging emphasis on identifying transdiagnostic dimensions of psychopathology that not only span disorders, but occur across the general population more broadly. This emerging trend is reflected in the recent Research Domain Criteria initiative of the National Institute of Mental Health (Insel et al., 2010), along with proposals for new diagnostic schema grounded in transdiagnostic dimensions in which diagnoses are only one level of multilevel structural hierarchy for describing psychopathology (Kotov et al., 2017).

Despite only recently receiving widespread attention, dimensional models of psychopathology have informed our understanding of psychopathology for decades. Watson and Clark's tripartite model of anxiety and depression symptomology has proven to be a particularly effective model in characterizing the behavioral structure of internalizing psychopathology (Clark & Watson, 1991; Watson et al., 1995a,b). Because we discussed this model in detail in

Chapter 1, we only briefly review it here. Watson and Clark proposed that anxiety and depression symptomology can be dissociated into three distinct factors: negative affect, anxious arousal, and low positive affect. Negative affect was borne out of the observation of high rates of comorbidity and symptom overlap between mood and anxiety disorders, and captures what is common across anxiety and depression, namely psychological distress. Anxious arousal was thought to be specific to anxiety disorders, capturing somatic states frequently associated with anxiety, particularly panic. Low positive affect, on the other hand, captures behaviors characterized by blunted reward processing and a diminution of positive affective states generally associated with depression.

Almost a decade after Watson and Clark's seminal paper introducing this model, Nitschke and colleagues (2001) proposed a four factor model that extended the tripartite model by including an additional anxiety dimension: anxious apprehension. Anxious apprehension, a construct analogous to worry, has been conceptualized as a form of anxiety grounded in cognitive behaviors, specifically the tendency for anxious individuals to perseverate on thoughts about future environmental stressors, often with debilitating consequences. In Watson and Clark's original model, anxious apprehension was largely captured by the item "worried a lot about things" and was considered part of the negative affect factor. While anxious apprehension is undoubtedly associated with both anxiety and depression, whether or not this association means this construct contributes to both classes of disorders equally remains in debate. Alternatively, the associations between anxious apprehension and depression may reflect the high rates of comorbidity between anxiety and depression, or it could reflect some general mechanism that may be driving similar yet dissociable behaviors in both anxiety and depression. In support of Nitschke and colleagues finding that anxious apprehension was distinct from the

other tripartite dimensions, additional evidence suggests that anxious apprehension may be preferentially associated with anxiety over and above depression. For example, employing SEM to simultaneously test the relationships of anxious apprehension with overall anxiety and depression symptomology, anxious apprehension prospectively predicted anxiety symptomology, not depression symptomology (Calmes & Roberts, 2007). This potential specificity of anxious apprehension to anxiety is also codified in the Diagnostic Statistical Manual, in which a criterial symptom of GAD is excessive worry, with no mention of worry in describing MDD (American Psychiatric Association, 2013).

Parsing the transdiagnostic dimensions within internalizing psychopathology need not stop with anxious apprehension. In fact, much like anxious apprehension is considered a cognitive dimension of anxiety, rumination has been put forth as a cognitive dimension preferentially associated with depression (Hong, 2007). Despite considerable overlap between the purported cognitive processes supporting rumination and anxious apprehension, substantial evidence exists suggesting that the two are indeed dissociable. Most notably, Hur and colleagues (2017) found that variance in rumination and anxious apprehension can be best accounted for under a three factor model, including a common bifactor dimension capturing repetitive negative thought processes that are shared across the two, as well as specific factors capturing residual variance unique to rumination and anxious apprehension, respectively. Taken together, these findings suggest that Nitschke and colleagues (2001) four-factor model of internalizing psychopathology can be extended to include not only rumination, but also repetitive negative thought. This repetitive negative thought factor allows for the decomposition of negative affect into more precise dimensions. That is, in Watson and Clark's initial framing of negative affect, it was a very broad dimension, capturing cognitive behaviors like worry, but also sensations of

bodily distress, which are likely driven by distinct mechanisms. By including a repetitive negative thought dimension that captures common cognitive processes shared across anxiety and depression-specific behaviors, we may gain additional insight into the specific behavioral architecture underlying internalizing psychopathology, and dissociate cognitive dimensions from those that are sensorial or bodily-based.

In the current study, we employ structural equation modeling (for a review see Ullman & Bentler, 2003) to perform a confirmatory factor analysis (CFA) of this novel six-factor model of internalizing psychopathology (see figure 1). As shown in figure 1, this model posits two primary gradients that can be used to characterized the six dimensions. The first gradient describes behaviors in accordance to automatic affective to cognitive mechanisms, including behaviors grounded in automatic, affective process (i.e., anxious arousal and low positive affect) to behaviors grounded in higher level cognitive processes (i.e., repetitive negative thought, rumination, and anxious apprehension), with behaviors that emerge through the integration of multiple levels lying in the middle (i.e., negative affect). The second gradient describes the degree to which behaviors are associated with depression (i.e., low positive affect and rumination) versus anxiety, (i.e., anxious arousal and anxious apprehension) with behaviors shared across anxiety and depression (i.e., negative affect and repetitive negative thought) falling in between. We then test whether the underlying factor structure of these internalizing dimension differs in accordance with sex and evaluate the degree to which each dimension shows specific relationships with distinct psychiatric disorders.

The current internalizing model builds off of the four-factor model put forth by Nitschke and colleagues (2001) in three important ways. First, we employ bifactor modeling to produce a single latent factor capturing covariation across all internalizing behaviors measured, termed

"negative affect". This negative affect factor is analogous to the negative affect dimension proposed by Watson and Clark, but instead of treating negative affect as being correlated with all other factors in the model, we explicitly partition covariation between behaviors into a single latent construct, creating six orthogonal factors. The use of bifactor modeling affords us the ability to partition variance associated with dimension-specific residuals over and above this common factor, improving the precision and purity of our dimensional measures. Second, much like Nitschke and colleagues (2001) amended the tripartite model to include anxious apprehension, we amend their model to include rumination as an additional dimension, given strong evidence that rumination may not only be central to MDD symptomology, but dissociable from anxious apprehension (Fresco et al. 2002; Goring & Papageorgiou, 2008; Gustavson et al., 2018; Hong, 2007; Hughes et al. 2008; Hur et al., 2017; Watkins et al., 2005). Finally, we include a second bifactor dimension capturing covariation between anxious apprehension and rumination that is not accounted for by the common internalizing factor. This additional dimension, termed "repetitive negative thought", is grounded in strong evidence linking rumination and anxious apprehension to similar, if not overlapping, cognitive processes (Hur et al., 2016).

Importantly, we evaluate the degree to which the resulting six dimensions are invariant across the sexes as well as related to clinical diagnostic status for two internalizing disorders, MDD and GAD, and an externalizing disorder, antisocial personality disorder (ASPD). In doing so, we hope to provide evidence that the six internalizing dimensions in the current project have diagnostic utility, showing specific relationships to specific disorders, even when accounting for comorbidity between disorders. Because negative affect likely captures some variance that is not just unique to internalizing disorders but shared across all psychopathology, we predict that

negative affect will be associated with all three disorders, including ASPD. Indeed, in Clark and Watson (1991a), the authors argue that negative affect is not just non-specific across anxiety and depression, but a contributor to all negative mood states, including anger, a mood often ascribed to externalizing disorder. However, we predict that all of the other dimensions besides negative affect will show preferential relationships to MDD or GAD status, but not ASPD, in line with models of behavioral distinctions between internalizing and externalizing psychopathology. We predict these relationships will include associations of MDD status with low positive affect-specific, rumination-specific, and repetitive negative thought, as well as associations of GAD status with anxious arousal-specific, anxious apprehension-specific and repetitive negative thought over and above any relationship with negative affect.

3.2. Methods

3.2.1. Participants

Participants were drawn from three age samples spanning two distinct studies (see table 1), including an adolescent (N= 121; 61 male/60 female; age= 17.1 (1.5) years) and a middle adult female sample (N= 64; Age= 47.9 (6.7) years) from the Colorado Cognitive Neuroimaging Family Emotion Research Study (CoNiFER Study), as well as a young-adult sample consisting of same-sex twin pairs from the Institute for Behavioral Genetics' Longitudinal Twin Study (LTS) (N= 630; 284 males/346 females; Age= 28.7 (.8)).

Sample	N (female)	Age range	Mean age (SD)
adolescent	121 (60)	14.1-22.9 years	17.1 (1.5) years
young adult	627 (345)	28.0-34.5 years	28.7 (.8) years
middle adult	64 (64)	35.3-64.6 years	47.9 (6.7) years
total	*812 (469)*	*14.1-64.6* years	*28.5 (7.3)* years

Table 1. Samples employed in confirmatory factor analysis. Sample size, age, and sex descriptive statistics for the three age samples used in confirmatory factor analyses. "N (female)" column indicates sample size with number of females in parentheses. "Age Range" indicates minimum and maximum age within each sample in years. "Mean Age (SD)" column indicates the mean age of each sample as well as the standard deviation in parentheses.

3.2.2. Internalizing Psychopathology Indicators

Three well-validated questionnaires were employed as manifest indicators for the internalizing dimensions, including the Mood and Anxiety Symptom Questionnaire (MASQ) (Watson & Clark, 1991) the Penn State Worry Questionnaire (PSWQ) (Meyer et al. 1990), and the Ruminative Response Scale (RRS) (Treynor et al., 2003). The MASQ is a 90- or 62-item questionnaire capturing multiple internalizing dimensions associated with anxiety and depression divided into six distinct subscales, including general distress-mixed (90-item version only), general distress-depression (GDD), general distress-anxiety (GDA), anxious arousal (AA), low positive affect (LPA), and loss of interest (LI). The adolescent and middle adult samples completed the 90-item version of the MASQ, whereas the young adult sample completed the 62-item version. To be able to equate manifest indicators across the different samples, only questions from the 62-item version were used across the three samples. The PSWQ is a 16-item questionnaire capturing trait levels of worry. The RRS is a 22- or 10-item questionnaire capturing trait levels of rumination, including distinct brooding and reflection subscales. The adolescent and middle adult samples completed the 22-item version of the RRS, whereas the young adult sample completed the 10-item version. To be able to equate manifest indicators across the different samples, only questions from the 10-item version were used across the three

samples. For all questionnaires, participants responded according to a Likert scale. On a subset of 505 young adults, we utilized the Diagnostic Interview Schedule (DIS) (Robins et al., 1981) to also obtain diagnostic status for MDD, GAD, and ASPD. Diagnostic status for these disorders were on a three-level scale: 0= no symptoms, 1= subclinical symptoms, and 2= meets criteria for diagnosis as determined by the DIS.

3.2.3. Confirmatory Factor Analysis

Structural equation modeling was carried out using MPlus software (Muthén & Muthén, 2012). Analyses evaluating the underlying factor structure of internalizing psychopathology employed a confirmatory factor analyses of a six-factor, bifactor dimensional model of internalizing psychopathology, using CFI > .90 and RMSEA < .08 as criteria for good model fit (Hu & Bentler, 1999). We chose to perform this model as a bifactor model instead of some other parameterization because we were explicitly interested in partitioning the covariation between items into discrete factors, with these factors being orthogonal, for later use in gray matter morphometry analyses (see Chapter 4). Of particular interest was the degree to which this six-factor model provided a better fit than a bifactor parameterization of other potential models. In particular, we were interested in comparing the six-factor model (see panel D in figure 2) to three other a models (see panels A, B, and C in figure 2).

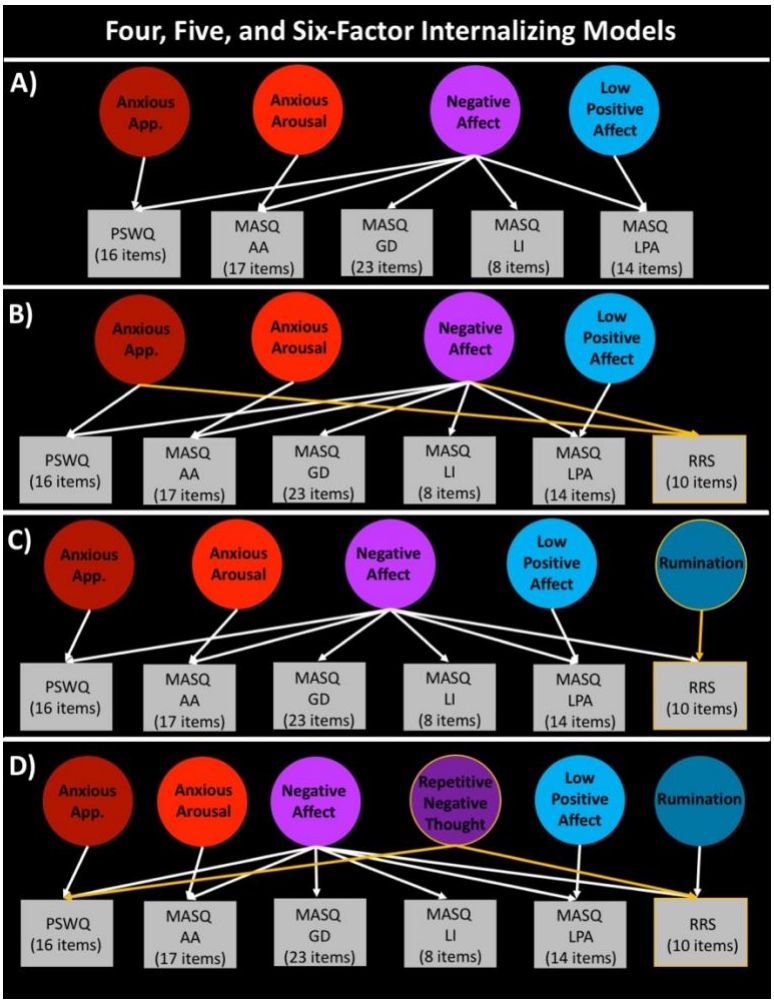

Figure 2. Four theoretical models of internalizing psychopathology. For all models, the gray squares represent multiple indicators, with the number of individual items indicators shown under the name of the relevant questionnaire. Yellow lines indicate the additional parameters added to the previous model. *Panel A) Four-factor A.* Bifactor parameterization of the four factors suggested by Nitschke & colleagues (2001) and utilized in Banich et al., (2020). *Panel B) Four-factor B.* Modified four factor model that posits that rumination and anxious apprehension are identical constructs. *Panel C) Five-factor*. Five factor model that posits that rumination and anxious apprehension are dissociable constructs, but non-overlapping after what is shared due to negative affect. *Panel D) Six-factor.* Six factor model that posits that rumination and anxious apprehension have shared and distinct variance, with the shared variance capturing repetitive negative thought. Anxious App.= anxious apprehension-specific; PSWQ= Penn. State Worry Questionnaire items; MASQ AA= Mood and Anxiety Symptom Questionnaire- anxious arousal subscale items; MASQ GD= Mood and Anxiety Symptom Questionnaire- general distress subscale items; MASQ LI= Mood and Anxiety Symptom Questionnaire- low of interest subscale items; MASQ LPA= Mood and Anxiety Symptom Questionnaire- low positive affect subscale items; RRS= ruminative response scale items.

We refer the reader to figure 2 for a graphical representation of these alternative models. They included a four-factor bifactor parameterization of the model put forth by Nitschke and colleagues (2001) in which internalizing psychopathology is decomposed into four factors, including negative affect, anxious arousal-specific, anxious apprehension-specific, and low

positive affect-specific (panel A of figure 2). Additionally, we test the fit of a second four-factor model that assumes anxious apprehension and rumination are the same construct (panel B in figure 2). This model adds rumination-tapping items to the Nitschke (2001) model (indicated by the orange border around RRS indicators in panel B of figure 2) but constrains these items to load solely on negative affect and anxious apprehension-specific (indicated by the orange arrows connecting RRS indicators to the negative affect and anxious apprehension-specific factors in panel B of figure 2). We also test a five-factor model that creates an additional rumination-specific factor and posits that, over and above negative affect, rumination-specific and anxious apprehension-specific are fully distinct constructs (panel C of figure 2). In panel C of figure 2, the new parametrizations of this model as compared to the model in panel B are indicated by the orange border around rumination-specific factor, an orange arrow marking loadings from the RRS indicators to this rumination-specific factor, and the removal of loadings between the RRS indicators and the anxious apprehension-specific factor. Finally, we compare these earlier models to the full six-factor model, in which we posit that anxious apprehension and rumination share common variance over and above negative affect, namely a common association with repetitive negative thought (panel D in figure 2). This model reparametrizes the five-factor model, including the addition of a new repetitive negative thought factor (indicated by orange outline around repetitive negative thought factor in panel D of figure 2), and factor loadings of anxious apprehension and rumination indicators on to this repetitive negative thought factor (indicated by orange arrows connecting PSWQ and RRS indicators to repetitive negative thought in panel D of figure 2). Because the four-factor B and five-factor models were nested within the six-factor model, we performed model comparison via chi-square differences tests, as implemented by the “DIFFTEST” option in Mplus.

All questions from the MASQ, PSWQ, and RRS were used as individual indicators, resulting in 88 total item level indicators. All items were treated as categorical indicators and weighted least square mean and variance adjusted estimation was used to account for non-normality in item-level responses. Sandwich estimation was carried out to account for non-independence within twin pairs by using the "TYPE=COMPLEX" option in Mplus.

For all models, the correlations between factors were set to 0 to make the factors orthogonal. In four-factor model A (panel A of figure 2), all items from the MASQ and PSWQ were set to load on to the negative affect factor, whereas the 17 MASQ- Anxious Arousal items were set to load the anxious arousal-specific factor, the 14 reversed-scored items within the MASQ- Positive Affect scale were set to load on the low positive affect-specific factor, and all 16 items from the PSWQ were set to load on the anxious apprehension-specific factor.

In the four-factor B model, the 10 rumination items from the RRS were added to the model and set to load on the negative affect and anxious apprehension-specific factors only (panel B of 2). In the five-factor model, the paths between anxious apprehension-specific and the RRS items were removed and the RRS items were set to load on their own factor, namely rumination-specific (panel C of figure 2). Finally, in the six-factor model an additional bifactor dimension was added, namely repetitive negative thought, and all PSWQ and RRS items were set to load on this factor (panel D of figure 2). In line with previous research on a similar bifactor model of internalizing psychopathology we did not include a loss of interest-specific factor, instead letting the MASQ- Loss of Interest items load solely on the common negative affect factor in all models (Banich et al., 2020). To evaluate sex differences in the underlying factor structure of the six internalizing dimensions, we ran invariance testing using the Mplus options "MODEL= configural metric scalar".

Factor scores for all six factors were saved for use in gray matter morphometry (see Chapter 4) and heritability analyses (see Chapter 5). Because Mplus does not produce factor determinacies values for models with categorical indicators, to evaluate the degree to which the factor scores captured the underlying latent variables, we ran the CFA again but treating all indicators as continuous in the context of robust maximum likelihood estimation. By treating the indicators as continuous, we were able to derive factor score indeterminacies for all six factors. By looking at the correlations between factor scores from the continuous indicator and the categorical indicator models, we are afforded some insight into the degree to which the factor scores from the categorical model were precisely capturing individual differences in the underlying latent factors.

3.2.4. Relationships between Internalizing Dimension Factor Scores and Diagnoses

We carried out a series of complementary analyses to evaluate the degree to which each dimension showed preferential associations with diagnostic status for two internalizing disorders, specifically MDD and GAD, and an externalizing disorder, ASPD. First, to evaluate whether internalizing factor scores differed in accordance with three levels of diagnostic status (i.e., no symptoms, subclinical symptoms, meets criteria for diagnosis) of MDD and GAD, we conducted mixed effects regression using the R function ‘nlme’ (Pinhero et al., 2020), predicting factor scores of each dimension by diagnostic status, controlling for sex and age. To evaluate significant differences in mean levels of internalizing dimensions for all pairwise comparisons of the different diagnostic status levels, we carried out Tukey tests utilizing the R function ‘glht’

(Hothorn et al., 2008), including comparisons of "no symptoms" to "subclinical symptoms", "no symptoms" to "clinical diagnosis", and "subclinical symptoms" to "clinical diagnosis".

Second, to evaluate the degree to which the internalizing dimensions showed preferential relationships to one class of disorders over the other, we ran mixed effects ordinal logistic regression models using the R-based 'clmm' package (Christensen, 2019) predicting MDD, GAD, and ASPD diagnostic status, separately, from factor scores for all six dimensions simultaneously while controlling for sex and age. To demonstrate diagnostic specificity, we additionally ran mixed effects logistic regression models predicting MDD, GAD, or ASPD diagnostic status while controlling for the status of the other two disorders. In doing so, we are able to test the degree to which each internalizing dimension is predictive of a given diagnosis over and above the other diagnoses, thus taking into account disorder comorbidity.

3.3. Results

3.3.1. Confirmatory Factor Analysis

The full six-factor model was deemed a good fit, with a $\chi^2(3657)= 8882.641$ (χ^2 $p<.001$), RMSEA= .041 (.040-.042 90% confidence interval), and CFI= .914 (model fit statistics for all tested models can be seen in table 2). Chi-square differences tests revealed that this six-factor model provided a significantly better fit than the five-factor ($\Delta\chi^2(27) = 286.64$; $p<.001$) and four-factor B model ($\Delta\chi^2(27) = 1519.70$; $p<.001$). While we could not use chi-square differences test to compare the six-factor model to the four-factor A model because they were not nested, the six-

factor model had a substantially lower RMSEA (.041 as compared to .049) and higher CFI (.915 as compared to .875), suggesting it was indeed a better fit.

Model	Chi-square (df)	RMSEA (90%)	CFI
6-factor	8882.64(3657)*	.041(.040-.042)	.914
5-factor	9172.43 (3684)	.042(.041-.043)	.910
4-factor b	11190.492 (3684)	.049(.048-.050)	.877
4-factor a	11302.43 (3694)	.049(.048-.050)	.875

Table 2. Confirmatory factor analysis model fit statistics. Model fit statistics for four models of internalizing psychopathology. "Model" column indicates which of the four theoretical models are being tested. "Chi-square (df)" column indicates chi-square value of the model with degrees of freedom in parentheses. "RMSEA" column indicates the Root Mean Square Error of Approximation estimate with parentheses showing 90% confidence interval. *= best fitting model as determined by chi-square differences tests. "CFI" column indicates comparative fit indices estimate.

Standardized factor loadings for all indicator items can be seen in Appendix 1. All 88-items loaded significantly on to the negative affect factor, with factor loadings ranging from .167 to .893. Negative affect appeared to be largely driven by the MASQ General Distress-Depression items, with the five highest factor loadings (ranging .893 to .825) coming from this subscale, with these five items including "felt like a failure", "felt hopeless", "was disappointed in myself", "felt worthless", and "felt depressed". All anxious arousal items significantly loaded on the anxious arousal-specific factor with factor loadings ranging from .207 to .640 with the five highest-loading items included "felt dizzy or light headed" (.640), "felt faint" (.625), "felt like I was choking" (.593), "was trembling or shaking" (.589), and "felt numbness or tingling in my body" (.568). All reverse scored MASQ- Positive Affect items significantly loaded on the low positive affect-specific factor with factor loadings ranging from .559 to .740 with the five highest-loading items including the reverse scores of "felt like I was having a lot of fun" (.740), "felt really up or lively" (.721), "felt like a had a lot to look forward to" (.705), "looked forward to things with enjoyment" (.703), and "felt like I had a lot of energy" (.683). All anxious apprehension items from the PSWQ significantly loaded on the anxious apprehension-specific factor, with factor loadings ranging from .298 to .736 with the five highest-loading items

including “I am always worrying about something” (.736), “I have been a worrier all my life” (.714), “I worry all the time” (.703), “I know I should not worry about things but I just can’t help it” (.699), and “many situations make me worry” (.699). All rumination items from the RRS, including both Brooding and Reflection subscale items, significantly loaded onto the rumination-specific factor, though this factor was largely driven by items belonging to the Reflection subscale as four out of five of the top loading items belonged to this subscale. Factor loadings for the rumination factor ranged between .403 to .831 and the five highest-loading items included “go away by yourself to think about why you feel this way” (.831), “go someplace alone to think about your feelings”, “analyze your personality to try to understand why you are depressed” (.651), “analyze recent events to try to understand why you are depressed” (.626), and “think “why do I always react this way?”” (.526). Finally, all of the RRS and PSWQ items significantly loaded onto the repetitive negative thought factor, except for two RRS-Reflection items, namely “go someplace alone to think about my feelings” and “Why can’t I handle things better?””. Across all RRS and PSWQ items, factor loadings ranged from -.127 to .577 with the highest loadings including the reverse score of “when this is nothing more I can do about a concern, I do not worry about it anymore” (.577), the reverse score of “I do not tend to worry about things” (.530), the reverse score of “I find it easy to dismiss worrisome thoughts” (.524), the reverse score of “I never worry about anything” (.495), and “write down what you are thinking and analyze it” (.441).

3.3.2. Invariance Testing

To test whether the underlying factor structure for internalizing dimensions was similar across males and females, we carried out gender invariance tests. Tests of configural invariance revealed that the underlying factor structure was not invariant across gender with a $\chi_2(7314)=$ 8882.641; χ_2 $p<.001$. Comparing factor loadings between males and females revealed that, while negative affect, anxious arousal-specific, low positive affect-specific, and rumination-specific had largely similar patterns of factor loadings in both genders, anxious apprehension-specific and repetitive negative showed largely divergent patterns of factor loadings between males and females. The differences in loading patterns appeared to be driven by certain items preferentially loading on anxious apprehension-specific in males but repetitive negative thought in females, and vice versa. For example, within males, all PSWQ items loaded significantly on to the anxious apprehension-specific factor, while in females, five of these items did not significantly load on to this factor. Instead, the items that did not significantly load onto anxious apprehension-specific had some of the highest loadings on the repetitive negative thought factor in females. Furthermore, whereas all rumination items loaded significantly onto the repetitive negative thought factor in females, three rumination-tapping items from the brooding subscale did not significantly load on repetitive negative thought in males. Looking across the general pattern of loadings, in males the repetitive negative thought factor seemed to be most driven by the RRS-brooding items, with the two strongest loading items coming from this subscale, whereas in females, repetitive negative thought appeared to be driven by PSWQ items, with the five strongest loading items all coming from the PSWQ. In line with recommendations from previous research, having established a lack of invariance at the configural level, we deemed it unnecessary to evaluate metric and scalar invariance (Putnick & Bornstein, et al., 2016). In light of the lack of gender invariance, we ran the six factor model split up by gender and found the

model to be a good fit in males (χ_2(3657)= 5531.235, χ_2 p<.001; RMSEA= .038; CFI= .913 and females (χ_2(3657)= 6415.28, χ_2 p<.001; RMSEA= .039; CFI= .920), separately.

3.3.3. Factor Scores

As noted earlier, we were interested in knowing the degree to which the factor scores from the model using the categorical indicators were correlated with factor scores from a model using continuous indicators for which we could obtain factor score determinacies. For the continuous indicator model, all factor score indeterminacies were high (common internalizing= .98, anxious arousal= .89, low positive affect= .95, worry= .96, rumination= .94, repetitive negative thought= .85) and the correlation of these factor scores with the factor scores from the categorical indicator model were also high (common internalizing: r= .94, anxious arousal: r= .82, low positive affect: r= .98, worry= .96, rumination: r= .97, repetitive negative thought: r= .83), suggesting that the factor scores used for the gray matter morphometry and twin analyses discussed in Chapters 4 and 5 are relatively precise estimates of individual differences in the underlying latent constructs.

3.3.4. Associations with Diagnostic Status

The number of young adult participants meeting the different levels of lifetime diagnostic status can be seen in table 3. For MDD and GAD, we observed prevalence rates of diagnoses that were a bit elevated (MDD: 22%; GAD: 10%), but largely in line with epidemiological studies of the prevalence of these disorders in the general population (MDD: 17%; GAD: 6%; Kessler et

al., 2005a). We note that the prevalence of ASPD diagnoses in our sample (ASPD: 30%) was substantially higher than what is frequently observed by clinicians (1-4%; Werner et al., 2015). However, this appears to be a result of how the DIS defines ASPD in the absence of clinical judgement, and has been observed elsewhere (Perry et al., 1987).

Level of symptomology from DIS	Major Depressive Disorder	Generalized Anxiety Disorder	Antisocial Personality Disorder
no symptoms	332 (177 female)	393 (211 female)	211 (143 female)
subclinical symptoms	60 (34 female)	61 (42 female)	141 (77 female)
meets criteria for diagnosis	113 (78 female)	51 (36 female)	153 (60 female)

Table 3. Number of participants meeting different levels of diagnoses based off the Diagnostic Interview Schedule (DIS). Breakdown of participants reporting no symptoms, subclinical symptoms, and diagnoses, based off of the DIS.

To visualize mean differences in internalizing factor scores by diagnostic status, we plotted box plots of internalizing factor scores across the three levels of diagnostic status for MDD and GAD, respectively (see figure 3).

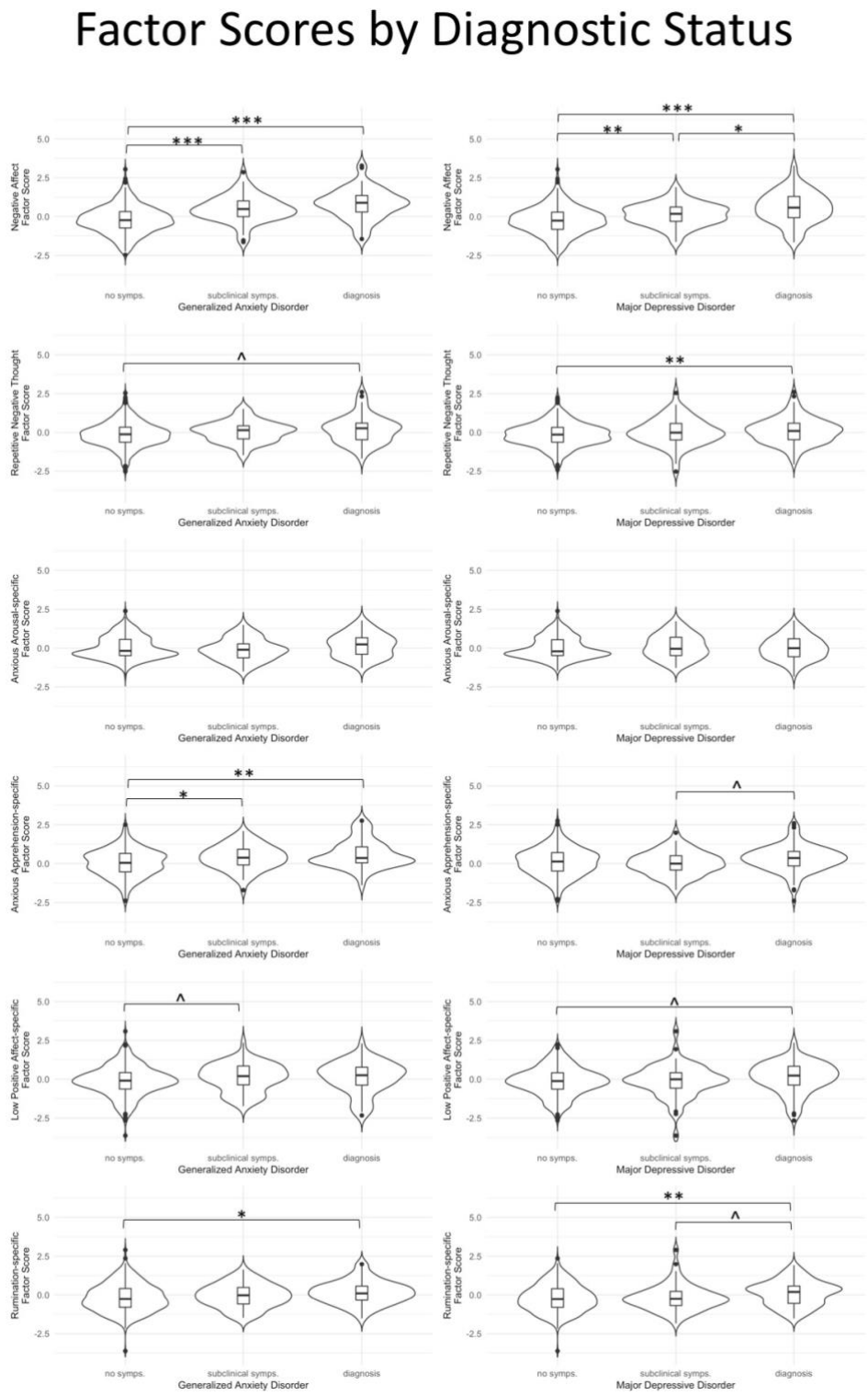

Figure 3. Differences in mean internalizing dimension factor scores by three levels of diagnostic status for generalized anxiety disorder and major depressive disorder. Violin plots of factor scores for all six dimensions for individuals showing no symptoms (no symps.), subclinical symptoms (subclinical symps.), and meeting symptom criteria for a diagnosis (diagnosis). Significant and marginally significant differences as determined by Tuley tests between symptom levels are indicated. ^= p<.10; *= p<.05; **= p<.01; ***= p <.001.

Mixed effects models evaluating mean differences in factor scores across MDD and GAD diagnostic status revealed that the factor scores differed in accordance with levels of diagnostic severity. To summarize, we found significant effects of MDD status on the following factors: *negative affect* (subclinical symptoms vs no symptoms: z-value = 3.202, p-value = .004; diagnosis vs no symptoms: z-value = 7.796, p-value <.001; diagnosis vs subclinical symptoms: z-value = 2.778, p-value = .015), *rumination-specific* (subclinical symptoms vs no symptoms: z-value = .249, p-value = .966; diagnosis vs no symptoms: z-value = 3.282, p-value = .003; diagnosis vs subclinical symptoms: z-value = 2.076, p-value = .092) and *repetitive negative thought* (subclinical symptoms vs no symptoms: z-value = 1.667, p-value = .213; diagnosis vs no symptoms: z-value = 2.594, p-value = .025 ; diagnosis vs subclinical symptoms: z-value = .358, p-value =.930), as well as a marginal effects on *low positive affect-specific* (subclinical symptoms vs no symptoms: z-value = -.181, p-value = .982; diagnosis vs no symptoms: z-value =2.184 , p-value = .072 ; diagnosis vs subclinical symptoms: z-value = 1.707, p-value = .198), *anxious apprehension-specific* (subclinical symptoms vs no symptoms: z-value = -1.137, p-value = .486; diagnosis vs no symptoms: z-value =1.663 , p-value = .215 ; diagnosis vs subclinical symptoms: z-value = 2.197, p-value = .070). There was not a significant effect of MDD diagnostic status on *anxious arousal-specific* (subclinical symptoms vs no symptoms: z-value = 1.090, p-value = .514; diagnosis vs no symptoms: z-value = .336, p-value = .938; diagnosis vs subclinical symptoms: z-value = -.772, p-value = .746).

For GAD, we found significant effects of diagnostic status on the factors of *negative affect* (subclinical symptoms vs no symptoms: z-value = 4.869, p-value <.001; diagnosis vs no symptoms: z-value = 6.985, p-value <.001; diagnosis vs subclinical symptoms: z-value = 1.859, p-value = .147), *anxious apprehension-specific* (subclinical symptoms vs no symptoms: z-value

= 2.590, p-value = .025; diagnosis vs no symptoms: z-value =3.564 , p-value = .001; diagnosis vs subclinical symptoms: z-value = .860, p-value = .660), and *rumination-specific* (subclinical symptoms vs no symptoms: z-value = .852, p-value = .664; diagnosis vs no symptoms: z-value = 2.418, p-value = .040; diagnosis vs subclinical symptoms: z-value = 1.280, p-value = .399). Marginal effects were observed for *low positive affect-specific* (subclinical symptoms vs no symptoms: z-value = 2.265, p-value = .059; diagnosis vs no symptoms: z-value = 1.830, p-value = .155; diagnosis vs subclinical symptoms: z-value = -.249, p-value = .966), and *repetitive negative thought* (subclinical symptoms vs no symptoms: z-value = 1.060, p-value = .531; diagnosis vs no symptoms: z-value = 2.243; p-value = .062; diagnosis vs subclinical symptoms: z-value = .986, p-value = .578). Surprisingly, there was no significant effect of GAD status on anxious arousal-specific (subclinical symptoms vs no symptoms: z-value = -1.078, p-value = .519; diagnosis vs no symptoms: z-value = 1.486, p-value = .290; diagnosis vs subclinical symptoms: z-value = 1.963, p-value = .118).

Results from ordinal logistic regression analyses simultaneously using all six internalizing dimension factor scores to predict diagnostic status for MDD, GAD, and ASPD can be seen in table 4. When not controlling for the other two disorders, MDD diagnostic status, was significantly associated with all dimensions but anxious apprehension-specific, including negative affect (z-value= 6.589, p<.001), anxious arousal-specific (z-value = 1.986, p= .047), low positive affect-specific (z-value= 2.191, p= .028), rumination-specific (z-value= 3.208, p=.001), and repetitive negative thought (z-value= 2.457, p=.014). However, when controlling for GAD and ASPD diagnostic status, MDD diagnostic status was only significantly associated with negative affect (z-value= 4.270; p<.001), rumination-specific (z-value= 2.445; p=.014), and repetitive negative thought (z-value= 2.457; p=.014).

	Major Depressive Disorder (Internalizing)			Generalized Anxiety Disorder (Internalizing)			Antisocial Personality Disorder (Externalizing)		
Dimension	**OR (SE)**	**z-value**	**p-value**	**Est. (SE)**	**z-value**	**p-value**	**Est. (SE)**	**z-value**	**p-value**
not controlling for comorbid disorder status									
Negative Affect	.962 (.146)	6.589	<.001	1.038 (.149)	6.957	<.001	.593 (.129)	4.582	<.001
Repetitive Negative Thought	.320 (.130)	2.457	.014	.138 (.140)	.986	.324	-.034 (.125)	-.273	.785
Anxious Arousal-specific	.231 (.116)	1.986	.047	.217 (.120)	1.812	.070	.301 (.119)	2.534	.011
Anxious Apprehension-specific	-.031 (.128)	-.239	.811	.486 (.142)	3.407	<.001	-.165 (.132)	-1.250	.211
Low Positive Affect-specific	.267 (.122)	2.191	.028	.303 (.136)	2.221	.026	.167 (.125)	1.335	.182
Rumination-specific	.401 (.125)	3.208	.001	.255 (.132)	1.929	.054	.157 (.121)	1.304	.192
controlling for comorbid disorder status									
Negative Affect	.637 (.149)	4.270	<.001	.640 (.149)	4.302	<.001	.334 (.133)	2.511	.012
Repetitive Negative Thought	.310 (.135)	2.294	.022	.089 (.142)	.632	.527	-.114 (.124)	-.913	.361
Anxious Arousal-specific	.105 (.123)	.852	.394	.120 (.126)	.948	.343	.244 (.117)	2.084	.037
Anxious Apprehension-specific	-.159 (.137)	-1.156	.247	.594 (.155)	3.841	<.001	-.221 (.131)	-1.691	.091
Low Positive Affect-specific	.161 (.126)	1.279	.201	.151 (.136)	1.113	.266	.103 (.123)	.838	.402
Rumination-specific	.316 (.129)	2.445	.014	.087 (.138)	.635	.525	.086 (.119)	.720	.472

Table 4. Results from ordinal logistic regression predicting diagnostic status from factor scores. Logistic regression models predicting diagnostic status of major depressive disorder, generalized anxiety disorder, and antisocial personality disorder from internalizing dimension factor scores, both with and without controlling for the other two disorders. All analyses controlled for age and sex. "OR (SE)" column indicates the odds ratio (OR) and standard error in parentheses. "z-value" indicates z-value of odds ratio. "p-value" column indicates p-value of OR.

When not controlling for the other two disorders, GAD diagnostic status was significantly (i.e., $p < .05$) associated with negative affect (z-value= 6.957, $p < .001$), low positive affect-specific (z-value= 2.221, $p = .026$), and anxious apprehension-specific (z-value= 3.407, $p < .001$), as well as marginally associated with anxious arousal-specific (z-value= 1.812, p= .070) and rumination-specific (z-value= 1.929, p= .054). However, when MDD and ASPD status were additionally controlled for, only negative affect (z-value= 4.302, $p<.001$) and anxious apprehension-specific (z-value= 3.841, $p< .001$) remained significantly associated with GAD

status. Finally, as a control to evaluate the degree to which the dimensions were tapping behaviors preferentially associated with internalizing disorders as opposed to externalizing disorders, we predicted ASPD status from all six internalizing dimension factor scores, both with and without controlling for GAD and MDD status. Without controlling for GAD or MDD status, ASPD was significantly associated with negative affect (z-value = 4.582; p-value <.001) and anxious arousal-specific (z-value = 2.534; p-value = .011). When controlling for MDD and GAD status, ASPD remained significantly associated with negative affect (z-value = 2.511; p-value = .012) and anxious arousal-specific (z-value= 2.084; p-value= .037), as well as marginally negatively associated with anxious apprehension-specific (z-value= -1.691; p-value= .091).

3.4. Discussion

3.4.1. Overview

In the current study, we carried out a confirmatory factor analysis on a novel bifactor model of internalizing psychopathology across three age groups. Results from these analyses suggest that the four-factor internalizing psychopathology model put forth by Nitschke and colleagues (2001) may be expanded to include two additional dimensions: rumination and repetitive negative thought. In line with evidence suggesting dissociations between internalizing psychopathology between the sexes, we find that factor loadings for this model are not invariant between males and females, particularly in regards to anxious apprehension-specific and repetitive negative thought. Finally, we found evidence that negative affect is capturing behaviors that are not just unique to internalizing disorders, but also associated with

externalizing disorders as well, while all other dimensions show some degree of associations with diagnostic status.

3.4.2. Factor Structure of Internalizing Dimensions

To better understand the specific behaviors that are driving each dimension, we evaluated the item-level factor loadings for each dimension and their relationship to each other. While these evaluations were qualitative in nature, they provide some insight into what behavioral items coalesce together when taking into account all other items. Beginning with negative affect, we found evidence that this common dimension was most highly associated with items from the general distress-depression subscale of the MASQ, with the five highest loading items on negative affect coming from this subscale. This coincides with findings from previous work on the tripartite model, in which the general distress-depression item "felt depressed" had the highest loading on the negative affect factor, and all general distress-depression items significantly loaded on the negative affect, which was not the case for the general distress-mixed or general distress-anxiety items (Watson et al., 1995a,b).

Anxious arousal-specific showed evidence of preferential associations with items tapping vestibular function, with the two highest loadings including "felt faint" and "felt dizzy or lightheaded". These results align with factor loadings from Watson and Clark (1995a), who found that the highest loading item on anxious arousal was "felt dizzy or lightheaded". Anxious arousal items tap a number of somatic complaints associated with panic, from widespread bodily processes (e.g., trembling/shaking, hot/cold spells) to focal sensations in particular parts of the body (e.g., chest pain, dry mouth), but the vestibular symptoms stand out for being part of the

most extreme end point of a stress response (Bracha, 2004). While vestibular symptoms are common across the range of anxiety disorders, they are particularly pronounced in panic disorder and phobias, with blood-injection-injury phobia being the only anxiety disorder consistently associated with *actually* fainting. As such, it is possible that the anxious arousal-specific dimension in the current project may be preferentially tapping anxiety symptomology that is preferentially associated with panic disorders and phobias as opposed to other anxiety disorders, such as GAD or social anxiety disorder, in which the dominating symptoms are predominately anxious apprehension-specific.

The anxious apprehension-specific factor showed the strongest loadings with three items tapping a particular temporal theme: that an individual's worry is constant and has been constant in the past (i.e., "I am *always* worrying", "I have been a worrier *all my* life", and "I worry *all the time*"). The temporal focus of these items is noteworthy in the context that one of the theorized distinctions between anxious apprehension and rumination is distinct temporal orientations. However, it is also important to note that there appears to be a distinct pattern in the way the PSWQ items were preferentially associated with anxious apprehension-specific and repetitive negative thought. Specifically, the five PSWQ items with lowest loadings on anxious apprehension-specific were the five reverse scored items, whereas they were the five highest loadings on the repetitive negative thought factor. It is unclear whether this pattern of results reflects instrumental properties of the items (i.e., reverse scoring) or a psychologically meaningful pattern and suggests that the current model could be bolstered by additional measures relevant to anxious apprehension, rumination, and repetitive negative thought.

The low positive affect-specific factor showed a relatively narrow range of loadings, suggesting largely similar contributions of all low positive affect items to this dimension, even

after taking into account variance that was partitioned into the negative affect factor. Despite the relative consistency of these loadings on low positive affect-specific, how the low positive affect items loaded on to negative affect is notable. While the low positive affect items had relatively low loadings on negative affect, the highest loading was for the reverse score of "felt really good about myself". The self-focused negative evaluation of the self that is captured by this item largely aligns with the interpretation of negative affect as being predominately driven by feelings of distress when thinking about oneself and their relationship to the world.

The rumination-specific factor showed the strongest associations with items from the RRS-reflection subscale. This subscale is thought to capture intentional thought regarding the cause of one's depression and while it is positively associated with *current* depression severity, it appears to be protective against *future* depression severity (Treynor et al., 2003). Follow up work suggests reflection and brooding exist as dissociable factors in never and formally depressed individuals, but are indistinguishable in currently depressed individuals (Whitmer & Gotlib, 2011). As such, it appears that the rumination-specific factor in the current project is likely capturing an adaptive response to depression that may contribute to depressive symptomology during the throes of a depressive episode, but diminish the likelihood or severity of future depressive episodes.

Finally, the repetitive negative thought factor had preferential associations with the reverse scored PSWQ items and, to a lesser but notable degree, the RRS-brooding items. Of note is the exceedingly low loadings of the RRS- reflection items on this factor, suggesting that what is shared between rumination and anxious apprehension is not the intentional, problem solving-oriented thought captured by reflection, but instead the largely spontaneous, self-judgmental thought captured by brooding. Indeed, preferential associations between brooding and anxious

apprehension over and above reflection have been observed previously. For example, Raes (2010) noted that while brooding and reflection were both significantly correlated with anxious apprehension, this relationship was over twice as strong in brooding than reflection (r=.53 vs r= .20).

Invariance tests across males and females showed distinct patterns of factor loadings for anxious apprehension-specific and repetitive negative thought. This finding coincides with an extensive body of literature reporting sex differences in the onset (Lewinsohn et al., 1998), prevalence (Bekker et al., 2007; Kessler et al., 1994; Vesga-Lopez et al., 2008) and severity (Bekker et al., 2007) of anxiety disorders, with some evidence suggesting that these disorder-level sex differences may be driven by sex differences in the nature of anxious apprehension (Robichaud et al., 2003; Zalta & Chambless, 2008). Identifying the differential mechanisms driving sex differences in anxious apprehension as well as anxiety more broadly is an area of considerable importance. To date, a number of mechanistic models have been proposed, including differential cultural expectations for males and females (e.g., Breslau et al., 2005), distinct patterns of exposure and reactivity to stress (e.g., Maeng & Milad, 2015), and differences between the sexes in the onset, trajectory, and biological targets of puberty (e.g., Giedd et al., 2006). Disentangling these possibilities is non-trivial, and not only are they all likely contributors, but also are likely interrelated.

3.4.3. Associations Between Internalizing Dimensions and Diagnoses

To further validate this model over and above model fit parameters, we evaluated the degree to which each of six dimensions showed diagnostic specificity to distinct disorders. A

central tenet of Watson and Clark's tripartite model is the idea that after taking into account the common factors, the specific factors should show preferential relationships with MDD or anxiety disorders. Such relationships would not only provide independent confirmation that the dimension are capturing meaningful variance in behavior, but they would also suggest that the dimensional framework may have clinical utility. To evaluate these possibilities, we ran logistic regression models using all internalizing dimensions as predictors of diagnostic status for three disorders, including two internalizing disorders (i.e., MDD and GAD) and an externalizing disorder (i.e., ASPD). To summarize, when controlling for comorbidity between disorders, we found that MDD status was associated with negative affect, rumination-specific, and repetitive negative thought, GAD status was associated with negative affect and anxious apprehension-specific, and ASPD was associated with negative affect and anxious arousal-specific. In the following, we discuss results from these analyses for each dimension.

In the context of the current model, variance in internalizing psychopathology that is attributable to a non-specific "p-factor" (Caspi et al., 2014) would be captured by our negative affect factor. As such, we hypothesized that negative affect should not just be associated with MDD and GAD status, two common internalizing disorders, but it should also be the only dimension associated with ASPD, an externalizing disorder. Logistic regression analyses predicting ordinal diagnostic status of these three disorders confirmed this hypothesis, revealing that increased negative affect was associated with increasing levels of MDD, GAD, and ASPD symptomology when controlling for age and sex. These relationships remained significant even when accounting for comorbidity between these three classes of disorders, suggesting that MDD, GAD, and ASPD diagnostic status are associated with at least partially distinct variance in negative affect. From this, we infer that the negative affect construct in the current model may

actually encapsulate a number of additional constructs that make independent contributions to distinct disorders. In Watson and Clark's original tripartite model, they noted dissociations within negative affect, which they proposed as being dividable into three subcomponents: general distress-anxiety, general distress-depression, and general distress-mixed. This highlights the important point that, thus far, dimensional models of psychopathology are still in their infancy. Though we propose a six-factor model, future research will likely uncover a myriad of additional dimensions that may be useful in accounting for the heterogeneity within psychopathology more broadly, as well as within specific classes of disorders. This multiplicity of behaviors that may be relevant to psychopathology is central to recent attempts to rethink the nosologies of psychopathology, as illustrated by the Hierarchical Taxonomy of Psychopathology (HiTOP; Kotov et al., 2017).

We hypothesize that repetitive negative thought captures behaviors emerging from cognitive mechanisms that are involved across all internalizing disorders. As such, we predicted that repetitive negative thought would show associations with both MDD and GAD status, but not ASPD. This hypothesis was only partially confirmed. Specifically, repetitive negative thought was indeed significantly associated with MDD status and not associated with ASPD, but we did not observe an association with GAD status as predicted. This pattern of results was consistent both when controlling and not controlling for diagnostic status of the other disorders. The apparent specificity of repetitive negative thought to MDD diagnostic status but not GAD status stands in contrast to previous research by suggesting that repetitive negative thought is a transdiagnostic dimension contributing to both mood and anxiety disorders. In one such study, McEvoy and Brans (2013) found that a bifactor estimate of repetitive negative thought was predictive of both depression and anxiety symptomology, even when controlling for one or the

other. While the reason for differences between this study and the current results is unclear, two potential explanations stand out. First, McEvoy and Brans (2013) did not explicitly model negative affect in their study. Thus, at least some of the variance in their repetitive negative thought factor is likely capturing negative affect, which our study found to be independently associated with both depression and anxiety diagnostic status. If this is indeed the case, the relationship between repetitive negative thought and both anxiety and depression symptomology may in fact be driven by variance that is partitioned into negative affect in the current project. Second, whereas we utilized a three level ordinal characterization of MDD and GAD diagnoses, McEvoy and Brans (2013) estimated latent general depression and anxiety symptomology using multiple continuous indicators. It is also worth noting that we had relatively few individuals meeting diagnostic criteria for GAD. Of the 505 participants involved in these analyses, over 70% reported no GAD symptoms and only 51 total participants met DIS GAD diagnostic criteria as compared to 113 who met diagnostic criteria for MDD. Furthermore, and of the 51 participants that did meet diagnostic status, 42 of them had concurrent MDD diagnoses. As such, we had the least power to detect relationships between GAD diagnostic status and internalizing dimensions, particularly when controlling for MDD status.

Because the current model posited that anxious arousal-specific and anxious apprehension-specific are preferentially associated with anxiety disorders, we predicted that they would both show evidence of relationships with GAD. While this was the case for anxious apprehension-specific, anxious arousal-specific showed preferential associations with ASPD, not GAD. Anxious arousal-specific was at least marginally positively associated with all three diagnoses when not controlling for comorbidity, but when comorbidity was controlled for, only the relationship with ASPD remained significant. Though not what we had predicted *a priori*, the

lack of a relationship between anxious arousal-specific and GAD is not entirely surprising as previous research suggests that anxious arousal may in fact be predictive of panic disorder, not GAD (Nitschke et al., 2001; Zinbarg & Barlow, 1996). However, why anxious arousal-specific would be associated ASPD over and above MDD and GAD status remains an open question. Previous research has shown that early-life panic attacks may be predictive of later-life ASPD, but this relationship was not specific to ASPD, instead suggesting that early life anxious arousal is a broad risk factor for later psychopathology in general (Goodwin & Hamilton, 2002). However, other research has shown that the severity and chronicity of panic attacks, and presumably anxious arousal, may drive increased levels of anger and aggression, central symptoms of ASPD. It also may be the case that some aspects of anxious arousal-specific are indeed associated with internalizing disorders (e.g., GAD), but this effect is masked when controlling for comorbidity with other internalizing (e.g., MDD) disorders, particularly due to the very few subjects who met GAD diagnoses without meeting MDD diagnoses. Further research should include additional diagnostic measures, including a broader array of diagnoses, to further validate the clinical utility of these dimensions.

Finally, we predicted that low positive affect-specific and rumination-specific would be specifically associated with MDD. The predicted relationship was observed for rumination-specific but not low positive affect-specific. In fact, much like anxious arousal-specific, low positive affect-specific was significantly associated with both MDD and GAD when not controlling for comorbidity, but when controlling for comorbidity both relationships became non-significant. Much like anxious arousal-specific, it may be that the high rates of comorbidity between MDD and GAD effectively washed out any significant relationship between low positive affect-specific and MDD diagnoses. It is noteworthy, however, that when not controlling

for comorbidity, low positive affect-specific was not associated with ASPD, suggesting a degree of specificity of low positive affect-specific to internalizing, not externalizing, disorders. The significant association between rumination-specific and MDD status is confirmation that the rumination-specific dimension is capturing meaningful covariance in behavior. In developing this six-factor model, there was concern that after taking into account covariation between rumination items through both the negative affect and repetitive negative thought factors, the rumination-specific residual would not be meaningful in terms of psychopathology. Instead, it may just capture uninteresting instrumental covariance emerging from the fact that all of the indicators were from the same questionnaire. The fact that we observe associations between rumination-specific and MDD status begins to ameliorates these concerns, suggesting that rumination-specific is capturing meaningful covariation in behaviors relevant to internalizing psychopathology.

3.4.4. Conclusions

In this study, we introduced a novel six-factor dimensional model of internalizing psychopathology. Employing bifactor modeling, we demonstrated that previous models of internalizing psychopathology may benefit from the inclusion of additional dimensions. Importantly, we showed that the underlying factor structure of internalizing psychopathology differs between the sexes, particularly in terms of higher level, cognitive dimensions. Finally, we demonstrated that such dimensional models have clinical utility and map on to case-control diagnoses in a pattern that was largely predicted a priori. However, understanding the dissociable factors driving internalizing psychopathology, as well as psychopathology more broadly, is by no

means complete. Future research may be well served to further dissect these dimensions into even more precise constructs, with an eye towards understanding how distinct diagnoses may exhibit distinct dimensional profiles. Of particular importance is understanding whether a single diagnosis may in fact be comprised of multiple dimensional profiles, in line with the considerable amount of heterogeneity in symptoms of a given disorder. Having demonstrated the plausibility of the current six-factor model of internalizing psychopathology, we now turn to better understanding the neurobiological mechanisms that may drive individual differences in these behaviors. In Chapter 4, we utilize factor scores derived from the six-factor CFA discussed in this chapter to test for relationships between individual differences in the internalizing dimensions and variability in neuroanatomical organization, and how these relationships may be influenced by age and sex.

CHAPTER 4

GRAY MATTER MORPHOMETRY OF INTERNALIZING DIMENSIONS

4.1. Introduction

Neuroimaging research into the neural correlates of psychopathology suggest that internalizing disorders emerge through the interaction of prefrontal brain regions supporting cognitive control and subcortical brain regions supporting emotion, as well as the insula (Disner et al., 2011; Ekin, 2009), which occupies an intermediate position between the two. Much of this research is grounded in case-control studies, in which the brains of individuals who meet diagnostic criteria for a given disorder are compared to the brains of healthy controls. While this approach has implicated alterations in a number of brain regions in patients, the mapping of specific regions to specific internalizing behaviors remains largely elusive. Despite potential clinical utility, it remains unclear the degree to which specific regions are preferentially associated with behaviors unique to one disorder over another, or associated with internalizing disorders more broadly. Furthermore, it is unknown the degree to which brain regions not classically implicated by case-control studies may indeed show associations with individual differences in internalizing behaviors. In this chapter, we present gray matter morphometry analyses evaluating the degree to which individual differences in the internalizing dimensions detailed in Chapter 3 are associated with individual differences in the structure of gray matter across two age groups.

In response to an overwhelming body of evidence suggesting that the distinctions between cases and controls in case-control frameworks are likely counter to the underlying

nature of psychopathology, there has been a recent emphasis on characterizing psychopathology as emerging through the interactions of transdiagnostic dimension that are distributed throughout the general population (Insel et al., 2010; Kotov et al., 2017). As discussed in Chapters 1 and, to a lesser degree, in Chapter 2, transdiagnostic dimensions are behaviors that span case-control diagnoses, often manifesting across multiple disorders, as well as in individuals who may not meet criteria for a given disorder. Such dimensional approaches afford researchers the ability to parse a monolithic construct like major depression into more precise, nuanced behaviors. In doing so, researchers may gain a better understanding of the specific biological correlates of pathological behaviors while simultaneously capturing the heterogeneity in behavior that occurs both between and within disorders.

Despite evidence of age and sex effects on neuroanatomy and internalizing behaviors, it is still largely unknown the degree to which the neuroanatomical correlates of internalizing psychopathology change across the lifespan and differ between males and females. Whereas the precise relationship between neuroanatomy and psychopathology has proven difficult to pin down, there is strong, well validated evidence of age and sex effects on both neuroanatomy (Gennatas et al., 2017; Gogtay et al., 2004; Taki et al., 2011; Tamnes et al., 2017) and psychopathology (Asher et al., 2017; de Lijster et al., 2017; Salk et al., 2017; Twenge & Nolen-Hoeksema, 2002). For example, adolescence marks a crucial shift in neuroanatomical development, with the cascade of sex hormones that are released in adolescence promoting widespread neuronal sculpting, including the pruning of gray matter and proliferation of white matter (Gogtay & Thompson, 2010; Peper et al., 2011; Spear, 2013). These developmental processes are thought to be largely complete by young adulthood (~30 years old), at which point gray matter levels sustain throughout middle adulthood, and then decrease as people enter into

older adulthood due to neuronal degeneration. Interestingly, age of first onset and severity of internalizing psychopathology follow a similar trajectory, with almost 50% of major depression patients ages 18 to 75 reporting that their first depressive episode occurred during adolescence (Zisook et al., 2007). While adolescence is characterized as a period of heightened risk for internalizing psychopathology (for a review, see Hankin, 2015), distinct internalizing disorders show differential age of onsets (de Lijster et al., 2017), suggesting that the expression of internalizing behaviors is dynamic across the lifespan.

In addition to age effects, there are also strong sex differences in both brain morphology and patterns of psychopathology. While the brains of males and females share much in common, males and females follow distinct neurodevelopmental trajectories (Gennatas et al., 2017; Tamnes et al., 2017), resulting in focal differences in gray matter structure during adulthood (Ruigrok et al., 2014). Some of the most pronounced differences in gray matter structure between males and females occur in brain regions thought to be central to internalizing psychopathology, including lateral prefrontal cortex, orbitofrontal cortex, and the amygdala (Ruigrok et al., 2014). In addition to neuroanatomical differences between the sexes, there are well documented sex differences in internalizing psychopathology (Altemus et al., 2014). For example, women are more likely than men to be diagnosed with MDD or an anxiety disorder (Altemus et al., 2014), with this dissociation between the sexes first manifesting during adolescence (Hankin, 2009; Hankin et al., 2007). This paints a picture in which the large scale, rapid changes in neural organization that occur during adolescence are often accompanied by a sudden onset of psychopathological behaviors, potentially in a sex-specific manner, begging the question as to the relationship between neurodevelopment and psychopathology. Indeed, a number of developmental theories of psychopathology mark adolescence as a critical period for

life-long mental health trajectories (Copeland et al., 2009; Kim-Cohen et al., 2003), with the dynamic neural reorganization that occurs during this short era of life potentially marking a particularly vulnerable period to the detrimental effects of stress and social influences on mental health (Hankin, 2009; Hankin et al., 2007; Steinberg, 2010).

As a result of the dynamic changes in both neuroanatomy and psychopathology across the lifespan and by sex, the insights gleaned in one age group or in one sex may not apply to the other. For example, in one of the largest surface-based morphometry studies of internalizing patients, adults with MDD showed reduced thickness in the orbitofrontal cortex, cingulate, insula, and temporal lobes, whereas MDD status in adolescence was associated with reduced surface area in the medial orbitofrontal cortex, superior frontal gyrus, pre- and postcentral gyri, as well as occipital and parietal regions (Schmaal et al., 2017). These results demonstrate considerable differences between adolescents and adults in the gray matter correlates of MDD, including differences between age groups in terms of the specific brain regions and neuroanatomical property associated with MDD status (i.e., thickness in adults/ area in adolescents). In fact, only one region was commonly implicated across both age groups, and that was the orbitofrontal cortex. Similar differences have also been observed between the sexes, with males and females within the same age range showing dissociable neuroanatomical correlates of internalizing disorders (Kong et al., 2013). For example, within an adult sample, Kong and colleagues (2013) found sex by MDD diagnosis interactions within subcortical structures, including the amygdala, hippocampus and caudate. Specifically, female patients showed reduced gray matter volume in the amygdala and hippocampus as compared to healthy controls, whereas male patients showed reduced caudate volume as compared to healthy controls. Taken together, it is apparent that to better understand the neural basis of internalizing psychopathology, it is

vital to carefully consider both age and sex, factors that are often neglected in studies evaluating the neuroanatomical correlates of internalizing psychopathology.

In this chapter, we test for associations between individual differences in gray matter morphometry and the six factor dimensional model of internalizing psychopathology presented in Chapter 3. Using the case-control literature as our guide, we carry out analyses at multiple levels of granularity, including analyses focused on a priori regions of interest from patient studies, as well as exploratory whole brain analyses. Because of potential moderating effects of age on the relationship between gray matter and internalizing psychopathology (e.g., Schmaal et al., 2017), we test for these relationships in two distinct age groups: adolescents and young adults. Additionally, in light of considerable sex influences on internalizing psychopathology and gray matter, we both control for sex and directly test for sex interactions on the relationship between gray matter morphometry and the internalizing dimensions.

4.2. Methods

4.2.1. Participants

Participants were drawn from two of the samples outlined in table 1, including the adolescent sample (N= 121; 61 male/60 female; mean age(SD)= 17.1(1.5)) from the Colorado Cognitive Neuroimaging Family Emotion Research Study (CoNiFER Study), and the adult sample consisting of same-sex twin pairs from the Institute for Behavioral Genetics' Longitudinal Twin Study (LTS) (N= 630; 284 males/346 females; mean age(SD)= 28.7(.8)). All

participants for gray matter morphometry analyses were included in the confirmatory factor analysis discussed in Chapter 3.

4.2.2. Internalizing Dimension Factor Scores

Factor scores of the six internalizing dimensions utilized in the gray matter morphometry analyses were drawn from the six factor confirmatory factor analysis (CFA) discussed in Chapter 3. To review, these dimensions included two bifactor dimensions, namely negative affect and repetitive negative thought, as well as four specific residual dimensions, including anxious arousal-specific, anxious apprehension-specific, low positive affect-specific, and rumination-specific. All indicators in the CFA were treated as categorical and factor scores were saved for each subject. Though factor indeterminacy values are not produced by MPlus when using categorical indicators, a CFA treating indicators as continuous found that the factor scores had high levels of indeterminacy (indeterminacy values ranging from .85 to .98) and the factor scores from these two models were highly correlated (r values ranging from .82 to .98). As such, it was determined that the factor scores utilized in the gray matter morphometry analyses were largely capturing the underlying latent constructs of interest.

4.2.3 Surface-Based Gray Matter Morphometry Analyses

4.2.3.1 Preprocessing

Analyses testing for relationships between individual differences in internalizing factor scores and surface-based morphometry employed the FreeSurfer analysis suite (http://surfer.nmr/mgh.harvard.edu/). SBM preprocessing included brain extraction using a hybrid watershed/surface deformation procedure (Segonne et al., 2004), followed by a transformation into Talaiarch space, intensity normalization (Sled et al., 1998), tessellation of the gray/white matter boundary (Fischl et al., 2001), and surface deformation along intensity gradients to optimally differentiate gray matter, white matter, and cerebral spinal fluid boundaries (Dale et al., 1999; Fischl and Dale, 2000). The resulting segmented surfaces were registered to a standard spherical inflated brain template (Fischl et al., 1999a,b), parcellated according to gyral and sulcal structure (Desikan et al., 2006; Fischl et al., 2004), and then used to compute a range of surface-based measurements, including cortical volume, surface area, and thickness. Prior to running surface-based analyses, data quality assurance was checked using FreeSurfer's standard QA tools (https://surfer.nmr.mgh.harvard.edu/fswiki/QATools). Surface-based measurements of volume, cortical thickness, and surface area were input into a general linear model, which tests for vertex-wise correlations between the aforementioned surface-based morphometry measures and the behavioral dimensions of interest.

4.2.3.2 General Analysis Plan

SBM analyses were conducted across different subsets of subjects, including each age group, separately, as well as a combined sample merging across the adolescent and young adult samples. Within both samples separately, we carried out two sets of analyses: main effect analyses controlling for sex and chronological age as well as sex interaction analyses which

tested for sex differences in the relationship between internalizing factor scores and gray matter morphometry. In all analyses looking across both age groups, we treated each age group as distinct within the general linear model, ensuring that our results are not biased by the variable sample sizes between the groups. Within the combined sample of adolescent and young adults, we tested for gray matter morphometry/internalizing factor score relationships that were consistent across the two age groups and sexes, using age group and sex as nuisance covariates. In separate analyses, we also tested for group differences in gray matter morphometry/internalizing factor score relationships between the two age groups by including an age group by internalizing factor score interaction term, treating sex as a nuisance covariate.

4.2.3.3 A Priori Region of Interest Analyses

Within both samples, we carried out two overarching sets of analyses: region of interest (ROI) analyses focusing on brain regions commonly implicated in case-control studies and exploratory whole brain, vertex-wise analyses. The ROI analyses evaluated the degree to which brain regions which frequently showed alterations in gray matter in internalizing patients show preferential associations with the internalizing dimensions employed in the current study. We hypothesized specific relationship between these regions and internalizing factor scores based on both previous findings but also the proposed theory regarding the functions of a given brain region in relationship to the mechanisms central to the different internalizing dimensions as conceptualized in Chapter 3 (for more information regarding hypotheses, see sections 1.7.2 to 1.7.4). For a graphical representation of ROIs from case-control studies and our a priori predictions regarding these ROIs, see figure 4. These hypotheses include significant associations

of negative affect with the insula and caudal anterior cingulate, repetitive negative thought with the middle frontal gyrus, anxious arousal-specific with the amygdala and thalamus, anxious apprehension-specific with the inferior frontal gyrus, low positive affect-specific with the orbitofrontal cortex, rostral anterior cingulate, and basal ganglia, and rumination-specific with the hippocampus.

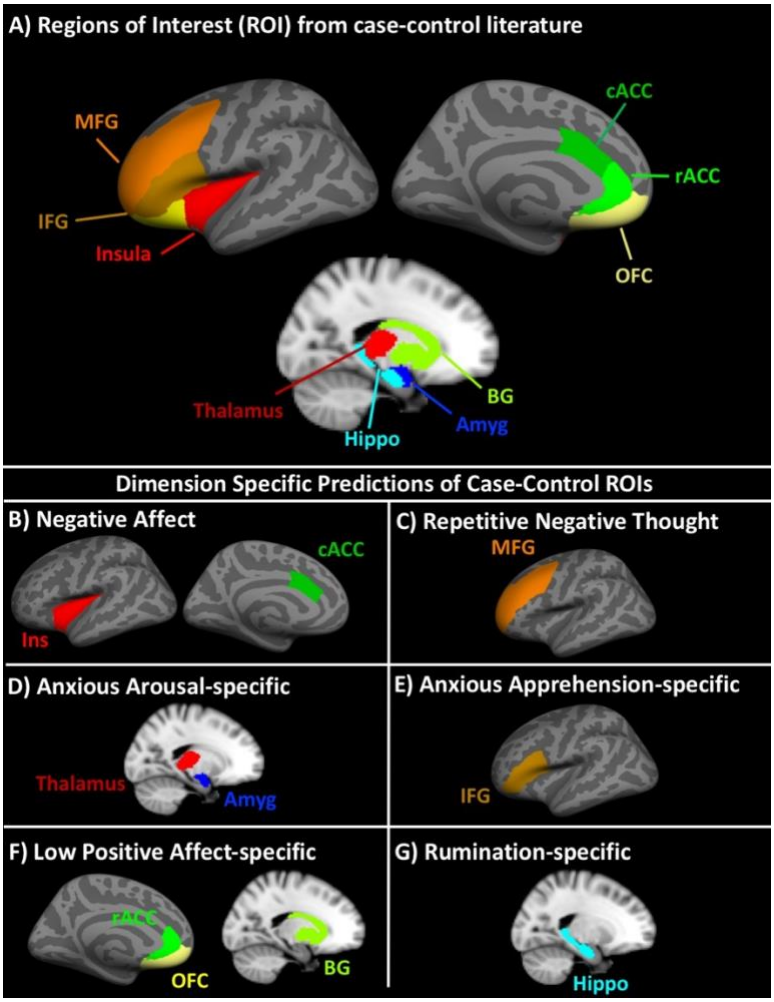

Figure 4. *A priori* regions of interest (ROI) from case-control studies and dimensional predictions. *Panel A:* ROIs from case-control literature; *Panel B:* predicted associations between negative affect and case-control ROIs; *Panel C:* predicted associations between repetitive negative thought and case-control ROIs; *Panel D:* predicted associations between anxious arousal-specific and case-control ROIs; *Panel E:* predicted associations between anxious apprehension-specific and case-control ROIs*; Panel F:* predicted associations between low positive affect-specific and case-control ROIs*; Panel G:* predicted associations between rumination-specific and case-control ROIs*;* MFG= middle frontal gyrus; IFG= inferior frontal gyrus; cACC= caudal anterior cingulate cortex; rACC= rostral anterior cingulate cortex; OFC= orbitofrontal cortex; BG= basal ganglia; Amyg= amygdala; hippo= hippocampus.

To compute individual differences in gray matter for each ROI, we utilized the FreeSurfer functions “aparcstats2table” and “asegstats2table” for cortical and subcortical ROIs, respectively. We parcellated the brain using the Killiany/Desikan atlas (Desikan et al., 2006), which partitions the brain into a total of 68 cortical ROIs across the left and right hemispheres. For our ROI analyses, we employed left and right homologs of the following ROIs from the Killiany/Desikan atlas: insula, caudal middle frontal gyrus, rostral middle frontal gyrus, pars opercularis (inferior frontal gyrus subregion), pars triangularis (inferior frontal gyrus subregion), pars orbitalis (inferior frontal gyrus subregion), rostral anterior cingulate, caudal anterior cingulate, lateral orbitofrontal cortex, medial orbitofrontal cortex, amygdala, hippocampus, caudate (basal ganglia subregion), putamen (basal ganglia subregion), pallidum, (basal ganglia subregion), accumbens (basal ganglia subregion), and thalamus.

To test for relationships between gray matter of the ROIs and internalizing factor scores, we utilized mixed-effect models as implemented by the R package “nlme” (Pinheiro et al., 2020), treating family as a random effect to account for non-independence between twin pairs in the young adult sample and siblings in the adolescent sample. For all cortical ROIs, we separately tested for associations of internalizing factor scores with surface area, volume, and thickness of a given ROI, whereas for all subcortical ROIs, we tested for associations with volume only. In each model, we predicted gray matter for a given ROI by all six internalizing dimensions simultaneously. Because we were interested in potential moderating effects of sex on the relationships between gray matter morphometry and internalizing factor scores, we also predicted gray matter for each ROI by each internalizing factor score, sex, and the interaction between factor scores and sex. All models controlled for total intracranial volume in analyses of volume, average surface area across the whole brain in analyses of surface area, and mean

thickness in analyses of thickness. Because data from this project were drawn from two distinct scanner software version, for all analyses we also included scanner platform as a nuisance regressor. Analyses were run separately for the two age samples (see section 4.3.1.1 for adolescent results; see section 4.3.2.1 for young adult results). Within the a priori ROIs, we additionally tested for interaction effects of age groups to determine the degree to which our hypothesized relationships between internalizing dimension and gray matter may statistically differ between the two age groups (see section 4.3.3.1).

To reduce the chance of type 1 errors, we employed a Bonferroni correction to determine statistical significance of observed effects. Specifically, for each ROI we carried out six distinct tests (volume, area, and thickness by left and right hemispheres). As such, we divided the standard $p < .05$ alpha level by six to arrive at a Bonferroni corrected p-value of $p < .0083$. However, for a priori predictions outlined in figure 4 panels B to G, we relaxed the significance threshold to $p < .05$.

4.2.3.4 Exploratory Whole Brain Analyses

In addition to the ROI-based analyses outlined above, we also carried out exploratory, whole brain analyses, testing for relationships between internalizing factor scores and fine-grained variability in gray matter morphometry on a vertex-wise basis. Importantly, these analyses allowed us to identify focal brain regions both within and outside of brain regions commonly implicated in case-control studies. Whole brain analyses employed the general linear model with permutation testing as implemented by the Permutation Analysis of Linear Models package (PALM; Winkler et al., 2014). To account for the non-independence between

participants, we utilized exchangeability blocks ("-eb" option in PALM) in conjunction with sign flipping and exchangeable errors ("-ise" and "-ee" options in PALM, respectively). Analyses were conducted within the adolescent (see section 4.3.1.2) and young adult samples (see section 4.3.2.2), separately, as well as across both samples combined. In analyses within each age sample, we tested for gray matter morphometry/internalizing factor score relationships within each age group controlling for sex, as well as testing for sex interactions on the relationship between gray matter morphometry and internalizing factor scores. As was the case in the ROI analyses, all whole brain analyses within each sample included sex, age, scanner version, and whole brain gray matter measures (i.e., total mean thickness, total surface area, and total intracranial volume) as nuisance covariates. We also carried out analyses across both samples, testing for effects that were significant across the age groups (see section 4.3.3.3), as well as significant age group interaction effects (see section 4.3.3.2).

For all exploratory whole brain models, permutations were carried out across 10,000 iterations. To determine cluster significance, we evaluated results at multiple thresholds, including False Discover Rate (FDR) and Familywise Error (FWE) corrections of $p < .05$, and uncorrected p-values of $p < .0002$ after permutation. An uncorrected p-value of $p < .0002$ was derived from dividing the standard $p < .05$ by the 216 distinct whole brain gray matter morphometry models that were run (i.e., 216). The breakdown of the 216 models is as follows: six internalizing dimension by three gray matter morphometry measures by two hemispheres by three age group samples (i.e., adolescent only, young adult only, adolescents and young adults) by two types of effects tested per age sample (i.e., controlling for sex/sex interactions in adolescent-only and young adult-only samples; controlling for age/age group interactions in combined adolescent and young adult sample). For uncorrected results after permutations, cluster

extent was determined by first thresholding permuted maps at a cluster forming threshold of p<.01. Then, if a cluster contained a peak vertex of p <.0002, it was considered significant. Because very few results passed the highly conservative FDR- and FWE- corrected thresholds and given the highly exploratory nature of these analyses, we report results at the uncorrected threshold after permutation testing.

4.3 Results

Throughout the results and discussion, we refer to effects as either being "positive" or "negative". When controlling for sex, "positive" means that increased internalizing factor scores were associated with greater volume, area, or thickness, whereas "negative" means that increased internalizing factor scores were associated with reduced volume, area, or thickness.

4.3.1. Adolescents

4.3.1.1. Region of Interest (ROI) Analyses

4.3.1.1.1. ROI Analyses Controlling for Sex

Results from multiple regression analyses predicting volume, area, and thickness of a priori ROIs in adolescents can be seen in Appendix 2 and figure 5 bottom panel. In the following, we summarize all relationships between ROI gray matter and the internalizing dimension factor scores that met an alpha threshold of p <.05 (as shown in Appendix 2) but focus

the discussion only on results that passed the Bonferroni corrected alpha of p<.0083 or that were p<.05 if they were the a priori predictions spelled out in figure 4 (Bonferroni correction/a priori results can be seen in figure 5). Within the adolescents, the only effect that met these criteria was a negative association between *low positive affect-specific* and volume of the left amygdala (ß(SE)= -.258(.072), t-value= -3.565, p-value=.004). Post-hoc analyses revealed that this relationship between low positive affect-specific and left amygdala volume identified in adolescents did not significantly differ between the two age groups (ß(SE)= .117(.074), t-value= 1.581, p-value=.115).

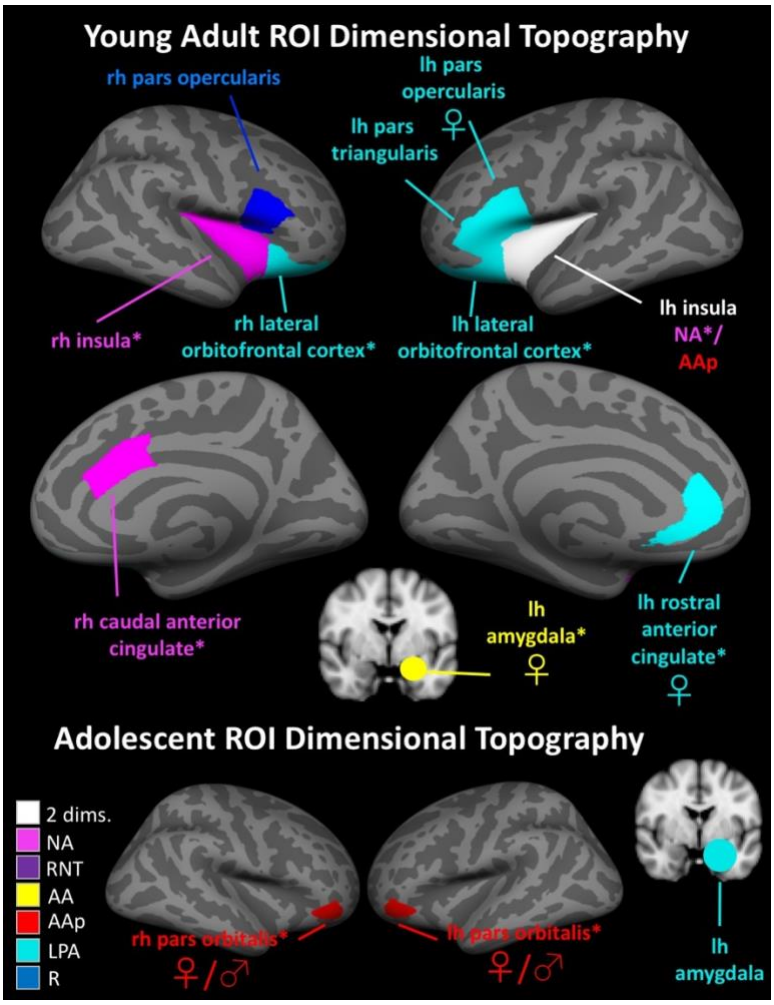

Figure 5. Dimensional topographies of ROI results in young adults and adolescents. Results from ROI analyses testing for relationships between internalizing dimension factor scores and gray matter morphometry from case-control study ROIs. All results were negative associations (i.e., increased internalizing factor scores associated with decreased gray matter properties). The color of each ROI specifies the specific dimension that was associated with

that ROI. White ROIs indicate two dimensions both showed associations with gray matter of that ROI. All results were either significant at p <.05 for predicted associations indicated in figure 4. (marked with *) or significant at a Bonferroni corrected p< .0083. ♀ indicates that the given effect was observed in females only. ♀/♂= cross-over interaction that is non-significantly positive in males and non-significantly negative in females. NA= negative affect; RNT= repetitive negative thought; AA= anxious arousal-specific; AAp= anxious apprehension-specific; LPA= low positive affect-specific; R= rumination-specific; lh= left hemisphere; rh= right hemisphere.

We now summarize all marginally significant results (i.e., p<.05 to p>.0083) (not shown in figure 5). *Negative affect* was positively associated with thickness of left pars triangularis (ß(SE)= .194(.077), t-value= 2.537, p-value=.028) and negatively associated with thickness of left pars orbitalis (ß(SE)= -.208(.079), t-value= -2.637, p-value=.023), as well as being negatively associated with volume of the left amygdala (ß(SE)= .153(.070), t-value= 2.187, p-value=.050).

Repetitive negative thought was positively associated with volume of the left pars orbitalis (ß(SE)= .239(.082), t-value= 2.923, p-value=.014) and thickness of the left caudal anterior cingulate (ß(SE)= .196(.088), t-value= 2.219, p-value=.048).

Anxious arousal-specific was positively associated with thickness of right rostral middle frontal gyrus (ß(SE)= .151(.063), t-value= 2.290, p-value=.036), volume (ß(SE)= .227(.092), t-value= 2.463, p-value=.032) and area (ß(SE)= .227(.087), t-value= 2.616, p-value=.024) of right pars triangularis, and thickness of right caudal anterior cingulate (ß(SE)= .205(.092), t-value= 2.241, p-value=.047).

Anxious apprehension-specific was positively associated with left rostral middle frontal gyrus area (ß(SE)= .157(.057), t-value= 2.728, p-value=.020).

Rumination-specific showed a negative association with area of the right pars triangularis (ß(SE)= -.204(.083), t-value= -2.462, p-value=.032).

4.3.1.1.2. Sex Interactions

Results from multiple regression analyses testing for sex interaction effects on the relationship between gray matter of a priori ROIs and internalizing dimensions in adolescents can be seen in table 5. No sex interaction effects met our Bonferroni threshold. However, *anxious apprehension-specific* showed sex interactions ($p<.05$) in left and right pars orbitalis subregions of the inferior frontal gyrus, in line with our a priori prediction that anxious apprehension-specific would be associated with the inferior frontal gyrus.

Dimension	ROI	Measure	Direction	Est.	SE	t-value	p-value
RNT	rh pars opercularis	area	♂= $+_{ns}$ ♀= $-_{ns}$	0.419	0.165	2.540	0.023
	rh lOFC	thickness	♂= $-_{ns}$ ♀= $+_{ns}$	-0.294	0.136	-2.162	0.047
AA	lh cMFG	thickness	♂= $+_{ns}$ ♀= $-_{ns}$	0.323	0.149	2.177	0.046
	rh rMFG	volume	♂= $-_{ns}$ ♀= $+_{ns}$	-0.352	0.149	-2.354	0.033
	lh pars orbitalis	volume	♂= $-_{ns}$ ♀= $+_{ns}$	-0.406	0.173	-2.353	0.033
	rh lOFC	thickness	♂= $-_{ns}$ ♀= $+_{ns}$	-0.312	0.146	-2.141	0.049
AAp	**lh pars orbitalis**	**thickness**	**♂= $+_{ns}$ ♀= $-_{ns}$**	**0.360**	**0.167**	**2.153**	**0.048**
	rh pars orbitalis	**volume**	**♂= $+_{ns}$ ♀= $-_{ns}$**	**0.435**	**0.177**	**2.451**	**0.027**
		area	**♂= $+_{ns}$ ♀= $-_{ns}$**	**0.375**	**0.157**	**2.389**	**0.031**
LPA	rh hippocampus	volume	♂= $+_{ns}$ ♀= $-_{ns}$	0.376	0.132	2.853	0.012
	lh cMFG	area	♂= $-^{\wedge}$ ♀= $+_{ns}$	-0.322	0.142	-2.279	0.038
	lh pars opercularis	volume	♂= $+_{ns}$ ♀= $-_{ns}$	0.385	0.164	2.339	0.034
R	rh lOFC	thickness	♂= $-_{ns}$ ♀= $+_{ns}$	-0.291	0.135	-2.155	0.048

Table 5. Adolescent ROI analyses – sex interactions. Significant ($p<.05$) results from multiple regression models testing for moderating effects of sex on the relationship between internalizing factor scores and ROI gray matter morphometry. All models controlled for sex, age, MRI scanner platform, and a whole brain morphometry measure, treating family as a random effect. Bold text indicates the results passed the Bonferroni correction threshold or was a result predicted a priori at a $p<.05$. "Direction" indicates results from post-hoc analyses testing for the relationship between a given internalizing dimension and ROI in both sexes, separately. "Est."= beta estimate of sex interaction effect; "SE"= standard error of beta estimate of sex interaction effect; RNT= repetitive negative thought; AA= anxious arousal-specific; LPA= low positive affect-specific; AAp= anxious apprehension-specific; R= rumination-specific; ♂ = males; ♀ = females; += Positive relationship (increased internalizing dimension factor score associated

with increased gray matter morphometry measures); - = Negative relationship (increased internalizing dimension factor score associated with decreased gray matter morphometry measure); *= effect is significant (p<.05); ^= effect is marginally significant (p<.1); ns = effect is non-significant (p>.1); lh= left hemisphere; rh= right hemisphere; lOFC= lateral orbitofrontal cortex; cMFG= caudal middle frontal gyrus; rMFG= rostral middle frontal gyrus.

In the following, we summarize all marginally significant (p<.05) sex interaction effects, as shown in table 5. *Negative affect* showed no sex interaction effects within the ROI analyses. *Repetitive negative thought* showed sex interactions with thickness of right lateral orbitofrontal cortex (ß(SE)= .419(.165), t-value= 2.540, p-value=.023) and area of right pars opercularis (ß(SE)= -.294(.136), t-value= -2.162, p-value=.047*). Anxious arousal-specific* showed sex interactions with thickness of left caudal middle frontal gyrus (ß(SE)= .323(.149), t-value= 2.177, p-value=.046) and left orbitofrontal cortex (ß(SE)= -.312(.146), t-value= -2.141, p-value=.049), as well as volume of left pars orbitalis (ß(SE)= -.406(.173), t-value= -2.353, p-value=.033) and right rostral middle frontal gyrus (ß(SE)= -.352(.149), t-value= -2.354, p-value=.033). *Anxious apprehension-specific* showed sex interactions within bilateral pars orbitalis, including thickness of left pars orbitalis (ß(SE)= .360(.167), t-value= 2.153, p-value=.048) and volume (ß(SE)= .435(.177), t-value= 2.451, p-value=.027) and area (ß(SE)= .375(.157), t-value= 2.389, p-value=.031) of right pars orbitalis. *Low positive affect-specific* showed sex interactions with volume of the right hippocampus (ß(SE)= .376(.132), t-value= 2.853, p-value=.012) and left pars opercularis (ß(SE)= .385(.164), t-value= 2.339, p-value=.034), as well as area of left caudal middle frontal gyrus (ß(SE)= -.322(.142), t-value= -2.279, p-value=.038). *Rumination-specific* showed a sex interaction with thickness of right lateral orbitofrontal cortex (ß(SE)= -.291(.135), t-value= -2.155, p-value=.048).

4.3.1.2. Exploratory Whole Brain Analyses

4.3.1.2.1. Controlling for Sex

In the following, we summarize significant results from the exploratory whole brain analyses controlling for sex in adolescents. For a summary figure showing results from all dimensions overlaid on a single brain, see figure 6. For full results, table 6 and figures 7 to 12.

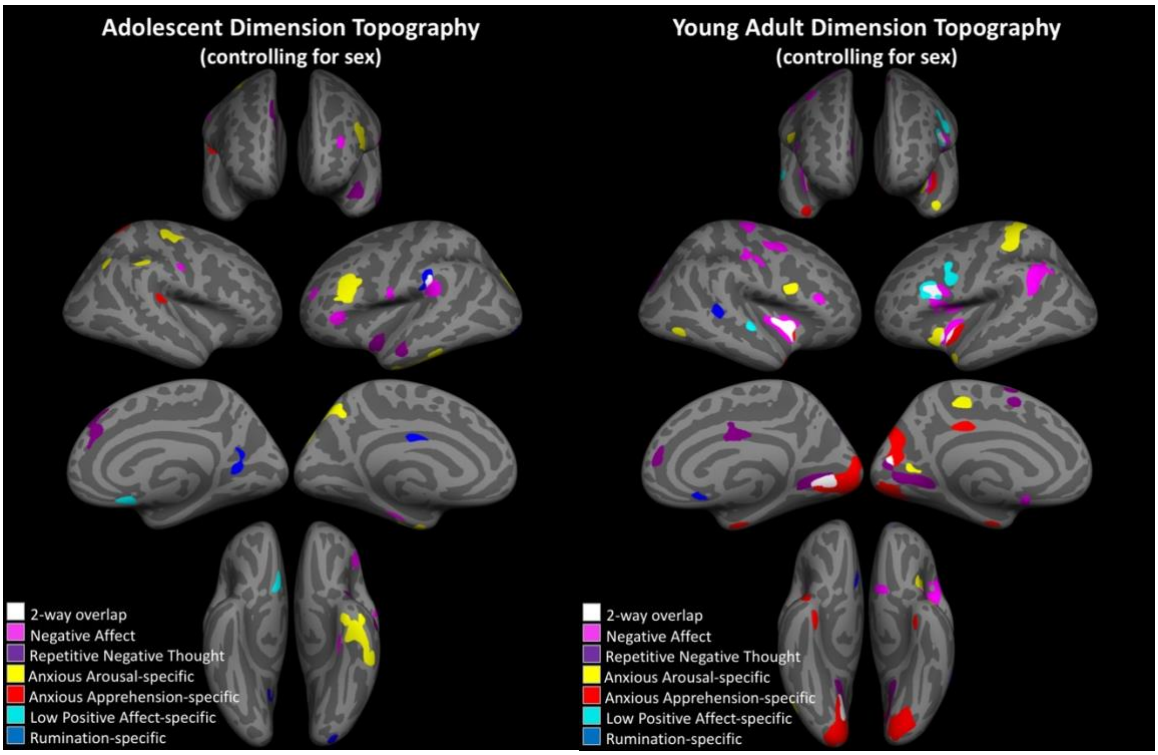

Figure 6. Age group specific dimensional topography from whole brain analyses. *Left panel:* Dimensional topography when controlling for sex within adolescents only. *Right panel:* Dimensional topography when controlling for sex in adolescents. Lh= left hemisphere; rh= right hemisphere.

Dimension	Measure	Direction	Hemi	Max p	Cluster Size (mm^2)	X	Y	Z	Region
NA	area	Positive	lh	.0002	510.4	-42.4	-34.9	23.4	parietal operculum
	area	Negative	rh	.0001	92.68	52	-11.7	33.4	postcentral gyrus
	volume	Positive	lh	.0001	372.08	-43.7	-35.2	24.6	parietal operculum
	volume	Positive	lh	.0001	124.64	-26	-23	-22.3	parahippocampal
	volume	Negative	lh	.0001	143.22	-30.2	43.3	14.3	frontal pole
	volume	Negative	lh	.0002	132.92	-59.8	-6.4	10	ventral central sulcus
	thickness	Positive	lh	.0001	287.46	-48.3	29.1	-2.4	ant. inferior frontal
	thickness	Positive	lh	.0002	129.57	-46	-38.9	25.8	parietal operculum
RNT	area	Negative	lh	.0002	319.49	-38.5	-7.4	-13.6	anterior insula
	volume	Positive	lh	.0001	198.2	-55.4	-9	-19.3	ant. middle temporal
	volume	Positive	rh	.0001	308.95	9.1	39.3	27.8	med. superior frontal
	thickness	Positive	rh	.0001	167.08	9.4	37.1	25.8	med. superior frontal

AA	area	Positive	lh	.0001	641.97	-39.8	27.9	20.4	inferior frontal sulcus
	area	Positive	lh	.0001	551.8	-15.3	-81.7	29.9	lateral occipital
	area	Negative	lh	.0002	789.85	-37.5	-12.2	-23.2	vent. inferior temporal
	area	Positive	rh	.0002	252.1	34	-20.1	49	central sulcus
	volume	Positive	lh	.0001	326.97	-36.9	24	21.7	inferior frontal sulcus
	volume	Negative	lh	.0001	407.39	-32.7	-4.1	-30.7	vent. inferior temporal
	volume	Positive	rh	.0001	355.82	35.9	-18.1	50.3	central sulcus
	volume	Negative	rh	.0002	136.92	37.5	-62.2	46.8	inferior parietal
	thickness	Negative	lh	.0002	375.61	-6.4	-63.3	47.5	precuneus
	thickness	Negative	rh	.0002	171.9	51.1	-35.8	42	supramarginal
LPA	area	Positive	rh	.0002	133.98	7.1	18.3	-12.5	medial orbitofrontal
AAp	thickness	Negative	rh	.0001	184.59	43.5	-34.3	14.9	parietal operculum
R	volume	Negative	lh	.0002	78.76	-4	-10.4	27.6	middle cingulate
	thickness	Positive	lh	.0001	291.23	-60.2	-26.5	27.7	supramarginal
	thickness	Positive	lh	.0002	162.26	-21.7	-93.7	-9.1	lateral occipital
	thickness	Positive	rh	.0001	242.11	26.1	-59.1	9.7	intracalcarine

Table 6. Adolescents exploratory whole brain analyses – controlling for sex. Results for exploratory whole brain analyses testing for vertex-wise associations between internalizing dimension factor scores and cortical volume, thickness, and area. All analyses controlled for sex, age, MRI scanner platform, and a whole brain morphometry measure. "X", "Y", "Z" are Talairach coordinates of the peak of given cluster. "Positive" direction means increased internalizing dimension factor scores was associated with increased gray matter morphometry measure. "Negative" direction means increased internalizing dimension factor scores was associated with decreased gray matter morphometry measure. "Max p" indicates the p-value of the peak voxel. lh= left hemisphere; rh= right hemisphere; ant.= anterior; med.= medial; vent.= ventral.

Negative affect (see figure 7) was significantly positively associated with volume (x= -43.7, y= -35.2, z= 24.6; cluster size= 372.08 mm^2), area (x= -42.4, y= -34.9, z= 23.4; cluster size= 510.4 mm^2), and thickness (x= -43.7, y= -35.2, z= 24.6; cluster size= 372.08 mm^2) of overlapping clusters in left parietal operculum, volume of a clusters in left parahippocampal gyrus (x= -26, y= -23, z= -22.3; cluster size= 124.64 mm^2), and thickness of a cluster in left anterior inferior frontal gyrus (x= -48.3, y= 29.1, z= -2.4; cluster size= 287.46 mm^2), as well as significantly negatively associated with volume of clusters in left frontal pole (x= -30.2, y= 43.4, z= 14.3; cluster size= 143.22 mm^2) and left ventral central sulcus (x= -59.8, y= -6.4, z= 10; cluster size= 132.92 mm^2) and area of a cluster in right postcentral gyrus (x= 52, y= -11.7, z= 33.4; cluster size= 92.68 mm^2).

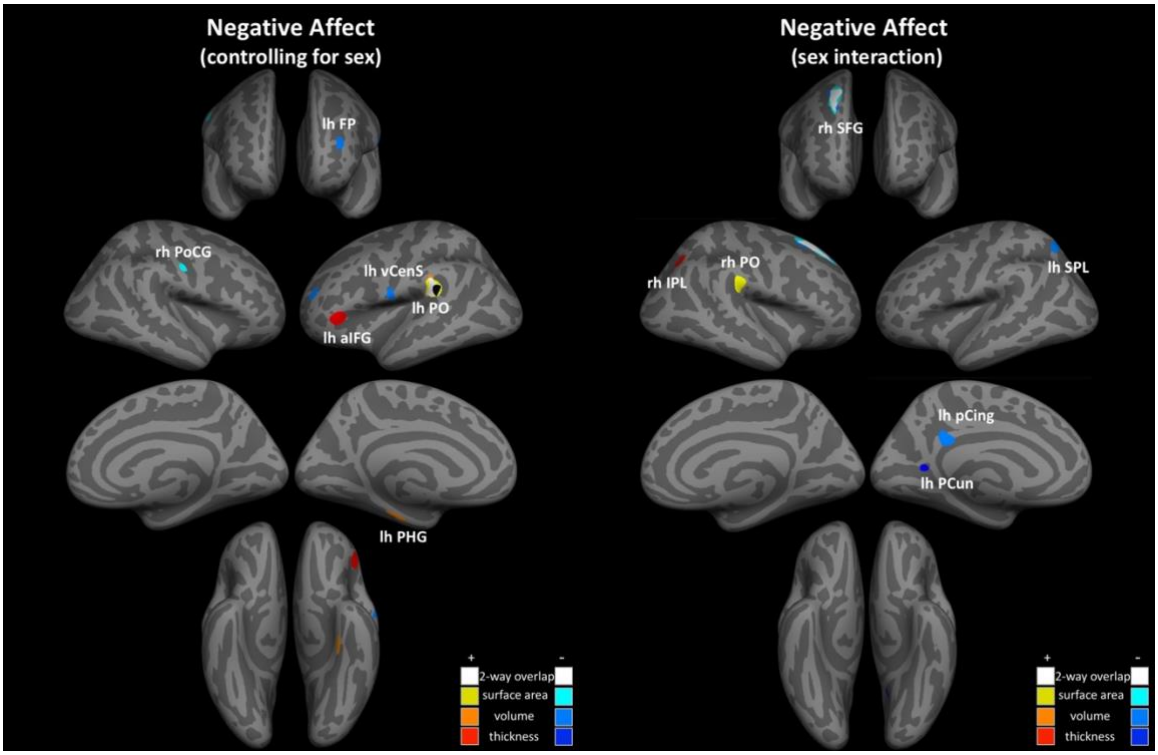

Figure 7. Adolescent whole brain results: Negative Affect. *Left panel:* results controlling for sex; *Right panel:* sex interactions on the relationship between factor scores and gray matter morphometry. Hot colors represent positive relationship between factor scores and gray matter morphometry. Cool colors represent negative relationship between factor scores and gray matter morphometry. White clusters indicate two distinct clusters are overlapping. Black clusters indicate three distinct clusters are overlapping. lh= left hemisphere; rh= right hemisphere; FP= frontal pole; vCenS= ventral central sulcus; PO= parietal operculum; aIFG= anterior inferior frontal gyrus; PHG= parahippocampal gyrus; PoCG= postcentral gyrus; SFG= superior frontal gyrus; IPL= inferior parietal lobe; SPL= superior parietal lobe; pCing= posterior cingulate; Pcun= precuneus

Repetitive negative thought (see figure 8) was positively associated with volume (x= 9.1, y= 39.3, z= 27.8; cluster size= 308.95 mm^2) and thickness of overlapping clusters in right medial superior frontal gyrus (x= 9.4, y= 37.1, z= 25.8; cluster size= 167.08 mm^2), as well as volume of a cluster in left anterior middle temporal gyrus (x= -55.4, y= -9, z= -19.3; cluster size= 198.2 mm^2), and negatively associated with volume of a cluster in left anterior insula (x= -38.5, y= -7.4, z= -13.6; cluster size= 319.49 mm^2).

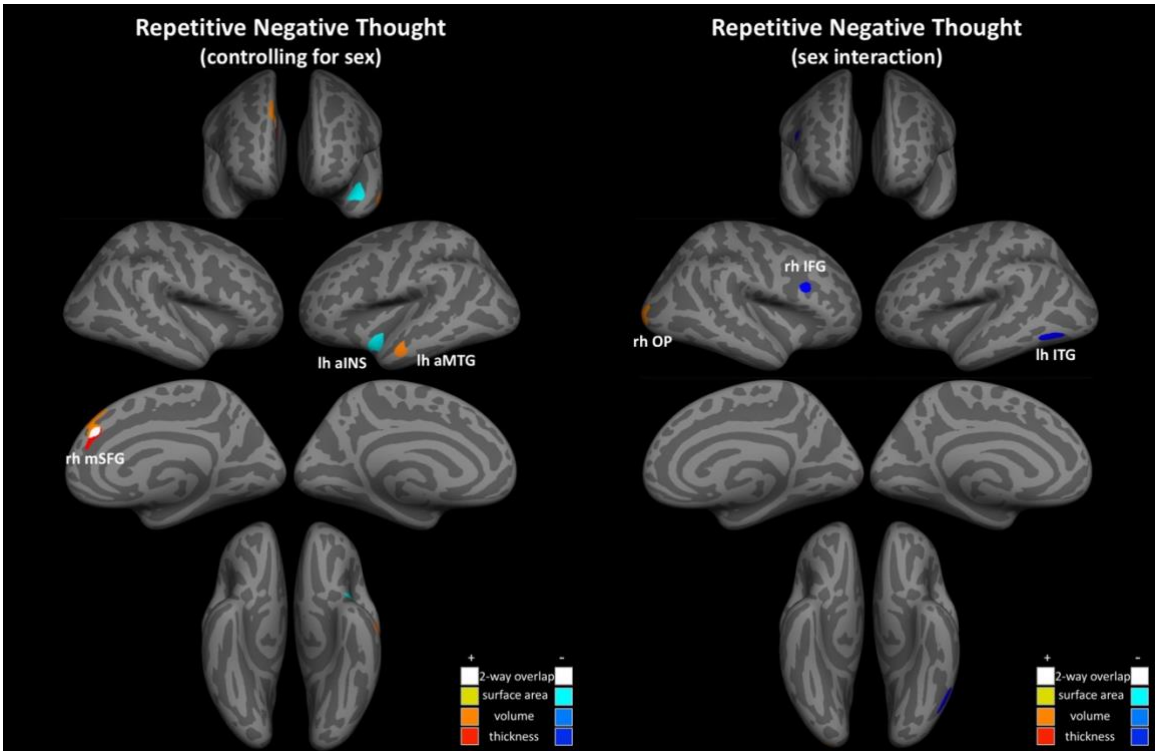

Figure 8. Adolescent whole brain results: Repetitive Negative Thought. *Left panel:* results controlling for sex; *Right panel:* sex interactions on the relationship between factor scores and gray matter morphometry. Hot colors represent positive relationship between factor scores and gray matter morphometry. Cool colors represent negative relationship between factor scores and gray matter morphometry. White clusters indicate two distinct clusters are overlapping. Black clusters indicate three distinct clusters are overlapping. lh= left hemisphere; rh= right hemisphere; aINS= anterior insula; aMTG= anterior middle temporal gyrus; mSFG= medial superior frontal gyrus; IFG; inferior frontal gyrus; OP= occipital pole; ITG= inferior temporal gyrus

Anxious arousal-specific (see figure 9) was negatively associated with area and volume of overlapping clusters in left ventral interior temporal gyrus (area: x= -37.5, y= -12.2, z= -23.2; cluster size= 789.85 mm^2; volume: x= -32.7, y= -4.1, z= -30.7; cluster size= 407.39 mm^2), volume of a cluster in right inferior parietal lobe (x= 37.5, y= -62.2, z= 46.8; cluster size= 136.92 mm^2), and thickness of clusters in left precuneus (x= -6.4, y= -63.3, z= 47.5; cluster size= 375.61mm^2) and right supramarginal gyrus (x= 51.1, y= -35.8, z= 42; cluster size= 171.9 mm^2) as well as positively associated with volume (x= -36.9, y= 24, z= 21.7; cluster size= 326.97 mm^2) and area (x= -39.8, y= 27.9, z= 20.4; cluster size= 641.97 mm^2) of overlapping clusters in left inferior frontal sulcus and right central sulcus (volume: x= 35.9, y= -18.1, z= 50.3; cluster

size= 355.82 mm2; area: x= 34, y= -20.1, z= 49; cluster size= 252.1 mm2), as well as area of a cluster in left lateral occipital cortex (x= -15.3, y= -81.7, z= 29.9; cluster size= 551.8 mm2).

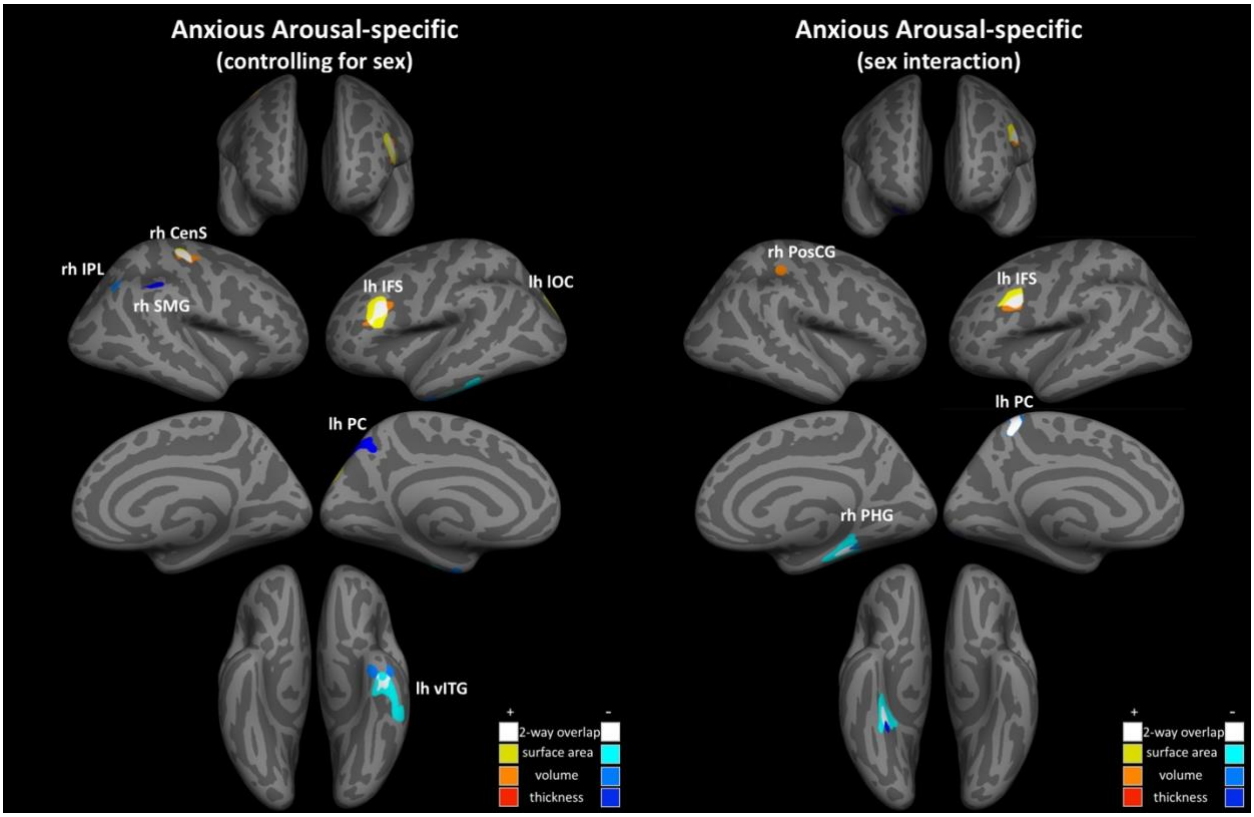

Figure 9. Adolescent whole brain results: Anxious Arousal-specific. *Left panel:* results controlling for sex; *Right panel:* sex interactions on the relationship between factor scores and gray matter morphometry. Hot colors represent positive relationship between factor scores and gray matter morphometry. Cool colors represent negative relationship between factor scores and gray matter morphometry. White clusters indicate two distinct clusters are overlapping. Black clusters indicate three distinct clusters are overlapping. lh= left hemisphere; rh= right hemisphere; lh IFS= left inferior frontal sulcus; lh lOC= left lateral occipital cortex; lh PC= left precuneus; lh vITG= left ventral inferior temporal gyrus; rh CenS= right central sulcus; rh IPL= right inferior parietal lobe; rh SMG= right supramarginal gyrus; rh PosCG= right post central gyrus; rh PHG= right parahippocampal gyrus.

Anxious apprehension-specific (see figure 10) was negatively associated with thickness of a cluster in right parietal operculum (x= 43.5, y= -34.3, z= 14.9; cluster size= 184.59 mm2).

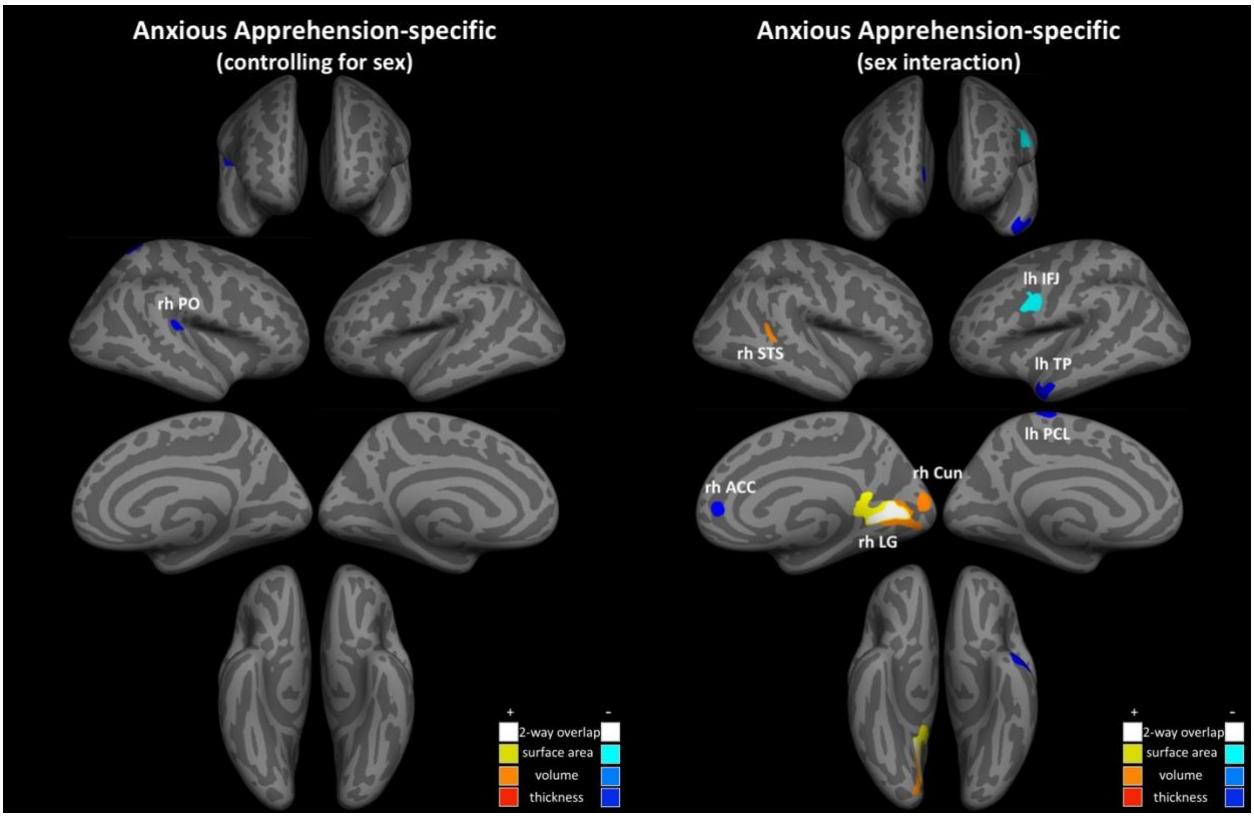

Figure 10. Adolescent whole brain results: Anxious Apprehension-specific. *Left panel:* results controlling for sex; *Right panel:* sex interactions on the relationship between factor scores and gray matter morphometry. Hot colors represent positive relationship between factor scores and gray matter morphometry. Cool colors represent negative relationship between factor scores and gray matter morphometry. White clusters indicate two distinct clusters are overlapping. Black clusters indicate three distinct clusters are overlapping. lh= left hemisphere; rh= right hemisphere; lh IFJ= left inferior frontal junction; lh TP= left temporal pole; lh PCL= left paracentral lobule; rh PO= right parietal operculum; rh STS= right superior temporal sulcus; rh ACC= right anterior cingulate cortex; rh LG= right lingual gyrus; rh Cun= right cuneus.

Low positive affect-specific (see figure 11) was positively associated with area of a cluster in right medial orbitofrontal cortex (x= 7.1, y= 18.3, z= -12.5; cluster size= 133.98 mm^2).

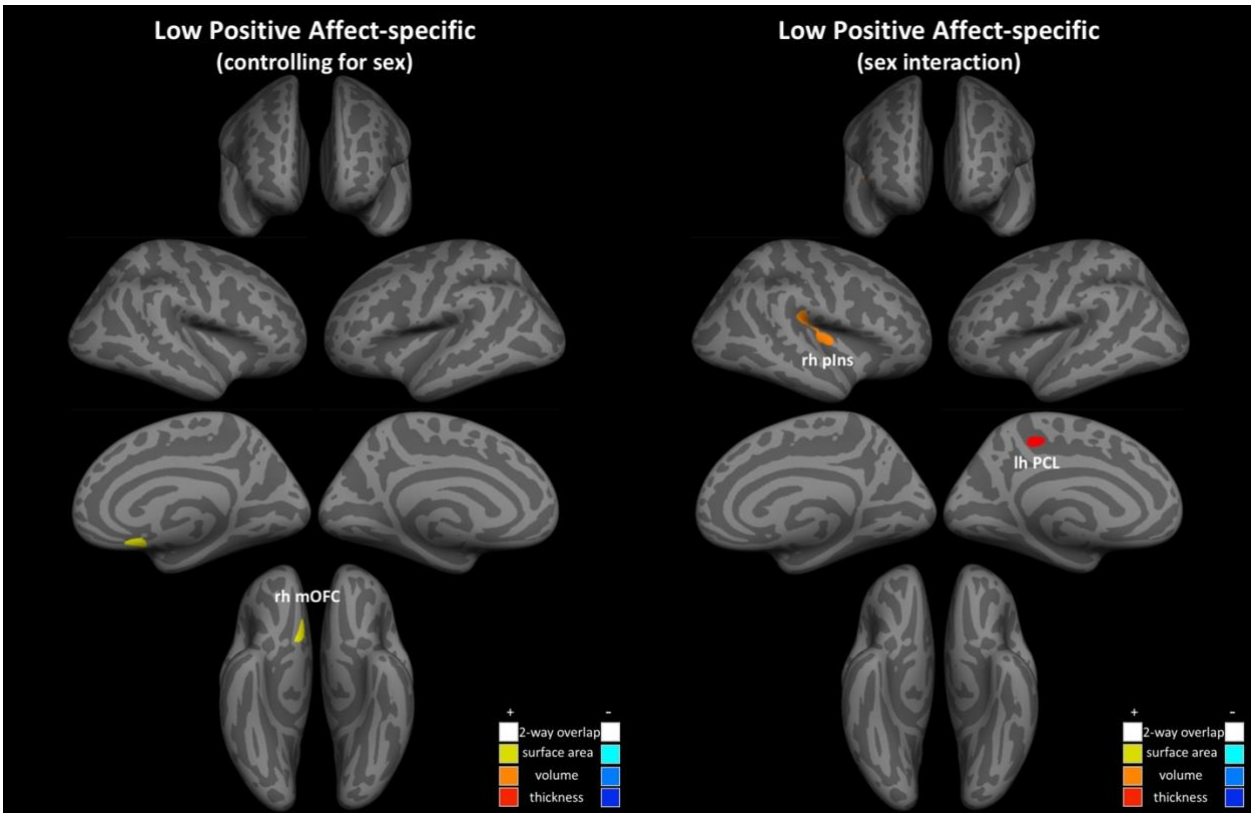

Figure 11. Adolescent whole brain results: Low Positive Affect-specific. *Left panel:* results controlling for sex; *Right panel:* sex interactions on the relationship between factor scores and gray matter morphometry. Hot colors represent positive relationship between factor scores and gray matter morphometry. Cool colors represent negative relationship between factor scores and gray matter morphometry. White clusters indicate two distinct clusters are overlapping. lh= left hemisphere; rh= right hemisphere; lh PCL= left paracentral lobule; rh mOFC= right medial orbitofrontal cortex.

Rumination-specific (see figure 12) was negatively associated with volume of a cluster in left middle cingulate (x= -4, y= -10.4, z= 27.6; cluster size= 78.76 mm^2) and positively associated with thickness of clusters in left supramarginal gyrus (x= -60.2, y= -26.5, z= 27.7; cluster size= 291.23 mm^2), left lateral occipital cortex (x= -21.7, y= -93.7, z= -9.1; cluster size= 162.26 mm^2), and right intracalcarine cortex (x= 26.1, y= -59.1, z= 9.7; cluster size= 242.11 mm^2).

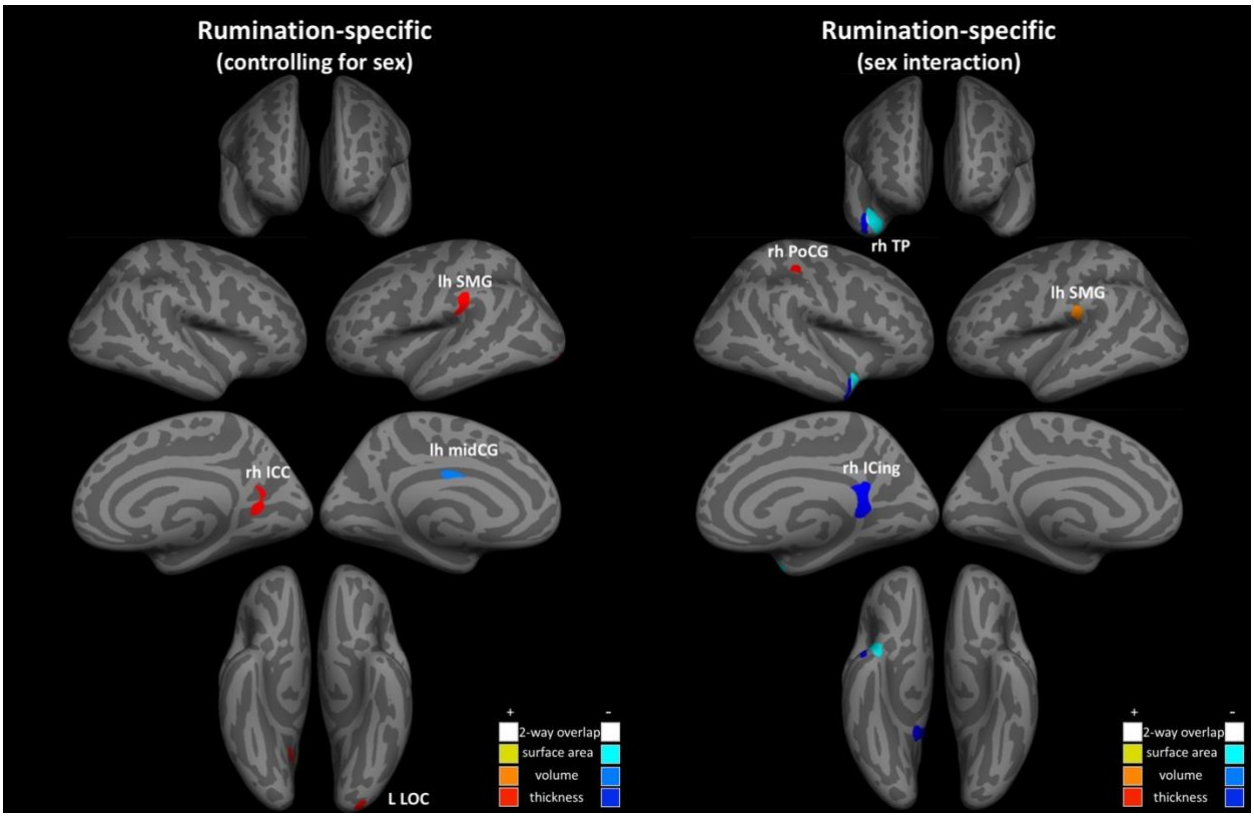

Figure 12. Adolescent whole brain results: Rumination-specific. *Left panel:* results controlling for sex; *Right panel:* sex interactions on the relationship between factor scores and gray matter morphometry. Hot colors represent positive relationship between factor scores and gray matter morphometry. Cool colors represent negative relationship between factor scores and gray matter morphometry. White clusters indicate two distinct clusters are overlapping. Black clusters indicate three distinct clusters are overlapping. lh= left hemisphere; rh= right hemisphere; lh SMG= left supramarginal gyrus; lh midCG= left mid cingulate; rh ICC= right intracalcarine cortex; rh PoCG= right postcentral gyrus; rh Icing= right isthmus cingulate.

4.3.1.2.1. Sex Interactions

In the following, we summarize significant results from the exploratory whole brain analyses testing for sex interactions on the relationships between internalizing factor scores and gray matter in adolescents. For full results, see table 7 and figures 7 to 12.

Dimension	Measure	Direction	Hemi	Max p	Cluster Size (mm^2)	X	Y	Z	Region
NA	area	♂= +^ ♀= -ns	rh	.0002	243.08	53.5	-24.4	26.6	parietal operculum
	area	♂= -^ ♀= +ns	rh	.0001	592.43	19.5	24.9	44.5	superior frontal gyrus
	volume	♂= -ns ♀=+^	lh	.0001	228.51	-17.7	-61.3	52.2	superior parietal
	volume	♂= -^ ♀= +ns	lh	.0002	151.57	-4.9	-40.8	30.6	posterior cingulate
	volume	♂= -^ ♀= + ns	rh	.0001	519.57	20.1	22.4	41.9	superior frontal gyrus
	thickness	♂= -* ♀= +ns	lh	.0002	77.25	-19.5	-54.3	9.8	precuneus
	thickness	♂= +^ ♀= - ^	rh	.0001	139.41	31.9	-61.1	36.4	inferior parietal
RNT	volume	♂= +^ ♀= -^	rh	.0001	643.95	22.5	-96	4.6	occipital pole
	thickness	♂= -* ♀= +^	lh	.0001	188.63	-49	-57.6	-4.6	inferior temporal gyrus
	thickness	♂= -* ♀= +^	rh	.0002	111.01	37.3	17	18.7	inferior frontal gyrus
AA	area	♂= +^ ♀= -ns	lh	.0002	395.62	-33.5	13.9	25.7	inferior frontal sulcus
	area	♂= -^ ♀= +ns	rh	.0001	625.06	32.4	-24.5	-17.8	parahippocampal gyrus
	volume	♂= +* ♀= -ns	lh	.0001	242.64	-33.8	14.7	22.4	inferior frontal sulcus
	volume	♂= -^ ♀= +ns	lh	.0002	348.93	-10.8	-45.3	61.9	precuneus
	volume	♂= +ns ♀= -ns	rh	.0001	152.61	36.3	-27.9	41.9	postcentral gyrus
	volume	♂= -^ ♀= +ns	rh	.0001	138.4	37.3	-33.3	-11.8	parahippocampal gyrus
LPA	volume	♂= +^ ♀= -^	rh	.0001	517.3	42.4	-27.7	21.7	posterior insula
	thickness	♂= +ns ♀= -*	lh	.0001	99.44	-18.2	-35.1	44.5	paracentral lobule
AAp	area	♂= -^ ♀= +ns	lh	.0001	342.29	-47.1	3.8	25.6	inferior frontal junction
	area	♂= +^ ♀= -ns	rh	.0002	1224.53	27	-61	4.6	lingual gyrus
	volume	♂= +^ ♀= -ns	rh	.0001	1324.73	19.3	-66.7	6.1	lingual gyrus
	volume	♂= +ns ♀= -ns	rh	.0002	393.86	4.9	-82.8	12.3	cuneus
	volume	♂= +ns ♀= -^	rh	.0002	163.01	45.4	-42.1	9	superior temporal sulcus
	thickness	♂= -^ ♀= +^	lh	.0001	587.51	-43.4	6.1	-29.6	temporal pole
	thickness	♂= -^ ♀= +ns	lh	.0002	198.07	-3.8	-26.8	64.2	paracentral lobule
	thickness	♂= -^ ♀= +ns	rh	.0002	87.64	15.2	40.6	1.7	anterior cingulate
R	area	♂= -^ ♀= +^	rh	.0001	481.55	40.3	9.2	-24.6	temporal pole
	volume	♂= +ns ♀= -ns	lh	.0001	170.58	-57.2	-24	19.5	supramarginal gyrus
	thickness	♂= +ns ♀= -*	rh	.0002	142.72	42.7	-26.6	49.9	postcentral gyrus
	thickness	♂= -^ ♀= +^	rh	.0001	359.96	10.2	-45.9	7	isthmus cingulate
	thickness	♂= -ns ♀= +*	rh	.0002	245.34	45.3	13.8	-21.5	temporal pole

Table 7. Adolescent exploratory whole brain analyses – sex interactions. Results for exploratory whole brain analyses testing for sex interactions of the vertex-wise associations between internalizing dimension factor scores

and cortical volume, thickness, and area. All analyses controlled for sex, age, MRI scanner platform, and a whole brain morphometry measure. "Direction" indicates results from post-hoc analyses testing for the relationship between a given internalizing dimension and ROI in both sexes, separately. "X", "Y", "Z" are Talairach coordinates of the peak of given cluster. "Max p" indicates the p-value of the peak voxel. ♂ = males; ♀ = females; += Positive relationship (increased internalizing dimension factor score associated with increased gray matter morphometry measures); - = Negative relationship (increased internalizing dimension factor score associated with decreased gray matter morphometry measure); *= effect is significant ($p<.05$); ^= effect is marginally significant ($p<.1$); ns = effect is non-significant ($p>.1$); lh= left hemisphere; rh= right hemisphere.

Sex interaction effects were found to significantly moderate the relationships between *negative affect* (see figure 7) and volume of clusters in left superior parietal (males: non-significant; females: marginal positive) and posterior cingulate (males: marginal negative; females: non-significant), volume and area of overlapping clusters in right superior frontal gyrus (males: marginal negative; females: non-significant), area of clusters in right parietal operculum, and thickness of clusters in left precuneus (males: significant negative; females: non-significant) and right inferior parietal lobe (males: marginal positive; females: marginal negative).

Sex interactions effects were found to significantly moderate the relationships between *repetitive negative thought* (see figure 8) and volume of a cluster in right occipital pole (males: marginal positive; females: marginal negative) and thickness of clusters in left inferior temporal gyrus (males: significant negative; females: marginal positive) and inferior frontal gyrus (males: marginal positive; females: marginal negative).

Sex interaction effects were found to significantly moderate the relationships between *anxious arousal-specific* (see figure 9) and volume (male: significant positive; female: non-significant) and area (male: marginal positive; female: non-significant) of overlapping clusters in left inferior frontal sulcus, volume and area of overlapping clusters in right parahippocampal gyrus (males: marginal negative; females: non-significant), and volume of clusters in left precuneus (male: marginal negative; female: non-significant), and right postcentral gyrus (male: non-significant positive; female: non-significant negative).

Sex interaction effects were found to significantly moderate the relationships between *anxious apprehension-specific* (see figure 10) and volume and area of overlapping clusters in right lingual gyrus (males: marginal positive; females: non-significant), volume of right superior temporal sulcus (males: non-significant; females: marginal negative) and cuneus (males: non-significant positive; females: non-significant negative), area of a cluster in left inferior frontal junction (males: marginal negative; females: non-significant), and thickness of clusters in left temporal pole (males: marginal negative; females: marginal positive), paracentral lobule (males: marginal negative; females: non-significant), and right anterior cingulate (males: marginal negative; females: non-significant).

Sex interaction effects were found to significantly moderate the relationships between *low positive affect-specific* (see figure 11) and volume of a cluster in right posterior insula (males: marginal positive; females: marginal negative) and thickness of a cluster in right paracentral lobule (males: non-significant; females: significant negative).

Sex interaction effects were found to significantly moderate the relationships between *rumination-specific* (see figure 12) and area (males: marginal negative; females: marginal positive) and thickness (males: non-significant; females significant positive) of overlapping clusters in the temporal pole, volume of a cluster in left supramarginal gyrus (males: non-significant positive; females: non-significant negative), and thickness of clusters in right isthmus cingulate (males: marginal negative; females: marginal positive).

4.3.2. Young Adults

4.3.2.1. Region of Interest Analyses

4.3.2.1.1. Controlling for Sex

Results from multiple regression analyses predicting volume, area, and thickness of a priori ROIs in young adults can be seen in Appendix 3 and figure 5. In the following, we summarize all relationships between ROI gray matter and the internalizing dimension factor scores that met an alpha threshold of p <.05 but focus the discussion only on results that passed the Bonferroni corrected alpha of p<.0083 or that were p<.05 but in line with our a priori predictions (see figure 5).

Results meeting our Bonferroni alpha level or a p<.05 in a priori ROIs included the following. *Negative affect* was associated with volume of the left (ß(SE)= -.060(.028), t-value= -2.110, p-value=.036) and right insula (ß(SE)= -.066(.028), t-value= -2.341, p-value=.020), as well as thickness of the left insula (ß(SE)= -.074(.032), t-value= -2.293, p-value=.023). Of these findings, post-hoc analyses revealed that the relationship between negative affect and right insula volume (ß(SE)= -.109(.087), t-value= -1.257, p-value=.210) and right caudal anterior cingulate thickness (ß(SE)= -.033(.117), t-value= -.283, p-value=.777) were not significantly different between young adults and adolescents.

Anxious apprehension-specific was negatively associated with thickness of the left insula (ß(SE)= -.100(.034), t-value=, -2.936, p-value= .004). Post-hoc analyses revealed that this relationships was marginally different between the adolescents and young adults (ß(SE)= -.123(.071), t-value= -1.723, p-value=.086).

Low positive affect-specific was negatively associated with area of the left lateral orbitofrontal cortex (ß(SE)= -.063(.026), t-value= -2.429, p-value= .016), area (ß(SE)= -

.064(.028), t-value= -2.254, p-value= .025) and volume (ß(SE)= -.066(.032), t-value= -2.069, p-value= .040) of right lateral orbitofrontal cortex, as well as area (ß(SE)= .065(.029), t-value= 2.236, p-value= .026) and thickness (ß(SE)= -.100(.038), t-value= -2.647, p-value= .009) of left rostral anterior cingulate, and volume of the left pars triangularis (ß(SE)= -.104(.038), t-value= -2.737, p-value= .007). Post-hoc analyses revealed the that relationships of low positive affect-specific with right lateral orbitofrontal cortex volume was significantly different between the two age groups (ß(SE)= -.158(.067), t-value= -2.345, p-value=.020), the relationships between low positive affect-specific and right lateral orbitofrontal area (ß(SE)= -.102(.061), t-value= -1.663, p-value=.097), left lateral orbitofrontal area (ß(SE)= -.100(.057), t-value= -1.753, p-value=.081), and left pars triangularis volume (ß(SE)= -.135(.081), t-value= -1.661, p-value=.098) were marginally different between the two age groups, and the relationship between low positive affect-specific and left rostral anterior cingulate area (ß(SE)= .099(.065), t-value= 1.526, p-value=.128) and thickness (ß(SE)= -.038(.081), t-value= -.472, p-value=.638) was not significantly different between the two age groups.

Rumination-specific was positively associated with area of right pars opercularis (ß(SE)= .094(.035), t-value= 2.669, p-value= .008). Post-hoc analyses revealed that this relationship was significantly different between the two age groups (ß(SE)= .221(.096), t-value= 2.305, p-value=.022).

Additionally, we observed the following relationships at an alpha level of $p<.05$: *negative affect* was negatively associated with volume of the right rostral middle frontal gyrus (ß(SE)= -.064(.031), t-value= -2.043, p-value= .042) and volume (ß(SE)= -.087(.036), t-value= -2.407, p-value= .017) and thickness (ß(SE)= -.063(.03), t-value= -2.126, p-value= .035) of the left pars opercularis.

Repetitive negative thought was negatively associated with volume of left pars opercularis (ß(SE)= -.089(.036), t-value= -2.407, p-value= .017), and thickness of left lateral orbitofrontal cortex (ß(SE)= .070(.035), t-value= 1.995, p-value= .047).

Anxious arousal-specific was negatively associated with volume of the right caudate (ß(SE)= -.060(.030), t-value= -2.009, p-value= .046).

Anxious apprehension-specific was positively associated with volume of the right pallidum (ß(SE)= .074(.034), t-value= 2.170, p-value= .031), negatively associated with volume of the left accumbens (ß(SE)= -.083(.037), t-value= -2.216, p-value= .028), and negatively associated with volume (ß(SE)= -.078(.030), t-value= -2.597, p-value= .010) and thickness (ß(SE)= -.081(.035), t-value= -2.302, p-value= .022) of the right insula, volume of the right medial orbitofrontal cortex (ß(SE)= -.072(.036), t-value= -1.991, p-value= .048), and thickness of left rostral middle frontal gyrus (ß(SE)= -.068(.030), t-value= -2.252, p-value= .025).

Low positive affect-specific was negatively associated with volume of right pars triangularis (ß(SE)= -.079(.038), t-value= -2.066, p-value= .040) and thickness of left caudal middle frontal gyrus (ß(SE)= -.07(.029), t-value= -2.384, p-value= .018).

Rumination-specific was positively associated with volume of right pars opercularis (ß(SE)= .082(.037), t-value= 2.193, p-value= .029) and area of the right caudal middle frontal gyrus (ß(SE)= .069(.032), t-value= 2.168, p-value= .031).

4.3.1.2.2. Sex Interactions

Results from multiple regression analyses testing for sex interaction effects on the relationship between gray matter of a priori ROIs and internalizing dimensions in young adults can be seen in table 8 and figure 5. In the following, we summarize all relationships between

ROI gray matter and the internalizing dimension factor scores that met an alpha threshold of p <.05 (as shown in table 8) but focus the discussion only on results that passed the Bonferroni corrected alpha of p<.0083 or that were p<.05 if they were the a priori predictions (see figure 5).

Dimension	ROI	Measure	Direction	Est.	SE	t-value	p-value
NA	rh amygdala	volume	♂= +ns ♀= -^	0.139	0.068	2.054	0.041
NA	lh caudate	volume	♂= +^ ♀= -ns	0.131	0.062	2.114	0.035
RNT	rh pars orbitalis	area	♂ = -* ♀ = +ns	-0.148	0.063	-2.342	0.020
RNT	rh pars opercularis	thickness	♂ = +* ♀ = -ns	0.133	0.065	2.047	0.042
RNT	rh lOFC	area	♂ = -^ ♀ = +ns	-0.123	0.056	-2.222	0.027
AA	lh insula	volume	♂= +ns ♀= -^	0.116	0.054	2.173	0.031
AA	rh pars orbitalis	area	♂= -* ♀= +ns	-0.127	0.062	-2.044	0.042
AA	lh mOFC	area	♂ = -ns ♀ = +*	-0.141	0.055	-2.569	0.011
AA*	**lh amygdala**	**volume**	**♂ = +ns ♀ = -***	**0.150**	**0.064**	**2.357**	**0.019**
AAp	rh lOFC	volume	♂ = -^ ♀ = +ns	-0.143	0.066	-2.169	0.031
AAp	lh lOFC	thickness	♂ = +ns ♀ = -*	0.154	0.071	2.164	0.031
LPA	**lh pars opercularis**	**thickness**	**♂ = +ns ♀ = -***	**0.166**	**0.059**	**2.826**	**0.005**
LPA	rh pars opercularis	thickness	♂ = +^ ♀ = -ns	0.137	0.064	2.147	0.033
LPA*	**lh rACC**	**thickness**	**♂= -* ♀= -ns**	**-0.158**	**0.077**	**-2.039**	**0.042**
LPA	lh cACC	area	♂ = -^ ♀ = +^	-0.135	0.057	-2.379	0.018
LPA	rh cACC	thickness	♂ = -* ♀ = +ns	-0.182	0.08	-2.277	0.024
R	rh pars triangularis	thickness	♂ = ♀ =	-0.135	0.067	-2.025	0.044
R	rh caudate	volume	♂ = +ns ♀= -ns	0.125	0.058	2.141	0.033
R	lh caudate	volume	♂ = +ns ♀= -ns	0.115	0.056	2.042	0.042

Table 8. Young adult ROI analyses – sex interactions. Significant (p<.05) results from multiple regression models testing for moderating effects of sex on the relationship between internalizing factor scores and ROI gray matter morphometry. All models controlled for sex, age, MRI scanner platform, and a whole brain morphometry measure, treating family as a random effect. Bold text indicates the results passed the Bonferroni correction threshold or was a result predicted a priori at a p<.05. "Direction" indicates results from post-hoc analyses testing for the relationship between a given internalizing dimension and ROI in both sexes, separately. "Est."= beta estimate of sex interaction effect; "SE"= standard error of beta estimate of sex interaction effect; NA= negative affect; RNT= repetitive negative thought; AA= anxious arousal-specific; LPA= low positive affect-specific; AAp= anxious apprehension-specific; R= rumination-specific; ♂ = males; ♀ = females; += Positive relationship (increased internalizing dimension factor score associated with increased gray matter morphometry measures); - = Negative

relationship (increased internalizing dimension factor score associated with decreased gray matter morphometry measure); *= effect is significant (p<.05); ^= effect is marginally significant (p<.1); ns = effect is non-significant (p>.1); lh= left hemisphere; rh= right hemisphere; lOFC= lateral orbitofrontal cortex; mOFC= medial orbitofrontal cortex; rACC= rostral anterior cingulate cortex; cACC= caudal anterior cingulate cortex.

Results meeting our Bonferroni corrected alpha level or a p<.05 for a prior predictions included a sex interaction effect on the relationship between *anxious arousal-specific* and volume of the left amygdala (ß(SE)= .150(.064), t-value= 2.357, p-value= .019; males= non-significant, females= negatively significant) and a sex interaction effect on the relationship between *low positive affect-specific* and thickness of the left pars opercularis (ß(SE)= .166(.059), t-value= 2.826, p-value= .005; males= non-significant, females= negatively significant) as well as low positive affect-specific and thickness of left rostral anterior cingulate (ß(SE)= -.158(.077), t-value= -2.039, p-value= .042; males= non-significant, females= negatively significant).

Additionally, we observed the following relationships at an alpha level of p<.05: *negative affect* showed sex interactions with volume of the right amygdala (ß(SE)= .139(.068), t-value= 2.054, p-value= .041) and left caudate (ß(SE)= .131(.062), t-value= 2.114, p-value= .035).

Repetitive negative thought showed sex interactions with area of right pars orbitalis (ß(SE)= -.148(.063), t-value= -2.342, p-value= .020), thickness of right pars opercularis (ß(SE)= .133(.065), t-value= 2.047, p-value= .042) and area of right lateral orbitofrontal cortex (ß(SE)= -.123(.056), t-value= -2.222, p-value= .027).

Anxious arousal-specific showed sex interactions with insula (ß(SE)= .116(.054), t-value= 2.173, p-value= .031), as well as area of the left medial orbitofrontal cortex (ß(SE)= -.141(.055), t-value= -2.569, p-value= .011) and right pars orbitalis (ß(SE)= -.127(.062), t-value= -2.044, p-value= .042).

Anxious apprehension-specific showed sex interactions in bilateral lateral orbitofrontal cortex, including volume of the right (ß(SE)= -.143(.066), t-value= -2.169, p-value= .031) and thickness of left (ß(SE)= .154(.071), t-value= 2.164, p-value= .031) lateral orbitofrontal cortex.

Low positive affect-specific showed sex interactions with thickness of the left (ß(SE)= .166(.059), t-value= 2.826, p-value= .005) and right pars opercularis (ß(SE)= .137(.064), t-value= 2.147, p-value= .033), thickness of the right (ß(SE)= -.182(.08), t-value= -2.277, p-value= .024) and area of the left (ß(SE)= -.135(.057), t-value= -2.379, p-value= .018) caudal anterior cingulate.

Rumination-specific showed sex interactions with volume of the left (ß(SE)= .115(.056), t-value= 2.042, p-value= .042) and right (ß(SE)= .125(.058), t-value= 2.141, p-value= .033) caudate, as well as thickness of right pars triangularis (ß(SE)= -.135(.067), t-value= -2.025, p-value= .044).

4.3.2.2. Exploratory Whole Brain Analyses

4.3.2.2.1. Controlling for Sex

In the following, we summarize significant results from the exploratory whole brain analyses controlling for sex in young adults. For a summary figure showing results from all dimensions overlaid on a single brain, see figure 6. For full results, see table 9 and figures 13 to 18.

Dimension	Measure	Direction	Hemi	Max p	Cluster Size (mm^2)	X	Y	Z	Region
NA	area	Negative	lh	.0002	835.25	-55.7	-48.3	28.4	temporoparietal junction
	volume	Negative	lh	.0001	604.18	-41.2	3.4	10.4	central operculum

	volume	Negative	rh	.0001	341.85	18.4	-19.4	61	precentral gyrus
	thickness	Negative	lh	.0001	306.84	-36.1	0.3	-5.3	insula
	thickness	Negative	lh	.0002	493.57	-42.5	7	16.7	inferior frontal sulcus
	thickness	Negative	lh	.0002	108.99	-6.6	6.6	-11	medial orbitofrontal
	thickness	Negative	rh	.0001	695.97	33.8	8.8	1.5	insula
	thickness	Negative	rh	.0001	375.81	33.7	0	40.8	precentral gyrus
	thickness	Negative	rh	.0002	324.95	41	-14.3	30.5	postcentral gyrus
	thickness	Negative	rh	.0002	136.43	44.3	26.7	13	inferior frontal gyrus
RNT	area	Negative	rh	.0002	417.31	5	-68.2	6.6	lingual gyrus
	volume	Positive	lh	.0002	87.98	-8.2	3	60.9	superior frontal gyrus
	volume	Negative	lh	.0001	986.34	-10.9	-57.4	1.1	lingual gyrus
	volume	Negative	rh	.0001	760.94	13.6	-49.1	-0.8	lingual gyrus
	volume	Negative	rh	.0001	604.79	17.5	-83	28	inferior parietal lobe
	volume	Negative	rh	.0001	177.73	7.1	-7.7	29.3	posterior cingulate
	thickness	Negative	lh	.0002	134.39	-9.4	6.2	51.4	med. sup. Frontal gyrus
	thickness	Negative	rh	.0002	218.34	15.1	-56	2.6	lingual gyrus
	thickness	Negative	rh	.0002	150.86	12.4	44	12.3	anterior cingulate
AA	area	Negative	lh	.0002	648.74	-19.4	-35.1	60	postcentral gyrus
	volume	Negative	lh	.0002	767.49	-32.3	-33.1	51.5	postcentral gyrus
	volume	Negative	lh	.0002	137.93	-42	12.6	-25.1	temporal pole
	volume	Negative	rh	.0002	136.93	42.5	-64	-1.2	lateral occipital cortex
	thickness	Negative	lh	.0001	303.16	-33.9	12.5	-3.2	anterior insula
	thickness	Negative	lh	.0001	150.9	-14.8	-28.9	45.6	paracentral lobule
	thickness	Negative	lh	.0001	131.29	-21.6	-70	9.8	calcarine fissure
	thickness	Negative	rh	.0001	194.21	42.4	5.8	19.2	inferior frontal junction
LPA	volume	Negative	rh	.0001	124.58	61.6	-13.1	-1.3	superior temporal gyrus
	thickness	Negative	lh	.0001	437.05	-45.4	16.2	20	po. Inferior frontal gyrus
	thickness	Negative	lh	.0001	311.01	-48.7	3.5	26.7	inferior frontal junction
AAp	area	Positive	lh	.0001	1225.16	-19.9	-81.4	-2.9	lingual gyrus
	area	Positive	lh	.0002	962.56	-7.8	-65.5	13.3	cuneus
	area	Positive	rh	.0002	2811.73	6.7	-82	2.7	medial occipital cortex
	volume	Positive	lh	.0001	603.15	-10.2	-86.1	-5.8	lingual gyrus
	volume	Positive	lh	.0001	83.28	-26.1	-10	-27.9	entorhinal cortex
	volume	Negative	lh	.0001	241.16	-34.4	-9.4	-7.6	ventral insula
	volume	Negative	lh	.0001	148.14	-5.5	-26.3	36.2	posterior cingulate
	volume	Negative	rh	.0001	379.77	35.8	5.5	0	insula
	thickness	Positive	lh	.0001	118.38	-24	-8.2	-28.1	entorhinal cortex
	thickness	Positive	rh	.0001	170.86	27.1	-4.8	-28.7	entorhinal cortex
	thickness	Negative	rh	.0002	194.08	36	13.1	-29.2	temporal pole
R	volume	Negative	rh	.0002	49.89	6	14.5	-8.1	subgenual cingulate
	thickness	Negative	lh	.0001	211.02	47.6	-36.6	9.6	superior temporal sulcus

Table 9. Young adult whole brain analyses – controlling for sex. Results for exploratory whole brain analyses testing for vertex-wise associations between internalizing dimension factor scores and cortical volume, thickness, and area. All analyses controlled for sex, age, MRI scanner platform, and a whole brain morphometry measure. "X", "Y", "Z" are Talairach coordinates of the peak of given cluster. "Positive" direction means increased internalizing dimension factor scores was associated with increased gray matter morphometry measure. "Negative" direction means increased internalizing dimension factor scores was associated with decreased gray matter morphometry measure. "Max p" indicates the p-value of the peak voxel. NA= negative affect; RNT= repetitive negative thought; AA= anxious arousal-specific; LPA= low positive affect-specific; AAp= anxious apprehension-specific; R= rumination-specific; lh= left hemisphere; rh= right hemisphere; med.= medial; sup.= superior; po.= posterior.

In young adults, when controlling for sex, *negative affect* (see figure 13) was significantly negatively associated with volume and thickness of overlapping clusters in left inferior frontal sulcus/central operculum (thickness: x= -42.5, y= 7, z= 16.7, cluster size= 493.57 mm^2; volume: x= -41.2, y= 3.4, z= 10.4, cluster size= 604.18 mm^2), volume of a cluster in right

precentral gyrus (x= 18.4, y= -19.4, z= 61, cluster size= 341.85 mm2), area of a cluster in left temporoparietal junction/supramarginal gyrus (x= -55.7, y= -48.3, z= 28.4, cluster size= 835.25 mm2), and thickness of clusters in left insula (x= -36.1, y= .3, z= -5.3, cluster size= 306.84 mm2), medial orbitofrontal cortex (x= -6.6, y= 6.6, z= -11, cluster size= 108.99 mm2), right insula (x= 33.8, y= 8.8, z= 1.5, cluster size= 695.97 mm2), precentral gyrus (x= 33.7, y= 0, z= 40.8, cluster size= 375.81 mm2), postcentral gyrus (x= 41, y= -14.3, z= 30.5, cluster size= 324.95 mm2) and inferior frontal gyrus (x= 44.3, y= 26.7, z= 13, cluster size= 136.43 mm2).

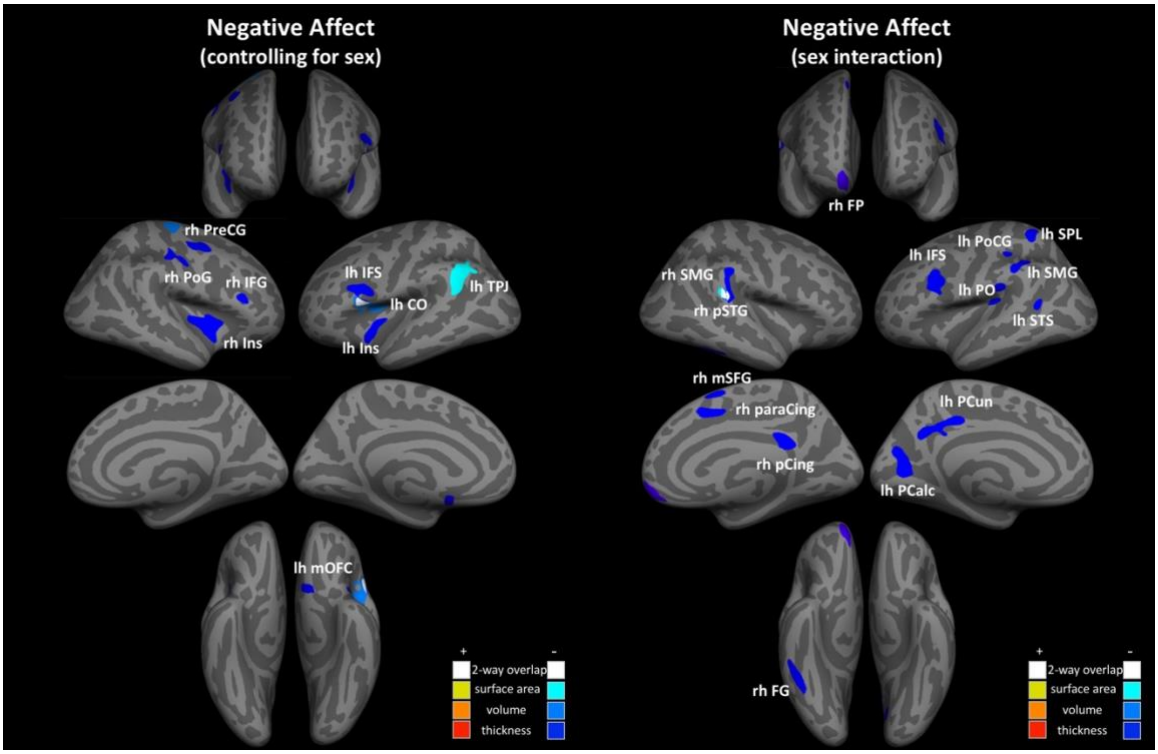

Figure 13. Young adult whole brain results: Negative Affect. *Left panel:* results controlling for sex; *Right panel:* sex interactions on the relationship between factor scores and gray matter morphometry. Hot colors represent positive relationship between factor scores and gray matter morphometry. Cool colors represent negative relationship between factor scores and gray matter morphometry. White clusters indicate two distinct clusters are overlapping. lh= left hemisphere; rh= right hemisphere; lh IFC= left inferior frontal sulcus; lh CO= left central operculum; lh Ins= left insula; lh TPJ= left temporoparietal junction; lh mOFC= left medial orbitofrontal cortex; lh PoCG= left postcentral gyrus; lh SPL= left superior parietal lobule; lh SMG= left supramarginal gyrus; lh PO= left parietal operculum; lh STS= left superior temporal sulcus; lh Pcun= left precuneus; lh Pcalc= left pericalcarine cortex; rh PreCG= right precentral gyrus; rh PoG= right postcentral gyrus; rh IFG= right inferior frontal gyrus; rh Ins= right insula; rh SMG= right supramarginal gyrus; rh pSTG= right posterior superior temporal gyrus; rh mSFG= right medial superior frontal gyrus; rh paraCing= right paracingulate gyrus; rh pCing= right posterior cingulate; rh FG= right fusiform gyrus.

Repetitive negative thought (see figure 14) was significantly negatively associated with volume (x= 13.6, y= -49.1, z= -.8, cluster size= 760.94 mm^2), area (x= 5, y= -68.2, z= 6.6, cluster size= 417.31 mm^2), and thickness (x= 15.1, y= -56, z= 2.6, cluster size= 218.34 mm^2) of overlapping clusters in right lingual gyrus, volume of a cluster in left lingual gyrus (x= -10.9, y= -57.4, z= 1.1, cluster size= 986.34 mm^2), volume of a cluster in right middle cingulate (x= 7.1, y= -7.7, z= 29.3, cluster size= 177.73 mm^2) and inferior parietal lobe (x= 17.5, y= -83, z= 28, cluster size= 604.79 mm^2), thickness of a cluster in left medial superior frontal gyrus (x= -9.4, y= 6.2, z= 51.4, cluster size= 134.39 mm^2), right anterior cingulate cortex/medial superior frontal gyrus (x= 12.4, y= 44, z= 12.3, cluster size= 150.86 mm^2), and positively associated with volume of a cluster in left medial superior frontal gyrus (x= -8.2, y= 3, z= 60.9, cluster size= 87.98 mm^2).

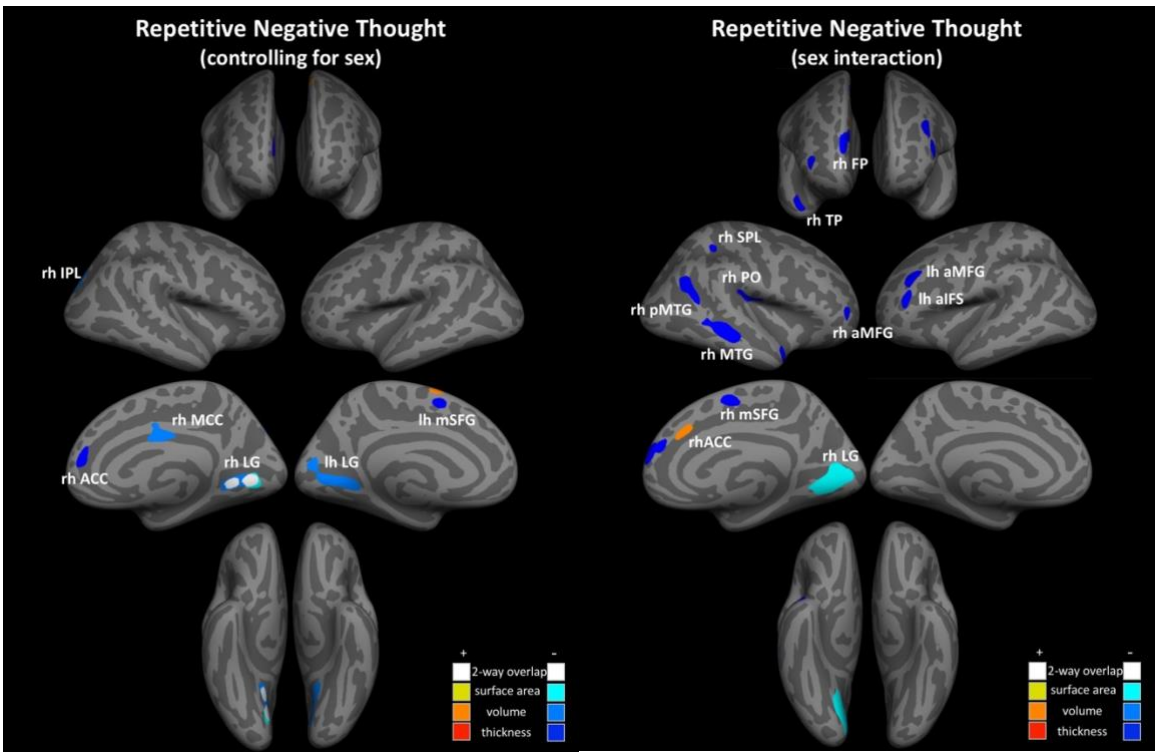

Figure 14. Young adult whole brain results: Repetitive Negative Thought. *Left panel:* results controlling for sex; *Right panel:* sex interactions on the relationship between factor scores and gray matter morphometry. Hot colors represent positive relationship between factor scores and gray matter morphometry. Cool colors represent negative relationship between factor scores and gray matter morphometry. White clusters indicate two distinct clusters are overlapping. lh= left hemisphere; rh= right hemisphere; lh mSFG= left medial superior frontal gyrus; lh LG= left lingual gyrus; lh aMFG= left anterior middle frontal gyrus; lh aIFS= left anterior inferior frontal sulcus; rh IPL= right inferior parietal lobule; rh MCC= right mid cingulate cortex; rh ACC= right anterior cingulate cortex; rh LG= right lingual gyrus; rh FP= right frontal pole; rh TP= right temporal pole; rh aMFG= right anterior middle frontal

gyrus; rh SPL= right superior parietal lobe; rh PO= right parietal operculum; rh pMTG= right posterior middle temporal gyrus; rh MTG= right middle temporal gyrus; rh mSFG= right medial superior frontal gyrus; rh LG= right lingual gyrus.

Anxious arousal-specific (see figure 15) was significantly negatively associated with volume (x= -32.3, y= -33.1, z= 51.5, cluster size= 767.49 mm^2) and area (x= -19.4, y= -35.1, z= 60, cluster size= 648.74 mm^2) of overlapping clusters in left postcentral gyrus, volume of a clusters in left temporal pole (x= -42, y= 12.6, z= -25.1, cluster size= 137.93 mm^2) and right lateral occipital cortex (x= 42.5, y= -64, z= -1.2, cluster size= 136.93 mm^2), and thickness of a clusters in left anterior insula (x= -33.9, y= 12.5, z= -3.2, cluster size= 303.16 mm^2), paracentral lobule (x= -14.8, y= -28.9, z= 45.6, cluster size= 150.9 mm^2), calcarine fissure (x= -21.6, y= -70, z= 9.8, cluster size= 131.29 mm^2), and right inferior frontal junction (x= 42.4, y= 5.8, z= 19.2, cluster size=194.21 mm^2).

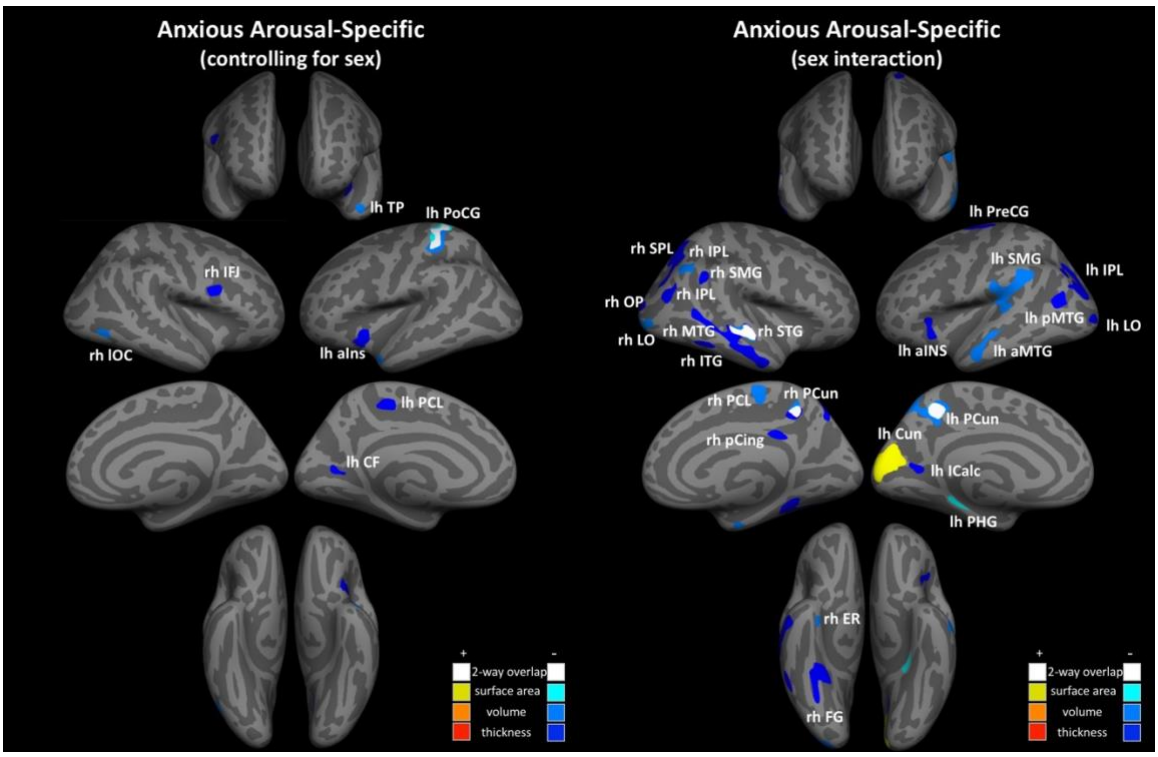

Figure 15. Young adult whole brain results: Anxious Arousal-specific. *Left panel:* results controlling for sex; *Right panel:* sex interactions on the relationship between factor scores and gray matter morphometry. Hot colors represent positive relationship between factor scores and gray matter morphometry. Cool colors represent negative relationship between factor scores and gray matter morphometry. White clusters indicate two distinct clusters are overlapping. Black clusters indicate three distinct clusters are overlapping. lh= left hemisphere; rh= right hemisphere; lh TP= left temporal pole; lh PoCG= left postcentral gyrus; lh aIns= left anterior insula; lh PCL= left

paracentral lobule; lh CF= left calcarine fissure; lh PreCG= left precentral gyrus; lh SMG= left supramarginal gyrus; lh IPL= left inferior parietal lobe; lh pMFG= left posterior middle temporal gyrus; lh LO= left lateral occipital cortex; lh aMTG= left anterior middle temporal gyrus; lh Pcun= left precuneus; lh Cun= left cuneus; lh Icalc= left intracalcarine cortex; lh PHG= left parahippocampal gyrus; rh IFJ= right inferior frontal junction; rh lOC= right lateral occipital cortex; rh SPL= right superior parietal lobe; rh IPL= right inferior parietal lobe; rh SMG= right supramarginal gyrus; rh IPL= right inferior parietal lobe; rh OP= right occipital pole; rh LO= right lateral occipital; rh MTG= right middle temporal gyrus; rh STG= right superior temporal gyrus; rh IGH= right inferior temporal gyrus; rh PCL= right paracentral lobule; rh Pcun= right preceuneus; rh pCing= right posterior cingulate; rh ER= right entorhinal cortex; rh FG= right fusiform gyrus

Anxious apprehension-specific (see figure 16) was significantly negatively associated with volume of clusters in left ventral insula (x= -34.4, y= -9.4, z= -7.6, cluster size= 241.16 mm^2), posterior cingulate (x= -5.5, y= -26.3, z= 36.2, cluster size= 148.14 mm^2), and right insula (x= 35.8, y= 5.5, z= 0, cluster size= 379.77 mm^2), and thickness of a cluster in right temporal pole (x= 36, y= 13.1, z= -29.2, cluster size= 194.08 mm^2), as well as significantly positively associated with volume (x= -10.2, y= -86.1, z= -5.8, cluster size= 603.15 mm^2) and area (x= -19.9, y= -81.4, z= -2.9, cluster size= 1225.16 mm^2) of overlapping clusters in left lingual gyrus, volume (x= -26.1, y= -10, z= -27.9, cluster size= 83.28 mm^2) and thickness (x= -24, y= -8.2, z= -28.1, cluster size= 118.38 mm^2) of overlapping clusters in left entorhinal cortex, area of clusters in left cuneus (x= -7.8, y= -65.5, z= 13.3, cluster size= 962.56 mm^2) and right medial occipital cortex (x= 6.7, y= -82, z= 2.7, cluster size= 2811.73 mm^2), and thickness of a cluster in right entorhinal cortex (x= 27.1, y= -4.8, z= -28.7, cluster size= 170.86 mm^2).

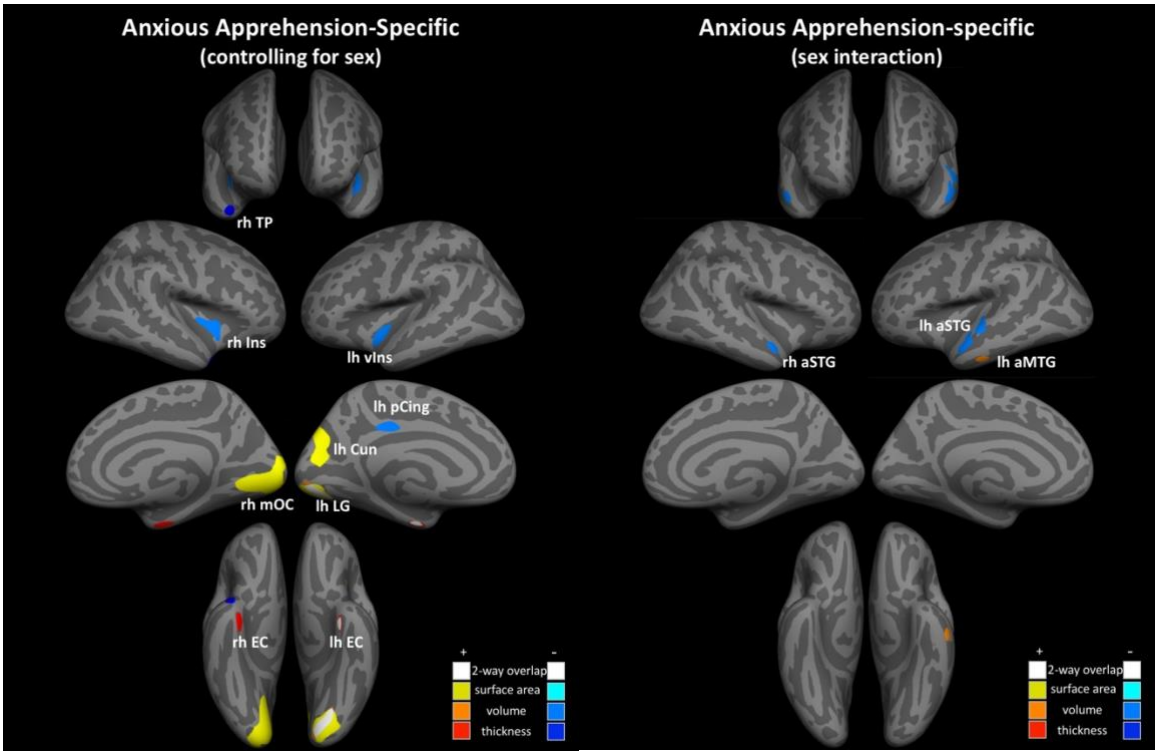

Figure 16. Young adult whole brain results: Anxious Apprehension-specific. *Left panel:* results controlling for sex; *Right panel:* sex interactions on the relationship between factor scores and gray matter morphometry. Hot colors represent positive relationship between factor scores and gray matter morphometry. Cool colors represent negative relationship between factor scores and gray matter morphometry. White clusters indicate two distinct clusters are overlapping. lh= left hemisphere; rh= right hemisphere; lh vIns= left ventral insula; lh pCing= left posterior cingulate; lh Cun= left cuneus; lh LG= left lingual gyrus; lh EC= left entorhinal cortex; lh aSTG= left anterior superior temporal gyrus; lh aMTG= left anterior middle temporal gyrus; rh TP= right temporal pole; rh Ins= right insula; rh mOC= right medial occipital cortex; rh EC= right entorhinal cortex; rh aSTG= right anterior superior temporal gyrus.

Low positive affect-specific (see figure 17) was significantly negatively associated with thickness of clusters in left inferior frontal junction (x= -48.7, y= 3.5, z= 26.7, cluster size= 311.01mm2) and posterior inferior frontal gyrus (x= -45.4, y= 16.2, z= 20, cluster size= 437.05 mm2), as well as volume of a cluster in right superior temporal gyrus (x= 61.6, y= -13.1, z= -1.3, cluster size= 124.58mm2).

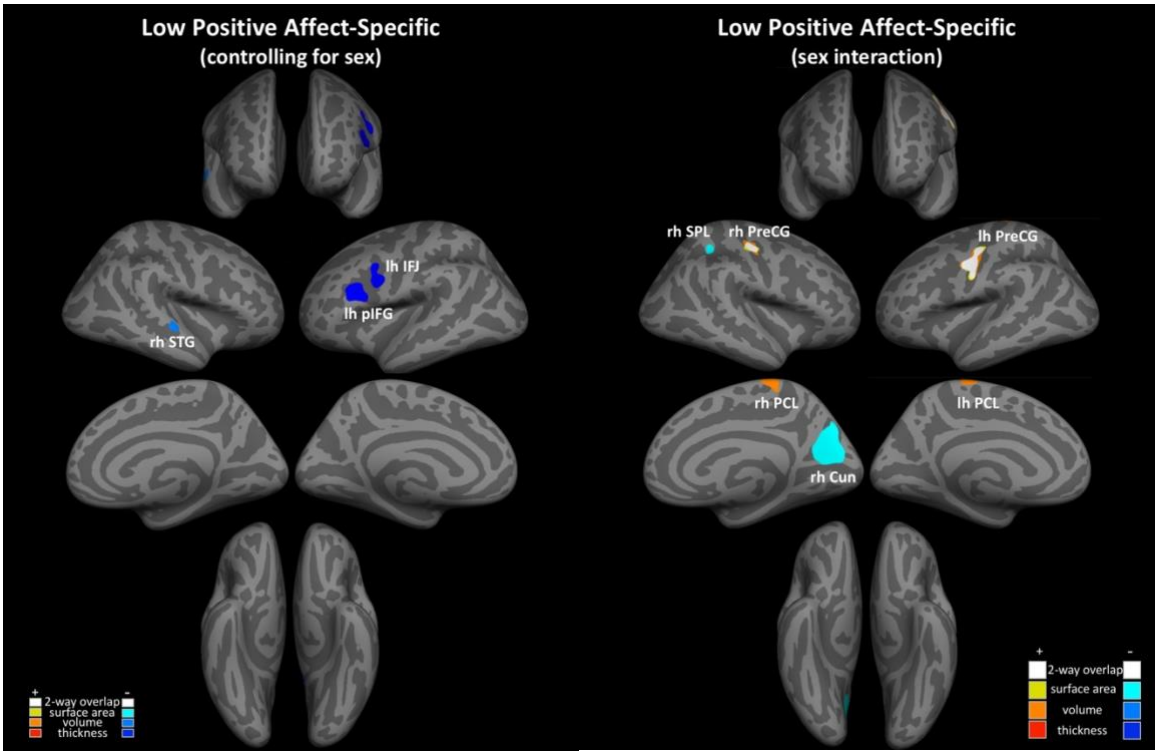

Figure 17. Young adult whole brain results: Low Positive Affect-specific. *Left panel:* results controlling for sex; *Right panel:* sex interactions on the relationship between factor scores and gray matter morphometry. Hot colors represent positive relationship between factor scores and gray matter morphometry. Cool colors represent negative relationship between factor scores and gray matter morphometry. White clusters indicate two distinct clusters are overlapping. lh= left hemisphere; rh= right hemisphere; lh IFJ= left inferior frontal junction; lh pIFG= left posterior inferior frontal gyrus; lh PreCG= left precentral gyrus; lh PCL= left paracentral lobule; rh STG= right superior temporal gyrus; rh PreCG= right precentral gyrus; rh SPL= right superior parietal lobe; rh PCL= right paracentral lobule; rh Cun= right cuneus.

Rumination-specific (see figure 18) was significantly negatively associated with volume of a cluster in right subgenual anterior cingulate cortex (x= 6, y= 14.5, z= -8.1, cluster size= 49.89 mm^2) and thickness of a cluster in right superior temporal sulcus (x= 47.6, y= -36.6, z= 9.6, cluster size= 211.02 mm^2).

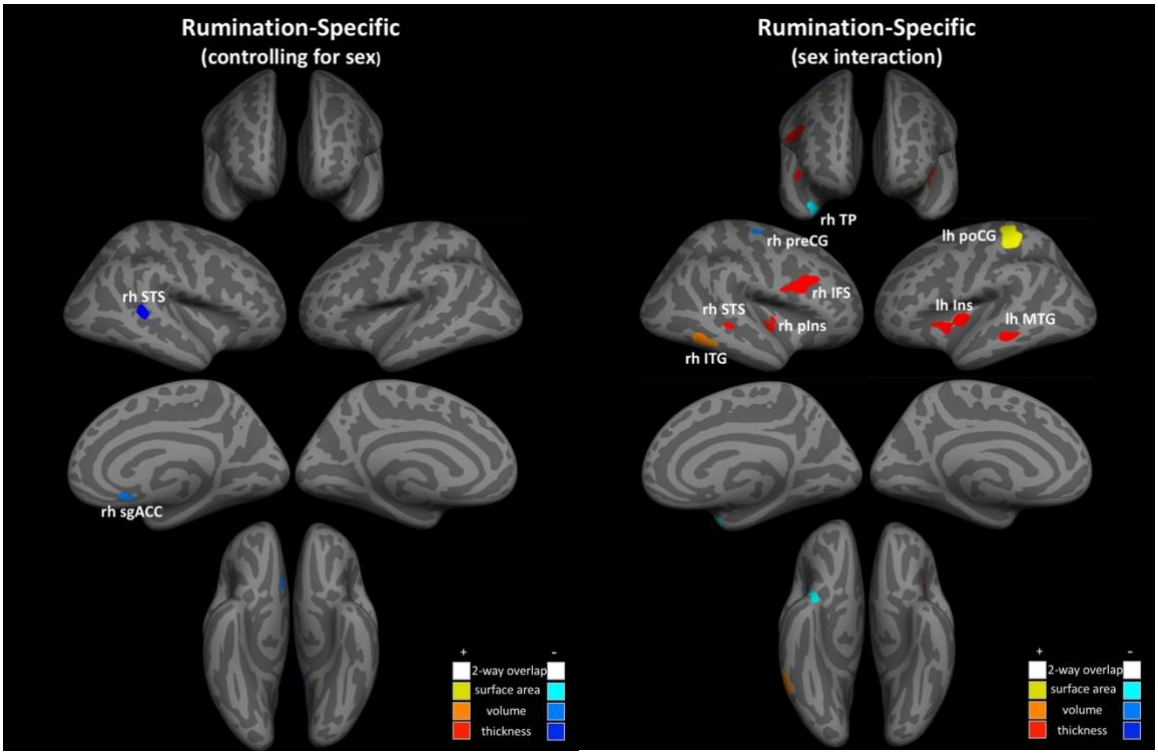

Figure 18. Young adult whole brain results: Rumination-specific. *Left panel:* results controlling for sex; *Right panel:* sex interactions on the relationship between factor scores and gray matter morphometry. Hot colors represent positive relationship between factor scores and gray matter morphometry. Cool colors represent negative relationship between factor scores and gray matter morphometry. White clusters indicate two distinct clusters are overlapping. lh= left hemisphere; rh= right hemisphere; lh poCG= left postcentral gyrus; lh Ins= left insula; lh MTG= left middle temporal gyrus; rh STS= right superior temporal sulcus; rh sgACC= right subgenual cingulate; rh TP= right temporal pole; rh preCG= right precentral gyrus; rh IFS= right inferior frontal sulcus; rh pIns= right posterior insula; rh STS= right superior temporal sulcus; rh ITG= right inferior temporal gyrus

4.3.2.2.2. Sex Interactions

In the following, we summarize significant results from the exploratory whole brain analyses testing for sex interactions on the relationships between internalizing factor scores and gray matter in young adults. For full results, see table 10 and figures 13 to 18.

Dimension	Measure	Direction	Max log(p)	Cluster Size	X	Y	Z	Region
NA	area	♂= -* ♀= +$_{ns}$	.0002	102.31	63.3	-36.1	16.7	rh supramarginal gyrus
	volume	♂= -* ♀= +$_{ns}$	.0001	130.58	63.3	-34	16	rh post. superior temporal
	thickness	♂= -* ♀= +*	.0001	646.93	-17.1	-71.3	5.7	lh pericalcarine cortex
	thickness	♂= -* ♀= +^	.0001	451.72	-11	-53.4	31	lh precuneus
	thickness	♂= -* ♀= +*	.0001	385.25	-35.4	15.7	27.3	lh inferior frontal sulcus
	thickness	♂= -* ♀= +*	.0001	351.65	-47.3	-41.1	41.2	lh supramarginal gyrus
	thickness	♂= -* ♀= +*	.0001	251.93	-30.5	-44.6	59.4	lh superior parietal lobe
	thickness	♂= -^ ♀= +*	.0001	166.71	-54.3	-27.5	17.9	lh parietal operculum

	thickness	♂= -* ♀= +*	.0002	130.18	-34.1	-30.5	20.4	lh parietal operculum
	thickness	♂= -* ♀= +*	.0002	97.18	-44.3	-48.5	10.5	lh superior temporal sulcus
	thickness	♂= -ns ♀= +*	.0002	77.93	-40	-26.6	39.8	lh postcentral gyrus
	thickness	♂= -* ♀= +ns	.0001	409.29	6.6	59.3	-11.5	rh frontal pole
	thickness	♂= -ns ♀= +*	.0001	194.04	5.2	-39.3	27	rh posterior cingulate
	thickness	♂= -* ♀= +*	.0001	183.71	10.4	12.7	40.8	rh paracingulate gyrus
	thickness	♂= -* ♀= +*	.0002	430.17	58.3	-32.4	15.1	rh supramarginal gyrus
	thickness	♂= -* ♀= +ns	.0002	262.75	41.6	-47.6	-8.6	rh fusiform gyrus
	thickness	♂= -^ ♀= +*	.0002	146.8	7.1	11.4	58.5	rh med. superior frontal
	area	♂= -* ♀= +*	.0001	1491.97	5	-68.2	6.6	rh lingual gyrus
	thickness	♂= -ns ♀= +*	.0001	270.41	-40	29.1	27.8	lh ant. middle frontal gyrus
	thickness	♂= -^ ♀= +*	.0001	180.63	-37.4	33.9	14.3	lh ant. inferior frontal sulcus
	thickness	♂= -* ♀= +*	.0001	652.96	57.9	-35.3	-4.3	rh middle temporal gyrus
	thickness	♂= -* ♀= +*	.0001	437.68	8.7	59.3	15.6	rh frontal pole
RNT	thickness	♂= -* ♀= +*	.0001	301.57	37.9	-21.2	20.1	rh parietal operculum
	thickness	♂= -* ♀= +*	.0001	169.68	8.5	3.1	52.3	rh med. superior frontal
	thickness	♂= -* ♀= +*	.0001	125.43	38.1	50.5	2.9	rh ant. middle frontal
	thickness	♂= -* ♀= +*	.0002	435.85	48	-60.2	26.6	rh pos. middle temporal
	thickness	♂= -* ♀= +*	.0002	193.83	43.9	13.9	-22.2	rh temporal pole
	thickness	♂= -* ♀= +*	.0002	96.6	31.2	-39.5	44.9	rh superior parietal lobe
	area	♂= +* ♀= -*	.0001	1490.01	-5	-76.1	20.1	lh cuneus
	area	♂= -* ♀= +*	.0002	219.32	-8.4	-44.5	46.8	lh precuneus
	area	♂= -^ ♀= +*	.0002	143.87	-21.8	-31.5	-9.4	lh parahippocampal gyrus
	volume	♂= -* ♀= +*	.0001	1411.1	-35.9	-33.8	18.2	lh supramarginal gyrus
	volume	♂= -* ♀= +*	.0001	732.04	-7.9	-44.6	48.7	lh precuneus
	volume	♂= -* ♀= +^	.0001	427.33	-55.5	-10	-18.7	lh ant. mid. Temporal gyrus
	volume	♂= -* ♀= +^	.0001	367.79	46.1	-22.1	-4	rh superior temporal gyrus
	volume	♂= -* ♀= +*	.0001	270.17	41.8	-59.5	40.7	rh inferior parietal lobe
	volume	♂= -* ♀= +*	.0001	70.43	25.1	-6.9	-28.3	rh entorhinal cortex
	volume	♂= -* ♀= +*	.0002	614.91	33.9	-86.9	0.9	rh lateral occipital cortex
	volume	♂= -* ♀= +ns	.0002	235.39	6	-19.9	60	rh paracentral lobule
	volume	♂= -* ♀= +^	.0002	167.37	7.1	-44.2	45	rh precuneus
	thickness	♂= -* ♀= +*	.0001	223.99	-27.6	20.5	-4.6	lh anterior insula
AA	thickness	♂= -* ♀= +*	.0002	1036.73	-35.1	-78.6	23.6	lh inferior parietal lobe
	thickness	♂= -* ♀= +*	.0002	248.89	-16.4	-6.3	57.9	lh precentral gyrus
	thickness	♂= -* ♀= +*	.0002	243.71	-25.6	-88.5	4.2	lh lateral occipital cortex
	thickness	♂= -* ♀= +*	.0002	211.76	-40.6	-63.5	15.1	lh inferior parietal lobe
	thickness	♂= -* ♀= +ns	.0002	193.95	-23.5	-62	10.8	lh intracalcarine
	thickness	♂= -* ♀= +*	.0001	1512.63	50.9	-14.3	-6.5	rh middle temporal gyrus
	thickness	♂= -* ♀= +*	.0001	1223.46	13.3	-65.4	52.5	rh superior parietal lobe
	thickness	♂= -* ♀= +*	.0001	532.82	34.7	-41.7	-11.1	rh fusiform gyrus
	thickness	♂= -ns ♀= +*	.0001	268.32	42.9	-70.8	20.8	rh inferior parietal lobe
	thickness	♂= -* ♀= +ns	.0001	203.35	6.4	-42.9	44.3	rh precuneus
	thickness	♂= -* ♀= +*	.0001	114.51	4.5	-34.4	28.7	rh posterior cingulate
	thickness	♂= -* ♀= +^	.0002	193.09	25	-90	16	rh occipital pole
	thickness	♂= -* ♀= +^	.0002	188.02	54.9	-48.3	30.8	rh supramarginal gyrus
	thickness	♂= -ns ♀= +*	.0002	183.01	54.8	-52.2	-12.6	rh inferior temporal gyrus
	volume	♂= +* ♀= -*	.0002	95.87	-51.8	-18.3	-20.3	lh ant. middle temporal
AAp	volume	♂= -* ♀= +^	.0001	314.3	-49.8	-1.8	-16.7	lh ant. superior temporal
	volume	♂= -* ♀= +*	.0002	251.86	-58.3	-12.8	-3	lh ant. superior temporal
	volume	♂= +* ♀= -*	.0002	175.34	52.5	0.7	-14.4	rh ant. superior temporal
	area	♂= +* ♀= -ns	.0002	520.75	-51.9	-4.6	35.7	lh precentral gyrus
	area	♂= +* ♀= -^	.0001	211.42	33.7	-18.7	39.9	rh central sulcus
	area	♂= -* ♀= +^	.0001	1580.63	14.3	-63.3	17.1	rh cuneus
LPA	volume	♂= +* ♀= -^	.0001	576.08	-51.9	-4.6	35.7	lh precentral gyrus
	volume	♂= +* ♀= -*	.0002	273.46	-6.2	-24.1	67.5	lh paracentral lobule
	volume	♂= +* ♀= -*	.0001	262.38	33.7	-18.7	39.9	rh precentral gyrus
	volume	♂= +* ♀= -ns	.0001	251.97	2.7	-30	64.4	rh paracentral lobule

R	area	♂= +* ♀= -ns	.0001	815.88	-32.3	-33.1	51.5	lh postcentral gyrus
	area	♂= -* ♀= +*	.0001	235.35	36.7	1	-20.8	rh temporal pole
	volume	♂= +* ♀= -^	.0002	357.44	55.7	-55	-7.4	rh inferior temporal gyrus
	thickness	♂= +* ♀= -*	.0001	227.54	-56.1	-31.1	-8.2	lh middle temporal gyrus
	thickness	♂= +* ♀= -*	.0002	424.97	-35.7	-12.9	0.8	lh insula
	thickness	♂= +* ♀= -*	.0001	502.87	38.5	11.1	19.8	rh inferior frontal sulcus
	thickness	♂= +* ♀= -ns	.0002	169.56	45.8	-17	-4.2	rh posterior insula
	thickness	♂= +ns ♀= -*	.0002	67.42	44.5	-33.4	-2.1	rh superior temporal sulcus

Table 10. Young adult whole brain analyses – sex interactions. Results for exploratory whole brain analyses testing for sex interactions of the vertex-wise associations between internalizing dimension factor scores and cortical volume, thickness, and area. All analyses controlled for sex, age, MRI scanner platform, and a whole brain morphometry measure. "Direction" indicates results from post-hoc analyses testing for the relationship between a given internalizing dimension and ROI in both sexes, separately. "X", "Y", "Z" are Talairach coordinates of the peak of given cluster. "Max p" indicates the p-value of the peak voxel. NA= negative affect; RNT= repetitive negative thought; AA= anxious arousal-specific; LPA= low positive affect-specific; AAp= anxious apprehension-specific; R= rumination-specific; ♂ = males; ♀ = females; += Positive relationship (increased internalizing dimension factor score associated with increased gray matter morphometry measures); - = Negative relationship (increased internalizing dimension factor score associated with decreased gray matter morphometry measure); *= effect is significant ($p<.05$); ^= effect is marginally significant ($p<.1$); ns = effect is non-significant ($p>.1$); lh= left hemisphere; rh= right hemisphere; post.= posterior; ant.= anterior; med.= medial.

In young adults, *negative affect* (see figure 13) showed significant sex interactions with volume (males: significant negative; females: non-significant), area (males: significant negative; females: non-significant), and thickness (males: significant negative; females: significant positive) of overlapping clusters in right supramarginal gyrus/posterior superior temporal gyrus, and thickness of clusters in left pericalcarine cortex (males: significant negative; females: significant positive), precuneus (males: significant negative; females: marginal positive), inferior frontal sulcus (males: significant negative; females: significant positive), superior parietal lobe (males: significant negative; females: significant positive), parietal operculum (cluster 1: males: marginal negative; females: significant positive; cluster 2: (males: significant negative; females: significant positive), superior temporal sulcus (males: significant negative; females: significant positive), postcentral gyrus (males: non-significant; females: significant positive), as well as right frontal pole (males: significant negative; females: non-significant), posterior cingulate (males: non-significant; females: significant positive), paracingulate gyrus (males: significant negative; females: significant positive), fusiform gyrus (males: significant negative; females:

non-significant), and medial superior frontal gyrus (males: marginal negative; females: significant positive).

Repetitive negative thought (see figure 14) showed significant sex interactions with area of a cluster in right lingual gyrus (males: significant negative; females: significant positive), and thickness of clusters in left anterior middle frontal gyrus (males: non-significant; females: significant positive), left inferior frontal sulcus (males: marginal negative; females: significant positive), right middle temporal gyrus (males: significant negative; females: significant positive), frontal pole (males: significant negative; females: significant positive), parietal operculum (males: significant negative; females: significant positive), medial superior frontal gyrus (males: significant negative; females: significant positive), anterior middle frontal gyrus (males: significant negative; females: significant positive), posterior middle temporal gyrus (males: significant negative; females: significant positive), temporal pole (males: significant negative; females: significant positive), and superior parietal lobe (males: significant negative; females: significant positive).

Anxious arousal-specific (see figure 15) showed significant sex interactions with volume (males: significant negative; females: significant positive) and area (males: significant negative; females: significant positive) over overlapping clusters in left precuneus, volume (males: significant negative; females: significant positive) and thickness (males: significant negative; females: non-significant) of overlapping clusters in right precuneus, volume of clusters in left supramarginal gyrus (males: significant negative; females: significant positive), anterior middle temporal gyrus (males: significant negative; females: marginal positive), right superior temporal gyrus (males: significant negative; females: marginal positive), inferior parietal lobe (males: significant negative; females: significant positive), entorhinal cortex (males: significant negative;

females: significant positive), lateral occipital cortex (males: significant negative; females: significant positive), paracentral lobule (males: significant negative; females: non-significant) and thickness of clusters in left anterior insula (males: significant negative; females: significant positive), inferior parietal lobe (males: significant negative; females: significant positive), intracalcarine cortex (males: significant negative; females: non-significant), and right middle temporal gyrus (males: significant negative; females: significant positive), superior parietal lobe (males: significant negative; females: significant positive), fusiform gyrus (males: significant negative; females: significant positive), inferior parietal lobe (males: non-significant; females: significant positive), precuneus (males: significant negative; females: non-significant), posterior cingulate (males: significant negative; females: significant positive), occipital pole (males: significant negative; females: marginal positive), supramarginal gyrus (males: significant negative; females: marginal positive), and inferior temporal gyrus (males: non-significant; females: significant positive).

Anxious apprehension-specific (see figure 16) showed significant sex interactions with volume of the left anterior middle temporal gyrus (males: significant positive; females= significant negative), two clusters in left anterior superior temporal gyrus (cluster 1: males: significant negative; females: marginal positive) (cluster 2: males: significant negative; females: marginal positive), and right anterior superior temporal lobe (males: significant positive; females: significant negative).

Low positive affect-specific (see figure 17) showed significant sex interactions with volume of clusters in left precentral gyrus (males: significant positive; females: marginal negative), left paracentral lobule (males: significant positive; females: significant negative), right precentral gyrus (males: significant positive; females: significant negative) and right paracentral

lobule (males: significant positive; females: non-significant), as well as area of clusters in left precentral gyrus (males: significant positive; females: non-significant), right central sulcus (males: significant positive; females: marginal negative), and right cuneus (males: significant negative; females: marginal positive).

Rumination-specific (see figure 18) showed significant sex interactions with volume of a cluster in right inferior temporal gyrus (males: significant positive; females marginal negative), area of clusters in left postcentral gyrus (males: significant positive; females: non-significant) and right temporal pole (males: significant negative; females: significant positive), and thickness of clusters in left middle temporal gyrus (males: significant positive; females: significant negative), left insula (males: significant positive; females: significant negative), right inferior frontal sulcus (males: significant positive; females: significant negative), right posterior insula (males: significant positive; females: non-significant), and right superior temporal sulcus (males: non-significant; females: significant negative).

4.3.3. Adolescents and young adults

4.3.3.1. Age group differences in a priori ROIs

For our a priori predictions (see figure 4 panels B to G), we carried out age moderation analyses to test whether the relationship between gray matter of these ROIs and the internalizing dimensions were significantly different between adolescents and young adults (see table 11 and figure 19).

Dimension	ROI	Measure	Direction	Est.	SE	t-value	p-value
NA	**lh insula**	**thickness**	**Adol= +$_{ns}$ YA= -$_{*}$**	**-0.254**	**0.093**	**-2.738**	**.007**
RNT	**rh rMFG**	**volume**	**Adol= +$_{ns}$ YA= -$_{ns}$**	**-0.134**	**0.067**	**-1.973**	**.049**
AAp	**lh pars triangularis**	**thickness**	**Adol= +$_{ns}$ YA= -$_{ns}$**	**-0.149**	**0.073**	**-2.034**	**.043**

Table 11. Differences between adolescents and young in adults in a priori ROI predictions. Results of ROI analyses testing for age group interactions for our a priori predictions. Bold text indicates the results passed the Bonferroni correction threshold or was a result predicted a priori at a p<.05. "Est."= beta estimate of age group interaction effect; "SE"= standard error of beta estimate of age group interaction effect; "Direction"= summary of effects in adolescents (Adol) and young adults (YA); NA= negative affect; RNT= repetitive negative thought; Asap= anxious apprehension-specific; lh= left hemisphere; rh= right hemisphere; cMFG= caudal middle frontal gyrus; rMFG= rostral middle frontal gyrus; += positive associations between internalizing dimension factor scores and gray matter; -= negative association between internalizing dimension factor scores and gray matter; ns= non-significant effect; *= significant effect.

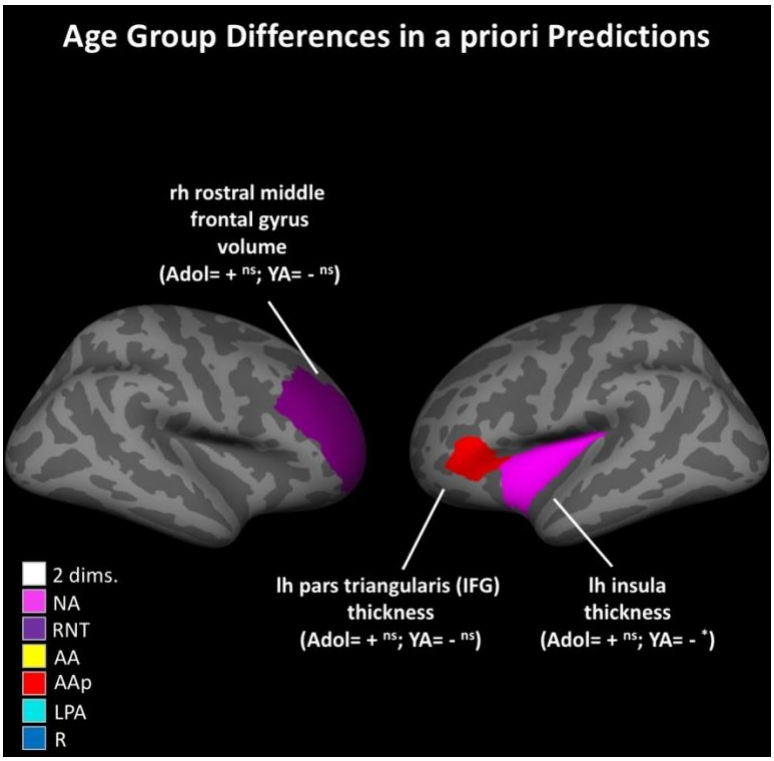

Figure 19. Adolescent and young adult differences from a *priori* ROI analyses. Results from analyses testing for age group interactions in our a priori ROI predictions. ROI's shown had a significant (p<.05) or marginally significant (p<.1) age group interaction effect on the relationship between the internalizing dimension (indicated by color of ROI) and gray matter of that ROI (specific ROI and gray matter measure indicated in white text). In parentheses, we show the direction and significance of these effects broken out by age group while controlling for sex. No significant or marginally significant effects were observed for anxious arousal-specific, low positive affect-specific, or rumination-specific. Lh= left hemisphere; rh= right hemisphere; IFG= inferior frontal gyrus; NA= negative affect; RNT= repetitive negative thought; AA= anxious arousal-specific; LPA= low positive affect-specific; Aap= anxious apprehension-specific; R= rumination-specific; Adol= effect in adolescents only; YA= effect in young adults only; += positive association between internalizing dimension and gray matter; -= negative association between internalizing dimension and gray matter; ns= non-significant; *= significant.

These analyses revealed that the following a priori predicted relationships were significantly different between the two age groups: *negative affect* and thickness of left insula was significantly different between adolescents and young adults (ß(SE)= -.254(.093), t-value= -2.738, p-value= .007; adolescents: non-significant, young adults: significantly negative), *repetitive negative thought* and volume of the right rostral middle frontal gyrus (ß(SE)= -.134(.067), t-value= -1.973, p-value= .049; adolescents: non-significant positive, young adults: non-significant negative), and *anxious apprehension-specific* and thickness of left pars triangularis (ß(SE)= -.149(.073), t-value= -2.034, p-value= .043; adolescents: non-significant positive, young adults: non-significant negative). These analyses also revealed a marginally significant difference between the age groups in the relationships between *negative affect* and left insula volume (ß(SE)= -.151(.088), t-value= -1.720, p-value=.086) as well as *repetitive negative thought* and thickness of left caudal middle frontal gyrus (ß(SE)= -.150(.085), t-value= -1.761, p-value= .079; adolescents: non-significant positive, young adults: non-significant negative).

4.3.3.2. Age group differences in whole brain analyses

In the following, we summarize significant results from the exploratory whole brain analyses testing for age group interactions between adolescent and young adults on the relationship between internalizing factor scores and gray matter. For a summary figure showing results for all dimensions overlaid on a single brain, see figure 20. For full results, see table 12 and figures 21 to 26).

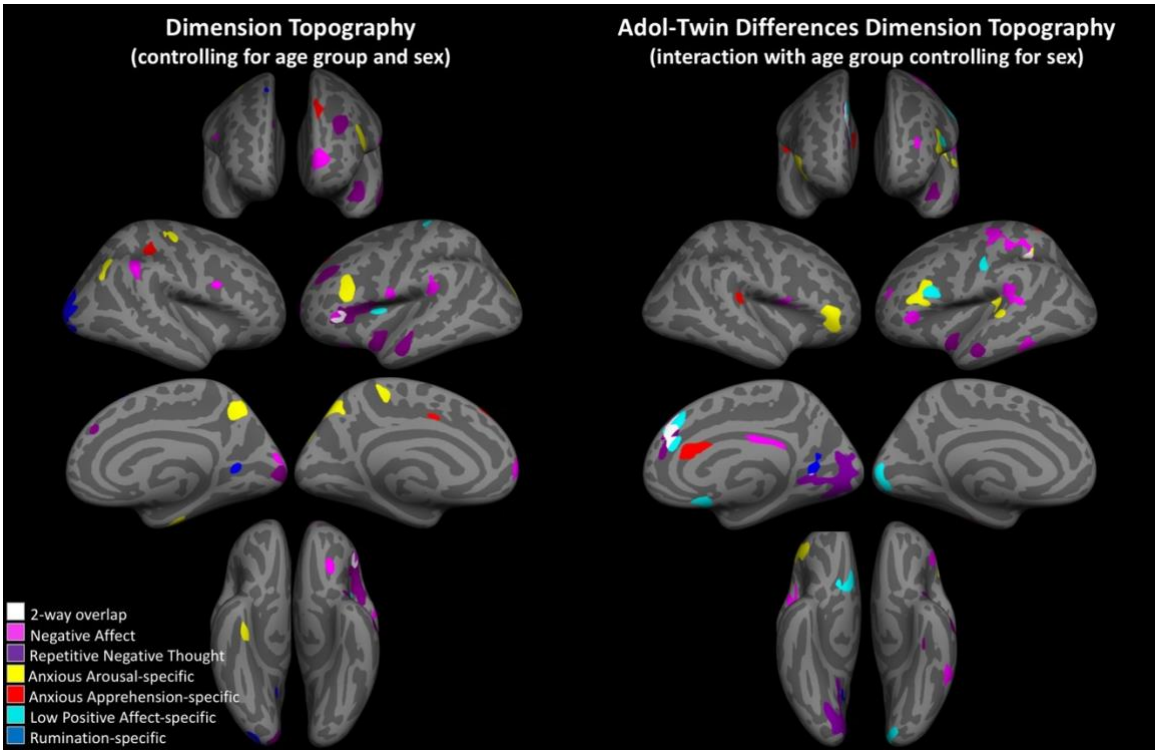

Figure 20. Whole brain dimensional topography across and between young adult and adolescents. *Left panel:* dimensional topography results controlling for sex and age group; *Right panel:* dimensional topography of age group interactions on the relationship between factor scores and gray matter morphometry controlling for sex. White clusters indicate two distinct clusters are overlapping. lh= left hemisphere; rh= right hemisphere.

Dimension	Measure	Direction	Hemi	Max p-value	Cluster Size (mm^2)	X	Y	Z	Region
NA	area	Adol= $+_{ns}$ YA= $-_{ns}$	lh	.0002	355.15	-27.5	-22.9	46.8	central sulcus
	volume	Adol= $+_{*}$ YA= $-_{ns}$	lh	.0002	486.3	-44.2	-36.3	24.9	parietal operculum
	volume	Adol= $+_{ns}$ YA= $-_{ns}$	lh	.0002	338.62	-28.2	-26.7	48.1	central sulcus
	volume	Adol= $-_{ns}$ YA= $+_{ns}$	lh	.0002	105.88	-29.4	45	12.5	frontal pole
	volume	Adol= $+_{ns}$ YA= $-_{ns}$	rh	.0001	353.69	50.3	4.3	2.9	central operculum
	volume	Adol= $-_{ns}$ YA= $+_{ns}$	rh	.0002	170.8	4.4	-35.9	23.8	posterior cingulate
	thickness	Adol= $+_{*}$ YA= $-_{ns}$	lh	.0001	257.49	-48.3	29.1	-2.4	ant. inferior front
	thickness	Adol= $+_{ns}$ YA= $-_{ns}$	lh	.0002	634.59	-36.5	-42.7	33.8	superior parietal
	thickness	Adol= $+_{ns}$ YA= $-_{ns}$	lh	.0002	306.98	-54	-49.1	-14.7	inferior temporal
	thickness	Adol= $+_{*}$ YA= $-_{ns}$	lh	.0002	162.12	-44.8	-37.4	25.1	parietal operculum
RNT	area	Adol= $-_{*}$ YA= $+_{ns}$	lh	.0001	271.2	-37.1	-5.5	-11.6	vent. insula
	volume	Adol= $+_{*}$ YA= $-_{ns}$	lh	.0002	236.24	-52.7	-10.6	-18.4	middle temporal
	volume	Adol= $+_{ns}$ YA= $-_{ns}$	rh	.0001	2210.32	15.6	-82.2	8.9	medial occipital
	volume	Adol= $+_{*}$ YA= $-_{ns}$	rh	.0001	292.51	9.1	37	27.8	med. superior frontal
	thickness	Adol= $+_{ns}$ YA= $-_{ns}$	lh	.0002	58.01	-37.9	-20.7	-18.2	fusiform gyrus
	thickness	Adol= $+_{*}$ YA= $-_{ns}$	rh	.0001	273.12	11.9	42.2	17	med. superior frontal
	thickness	Adol= $-_{ns}$ YA= $+_{ns}$	rh	.0002	185.57	5.2	-26.5	66.7	precentral gyrus
AA	area	Adol= $+_{ns}$ YA= $-_{ns}$	rh	.0002	699.38	46.7	34.6	-10.6	ant. inferior frontal
	volume	Adol= $+_{*}$ YA= $-_{ns}$	lh	.0001	512.11	-37.3	29	12.6	inferior frontal sulcus
	volume	Adol= $+_{ns}$ YA= $-_{ns}$	lh	.0002	139.78	-35.7	-32.5	12.2	planum temporale
	volume	Adol= $+_{ns}$ YA= $-_{ns}$	rh	.0001	242.88	49.6	32.9	0	ant. inferior frontal
	thickness	Adol= $+_{ns}$ YA= $-_{ns}$	lh	.0001	167.25	-33.5	-41.5	35.4	superior parietal
	thickness	Adol= $+_{ns}$ YA= $-_{ns}$	lh	.0001	134.81	-61	-25.5	6	superior temporal
AAp	volume	Adol= $+_{ns}$ YA= $-_{ns}$	lh	.0002	76.9	-19.9	-49.8	57.3	superior parietal

	thickness	Adol= $+_{ns}$ YA= $-_{ns}$	rh	.0001	238.56	7.2	28	16.1	anterior cingulate
	thickness	Adol= $+_{ns}$ YA= $-_{ns}$	rh	.0001	180.28	45.2	-33.2	13.3	parietal operculum
LPA	area	Adol= $+_{*}$ YA= $-_{ns}$	rh	.0001	229.72	7	16.4	-11.8	medial orbitofrontal
	area	Adol= $+_{*}$ YA= $-_{ns}$	rh	.0001	536.42	6.8	39.3	40.5	med. superior frontal
	thickness	Adol= $+_{ns}$ YA= $-_{ns}$	lh	.0002	250.89	-44.2	15.8	20.1	pos. inferior frontal
	thickness	Adol= $-_{ns}$ YA= $+_{ns}$	lh	.0001	600.75	-13.3	-88.2	7.9	pericalcarine
	thickness	Adol= $-_{ns}$ YA= $+_{ns}$	lh	.0001	206.9	-49.2	-16.3	35.9	postcentral gyrus
R	thickness	Adol= $+_{*}$ YA= $-_{ns}$	rh	.0001	200.75	26.1	-59.1	9.7	precuneus

Table 12. Adolescent and young adults whole brain analyses – age group interactions. Results for exploratory whole brain analyses testing for age group interactions between adolescents and young adults on the vertex-wise associations between internalizing dimension factor scores and cortical volume, thickness, and area. All analyses controlled for sex, age group, MRI scanner platform, and a whole brain morphometry measure. "Direction" indicates the direction and significance of effects in adolescents (Adol) and young adults (YA). "X", "Y", "Z" are Talairach coordinates of the peak of given cluster. "Max p" indicates the p-value of the peak voxel. NA= negative affect; RNT= repetitive negative thought; AA= anxious arousal-specific; LPA= low positive affect-specific; AAp= anxious apprehension-specific; R= rumination-specific; += Positive relationship (increased internalizing dimension factor score associated with increased gray matter morphometry measures); - = Negative relationship (increased internalizing dimension factor score associated with decreased gray matter morphometry measure); $_{*}$= effect is significant ($p<.05$); $_{\wedge}$= effect is marginally significant ($p<.1$); $_{ns}$ = effect is non-significant ($p>.1$); lh= left hemisphere; rh= right hemisphere; ant.= anterior; med.= medial; vent.= ventral.

Age group significantly moderated the relationships between *negative affect* (see figure 21) and volume, area, and thickness of overlapping clusters in left central sulcus (adolescents: marginal positive; young adults: marginal negative), with the thickness cluster spanning into superior parietal lobe, volume and thickness of overlapping clusters in left parietal operculum (adolescents: significant positive; young adults: non-significant), volume of a cluster in left frontal pole (adolescents: marginal negative; young adults: marginal positive), right posterior cingulate (adolescents: marginal negative; young adults: marginal positive), right central operculum (adolescents: marginal positive; young adults: marginal negative), and thickness of clusters in left anterior inferior frontal gyrus (adolescents: significant positive; young adults: non-significant) and inferior temporal gyrus (adolescents: marginal positive; young adults: marginal negative).

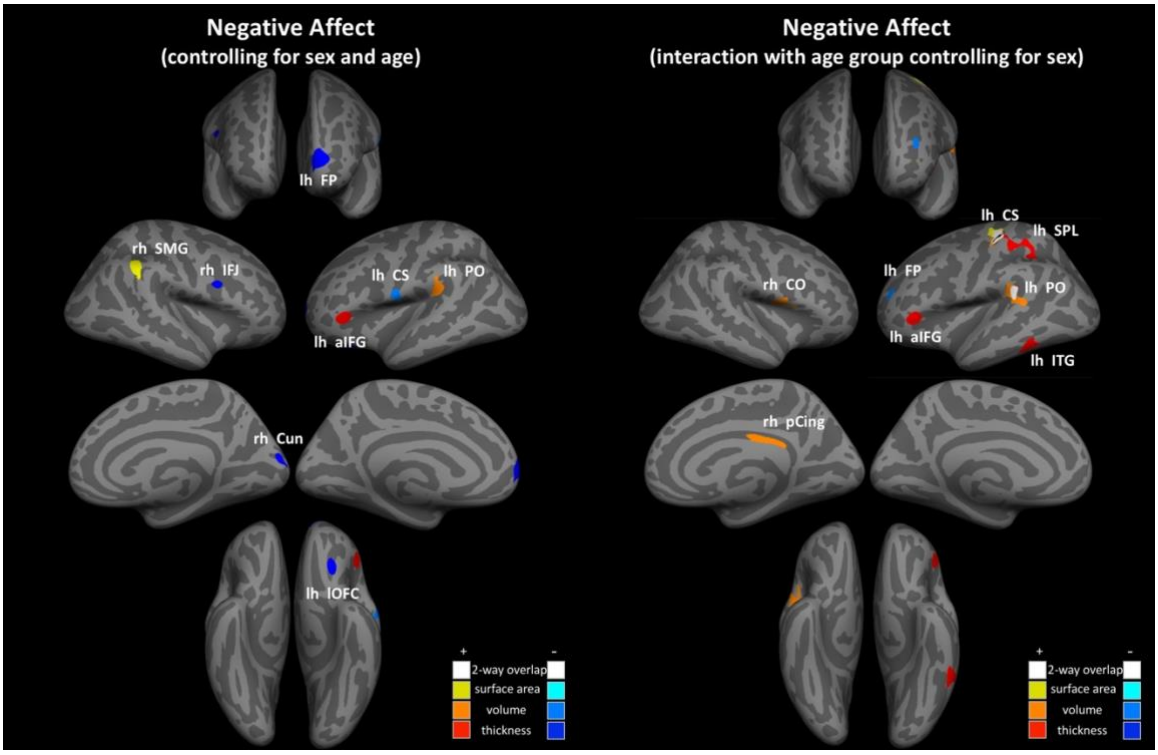

Figure 21. Young adult and adolescents whole brain results: Negative Affect. *Left panel:* results controlling for sex and age group; *Right panel:* age group interactions on the relationship between factor scores and gray matter morphometry controlling for sex. In left panel, hot colors represent positive relationship between factor scores and gray matter morphometry and cool colors represent negative relationship between factor scores and gray matter morphometry. In right panel, hot colors indicate the relationship is more positive in adolescents than young adults and cool colors indicate the relationship is more negative in adolescents than young adults. White clusters indicate two distinct clusters are overlapping. lh= left hemisphere; rh= right hemisphere; lh FP= left frontal pole; lh aIFG= left anterior inferior frontal gyrus; lh CS= left central sulcus; lh PO= left parietal operculum; lh lOFC= left lateral orbitofrontal cortex lh SPL= left superior parietal lobe; lh ITG= left inferior temporal gyrus; rh SMG= right supramarginal gyrus; rh IFJ= right inferior frontal junction; rh Cun= right cuneus; rh CO= right central operculum; rh pCing= right posterior cingulate.

Age group significantly moderated the relationships between *repetitive negative thought* (see figure 22) volume and thickness of overlapping clusters in right medial superior frontal gyrus (adolescents: significant positive; young adults: non-significant), volume of clusters in left middle temporal gyrus (adolescents: significant positive; young adults: non-significant), right medial occipital cortex (adolescents: marginal positive; young adults: marginal negative), area of a cluster in left ventral insula (adolescents: significant negative; young adults: non-significant), and thickness of a cluster in left fusiform gyrus (adolescents: marginal positive; young adults:

marginal negative) and right precentral gyrus (adolescents: marginal positive; young adults: marginal negative).

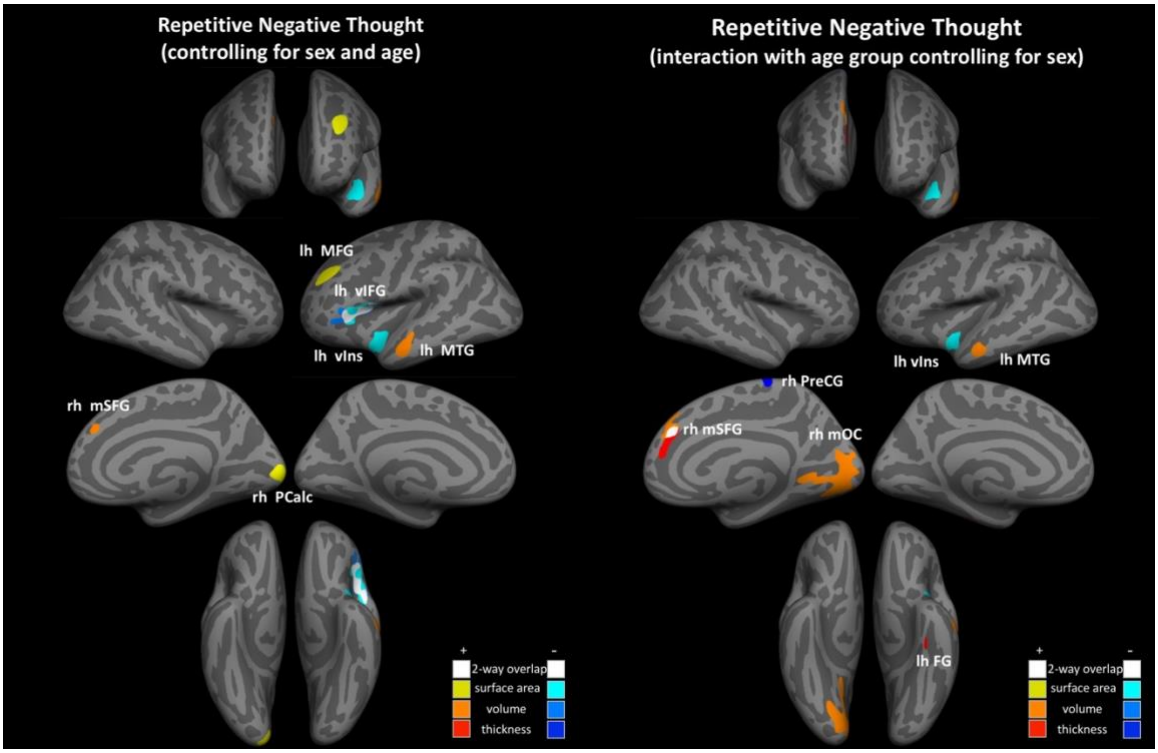

Figure 22. Young adult and adolescents whole brain results: Repetitive Negative Thought. *Left panel:* Results controlling for sex and age group. Hot colors represent positive relationship between factor scores and gray matter morphometry and cool colors represent negative relationship between factor scores and gray matter morphometry. White clusters indicate two distinct clusters are overlapping. *Right panel:* age group interactions on the relationship between factor scores and gray matter morphometry controlling for sex. Hot colors indicate the relationship is more positive in adolescents than young adults and cool colors indicate the relationship is more negative in adolescents than young adults. White clusters indicate two distinct clusters are overlapping. lh= left hemisphere; rh= right hemisphere; lh MFG= left middle frontal gyrus; lh vIFG= left ventral inferior frontal gyrus; lh vIns= left ventral insula; lh FG= left fusiform gyrus; rh mSFG= right medial superior frontal gyrus; rh Pcalc= right pericalcarine cortex; rh PreCG= right precentral gyrus; rh mOC= right medial occipital cortex.

Age group significantly moderated the relationships between *anxious arousal-specific* (see figure 23) and volume and area of overlapping clusters in right anterior inferior frontal gyrus (adolescents: marginal positive; young adults: marginal negative), volume of clusters in left inferior frontal sulcus (adolescents: significant positive; young adults: non-significant) and planum temporale (adolescents: marginal positive; young adults: marginal negative), and thickness of clusters in left superior parietal lobe (adolescents: marginal positive; young adults:

marginal negative) and superior temporal gyrus (adolescents: marginal positive; young adults: marginal negative).

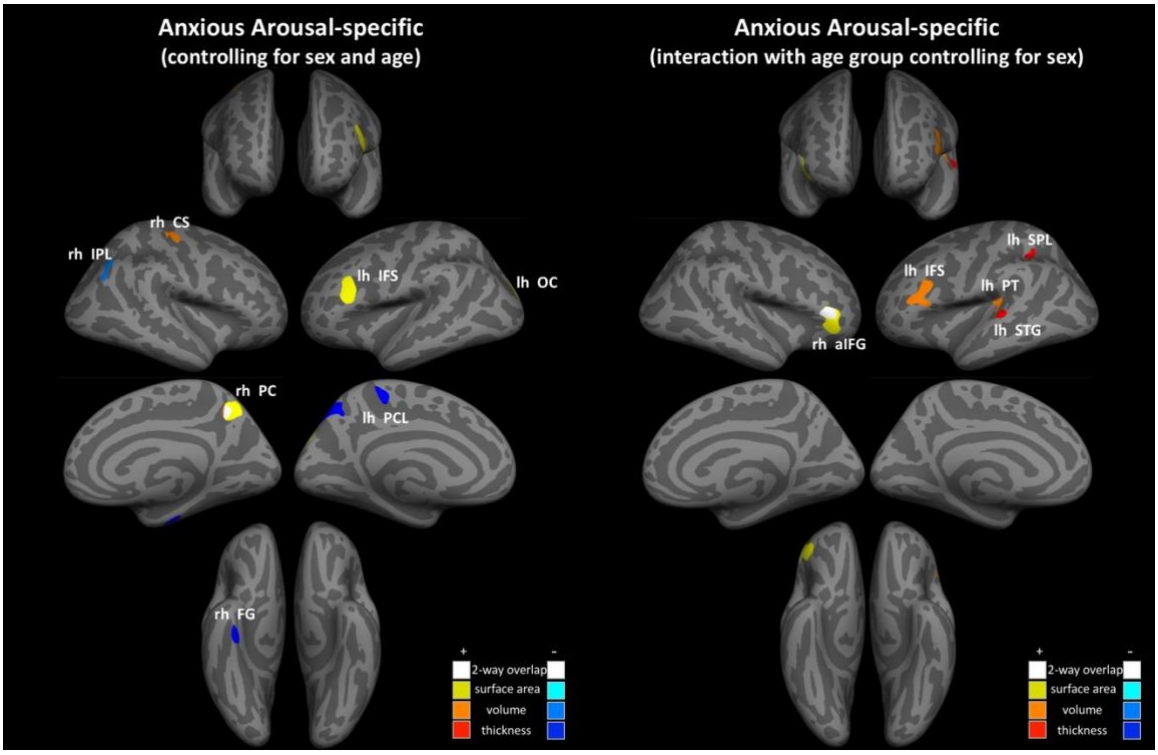

Figure 23. Young adult and adolescents whole brain results: Anxious Arousal-specific. *Left panel:* Results controlling for sex and age group. Hot colors represent positive relationship between factor scores and gray matter morphometry and cool colors represent negative relationship between factor scores and gray matter morphometry. White clusters indicate two distinct clusters are overlapping. *Right panel:* age group interactions on the relationship between factor scores and gray matter morphometry controlling for sex. Hot colors indicate the relationship is more positive in adolescents than young adults and cool colors indicate the relationship is more negative in adolescents than young adults. White clusters indicate two distinct clusters are overlapping. lh= left hemisphere; rh= right hemisphere; lh IFS= left inferior frontal sulcus; lh OC= left occipital cortex; lh PCL= left paracentral lobule; lh SPL= left superior parietal lobe; lh PT= left planum temporale; lh STG= left superior temporal gyrus; rh CS= right central sulcus; rh IPL= right inferior parietal lobe; rh PC= right precuneus; rh FG= right fusiform gyrus; rh aIFG= right anterior inferior frontal gyrus.

Age group significantly moderated the relationships between *anxious apprehension-specific* (see figure 24) and volume of a cluster in left superior parietal lobe (adolescents: marginal positive; young adults: marginal negative), as well as thickness of clusters in right caudal anterior cingulate (adolescents: marginal positive; young adults: marginal negative) and parietal operculum (adolescents: significant negative; young adults: non-significant).

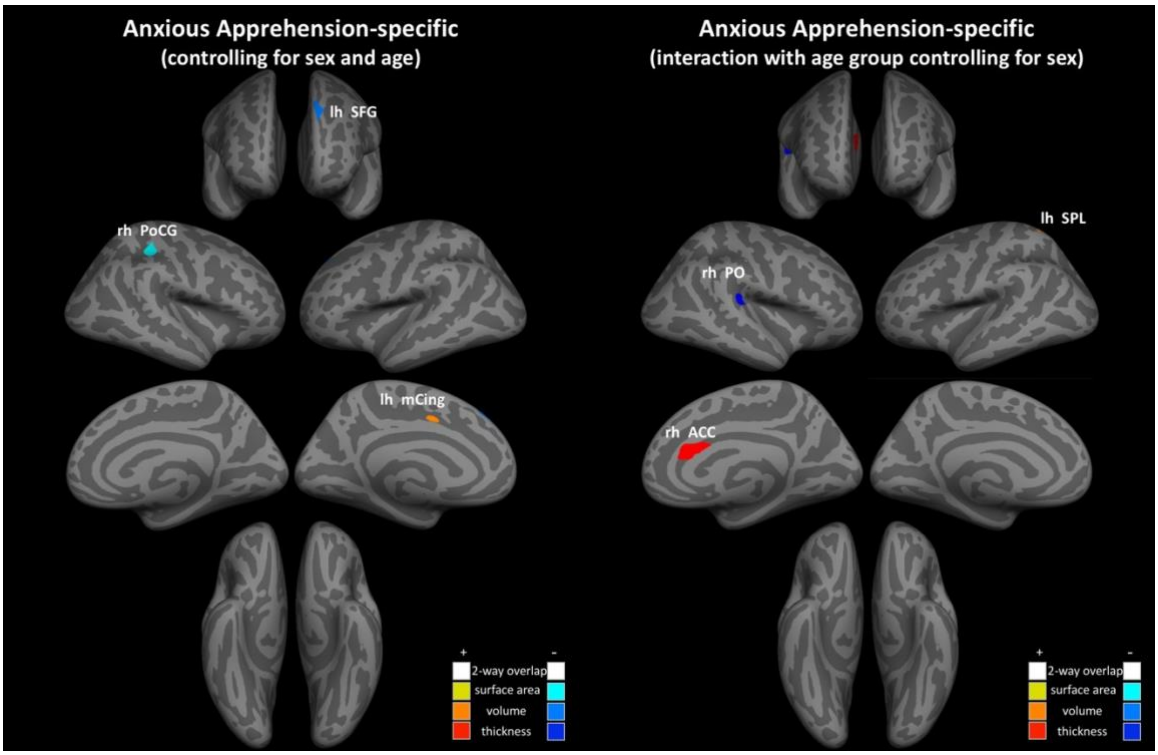

Figure 24. Young adult and adolescents whole brain results: Anxious Apprehension-specific. *Left panel:* Results controlling for sex and age group. Hot colors represent positive relationship between factor scores and gray matter morphometry and cool colors represent negative relationship between factor scores and gray matter morphometry. White clusters indicate two distinct clusters are overlapping. *Right panel:* age group interactions on the relationship between factor scores and gray matter morphometry controlling for sex. Hot colors indicate the relationship is more positive in adolescents than young adults and cool colors indicate the relationship is more negative in adolescents than young adults. White clusters indicate two distinct clusters are overlapping. lh= left hemisphere; rh= right hemisphere; lh SFG= left superior frontal gyrus; lh mCing= left mid cingulate; lh SPL= left superior parietal lobe; rh PoCG= right postcentral gyrus; rh PO= right parietal operculum; rh ACC= right anterior cingulate cortex.

Age group significantly moderated the relationships between *low positive affect-specific* (see figure 25 and area of right superior frontal gyrus and medial orbitofrontal cortex (adolescents: significant positive; young adults: non-significant), as well as thickness of clusters in left posterior inferior frontal gyrus (adolescents: marginal positive; young adults: marginal negative), postcentral gyrus (adolescents: marginal negative; young adults: marginal positive), and pericalcarine cortex (adolescents: marginal negative; young adults: marginal positive).

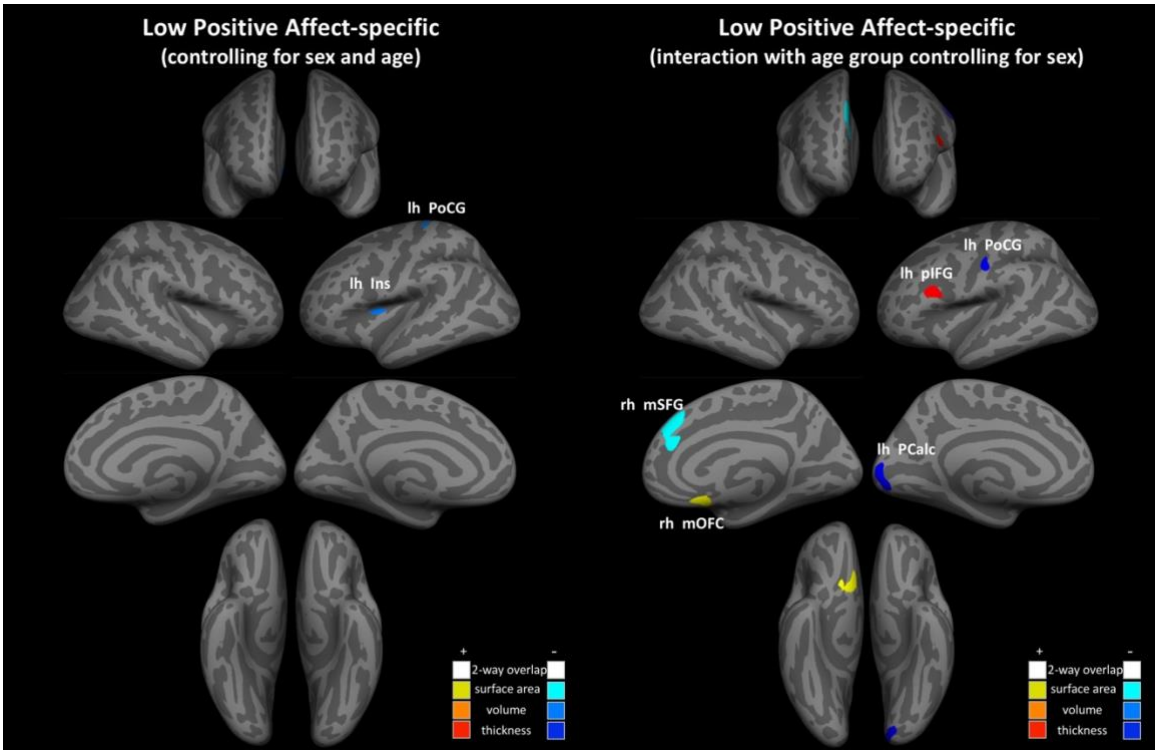

Figure 25. Young adult and adolescents whole brain results: Low Positive Affect-specific. *Left panel:* Results controlling for sex and age group. Hot colors represent positive relationship between factor scores and gray matter morphometry and cool colors represent negative relationship between factor scores and gray matter morphometry. White clusters indicate two distinct clusters are overlapping. *Right panel:* age group interactions on the relationship between factor scores and gray matter morphometry controlling for sex. Hot colors indicate the relationship is more positive in adolescents than young adults and cool colors indicate the relationship is more negative in adolescents than young adults. White clusters indicate two distinct clusters are overlapping. lh= left hemisphere; rh= right hemisphere; lh PoCG= left postcentral gyrus; lh Ins= left insula; lh PoCG= left postcentral gyrus; lh pIFG= left posterior inferior frontal gyrus; lh Pcalc= left pericalcarine cortex; rh mSFG= right medial superior frontal gyrus; rh mOFC= right medial orbitofrontal cortex.

Age group significantly moderated the relationship between *rumination-specific* (see figure 26) and a thickness of a cluster in right precuneus (adolescents: significant positive; young adults: non-significant).

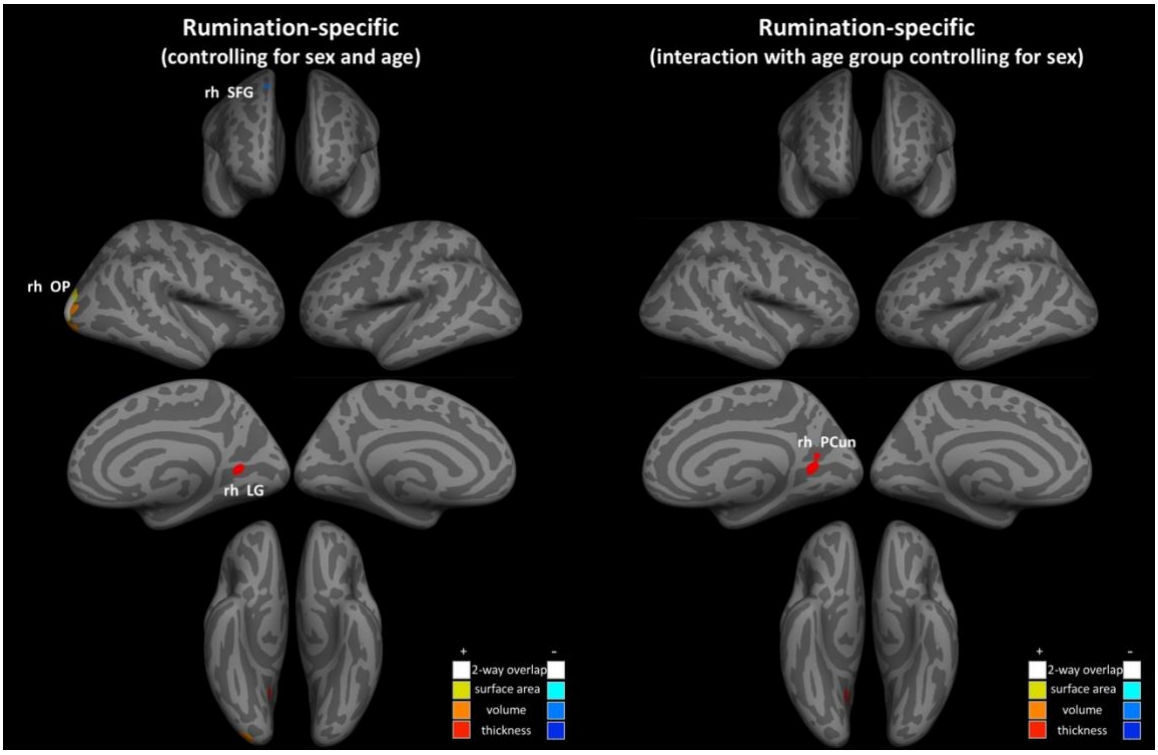

Figure 26. Young adult and adolescent whole brain results: Rumination-specific. *Left panel:* Results controlling for sex and age group. Hot colors represent positive relationship between factor scores and gray matter morphometry and cool colors represent negative relationship between factor scores and gray matter morphometry. White clusters indicate two distinct clusters are overlapping. *Right panel:* age group interactions on the relationship between factor scores and gray matter morphometry controlling for sex. Hot colors indicate the relationship is more positive in adolescents than young adults and cool colors indicate the relationship is more negative in adolescents than young adults. White clusters indicate two distinct clusters are overlapping. lh= left hemisphere; rh= right hemisphere; rh SFG= right superior frontal gyrus; rh OP= right occipital pole; rh LG= right lingual gyrus; rh Pcun= right precuneus.

4.3.3.3. Controlling for age group and sex in whole brain analyses

In the following, we summarize significant results from the exploratory whole brain analyses across adolescents and young adults, controlling for age group and sex. For a summary figure showing results for all dimensions overlaid on a single brain, see figure 20. For full results, see table 13 and figures 21 to 26. We caution the reader when interpreting these effects because many of these clusters were driven by a significant effect in one age group alone.

Dimension	Measure	Direction	Hemi	Max log(p)	Cluster Size (mm^2)	X	Y	Z	Region
NA	area	Positive	rh	.0001	346.44	51.4	-41.7	37.5	supramarginal gyrus
	volume	Positive	lh	.0001	319.03	-47	-31.3	23.7	parietal operculum
	volume	Negative	lh	.0001	166.95	-59.1	-5.6	9.8	central sulcus
	thickness	Positive	lh	.0001	248.84	-48.3	29.1	-2.4	ant. inferior frontal gyrus
	thickness	Negative	lh	.0001	410.28	-11.7	62.2	3.3	frontal pole
	thickness	Negative	lh	.0002	130.15	-24.1	23.6	-13.4	lateral orbitofrontal
	thickness	Negative	rh	.0002	200.72	6	-84.1	16.6	cuneus
	thickness	Negative	rh	.0002	76.93	39	6.4	20.8	inferior frontal junction
RNT	area	Positive	lh	.0002	542.09	-25.8	32.7	23.9	middle frontal gyrus
	area	Negative	lh	.0001	773.62	-35.3	18.3	9.9	vent. inferior frontal gyrus
	area	Negative	lh	.0001	426.12	-40.8	-7.9	-14.8	vent. insula
	area	Positive	rh	.0001	531.25	14.1	-88.3	10.3	pericalcarine
	volume	Positive	lh	.0001	369.43	-49.6	-9.8	-18.1	middle temporal gyrus
	volume	Negative	lh	.0001	671.35	-33.3	16.9	11	vent. inferior frontal gyrus
	volume	Positive	rh	.0002	81.86	9.1	39.3	27.8	med. superior frontal gyrus
AA	area	Positive	lh	.0001	483.42	-13.9	-81.9	32.5	occipital cortex
	area	Positive	lh	.0002	479.94	-39.2	25.6	17	inferior frontal sulcus
	area	Positive	rh	.0001	381.14	9.1	-55.1	43.5	preceuneus
	volume	Positive	rh	.0001	116	7.6	-53	44	precuneus
	volume	Positive	rh	.0002	208.5	34.4	-20	47.9	central sulcus
	volume	Negative	rh	.0001	282.78	37.5	-62.2	46.8	inferior parietal lobe
	thickness	Negative	lh	.0001	145.07	-11	-32	51.1	paracentral lobule
	thickness	Negative	lh	.0002	410.35	-7.7	-68.4	46	precuneus
	thickness	Negative	rh	.0002	200.64	34.4	-16.9	-25.1	fusiform gyrus
AAp	area	Negative	rh	.0001	226.81	34.4	-28.6	38.3	postcentral gyrus
	volume	Positive	lh	.0001	48.94	-10.1	2.5	35.5	middle cingulate
	volume	Negative	lh	.0002	200.35	-11.5	42.9	38.3	superior frontal gyrus
LPA	volume	Negative	lh	.0002	92.27	-32.4	4.9	12	insula
	volume	Negative	lh	.0002	89.78	-19.3	-29.1	54.5	postcentral gyrus
R	area	Positive	rh	.0001	886.05	23.8	-93.1	7.9	occipital pole
	volume	Positive	rh	.0001	1074.45	25	-90	16	occipital pole
	volume	Negative	rh	.0001	61.61	14.5	18.3	53.3	superior frontal gyrus
	thickness	Positive	rh	.0001	121.12	28.5	-60	7.8	lingual gyrus

Table 13. Adolescent and young adults whole brain analyses – controlling for age group and sex. Results for exploratory whole brain analyses across both adolescents and young adults testing for association of the vertex-wise associations between internalizing dimension factor scores and cortical volume, thickness, and area. All analyses controlled for sex, age group, MRI scanner platform, and a whole brain morphometry measure. "Direction" indicates whether the relationship was positive or negative in nature. "X", "Y", "Z" are Talairach coordinates of the peak of given cluster. "Max p" indicates the p-value of the peak voxel. NA= negative affect; RNT= repetitive negative thought; AA= anxious arousal-specific; LPA= low positive affect-specific; AAp= anxious apprehension-specific; R= rumination-specific; lh= left hemisphere; rh= right hemisphere; ant.= anterior; med.= medial; vent.= ventral.

Looking across adolescents and young adults while controlling for sex, *negative affect* (see figure 21) was significantly negatively associated with volume of a cluster in left central sulcus (x= -59.1, y= -5.6, z= 9.8, cluster size= 166.95 mm^2) and thickness of clusters in left lateral orbitofrontal cortex (x= -24.1, y= 23.6, z= -13.4, cluster size= 130.15 mm^2), frontal pole (x= -11.7, y= 62.2, z= 3.3, cluster size= 410.28 mm^2), right inferior frontal junction (x= 39, y= 6.4, z= 20.8, cluster size= 76.93 mm^2), cuneus (x= 6, y= -84.1, z= 16.6, cluster size= 200.72

mm^2), as well as significantly positively associated with volume of a cluster in left parietal operculum (x= -47, y= -31.3, z= 23.7, cluster size= 319.03 mm^2), area of a cluster in right supramarginal gyrus (x= 51.4, y= -41.7, z= 37.5, cluster size= 346.44 mm^2), and thickness of a cluster left anterior inferior frontal gyrus (x= -48.3, y= 29.1, z= -2.4, cluster size= 248.84 mm^2). However, the associations between negative affect and the left anterior inferior frontal gyrus, ventral central sulcus, and parietal operculum were all driven by significant relationships in the adolescents only.

Repetitive negative thought (see figure 22) was significantly negatively associated with volume (x= ,-33.3 y= 16.9, z= 11, cluster size= 671.35 mm^2) and area (x= -35.3, y= 18.3, z= 9.9, cluster size= 773.62 mm^2) of overlapping clusters in left ventral inferior frontal gyrus, and area of left ventral insula (x= -40.8, y= -7.9, z= -14.8, cluster size= 426.12 mm^2), as well as positively associated with volume of clusters in left middle temporal gyrus (x= -49.6, y= -9.8, z= -18.1, cluster size= 369.43 mm^2) and right medial superior frontal gyrus (x= 9.1, y= 39.3, z= 27.8, cluster size= 81.86 mm^2), and area of clusters in left middle frontal gyrus (x= -25.8, y= 32.7, z= 23.9, cluster size= 542.09 mm^2) and right pericalcarine cortex (x= 14.1, y= -88.3, z= 10.3, cluster size= 531.25 mm^2). However, the associations between repetitive negative thought and left ventral insula, middle temporal gyrus, and right medial superior frontal gyrus were driven by significant relationships in the adolescents only.

Anxious arousal-specific (see figure 23) was negatively associated with volume of a cluster in right inferior parietal lobe (x= 37.5, y= -62.2, z= 46.8, cluster size= 282.78 mm^2), and thickness of clusters in left paracentral gyrus (x= -11, y= -32, z= 51.1, cluster size= 145.07 mm^2) and precuneus (x= -7.7, y= -68.4, z= 46, cluster size= 410.35 mm^2), as well as positively associated with volume (x= 7.6, y= -53, z= 44, cluster size= 116 mm^2) and area (x= 9.1, y= 39.3,

z= 27.8, cluster size= 381.14 mm^2) of clusters in right precuneus, volume of a cluster in right central sulcus (x= 34.4, y= -20, z= 47.9, cluster size= 208.5 mm^2), and area of a clusters left inferior frontal sulcus (x= -39.2, y= 25.6, z= 17, cluster size= 479.94 mm^2) and occipital cortex (x= -13.9, y= -81.9, z= 32.5, cluster size= 483.42 mm^2). However, the associations between anxious arousal-specific and left inferior frontal sulcus, occipital cortex, precuneus, right central sulcus and inferior parietal lobe were driven by significant associations in the adolescents only, and the association with left paracentral lobule were driven by significant relationships in the young adults only.

Anxious apprehension-specific (see figure 24) was significantly negatively associated with volume of a cluster in left superior frontal gyrus (x= -11.5, y= 42.9, z= 38.3, cluster size= 200.35 mm^2) and area of a cluster in right postcentral gyrus (x= 34.4, y= -28.6, z= 38.3, cluster size= 226.81 mm^2), as well as positively associated with volume of a cluster in left middle cingulate (x= -10.1, y= 2.5, z= 35.5, cluster size= 48.94 mm^2).

Low positive affect-specific (see figure 25) was significantly negatively associated with volume of clusters in left insula (x= -32.4, y= 4.9, z= 12, cluster size= 92.27 mm^2) and postcentral gyrus (x= -19.3, y= -29.1, z= 54.5, cluster size= 89.78 mm^2).

Rumination-specific (see figure 26) was negatively associated with volume of a cluster in right superior frontal gyrus (x= 14.5, y= 18.3, z= 53.5, cluster size= 61.61 mm^2), as well as positively associated with volume (x= 25, y= -90, z= 16, cluster size= 1074.45 mm^2) and area (x= 23.8, y= -93.1, z= 7.9, cluster size= 886.05 mm^2) of overlapping clusters in right occipital pole and thickness of a cluster in right lingual gyrus (x= 28.5, y= -60, z= 7.8, cluster size= 121.12 mm^2). However, the association with the right lingual gyrus was significant in adolescents only.

4.4. Discussion

In the current study, we tested whether individual differences in factor scores of six internalizing dimensions discussed in Chapter 3 were associated with individual differences in gray matter morphometry at multiple levels of spatial granularity. Because of evidence that the dynamic neurodevelopmental processes that occur throughout adolescences and young adulthood may dramatically change the brain regions supporting internalizing psychopathology (e.g., Schmaal et al., 2017), we tested for relationships of internalizing dimensions and gray matter morphometry in two age groups: a sample of over 100 adolescents, ages 14 to 22, and a sample of over 600 young adult twins, tightly centered around 29 years old. Because of strong evidence suggesting sex differences in the timing, severity, and nature of internalizing psychopathology, we also tested for interactions of sex on internalizing dimensions/gray matter relationships in both samples, separately. Our results suggest three overarching themes. First, adolescents and young adults show largely divergent patterns of relationships between internalizing psychopathology and gray matter. Second, our individual differences approach finds evidence that internalizing behaviors are associated with brain regions spanning much of the brain, not just the prefrontal and limbic brain regions implicated in case-control studies. Third, though males and females show some common gray matter correlates of internalizing behaviors, there are considerable sex differences in the pattern of brain regions associated with any given internalizing dimensions and this is true in both adolescents and young adults.

In the following, we discuss results from each dimension in turn. We begin our discussion of each dimension by providing an overview of our a priori hypotheses for that

dimension, including which brain regions we expected to be associated with that dimension and whether or not we expected to see age differences in the pattern of results. Then, for each dimension, we discuss results for each age group separately, ending with a summary that highlights the general takeaways looking across both adolescents and young adults.

4.4.1. Negative Affect

Based on the preexisting case-control literature, we hypothesized that negative affect would be associated with gray matter in a limited set of brain regions which are consistently altered across internalizing disorders, namely the caudal anterior cingulate and the insula (Goodkind et al., 2015). Because of the relative late maturation of the frontal lobe, however, we hypothesized that the association between negative affect and caudal anterior cingulate would be unique to the young adult group and not present in adolescents.

4.4.1.1. Adolescence

In adolescence, when controlling for sex, we found no evidence of associations between negative affect and gray matter morphometry in the insula or caudal anterior cingulate regions, our a priori regions of interest. We instead found evidence that during adolescence, negative affect is associated with gray matter in left lateral prefrontal cortex, particularly the inferior frontal gyrus, as well as in sensorimotor regions. We also observed interactions with sex in medial prefrontal portions of the default mode network, as well as regions supporting visual attention and the secondary somatosensory cortex. The current results extend our understanding

of the brain systems broadly associated with internalizing psychopathology, suggesting that, at least in adolescence, negative affect may not be associated solely with brain systems supporting cognitive control and affect, but may also be associated with alterations in sensorimotor and visual regions, potentially in a sex-specific manner.

While we did not find associations between negative affect and the insula and caudal anterior cingulate as predicted, we did observe associations of negative affect with other brain regions frequently implicated in case-control studies. Beginning in the prefrontal cortex, when controlling for sex, ROI and exploratory analyses both implicated gray matter in left inferior frontal gyrus, with exploratory analyses also implicating the left frontal pole/anterior middle frontal gyrus. While the ROI findings were only marginally significant after Bonferroni correction, they are reinforced by the significant whole brain effects. The left inferior frontal gyrus has been commonly implicated in higher-level language processes, with anterior portions implicated in the selection and retrieval of semantic information into working memory (Badre et al., 2005; Snyder et al., 2011, 2014) and posterior portions associated with language production (for a review, see Friederici & Gierhan, 2013). Though we had predicted that the inferior frontal gyrus would show preferential associations with levels of the anxious apprehension-specific factor, the observed association between this region and negative affect align with case-control studies showing altered inferior frontal gyrus gray matter in anxiety patients (Andreescu et al., 2017; Kang et al., 2017; Shang et al., 2014; Strawn et al., 2015), depression patients (Na et al., 2016; Qiu et al., 2014; Zhao et al., 2017), as well as individuals with comorbid anxiety and depression (Peng et al., 2017; Zhao et al., 2017). Furthermore, individual differences studies often report correlations between individual differences in inferior frontal gyrus gray matter and continuous measures of anxiety (Besteher et al., 2017; Hu & Dolcos, 2017; Spampinato et al.,

2009) and depression (Besteher et al., 2017; Salvadore et al., 2011; Vasic et al., 2008) symptom severity. While none of these studies employed a bifactor model to parse covariation between internalizing behaviors, as was done in the current study, previous research utilizing a bifactor model of psychopathology more broadly report associations between left inferior frontal gyrus neuroanatomy and the p-factor in children ages 6 to 11 (Snyder et a., 2017). Because we did not include a p-factor in our internalizing model, the negative affect factor may contain some variance that is better explained by a more general p-factor, variance that might be driving the association with left inferior frontal anatomy. While the specific neuroanatomy metric and direction of the effect differ between our current findings and what was observed by Snyder et al. (2017), Snyder and colleagues had a substantially younger sample of largely prepubescent children who are likely still undergoing neuronal proliferation. In contrast, our adolescent sample likely contains at least some individuals who are undergoing rapid neuronal pruning. Though speculative, in adolescents, the positive association between inferior frontal gyrus gray matter and negative affect may indicate a delayed or stunted pruning process with downstream effects on an individual's ability to modulate negative emotional experiences.

Remaining within left lateral prefrontal cortex, we also observed a relationship between negative affect and volume of the left frontal pole/rostral middle frontal gyrus, with increased negative affect associated with reduced volume. Though the precise role of the frontal pole remains in questions, it is generally thought to support abstract goal representations, potentially managing the focus of attention between internal and external stimuli in accordance with task goals (Burgess et al., 2007; Orr et al., 2015). The frontal pole has received considerably less attention than other prefrontal regions in terms of its potential role in internalizing psychopathology, but may play a role none the less. Not only have some studies suggested

alterations in frontal pole anatomy in internalizing patients (Bludau et al., 2016), this region has direct connections to other brain regions considered central to internalizing psychopathology, including the amygdala, anterior cingulate, and lateral prefrontal cortex (Orr et al., 2015), and may play a supervisory role over these regions.

After partitioning covariation between internalizing behaviors into discrete factors, we had anticipated that exploratory whole brain analyses would reveal that gray matter morphometry in sensorimotor regions is exclusively associated with anxious arousal-specific. While we did indeed find associations between anxious arousal-specific and sensorimotor regions (see section 4.4.3.1), we also observed quite a few associations of negative affect with these regions. Increased negative affect was associated with reduced volume in the most ventral portion of the left central sulcus, reduced area of a ventral portion of right postcentral gyrus, and increased area, volume, and thickness of clusters in left parietal operculum, portions of the primary motor, primary somatomotor, and secondary somatomotor cortices, respectively. These findings provide some context to the range of unpleasant bodily states found across internalizing disorders, suggesting that, despite bodily symptoms appearing to vary between disorders, there may be some sensorimotor commonalities across internalizing psychopathologies. Indeed, of the specific questionnaire items employed in the internalizing confirmatory factor analysis, a number of items tapping bodily states stand out for showing strong relationships with the negative affect factor. These include questions tapping hyperactive states, like “felt uneasy” (standardized loading on negative affect of .731), “was unable to relax” (standardized loading on negative affect of .713), and “was trembling or shaking” (standardized loading on negative affect of .650), as well as hypoactive states, like “felt really slowed down” (standardized loading on negative affect of .690) and “felt like it took an extra effort to get started” (standardized loading on

negative affect of .654). While we had predicted that the bodily component of negative affect would show up as preferential associations with insular gray matter, with the insula often attributed to the conscious awareness of bodily states, instead we found associations in more low-level brain regions supporting movement and sensation. One speculative yet intriguing possibility is that the bodily component of negative affect may, in part, be driven by the over or under representation of certain portions of the body within the homunculi that make up the primary and secondary somatomotor systems.

One of the central questions surrounding internalizing psychopathology is what mechanisms may be driving sex differences in the trajectory of internalizing behaviors across the lifespan. Our analyses did not find any sex differences during adolescence in the relationships between gray matter and negative affect in our a priori ROIs. Instead, exploratory whole brain analyses revealed divergent patterns of associations in males and females in multiple portions of the default mode network, including right dorsal superior frontal gyrus and left posterior cingulate, portions of the right secondary somatosensory cortex, and bilateral portions of the parietal lobe. Given models of internalizing psychopathology as emerging through properties of the default mode network (e.g., Whitfield-Gabrieli & Ford, 2012), the sex differences observed in portions of this network stand out in particular. In the right dorsal superior frontal gyrus, males showed a marginally significant negative relationship between area and volume of this region and negative affect, whereas girls showed a nonsignificant, though trending to positive relationship. Similarly, in the left posterior cingulate, males showed a significant negative relationship between volume and negative affect whereas females showed a non-significant relationship. Though we interpret these relatively weak effects with caution, they tentatively

suggest that anatomy of default mode network may be preferentially related to negative affect in adolescent males but not adolescent females.

In addition to this sex-related dissociation in portions of the default mode network, we found that males showed a marginally positive association between negative affect and area of the right supramarginal gyrus spanning into the parietal operculum, whereas females showed a non-significant relationship. This finding is interesting in the context of what was observed when controlling for sex. Specifically, we found that increased negative affect was positively associated with area, thickness, and volume of the left parietal operculum, regardless of sex, yet it appears that the right homolog of this region may have preferential associations with negative affect in males only. As such, this constellation of main effects and sex interactions in the left and right homologs of this region point to a complicated relationship between the secondary somatosensory cortex and negative affect, while simultaneously highlighting this region as a relatively novel region of interest for future research into internalizing psychopathology.

4.4.1.2 Young adults

In young adults, in line with our predictions, we observed associations of negative affect with gray matter in the bilateral insula and right caudal anterior cingulate. Similar to adolescents, we also unexpectedly found associations of negative affect with the inferior frontal gyrus and sensorimotor regions, including negative relationships between negative affect and right pre- and postcentral gyrus thickness and volume, and area of the parietal operculum, spanning into the temporoparietal junction. However, contrary to our predictions and what was observed in

adolescents, we also found that negative affect was associated with right lateral prefrontal cortex and left medial orbitofrontal cortex, brain regions frequently implicated in psychopathology.

As discussed previously, a meta-analysis of case-control studies across all major Axis 1 disorders found that the reductions in bilateral insula volume and predominately right caudal anterior cingulate were associated with all disorders (Goodkind et al., 2015) thus making them candidate regions to show associations with negative affect. We found converging evidence from ROI and whole brain analyses that the insula is associated with negative affect in young adults.

Nailing down the precise function of the insula has proven quite problematic, potentially due to a multifaceted, integrative role across a number of behaviors. However, it appears to play a critical role in interoception, or the awareness of bodily states. Distinct portions of the insula are responsible for representing interoception of distinct sensory modalities, as well as the integration of these modalities into abstract representation of the overall state of the body (Craig et al., 2011; Shura et al., 2014). Organized along an anterior to posterior gradient, posterior portions of the insula receive information regarding homeostatic, somatosensory information, including warmth and pain; more middle portions integrate this information with motoric signals; more anterior portions supporting holistic representation of the body integrate across distinct somatomotor systems, supporting the conscious awareness of our body with direction connections to prefrontal cognitive control systems (Craig et al., 2011). In the current study we found evidence that negative affect is preferentially associated with more middle to anterior portions of the insula, not the more posterior portion. This suggests that the relationship between negative affect and the insula may be unique to areas of the insula where we begin to see integration of sensory and motor signals, as well as more anterior portions supporting a general bodily awareness. If the insula is indeed the center of general bodily awareness, it makes sense

that we would see associations between negative affect, a dimension characterized by general feelings of distress, distress that is often not localized to specific parts of the body.

Functional imagining studies suggest that the caudal anterior cingulate supports a broad range of processes, including reward, fear, pain, as well as cognitive functions (de la Vega et al., 2016). Strong evidence exists linking the caudal anterior cingulate to executive function more specifically, supporting both the selection and evaluation of goal-relevant behaviors (Banich, 2009). Meta-analytic work focusing on the role of the anterior cingulate cortex in emotional processes suggest that caudal portions largely support the appraisal and expression of emotion (Etkin et al., 2011). Our results support a model of the caudal anterior cingulate supporting processes that are relevant across all internalizing disorder, potentially contributing to the cognitive impairments that are characteristic of nearly all internalizing disorders.

While we found no evidence of this in the adolescent sample, in young adults, exploratory whole brain analyses revealed associations of negative affect with gray matter of the medial orbitofrontal cortex. The orbitofrontal cortex has been broadly implicated in processes relevant to emotion- and reward-related decision making, the regulation of emotional states, and social cognition, all of which are disrupted to varying degrees across psychopathologies, particularly internalizing disorders (for a review, see Hiser & Koenigs, 2018). Though partitioning the precise role of subregions of the orbitofrontal cortex has proven challenging, one model of orbitofrontal cortex function suggests a medial to lateral distinction, with more medial portions supporting the monitoring and learning of reward contingencies and is thus involved in supporting reward-motivated behaviors, whereas more lateral aspects are associated with processing punishment (for a review, see Kringelbach et al., 2005). Substantial additional research is needed to understand the exact role of the medial orbitofrontal cortex in internalizing

psychopathology, but it is well situated to influence a broad range of internalizing symptom domains through direct connections to much of the rest of the brain, including subcortical affective regions. The current results contribute to our understanding of the orbitofrontal cortex's role in internalizing psychopathology by reinforcing theories of a transdiagnostic role of this region across internalizing disorders, with alterations in this region potentially contributing to a general susceptibility to internalizing disorders, as opposed to one disorder specifically.

Staying within the prefrontal cortex, we also found that increased negative affect was associated with decreased gray matter thickness and volume in bilateral inferior frontal gyrus, including marginal evidence in ROI analyses and bilateral clusters in whole brain analyses. There are purported functional differences between the left and right inferior frontal gyrus, with the left homolog thought to support semantic and linguistic processes, including the selection and retrieval of semantic information (Moss et al., 2005; Thompson-Schill et al., 1997), and the right homolog supporting context monitoring, potentially interrupting ongoing goal-relevant behaviors when important stimuli are detected (Wessel & Aron, 2017). While the precise role of these regions in internalizing disorders is unclear, they likely play multifaceted roles across internalizing psychopathology broadly, as suggested by the observed associations with negative affect. However, to preview, we found evidence that the inferior frontal gyrus is not only associated with negative affect in young adults, but nearly all other internalizing dimensions included in the current dimensional model.

Finally, when controlling for sex, we found evidence that negative affect is associated with gray matter in the left parietal operculum, spanning posteriorly into temporoparietal junction. This cluster was partially overlapping with similar clusters observed in adolescence, but was distinguished by its posterior extent into the temporoparietal junction. The temporoparietal

junction is thought to play a crucial role in social cognition, though there is considerable debate as to what its role might be. One prominent model suggests that this region provides an overarching representation of social context to guide behavior (Carter & Huettel, 2013). Sitting at the convergence of brain regions supporting vision, language, and attention, the temporoparietal junction is well situated to integrate bottom-up sensory information with semantic meaning to infer the current context of a given situation. Though it is not commonly discussed in terms of a core region in psychopathology, an emerging body of research indeed finds that properties of both the parietal operculum and temporoparietal junction appear to be associated with facets of internalizing psychopathology in both patients (Poeppl et al., 2016), as well as healthy controls (Hwang et al., 2015).

In addition to the associations discussed above when controlling for sex, the relationship between negative affect and gray matter morphometry showed a large number of interactions with sex, distributed throughout much of the brain. These included sex interactions within the subcortex, namely the amygdala and caudate, the prefrontal cortex, including the frontal pole, inferior frontal sulcus, and medial superior frontal gyrus, medial posterior brain regions, including the posterior cingulate, precuneus, and medial occipital lobe, posterior temporal regions, and portions of the primary and secondary somatosensory cortices.

Beginning within the subcortex, males and females showed opposing relationships between negative affect and volume of the right amygdala and left caudate, respectively. Within the amygdala, females showed a marginally significant negative relationship between negative affect and volume, whereas males showed a non-significant positive association, while within the caudate males showed a marginally significant positive association and females showed a non-significant negative association.

For all of cortical clusters, males showed either a significant or trend towards a negative relationship between gray matter morphometry and negative affect, whereas females showed the opposite. For all clusters but one, the sex interaction was observed with thickness, with a single cluster showing an association with volume. These results suggest that negative affect shows opposing relationships between the sexes with cortical thickness across much of the brain. While the specific mechanisms driving this dissociation between the sexes is unclear, it represents an interesting avenue of further research. When the location of these clusters was compared to a map of where in the brain males and females in the current sample showed differences in underlying thickness, no consistent trend was observed (see Appendix 4). That is, only some of the clusters showing sex interactions between thickness and negative affect fell within regions that were relatively thicker or thinner in males as compared to females. However, taken together with the general observation that females are more susceptible to internalizing disorders than males, the widespread moderating effect of sex on the relationships between negative affect and gray matter suggest that the neural systems associated with internalizing psychopathology may fundamentally differ between the sexes.

4.4.1.3. Negative affect summary

We found evidence supporting our hypotheses that negative affect would be associated with the insula and caudal anterior cingulate, but in young adults only. However, in post-hoc analyses testing the degree to which these results different between young adults and adolescents, only thickness of the left insula was found to be significantly different between the two age groups. Thus, we cannot exclude the possibility that the association between negative

affect and the caudal anterior cingulate was indeed present in the adolescents, and that we just lacked the power to detect the effect. Unexpectedly, we also found that negative affect was associated with additional prefrontal regions, particularly the inferior frontal gyrus, with more anterior portions associating with negative affect in adolescents and more posterior portions associating with negative affect in young adult. When directly comparing the two groups in whole brain analyses, however, we found that the relationship between inferior frontal gyrus anatomy and negative affect was significantly different between the age groups in the left anterior inferior frontal gyrus, only showing a significant effect in the adolescents. Finally, though we had predicted we would find preferential associations of sensorimotor brain systems with anxious arousal-specific, we observed a number of effects of negative affect within the primary motor, primary somatosensory, and secondary somatosensory cortices within both adolescents and young adults, suggesting alterations in sensorimotor systems in across internalizing psychopathology broadly.

4.4.2. Repetitive Negative Thought

Models of the interrelationships between rumination and anxious apprehension suggest that what is shared between these two dimensions is an impaired ability to disengage attention away from negatively-valenced thoughts (Vanderhasslet et al., 2011) that are temporally distal (Papageorgiou & Wells, 1999). Expounding upon this, some have argued that was is shared between rumination and anxious apprehension are *processes* of thought and thought control, whereas what differs between the two are the *content* of these thoughts (McEvoy et al., 2013). As such, we hypothesized that repetitive negative thought, a dimension capturing commonalities

between rumination and anxious apprehension, would be preferentially associated with gray matter of brain regions supporting high-level processes relevant to attentional control. Evidence from neuroimaging studies suggest that lateral prefrontal regions, specifically the dorsolateral prefrontal cortex are crucial to cognitive control over the current focus of working memory and attention (for a review, see Banich, 2009), whereas frontopolar regions support thinking about temporally distant events (Addis et al., 2007; Underwood et al., 2015), whether that be remembering the past or simulating the future. Because we believe out repetitive negative thought dimension captures these constructs, we hypothesized that repetitive negative thought would be associated with the middle frontal gyrus and frontal pole.

4.4.2.1 Adolescents

In adolescents, we did not find evidence of our hypotheses that repetitive negative thought would be associated with portions of the middle frontal gyrus. Instead, when controlling for sex, repetitive negative thought showed exploratory whole brain associations with anterior brain regions, including right medial prefrontal regions of the default mode network, the anterior insula, and anterior temporal lobe. Within the right medial superior frontal gyrus, increased repetitive negative thought was associated with greater volume and thickness of overlapping clusters which spanned multiple subregions of the medial superior frontal gyrus identified in a meta-analytic parcellation of the medial prefrontal cortex (de la Vega et al., 2016). However, the bulk of these two clusters, including their overlap, sat within a region that has been preferentially associated with social perception and self-referential thought (de la Vega, et al., 2016). Though we had hypothesized repetitive negative thought would be associated with lateral, not medial,

prefrontal regions, the association between repetitive negative thought and medial prefrontal regions supporting self-referential thought is not entirely surprising. Self-referential thought is considered a hallmark of rumination, one of the two internalizing dimensions we propose as being driven by repetitive negative thought. The second internalizing dimension, anxious apprehension or worry, is generally discussed in terms of more externally directed attention, but this does not preclude a role of internally directed mentation. For example, in anxious apprehension in social anxiety disorder, there is an interesting mix of both externally directed and self-referential thought processes. That is, social anxiety disorder is associated with a very particular form of anxious apprehension in which individuals worry about other people's (i.e., externally directed) opinion of them, often resulting in an increased incidence of negative opinions of the themselves (i.e., self-referential thought) (Clark & Wells, 1995; Yoon et al., 2019). Similar distinctions can be made about anxious apprehension more generally. While we argue that anxious apprehension is indeed driven by repetitive negative thoughts about external stressors, ultimately, the reason individuals worry about these stressors is because of perceived impacts on how these stressors may affect them. Thus, almost by definition, there is an inherent self-referential aspect to anxious apprehension that may or may not be reliant on similar mechanisms to the self-referential aspect of rumination. Though it is unclear the precise mechanisms driving the observed association in medial superior frontal gyrus region, the current results suggest that commonalities between rumination and anxious apprehension, as indexed by the repetitive negative thought factor, may be in part driven by dorsomedial prefrontal regions supporting self-referential processes.

In addition to the association between medial superior frontal gyrus, we also observed two clusters in anterior portions of the left temporal lobe that were associated with repetitive

negative thought: a cluster in anterior middle temporal gyrus that showed a positive relationship between volume and repetitive negative thought and a cluster in anterior superior temporal gyrus spanning into anterior ventral insula that showed a negative relationship. Whereas more posterior portions of the insula represent subjective feelings that are largely modality specific, the anterior insula is thought to be provide a more global representation of bodily states that are largely temporally specific, potentially serving as the seat of bodily awareness and human consciousness (for a review, see Craig et al., 2011). The more ventral portion of the anterior insula implicated with repetitive negative thought shows preferentially structural and functional connectivity with lateral prefrontal and limbic regions, suggesting this region may play a crucial role in the relay of information about global bodily states to regions supporting cognitive control and lower-level affective states (Cloutman et al., 2012; Shura et al., 2014). Recent fMRI research in adolescents suggests that alterations in the dynamics of a default mode subnetwork centered around anterior portions of the insula are associated with depressive symptomology, including rumination, a form of repetitive negative thought (Kaiser et al., 2019b). Though the insula remains one of the least well understood brain regions, our current results align with emerging models of adolescents internalizing psychopathology that suggest a prominent role of anterior portions of the insula in psychopathology related cognitive processes (Kaiser et al., 2018, 2019a).

Looking across the ROI and exploratory whole brain analyses, we found converging evidence that repetitive negative thought is associated with posterior portions of the right inferior frontal gyrus in a sex specific manner, though these associations were only marginal in the ROI analysis. The exploratory whole brain analysis revealed a cluster in the most posterior portions of right pars opercularis in which adolescent males showed a significant negative association whereas adolescent females showed a marginally significant positive association. These analyses

identified two other sex interaction clusters, including in the left inferior temporal gyrus and right occipital pole. Interestingly, none of these effects were in regions in which males or females differed in terms of underlying gray matter (see Appendix 5). As such, it appears that these sex interactions did not stem from sex differences in the underlying gray matter, but may rather represent distinctions in the instantiation of repetitive negative thought that are sex specific despite common underlying neuroanatomy. Of these three clusters, the inferior frontal gyrus is particularly noteworthy. First, the right inferior frontal gyrus sex interaction corresponds to a similar cluster showing a sex interaction with levels of the anxious apprehension-specific factor, albeit in the opposite hemisphere and with a different measures of gray matter morphometry. Evidence suggests that the role of the right inferior frontal gyrus in inhibition may not be to inhibit per se, but rather to detect salient information that may be goal-relevant and to reorient attention and subsequent behavior in accordance with this new information (for a review, see Banich & Depue, 2015; Wessel & Aron, 2017). Though speculative, such a mechanism may be at play in repetitive negative thought. Repetitive negative though can be conceptualized as emerging due to in ability to reorient attention away from a particular focus of attention, with that focus in anxious apprehension being external, future stressors and the focus in rumination being past, self-referential memories. Sustained repetitive negative thought may, in part, arise from dysfunction in right inferior frontal mechanism that, under normal circumstances, would disrupt the repetitive negative thinking, reorienting attention away to something else. However, the converse could be true as well. That is, repetitive negative thoughts are often intrusive, entering the focus of attention at inopportune times and disrupting normal goal-related activity. If the right inferior frontal gyrus is indeed responsible for disrupting ongoing goal-relevant behavior to reorient attention, it may be that this region is consistently

reorienting attention away from adaptive goal-directed activities and towards the focus of the repetitive negative thought. While these two scenarios provide possible explanations as to why we observed associations between repetitive negative thinking and the right inferior frontal gyrus, they are speculative and warrant further investigation.

4.4.2.2 Young adults

In young adults, we found evidence supporting our hypotheses that repetitive negative thought would be associated with gray matter in the rostral middle frontal gyrus, though the association between these regions were sex specific and only observed in the exploratory whole brain analyses. Specifically, females showed a significant positive association between repetitive negative thought and thickness of clusters in anterior portions of left and right rostral middle frontal gyrus, relationships that were non-significant and significantly negative in males. When controlling for sex, repetitive negative thought showed marginal associations with ROIs of left pars opercularis and lateral orbitofrontal cortex, though neither of these results were bolstered by exploratory whole brain analyses. Instead, exploratory whole brain analyses exclusively implicated brain regions along the medial wall, spanning anterior prefrontal regions, to the mid cingulate, to posterior medial occipital regions. Despite relatively little correspondence between adolescents and young adults for most dimensions, we found that repetitive negative thought in young adults was associated with a reduced thickness of a medial prefrontal region immediately adjacent to what was observed in adolescents, though in the opposite direction. As discussed previously, this region is key node in the default mode network, a brain region supporting internally directed thought, a key component of repetitive negative

thought. Thus, though not predicted, the association between this region align with models of repetitive negative thought as emerging through mechanisms relevant to the default mode network (Lydon-Staley et al., 2019).

Testing for interactions of sex on the relationship between gray matter morphometry and repetitive negative thought revealed that many of the same regions that showed effects when controlling for sex also showed sex interactions. These regions included portions of the right medial superior frontal gyrus and the right ventral medial occipital cortex. In addition to these sex interaction effects that were overlapping or immediately adjacent to regions implicated when controlling for sex, we found sex interactions affecting relationships between repetitive negative thought and cortical thickness across much of the right hemisphere, including the right frontal pole, right anterior inferior frontal gyrus, right temporal pole, right middle temporal gyrus, right parietal operculum, and right superior parietal lobe, as well as two clusters in right middle frontal gyrus. For all of these sex interactions, males and females showed opposing significant or marginally significant relationships, with males exclusively showing negatives associations and females exclusively showing positive associations. Furthermore, nearly all of these regions overlapped with portions of the brain that showed sex differences in the underlying gray matter (see Appendix 4). Taken together, these results provide compelling evidence that not only do males and females differ in gray matter properties in young adulthood, but that these differences may, in part, drive sex differences in the mechanisms supporting repetitive negative thought.

4.4.2.3. Repetitive negative thought summary

Though we did not observe relationships of repetitive negative thought with rostral middle frontal gyrus gray matter in adolescents, we did find associations within these regions in young adults, albeit in a sex specific fashion. Furthermore, ROI analyses testing for age group difference revealed a significant difference in the relationship of repetitive negative thought and volume of the right rostral middle frontal gyrus. This finding provides support for the idea that repetitive negative thought is indeed associated with anterior portions of the middle frontal gyrus, but because of the relatively late development of this region, this relationship is divergent between adolescents and young adults. Within adolescence, repetitive negative thought appears to be associated with properties of more cognitively oriented portions of the left insula and temporal lobe, suggesting that, while it may not be associated with cognitive control regions proper, repetitive negative thought does appear to be associated with regions that directly interface with cognitive control systems. Looking across adolescents and young adults, we found evidence that repetitive negative thought is also associated with medial superior frontal portions of the default mode network, though the direction of these effects differed between the age groups, suggesting developmental influences on the relationship between the default mode network and repetitive negative thought. Sex interactions were observed across much of the brain, particularly in young adults, including in temporal and occipital regions supporting semantic and visual processes, respectively. Our current results suggest that, at least in young adults, repetitive negative thought may be associated with properties of a number of brain systems throughout the brain in a largely sex specific manner.

4.4.3. Anxious arousal-specific

Because anxious arousal has been conceptualized as stemming from a hyperactive threat detection system, leading to increased vigilance and hyperactive sensorimotor systems, we hypothesized that levels of the anxious arousal-specific factor would be associated with brain regions supporting these functions, namely the amygdala, thalamus, and sensorimotor cortices. Because these functions are largely supported by early-developing brain systems, we hypothesized that would see considerable similarity in the results across adolescents and young adults.

4.4.3.1. Adolescents

In adolescents, we found evidence confirming our hypotheses that the levels of the anxious arousal-specific factor would be associated with the amygdala and sensorimotor regions. ROI analyses revealed a marginally significant negative association between anxious arousal-specific factor and volume of the left amygdala whereas exploratory whole brain analyses revealed associations between anxious arousal-specific and the primary and secondary sensorimotor regions. We also observed associations between levels of the anxious arousal-specific factor and a number of unexpected regions, including whole brain results in portions of the left inferior frontal sulcus, the left precuenus, and right inferior parietal lobe.

Overall, the pattern of results observed in the current adolescent whole brain analyses largely mirror what has been observed previously in a younger sample of children and adolescents ages 8 to 17. Specifically, using a manifest measure of anxious arousal, Castagna and colleagues (2018) reported associations in regions that almost perfectly overlapped with a number of clusters identified in our exploratory whole brain analysis, including the left inferior

frontal sulcus, right precentral gyrus/central sulcus, right supramarginal gyrus, and right superior parietal lobe. Furthermore, though the overlap was not as precise as the aforementioned clusters, Castagna and colleagues (2018) also found an association with right anterior temporal lobe, partially overlapping with the interior anterior temporal lobe cluster identified in the current study. Despite striking similarities between the regions identified in Castagna's study and the current report, the specific gray matter metric and, in some cases, the direction of effects differed between the two studies. In their younger sample, every cluster Castagna identified demonstrated a positive association between anxious arousal and cortical thickness. In the current study, while we did find positive associations in the inferior frontal sulcus and right central sulcus, in both cases these associations were with area and volume, not thickness. Additionally, we observed negative relationships between anxious arousal-specific and thickness in the right supramarginal gyrus and volume of the right superior parietal lobe as well as a negative association between volume and surface area of the anterior temporal lobe. Considering these studies together, there is compelling evidence that anxious arousal during childhood and adolescence is, indeed, associated with lateral prefrontal regions and regions supporting sensorimotor process, as these regions have now been replicated in independent samples, using different parameterizations of anxious arousal. With that being said, our use of a measure of anxious arousal that parsed covariation between other internalizing behaviors extends what was observed by Castagna and colleagues. Specifically, they reported that the left inferior frontal sulcus cluster was associated with both anxious arousal and anxious apprehension across sexes. In the current study, we find evidence that regions may be preferentially associated with behaviors specific to anxious arousal, at least when controlling for sex.

Our work also further extends Castagna and colleagues findings by not just controlling for sex, but by also testing for sex interactions. These interaction analyses in the current study revealed a number of interesting findings. First, though the relationship between inferior frontal sulcus gray matter and anxious arousal-specific was significant when controlling for sex, this relationship was in fact largely driven by males. Specifically, we observed that males showed a significant positive association between area and volume of this region, whereas these relationships were non-significant in females. In fact, across the ROI and whole brain analyses we observed a number of sex interactions in multiple regions of the prefrontal cortex, including the left inferior frontal gyrus, right middle frontal gyrus, and right lateral orbitofrontal cortex. These results suggest that the relationship between prefrontal cognitive control regions and anxious arousal-specific may be sex dependent. However, because all of these ROI-based sex interactions were cross over effects in which the relationship was non-significant in both sexes individually, we interpret these effects with caution. Second, though anxious-arousal specific was associated with gray matter in the right central sulcus when controlling for sex, portions of the right postcentral gyrus appear to show sex specific relationships with anxious arousal-specific. These sex specific relationships are non-significant in both sexes, but create a cross-over due to opposing positive and negative trends. Finally, within portions of right medial and lateral temporal lobe, males show significant or marginally significant negative associations between gray matter morphometry and anxious arousal-specific, whereas females show non-significant or significantly positive relationships. Coupled with our finding of a main effect in right anterior ventral temporal lobe, we find converging evidence linking multiple properties of the temporal lobe to levels of the anxious arousal-specific factor.

4.4.3.2. Young adults

In young adults, our hypotheses that anxious arousal-specific would be associated with regions supporting threat detection and sensorimotor processes were partially confirmed. First, we found evidence that anxious arousal-specific is associated with properties of the amygdala, the purported core of threat detection (Ohman, 2005), but only in females. Second, as predicted, we found that anxious arousal-specific is associated with gray matter of sensorimotor brain regions, including the postcentral gyrus and paracentral lobule. Third, in line with models of anxious arousal-specific as capturing largely somatic, non-cognitive behaviors, ROI analyses notably did not find any relationship between anxious arousal-specific and prefrontal gray matter when controlling for sex, instead only finding an association with volume of the caudate.

We hypothesized the amygdala would be central to anxious arousal-specific because of its role in the rapid, automatic detection of external threats, a function which triggers a cascade of physiological responses commonly referred to as the "fight or flight" response (Ohman, 2005). Many of the behaviors that load most highly on anxious arousal-specific are indeed capturing these physiological responses. While we expected this relationship between anxious arousal-specific to be consistent across the sexes, we found that it was only significant in female adolescents. Sex differences in the relationship between amygdalar volume and anxious arousal-related traits have been observed previously, though generally in younger samples and not with the specific pattern of sex difference we observed. For example, in children and adolescents, sex influenced the relationship between gray matter volume and somatic anxiety symptoms though in a different pattern than what we observed (Warnell et al., 2018). Specifically, increased gray matter volume in the amygdala was associated with decreased somatic anxiety symptoms in

males, and that relationship was significantly stronger than what was observed in females (Warnell et al., 2018). Though we are unaware of analogous morphometry/individual differences results in adults, case-control studies have demonstrated amygdalar sexual dimorphisms in anxiety patients. For example, Asami and colleagues (2009) reported that male and female adults with panic disorder show a difference in the relative reduction in amygdalar volume when compared to gender matched healthy controls. fMRI research has also highlighted sex-related effects in the relationship between anxiety and properties of the amygdala. When presented with fearful faces, females with high trait anxiety demonstrate a stronger amygdala response than females low on anxiety, a relationship that is not observed in men (Dickie & Armony, 2008). Thus, there is compelling evidence across modalities and analysis techniques suggesting that the amygdala may influence anxiety in sex specific ways. The contributing factors to these sex differences, however, remain elusive. One potential factor may be a mediating role of female gonadal hormones like estrogen, on stress and neuronal growth, with evidence in rats suggesting that estrogen may mediated the effects of chronic stress on neuronal structure in the amygdala (Shansky et al., 2010).

Second, in addition to observing associations between anxious arousal-specific and amygdalar neuroanatomy, we also found evidence that anxious arousal-specific was associated with gray matter in brain regions supporting both primary and somatosensory representations, including the postcentral gyrus and paracentral lobule, as well as higher level awareness of holistic bodily states and feelings, namely the anterior insula. Though the associations with primary somatosensory regions were anticipated, we had expected that the insula would be preferentially associated with negative affect, due to evidence implicating insular gray matter as being altered across all internalizing disorders, and not symptoms that are thought to be specific

to anxiety. However, given the anterior insula's role in the conscious awareness of bodily states and strong reciprocal connections to much of the brain, including the amygdala (Baur et al., 2013; Shura et al., 2014), this finding is not entirely surprising. In fact, models of amygdala's role in fear detection suggests that when the amygdala detects a threatening stimulus, a network of brain regions including the anterior insula and prefrontal regions comes online in order to consciously assess the threat and regulate behavior accordingly (Ohman, 2005). fMRI work suggests that connectivity between the amygdala and anterior insula is a key player in both state and trait anxiety, with measures of functional connectivity between these two regions explaining 40% and 15% of the variance in state anxiety immediately prior to scanning and trait anxiety measured outside of the scanner (Baur et al., 2013). As such, our current findings align with models of anxiety positing a central role of communication between the anterior insula and amygdala, while extending this literature to suggest that these two regions may play preferential roles in anxious arousal-specific, not just general internalizing behaviors more broadly.

We also found evidence of associations between anxious arousal-specific and brain regions outside of where we had predicted, with the most notable being the right inferior frontal junction spanning into the pars opercularis. Sitting at the convergence of multiple dissociable brain networks, including the frontoparietal control network, the ventral attention network, and the default mode network (Yeo et al., 2011), the inferior frontal junction is well situated to play a dynamic role in goal-oriented processes, attentional orientation processes, and internally directed thought. While it's specific relationship to anxious arousal-specific is unclear at this time, the inferior frontal junction and the adjacent middle- and inferior frontal gyri frequently show alterations in gray matter morphometry across internalizing disorders. One potential role of this region in anxious arousal-specific may be its purported function of monitoring the environment

for salient stimuli and integrating contextual environmental information with current goals (Banich & Depue, 2015). Though speculative, if anxious arousal-specific is, in part, a hypervigilance to threat, the right inferior frontal gyrus may be a key player in this hypervigilance, monitoring the environment for salient, threatening stimuli, and potentially integrating environmental context with the goal to avoid the perceived threat.

Similar to what we found in adolescents, we observed a number of associations between anxious arousal-specific and brain regions supporting multiple stages of visual processing in young adults. These findings included main effects while controlling for sex in the medial occipital lobe, namely the calcarine fissure, as well as lateral occipital lobe. Though gray matter in both regions showed negative associations with anxious arousal when controlling for sex, we observed quite a few sex interactions in a wide-range of visual processing regions, including the cuneus, precuneus, calcarine fissure, and lateral occipital lobe. We observed additional sex-interactions in brain regions within more anterior regions of the ventral visual processing stream, including portions of the inferior temporal lobe. These results suggest that, while anxious arousal-specific shows some evidence of relationships with primary visual cortex that are consistent across the sexes, its relationship with the primary visual cortex, as well as brain regions that processes visual information into increasing abstract representations, may be largely sex dependent.

4.4.3.3. Summary

In both adolescents and young adults, we largely confirmed our hypotheses that anxious arousal-specific is associated with gray matter of threat detection and sensorimotor systems. In

addition, we observed relationships between prefrontal portions of the frontoparietal network and ventral attention networks, as well as brain regions supporting vision and visual attention, and the temporal lobe. However, the specific pattern of results was largely age-dependent and there were considerable sex differences throughout much of the brain. Within adolescents, anxious arousal-specific demonstrated robust associations with left inferior frontal sulcus, relationships that were largely absent in young adults when controlling for sex. Instead, associations between anxious arousal-specific and prefrontal gray matter in young adults were in right inferior frontal gyrus, and largely sex-specific.

4.4.4. Anxious apprehension-specific

Previous fMRI research suggests that anxious apprehension is largely driven by linguistic and semantic brain regions, including left inferior frontal gyrus and anterior temporal lobe (Engels et al., 2007; Nitschke et al., 2001; Sharp et al., 2015), as well as portions of the default mode network supporting internally directed thought (Burdwood et al., 2016). However, because of a general role of the default mode network across of much of internalizing psychopathology, we predicted that anxious apprehension-specific would be preferentially associated with these linguistic/semantic brain systems, not the default mode network.

4.4.4.1. Anxious apprehension-specific in adolescence

Within adolescence, the gray matter correlates of the anxious apprehension-specific factor were largely divergent between the sexes. Looking across the sexes, only one cluster

reached significance in the exploratory whole brain analyses: a negative association between anxious apprehension-specific and thickness in the right parietal operculum, a region, as discussed previously, implicated in higher order sensorimotor integration. While the lack of effects across the sexes was surprising, this may in part be driven by both prominent sex differences in anxious apprehension, with females generally reporting greater anxious apprehension severity than males (Robichaud et al., 2003), as well as an earlier onset (McLean et al., 2011), potential due to differences in anxiety-related neurodevelopment. Indeed, in the current study, we found sex interactions with anxious apprehension-specific across much of the brain, including bilateral inferior frontal regions often associated with language processes, temporal regions supporting semantic processes, and occipital regions supporting visual processes.

There was considerable variability in the nature of the sex differences across the brain, with distinct patterns of sex difference emerging between more anterior as compared to more posterior brain regions. In more anterior brain regions, including the left inferior frontal junction, right anterior cingulate, and left temporal pole, boys showed evidence of negative relationships between anxious apprehension-specific and thickness or area, whereas girls showed evidence of positive relationships. Though the effects within each sex were generally only marginally significantly, they demonstrated crossover interactions, in which the difference between the opposing direction of effects in males and females constituted a significant sex interaction. Within the prefrontal cortex, we observed evidence that increased anxious apprehension-specific is associated with reduced area and thickness in boys, whereas it is associated with increased area and thickness in girls. Specifically, in a cluster in left inferior frontal junction, adolescent males showed a marginal negative association between anxious apprehension-specific and area

whereas adolescent females showed a non-significant positive association. A similar relationship was observed in the right anterior cingulate, where males showed a significant negative relationship between anxious apprehension-specific and thickness and females showed a non-significant negative relationship. Of note is the fact that both of these prefrontal cluster at least partially fell in regions that showed differences between the sexes in mean levels of area and thickness (see Appendix 5). As compared to females, males showed greater area in a portion of the precentral gyrus that overlapped with the inferior frontal junction cluster though they showed thinner gray matter in the anterior cingulate cortex. This constellation of results suggests that the observed prefrontal sex differences may stem from fundamental differences in neuroanatomy between the sexes, potentially speaking to ongoing debates regarding the etiological factor driving sex differences in psychopathology (for reviews, see Rutter et al., 2003; Zahn-Waxler et al., 2006).

In more posterior brain regions, we observed an opposite pattern of sex differences in anxious apprehension-specific/gray matter relationships than was observed in the prefrontal cortex. Within portions of the right posterior superior temporal sulcus and multiple clusters of the right medial occipital lobe, we once again found cross over interactions, but this time with increased anxious apprehension-specific associating with increased volume and area in boys, but decreased volume and area in girls. Post hoc regression analyses revealed that the effects within each sex were only marginally significant, but once again created a significant crossover interaction. Though we are cautious to make too strong of inferences from these crossover interactions, they may suggest that the relationship between anxious apprehension-specific and gray matter within a given region may not only differ between the sexes, but that the nature of these differences may by contingent on the general brain system involved. Anxious apprehension

has been conceptualized as a cognitive dimension of anxiety that is largely contingent upon linguistic and semantic processes (Behar et al., 2005), supported by prefrontal mechanisms including the left inferior frontal gyrus and the anterior temporal lobe (for a review, see Fedorenko & Thompson-Schill, 2014), both regions showing interaction effects in the current study. Interestingly, work within both anxiety patients and healthy controls suggest that anxious apprehension intensity can be modulated through the implementation of mental imagery (for a review, see Hirsch & Holmes, 2007), processes that largely rely on medial occipital and posterior temporal regions (for a review, see Thompson & Kosslyn, 2000). Despite mixed evidence as to whether or not mental imagery can increase or decrease anxious apprehension, mental imagery indeed appears to be highly relevant to anxiety disorders. For example, Stokes & Hirsch (2010) had individuals worry about a personally relevant topic, but either through verbal thought or mental imagery, followed by a five-minute breathing exercise. They found that individuals who engaged in verbal worry reported greater negative intrusions in the post-worry breathing exercise than those who engaged in mental imagery-based worry, whereas those who engaged in mental imagery-based worry reported greater positive intrusions. Thus, it may be that anterior prefrontal and temporal regions supporting verbal processes and medial occipital regions supporting imagery may interact to bring about individual differences in anxious apprehension. Though the relationship between gray matter morphometry and function remains elusive, our current results suggest that in adolescents, anxious apprehension-specific in males and females are differentially related to properties of prefrontal language systems and medial occipital imagery systems.

4.4.4.2. Anxious apprehension-specific in young adults

In young adults, anxious apprehension-specific was associated with gray matter morphometry in ROI-based measures of left insula, as well as whole brain analysis clusters in largely ventral portions of the brain, including the bilateral insula, anterior temporal lobe, medial occipital lobe, and posterior cingulate, with evidence of sex differences in the anterior temporal lobe. Despite our predictions that anxious apprehension-specific would be associated with lateral prefrontal anatomy, predictions which bore out in sex interactions in the adolescents, we found no evidence of associations between the lateral prefrontal cortex and anxious apprehension-specific in the young adult sample. Though we had hypothesized and confirmed that insular anatomy was associated with negative affect, we found that increased anxious apprehension-specific was associated with reduced volume in large swaths of the bilateral insula. These clusters largely overlapped with clusters observed with negative affect, though negative affect was associated with thickness, not volume, as was observed for anxious apprehension-specific. This correspondence between negative affect and anxious apprehension-specific in the insula suggest that anxious apprehension-specific may share some of the same neural substrates as negative affect, even after taking into account variance shared between the two dimensions, as is done in this study.

Previous fMRI research has indeed found associations between individual differences in anxious apprehension and the insula in adults. For example, employing an fMRI paradigm within female adults, increased self-reported anxious apprehension was associated with reduced activation in the insula when participants viewed aversive images (Schienle et al., 2009). Additionally, while not directly measuring trait-levels of anxious apprehension-specific per se, studies in which participants anticipate aversive stimuli can be thought of as inducing a state analogous to worry. Such studies have consistently shown that the anticipation of aversive

stimuli modulates reactivity in the insula (Lutz et al., 2013; Sarinopoulos et al., 2010; Simmons et al., 2004, 2006), with these effects present in individuals high on trait anxiety, as well as general population samples. Despite a number of studies implicating gray matter alterations in anxiety disorders characterized by excessive anxious apprehension (e.g., Hilbert et al., 2015), to date, far fewer studies have found relationships between individual differences in anxious apprehension-specific and gray matter morphometry in a general population sample. One such study in children and adolescence ages 8 to 17 found that both anxious arousal and anxious apprehension showed overlapping associations with increased cortical thickness in the left anterior insula, in a cluster overlapping with the insula clusters observed here (Castagna et al., 2018). It is unclear why we did not observe associations between anxious apprehension-specific and the insula in our current adolescent sample, as was observed by Castagna and colleagues (2018), instead observing relationships between the insula and anxious apprehension-specific in our young adult sample. Though our adolescent sample was older than that employed by Castagna and colleagues (2018), it is still puzzling that associations between the insula and anxious apprehension that Castagna and colleagues observed in childhood/young adolescents, didn't appear in our adolescence sample, but did appear in young adults. One speculative reason may be the unusual neuroanatomical trajectory of the insula across these three age groups. Specifically, a multisite, longitudinal study mapping changes in gray matter morphometry from ages 7 to 29 years showed that, unlike most of the brain that reduces in thickness, area, and volume across these ages, the insula remains similar across these age ranges, however the relationship between thickness, area, and volume changes (Tamnes et al., 2017). Further research is needed to understand the neurodevelopmental process that unfold in the insula and how they might relate to anxious apprehension.

As predicted, we observed a number of effects of anxious apprehension-specific on gray matter morphometry in anterior temporal lobe, a brain region generally supporting abstract semantic representations. Of these associations, effects in bilateral portions of the entorhinal cortex stand out. Specifically, when controlling for sex, increased anxious apprehension-specific was associated with increased thickness of left anterior and thickness and volume of right anterior entorhinal cortex. What makes this finding particularly notable is the purported role of the entorhinal cortex in the perception of time and our conceptualization of anxious apprehension as being repetitive negative thought about future stressors. Immediately adjacent to and sharing strong interconnections with the hippocampus, work in rodents suggest that the entorhinal cortex may play a critical role in associating temporally distinct events in the service of episodic memory (Suh et al., 2011; Tsao et al., 2018). Recently, these findings have been extended into humans. For example, Montchal and colleagues (2019) showed participants a roughly 30-minute video and then asked participants identify when specific still frames from the video occurred. Relative temporal precision of memory in this task was associated with increased entorhinal activation but not in other regions supporting episodic memory, suggesting that temporal information in episodic memory may be preferentially represented by the entorhinal cortex. Additionally, multivariate pattern analyses within entorhinal cortex can accurately recreate the timeline of encountered object in a virtual reality environment (Bellmund et al., 2018). Taken together, these studies, amongst others, provide compelling evidence of a temporally-specific function of the entorhinal cortex. It is unclear precisely why entorhinal cortex gray matter structure was related to anxious apprehension-specific but we speculate that this relationship may reflect the temporal component of anxious apprehension, specifically the focus on future events. Indeed, anxious apprehension can be conceptualized as experiencing substantial stress in

accordance with some imagined future stressor, almost as if the future stressor is being experienced at that moment. Because the entorhinal cortex has been shown as being central to the perception of temporal distance, it may be that the temporal phenomena associated with anxious apprehension are grounded in properties of this region. Though this explanation is speculative, research into the interrelationships between anxious apprehension, the perception of time, and properties of the entorhinal cortex may provide important insights into the etiological factors driving anxiety disorders.

Looking across both age groups, it is also notable the relative degree of correspondence with what was observed between adults and adolescents. Though much of the findings in adolescents involved sex interactions, many of the regions implicated in adolescence were also implicated in young adults, particularly the anterior temporal lobe and medial occipital lobe. Specifically, we observed that increased anxious apprehension-specific in young adults was associated with reduced thickness in the right temporal pole across genders, the right hemisphere homolog of where we found sex differences on the relationships between anxious apprehension-specific and gray matter in adolescents. We also observed positive associations of anxious apprehension-specific with thickness and volume of more inferior, medial portions of the anterior temporal lobe. In addition to these multiple association between anxious apprehension-specific and anterior temporal lobe anatomy that held across sexes, we also found a number of sex interactions within bilateral anterior temporal lobe that largely mirrored the sex interactions observed in adolescence. These sex differences included four distinct clusters in left and right anterior temporal lobe, all showing crossover interactions with males and females showing opposing relationships, with three of these clusters demonstrating the same pattern observed in the anterior temporal lobe in adolescents, namely negative associations in males and positive

associations in females. In addition to both adolescents and adults implicating portions of the anterior temporal lobe in anxious apprehension-specific, both samples showed associations with surface area and volume of the medial occipital lobe. While the medial occipital lobe showed sex differences with anxious apprehension-specific in adolescence, in young adults we observed that increased anxious apprehension-specific was associated with increased surface area and volume of large portions of the medial occipital lobe, with much of the right hemisphere cluster overlapping with the region observed in adolescence. The convergence of anxious apprehension-specific associations in the anterior temporal lobe and medial occipital regions across adolescence and young adults suggest that these regions may play critical roles in anxious apprehension regardless of age. While there was some variability across the age groups in terms of sex-related influences on these anxious apprehension-specific's relationship with these regions, they provide confirmatory evidence that anxious apprehension may be supported by two general sets of neural systems, those supporting semantic processes (i.e., anterior temporal lobe) and those supporting visual imagery (i.e., medial occipital lobe).

4.4.4.3. Anxious apprehension-specific summary

Our specific prediction that anxious apprehension-specific would be associated with gray matter of the inferior frontal gyrus was only partially confirmed. In ROI analyses, we did not observe any significant relationships between anxious apprehension-specific and inferior frontal gyrus gray matter in adolescents or young adults, separately, but did find a moderating effect of age group on the relationship between anxious apprehension-specific and left inferior frontal gray matter. This suggests that the role of the inferior frontal gyrus in anxious apprehension-

specific may differ with age, as we had predicted. Looking across both age groups, we also found evidence that anxious apprehension-specific is associated with brain regions supporting linguistic and semantic processes, albeit with different patterns of results across the age groups. However, though both age groups showed sex interactions on the relationship between anxious apprehension-specific and anterior temporal gray matter, consistent results in this region across males and females were only observed in the young adult group. Finally, both age groups showed relationships between anxious apprehension-specific and portions of the medial occipital cortex, suggesting a prominent role of the brain systems supporting visual imagery in anxious apprehension-specific.

4.4.5. Low Positive Affect-Specific

Low positive affect has been characterized as a depression-specific dimension capturing blunted reward processing. As such, we hypothesized that low positive affect would be associated with gray matter morphometry in brain regions that make up the mesolimbic dopaminergic reward circuit (for a review, see McGinty et al., 2011), a predominately subcortical collection of regions centered around the basal ganglia, as well as medial prefrontal regions which integrate this circuit with cognitive control mechanisms.

4.4.5.1 Adolescence

Though we had predicted that we would see associations between low positive affect-specific and the basal ganglia, in adolescents we instead found associations between low positive

affect-specific and the amygdala when controlling for sex. The amygdala has been classically associated with threat detection (for a review, see Ohman, 2005) but may play and important role in reward processing. It is also one of the most commonly implicated regions in internalizing disorders, yet an understanding of its specificity to one disorder or another remains unclear. Exploratory whole brain analyses further supported our predictions, revealing that low positive affect-specific was positively associated with area of a cluster in right medial orbitofrontal cortex spanning into the subgenual cingulate.

The amygdala is thought to be a central brain structure in internalizing psychopathology, showing atypical neuroanatomical properties across a number of internalizing disorders, including major depression (Hamilton et al., 2008), anxiety disorders (Hilbert et al., 2014), and comorbid depression and anxiety (Bora et al., 2012), as well as across internalizing disorders in general (Goodkind et al., 2015). Our current results suggest that amygdala volume is associated with low positive affect-specific when controlling for sex, a dimension generally associated with depression yet likely to occur to some degree across many internalizing disorders (Brown et al., 1998). Functionally, the amygdala is a key processing center for emotion and while it has been largely discussed in terms of fear circuitry, it has also been implicated in reward processing (for a review, see Janak & Tye, 2015), a factor hypothesized to drive individual differences in low positive affect (Forbes & Dahl, 2005). The amygdala's role in both fear and reward processing has been unified by evidence suggesting it may be a key player in detecting emotionally salient information, regardless of the valence (Liberzon et al., 2003; O'Neill et al., 2018). Given low positive affect is characterized by a lack of a response to positively valenced information and events, our current results suggest that at least part of this blunted reward processing may stem from properties of the amygdala, potentially atypical amygdalar responses to positively valenced

information in the environment. Such phenomena have been observed previously in fMRI studies. For example, comparing amygdala reactivity in depressed patients and healthy controls, Stuhrmann et al., (2013) reported that depressed patients showed elevated amygdala activation in response to sad but not happy faces, whereas the opposite was observed in healthy controls.

In addition to a main effect of low positive affect-specific on the amygdala, we also observed a marginal sex interaction between low positive affect-specific and hippocampal volume, with males and females showing opposing, albeit non-significant, negative and positive relationships, respectively. Though this result was only marginal, we highlight it due to particular interest in the literature as to the relationship between internalizing psychopathology and the hippocampus. The hippocampus sits immediately posterior to the amygdala, and the two share rich bilateral connections, with the amygdala providing input on the emotional salience of information while the hippocampus provides the context for that information. The hippocampus's role in the reward systems is thought to entail providing a mnemonic context during reward learning so individuals can effectively predict what scenarios may be rewarding in the future, based of hippocampal encoding of memories for what was rewarding the past (for a review, see Delgado & Dickerson, 2012). The orbitofrontal cortex has direct connections to both the amygdala and hippocampus (Kringelbach, 2015) and together these three regions support multiple aspects of reward processing that appear to be altered in internalizing psychopathology, including reward learning, emotion regulation, and motivation (Holland & Gallagher, 2004). In fact, evidence in rats suggests that when the pathway between these regions is disrupted, rats will no longer pursue what had previously been rewarding stimuli (Lichtenberg et al., 2017). Taken together, the current results reinforce an extensive body of work demonstrating the role of subcortical-orbitofrontal cortex circuitry in reward processing, while also demonstrating that, at

least in adolescents, the relationship between amygdalar structure and internalizing disorders may be specific to reward-related but not threat-related behaviors.

Exploratory analyses also revealed sex differences in the right parietal operculum spanning into the posterior insula and the left paracentral lobule. Both of these regions are considered part of the sensorimotor system (Yeo et al., 2011), with the parietal operculum and posterior insula implicated in somatosensory integration, including pain representations (Oh et al., 2018; Uddin et al., 2017; Wager et al., 2013), and the paracentral lobule supporting movement and sensation in the lower extremities (Newton et al., 2008). Low positive affect and depression more broadly show interesting relationships with pain and movement. Not only do depressed patients often report high levels of physical pain (Bair et al., 2003), but positive affect has been shown to diminish reported pain severity (Finan & Garland, 2015). Thus, it follows that low positive affect is associated with a reduced ability to effectively modulate pain. Additionally, activation in parietal operculum and posterior insula have been shown to be similar across physical pain and social rejection (Woo et al., 2014), with social rejection being one of the strongest predictors of the onset of depression as compared to other stressors (Kendler et al., 2003; Slavich et al., 2010). Importantly, females show a particularly strong stress response to social rejection as compared to males (Stroud et al., 2002). These findings, taken together with the observed sex interaction with low positive affect suggest that parietal operculum and posterior insula may play an important, sex-specific role in low positive affect, potentially through their mutual roles in supporting neural responses to social rejection and physical pain.

4.4.5.2. Young adults

As was the case in adolescence, very few significant clusters were associated with low positive affect-specific in young adults and, of those that were found, there was very little correspondence between the age groups. In ROI analyses, as predicted, we found evidence of a negative association between low positive affect-specific and volume and area of left rostral anterior cingulate and bilateral orbitofrontal cortex Though not predicted, we additionally observed associations between low positive affect-specific and left inferior frontal gyrus, including effects both controlling for sex as well as sex interactions. These ROI results were bolstered by whole brain analyses controlling for sex, in which we found two clusters in left inferior frontal gyrus/inferior frontal junction that demonstrated negative associations between thickness and low positive affect-specific. In addition to these two prefrontal clusters, a third negative association was observed with volume of a cluster in the right superior temporal gyrus.

The more anterior of the inferior frontal clusters, which sit predominately in pars opercularis, showed a negative association between low positive affect-specific and thickness. This region largely overlapped with the left inferior frontal cluster identified as associating with negative affect, with both clusters showing negative associations with thickness. As such, it appears that the posterior portions of the left inferior frontal gyrus show a multifaceted relationship with internalizing dimensions, even when these internalizing dimensions are parameterized to be orthogonal, as was done in the current study. Thus, the overlap in these clusters cannot be explained by covariation between low positive affect-specific and negative affect, but rather capture distinct variance in thickness of the left inferior frontal gyrus. Though the inferior frontal gyrus has been frequently implicated in internalizing disorders, it's specific role, as well as the degree to which it may show preferential associations with anxiety- or depression-related behaviors, remains in question. These current results suggest that the inferior

frontal gyrus may not just be associated with behaviors shared across internalizing disorders (i.e., negative affective), but may in fact also play a role in behaviors preferentially associated with depression, over and above this more general role. fMRI studies have implicated the inferior frontal gyrus across a range of cognitive functions and future studies may be well served to disentangle which inferior frontal gyrus functions appear to be altered across internalizing disorders, and which appear to be more specific to low positive affect and depression.

Sex interactions in the relationship between low positive affect-specific and gray matter morphometry revealed that males and females may show divergent relationships between low positive affect-specific and brain region supporting sensorimotor and visual functions. Specifically, within bilateral pre- and postcentral gyri, as well as bilateral paracentral lobule, males consistently showed significant positive relationships between low positive affect-specific and volume and area, whereas females generally showed a marginally significant negative relationship. As discussed previously, the central sulcus sits at the intersection of the primary motor and primary somatosensory cortices suggesting that there may be a considerable sensorimotor component to low positive affect-specific that is largely distinct between the sexes. Despite an emphasis on reward systems in models of depression, there appears to be a substantial sensorimotor aspects to depression (for a review, see Canbeyli, 2010), behaviors that may be captured by the low positive affect-specific factor. In the current study, of the 14 items loading on the low positive affect-specific factor, two are directly related to sensorimotor function, including “felt like I had a lot of energy” and “seemed to move quickly and easily”. Suggesting an intimate role of sensorimotor function in depression and related behaviors, substantial evidence suggests that activation of sensorimotor systems via exercise may help ameliorate depressive symptomology, including low positive affect, if only temporarily (Canbeyli, 2010). In

the current project, we extend the literature on the sensorimotor component of depression, suggesting that low positive affect may be associated with sensorimotor brain systems and that, at least in young adults, the relationship between these brain regions may be sex specific.

Within visual processing regions, we found a sex interaction in the cuneus, with males showing a significant negative, and females showing a marginally significant positive association between low positive affect-specific and surface area. While the cuneus has not been commonly implicated in gray matter morphometry studies of depression, depression and related mood states are associated with impaired visual processing (Adolphs, 2004; Bar & Neta, 2007; Meier et al., 2007), a primary function of the cuneus. For example, depressed patients, show impaired visual search performance, particularly when effortful attention is required (Hammar et al., 2003a, 2003b). Evidence from fMRI evidence suggesting that cuneal activity is central to visual search performance (Makino et al., 2004; Parker et al., 2014). Within patients with major depression, increased anhedonia is associated with increased functional connectivity between the caudate and the cuneus, providing evidence that properties of the cuneus may not only be altered in major depression, but maybe specifically associated with anhedonia, a construct highly related to low positive affect-specific.

4.4.5.3. Low positive affect-specific summary

Low positive affect-specific was associated with both cortical and subcortical regions supporting reward processing, though these findings were observed exclusively in adolescents. Specifically, in adolescents, we observed associations between gray matter in the medial orbitofrontal cortex and amygdala, as well as marginal evidence of a sex interaction in the

hippocampus. In the young adults, however, low positive affect-specific appeared to be associated with gray matter of brain regions not commonly discussed in terms of reward processing, including lateral prefrontal and temporal regions, as well as a number of sex interactions in sensorimotor and visual processing regions. As such, it appears that the gray matter correlates of behaviors specific to low positive affect may shift across the first three decades of life, and this shift may be sex specific.

4.4.6. Rumination-specific

Rumination has been conceptualized as repetitive negative thought about past events and perceived self-failures. Within the brain, we frame rumination as stemming from interactions between internally focused default mode network, hippocampal and related medial temporal lobe structures supporting episodic memory, and cognitive control regions that regulate attention. However, because our rumination-specific measure excluded variance shared with other internalizing psychopathology behaviors, we suspected that we would only observed associations with rumination-specific and brain region specifically supporting episodic memory, namely the hippocampus, and not brain regions that appear to be affected more generally across internalizing psychopathology (i.e., default mode network, cognitive control regions). Furthermore, because the hippocampus and related memory systems are thought to develop relatively early, we suspected that we would observe similar relationships across adolescents and young adults.

4.4.6.1 Adolescence

In adolescence, analyses controlling for sex as well as sex interactions revealed that rumination-specific was associated with a collection of regions including visual processing regions associated with autobiographical memory, somatosensory regions, and, to a lesser degree, brain regions supporting semantic processes. These regions largely align with the self-reported nature of rumination, with depressed patients reporting that ruminative experiences overwhelmingly involve mental imagery, feelings, and, to a lesser but non-trivial degree, verbal thought (Newby & Moulds, 2012). Though we did not find evidence of associations between rumination-specific and the hippocampus proper a number of the observed results fell within a network of brain systems involved in autobiographical memory, a key contributor to the ruminative experience in which individuals often perseverate on past events in a self-referential, often self-deprecating manner (Svoboda et al., 2006).

Beginning in visual processing regions, rumination-specific was associated with increased cortical thickness in an anterior cluster of right medial occipital lobe, spanning portions of the cuneus, lingual gyrus, and calcarine fissure. As discussed in the context of anxious apprehension-specific, medial occipital regions support visual representation, with the calcarine fissure being the site of the primary visual cortex. Considered part of the secondary autobiographical memory network (Svoboda et al., 2016), properties of this and adjacent regions are associated with the vividness of memory. For example, in a sample of children and adolescents ages 8 to 17, increased individual differences in vividness of remembered events was associated with reduced functional connectivity in the default mode network in a portion of the medial occipital/parietal lobes, partially overlapping and adjacent to this rumination-specific cluster (Ostby et al., 2012). Relatedly, individual differences in manifest measures of rumination

have been associated with brain activation in occipital regions while participants were at rest (Piguet et al., 2014).

Immediately anterior to the medial occipital lobe cluster, we also observed sex-interactions in a cluster spanning portions of the isthmus cingulate, precuneus, and into the parahippocampal gyrus. Specifically, in this region, males showed a significant negative association between rumination-specific and thickness whereas females showed a marginally significant negative association. This region sits squarely within a cluster that showed increased thickness in males as compared to females when testing for sex-differences in neuroanatomy within the adolescent sample, suggesting that sex differences in rumination may in fact be supported by distinct neuroanatomical organization between males and females. Functionally, much of this region is considered to be a posterior hub in the default mode network, a collection of brain regions that preferentially coactivate in accordance with internally directed thought, including memory retrieval (for a review, see Rugg & Vilberg, 2013). Furthermore, this region is thought to be a major component in the autobiographical memory network through its role in visuospatial processing (Svoboda et al., 2006). The fact that this cluster spanned into the parahippocampal gyrus provides compelling evidence that brain systems supporting visual aspects of memory are central to rumination, even if the hippocampus proper is not. The parahippocampal gyrus is considered a bridge between the hippocampus, a central hub in memory formation and retrieval, the visual cortex, with fMRI studies suggesting the parahippocampal gyrus plays a preferential role in the retrieval of visual memories. For example, in an fMRI study of visual memory retrieval, portions of the parahippocampal gyrus showed increased activation when participants were asked to recall previously viewed as compared to novel visual stimuli (Duzel et al., 2003). Taken together, the relationships between rumination-

specific and brain systems supporting autobiographical memory reinforce rumination as emerging in association with brain systems supporting self-referential thought and memory retrieval. Interestingly, these associations were not with medial prefrontal regions involved in autobiographical memory, suggesting that, when shared covariation between rumination and other internalizing dimensions is taken to account, what is specific to rumination is largely supported by posterior, medial brain systems.

In addition to finding associations between rumination-specific and portions of the autobiographical memory network, we also found effects of rumination-specific in somatosensory regions, including main and sex-interaction effects in the primary and secondary somatosensory cortices. Specifically, we observed that, when controlling for sex, increased rumination-specific was associated with increased thickness in a portion of the left supramarginal gyrus, a key brain region in the integration of sensation. Interactions with sex were observed in this same supramarginal gyrus region, with males showing a non-significant negative association between rumination-specific and volume and females showing a non-significant positive association, as well as in the right postcentral gyrus, where females showed a significant negative association and males showed a marginal positive association. A meta-analysis across emotional memory encoding studies implicated supramarginal gyrus activation in emotional memories (Murty et al., 2010), a key component of rumination. Though not commonly discussed in reference to rumination, limited evidence suggests that the postcentral gyrus may indeed be involved in rumination, with adults showing increased activation in the postcentral gyrus when asked to ruminate as opposed to a control condition (Cooney et al., 2010). As such, our current findings add to this emerging body of literature suggesting that rumination and associated

emotional memories may be related to brain systems supporting sensation, with such regions potentially supporting bodily states associated with emotional memories.

Finally, we also observed sex-interactions in overlapping clusters in the right temporal pole, with males showing a non-significant and marginally significant positive association and females showing a significant and marginally significant negative association with thickness and surface area, respectively. Whereas the left temporal pole has been implicated in abstract semantic processes, the right temporal pole has been commonly implicated in higher order socio-emotional process, potentially coupling abstract sensory information, including auditory, visual, and olfactory information, with emotional responses (Olson et al., 2007). Indeed, some evidence further suggests that, in this role, the temporal pole plays an important part in the recall of emotionally charged memories, particularly memories with a social component. As was the case with a number of regions that showed sex-interactions with rumination-specific in adolescents, we found that the right temporal pole showed underlying difference in gray matter between males and females, with males showing greater thickness and area in clusters spanning from the anterior insula into the portions of the temporal pole where we observed these sex-interactions. Taken together, this correspondence between sex-interactions between rumination-specific and gray matter within regions showing different patterns of underlying gray matter between the sexes suggest that rumination in adolescence may differ between the sexes due to underlying differences in neuroanatomical organization.

4.4.6.2 Young adults

In young adults, controlling for sex, rumination-specific showed associations with gray matter of the right opercularis ROI, whole brain clusters in the right subgenual anterior cingulate and right superior temporal sulcus, as well as a broad array of interactions with sex throughout much of the brain. The association with subgenual anterior cingulate stands out in particular. Though there is extensive research showing altered properties of the subgenual cingulate in major depression (for a review, see Drevets et al., 2008), it is unclear the degree to which the subgenual cingulate shows preferential associations with depression, comorbid anxiety, or internalizing psychopathology more broadly. Gray matter morphometry studies in internalizing disorder patients show that subgenual cingulate volume is not only reduced in major depression both with and without comorbid anxiety disorders, but also anxiety disorders without comorbid depression, (van Tol et al., 2010). While such findings call into question the specificity of the subgenual cingulate to depression, by employing a dimensional approach, we are better able to specify which behavioral component of internalizing disorders appears to be most closely tied to subgenual cingulate anatomy. Our results suggest that the relationship between subgenual cingulate anatomy and internalizing psychopathology in young adults may be preferentially associated with rumination-specific behaviors, over and above what is common across internalizing disorders (i.e., negative affect and repetitive negative thought). While similar theories linking the subgenual cingulate to rumination have been proposed elsewhere (Hamilton et al., 2015), to our knowledge, the current study is the first to show associations between rumination-specific behaviors and subgeneual cingulate anatomy when taking into account repetitive negative thought.

Working in close coordination with the immediately adjacent orbitofrontal cortex, the subgenual cingulate has been implicated in a range of functions relevant to the regulation,

evaluation, experience, and expression of emotion (Drevets et al., 2008). With direct connections to the amygdalar-hippocampal complex, the ventral striatum, and the hypothalamus, among other subcortical and cortical regions, animal models suggest that the subgenual cingulate is directly involved in controlling the "visceromotor network" responsible for autonomic responses to fear, stress, and reward (Drevets et al., 2008; Ongur & Price, 2000). In humans, this region appears to be a crucial player in a number of constructs highly relevant to depressive symptomology, particularly reward sensitivity (e.g., Manohar & Husain, 2016), attention towards emotional information (Elliot et al., 2000), and responses to stress (e.g., Thomason et al., 2011). The ventromedial prefrontal cortex, which includes the subgenual cingulate, is thought to influence emotional processes in part by shutting down or ramping up processing in subcortical structures, particularly the amygdala (Pizzi et al., 2017). Because the amygdala drives attention towards emotionally salient information (Ohman, 2005) and rumination is associated with an inability to disengage from emotional information (Donaldson et al., 2007), it follows that the circuitry supporting the regulation of the amygdala, namely the subgenual cingulate, may play a central role in rumination.

The importance of the subgenual cingulate in depression symptomology has been reinforced by recent innovations in mental health treatment. Ruminative behaviors appear to be a risk factor for the most severe instantiations of MDD, with increased rumination associating with worse treatment outcomes (Ciesla & Roberts, 2002). Previous gray matter morphometry studies suggest that treatment resistant depression is associated with reduced subgenual cingulate volume in patients as compared to healthy controls (Machino et al., 2014). Leveraging this associations between properties of the subgenual cingulate and depression, recent treatment methodologies that target subgenual cingulate function have proven successful in ameliorating

treatment resistant depression, providing evidence for previous hypotheses that the subgenual cingulate's role in depression may be, in part, due to its relationship with rumination (Hamilton et al., 2015). For example, deep brain stimulation of this region has been associated with marked clinical improvements in patients with treatment resistant depression (Johansen-Berg et al., 2008; Mayberg et al., 2005). Furthermore, there is emerging evidence that the therapeutic administration of ketamine may preferentially alter connectivity of the subgenual cingulate to other limbic regions (Wong et al., 2016). Our current results contribute to our understanding of the mechanistic action of these treatments on behavior, suggesting that, by altering properties of the subgenual cingulate, clinicians may be bolstering patient's ability to disengage from ruminative patterns of thought.

The other region that showed a main effect with rumination-specific when controlling for gender in the young adults fell within the right temporal lobe, a region that has been also associated with rumination in treatment resistant depression (Machino et al., 2014). Though the specific portion of the temporal lobe and the direction of effects with rumination observed by Machino and colleagues (2014) differed from what we observed in the current study, these studies together highlight lateral portions of the temporal lobe as being potential targets for further research into the etiological factors driving rumination. To date, considerable attention has been paid to medial temporal lobe structures (i.e., amygdala and hippocampus) in the pathophysiology of depression and internalizing psychopathology more broadly, but lateral temporal structures have received relatively little attention, despite some evidence suggesting alterations in gray matter of these regions in internalizing patients (e.g., Schmaal et al., 2017). Our current results point to lateral temporal regions as playing a role in rumination, potentially through this regions role in supporting semantic associations.

As was observed in the adolescent sample, young adults showed sex-interactions in the relationship between rumination-specific and gray matter morphometry in the right temporal pole and bilateral sensorimotor regions, but also in prefrontal and insular regions not observed in adolescents. In fact, in young adults, sex-interactions were so widespread that portions of six of the seven major brain networks identified by Yeo and colleagues (2011) were implicated, with the one exception being the visual network. Of these results, a few trends stand out. First, the sex-interaction observed in the right temporal pole is practically identical to what was observed in adolescents, including the location, the gray matter measure implicated (i.e., area), and the cross over patterns observed between males and females (i.e., males: positive relationship; females: negative relationship). This correspondence across the two age groups is particularly noteworthy given the overall lack of correspondence observed for all of the other dimensions. While similar and often overlapping brain regions were associated with internalizing dimensions across the two age groups, in general, the specific internalizing dimension and gray matter measure associated with a given region were largely divergent between the age groups. This similar pattern of results for rumination-specific in the right temporal pole suggest that this region may play a relatively stable role in internalizing psychopathology across adolescence and into young adulthood, something that cannot be said about other regions identified in this study.

A second notable sex-interaction result in young adults were in bilateral insula, where males showed a significant positive relationship between rumination-specific and thickness bilaterally and females showed a significant and non-significant relationship in the left and right insula, respectively. These results are noteworthy in large part due to the overarching question as to the role of the insula in internalizing psychopathology. In young adults looking across all internalizing dimensions, we observed a number of associations with the insula, suggesting a

rather complex, multifaceted role of the insula in internalizing psychopathology. However, across all of these insular findings, rumination-specific was the only dimension showing evidence that increased internalizing behavior was associated with increased gray matter properties, albeit in males only. When looking at underlying differences in neuroanatomy between the sexes, the bilateral insula shows markedly greater thickness in males as opposed to females (see Appendix 4), suggesting that the sex-interaction with rumination-specific may be driven by fundamentally different neuroanatomical organization between the sexes. Finally, we also note that we observed a sex-interaction on the relationship between rumination-specific and the right inferior frontal sulcus, with males and females showing opposing significant positive and negative relationships, respectively. This result is particularly notable in the context of the multitude of other findings implicating both the right and left inferior frontal sulcus across multiple dimensions suggesting that, like the insula, the inferior frontal sulcus may play a multifaceted role in internalizing psychopathology that cannot be reduced to a single behavioral dimension, even in the context of a bifactor model.

4.4.6.3. Rumination-specific summary

We predicted that rumination-specific would be associated with brain regions directly supporting episodic memory, specifically the hippocampus and related medial temporal lobe structures. Within both adolescents and young adults, we found very little evidence supporting this hypothesis, outside of sex interactions on the relationship between rumination-specific and gray matter of the most posterior partition of the parahippocampal gyrus. In fact, for both adolescents and young adults, we found relatively few associations between cortical gray matter

and rumination-specific, though notably found that it was associated with subgenual anterior cingulate gray matter, brain regions commonly affected in internalizing psychopathology that plays a modulatory role over medial temporal structures, including the hippocampus. However, for both age groups separately, we found widely distributed sex interactions, including in lateral prefrontal cortex, both lower-level and higher-level somatosensory regions, and lateral temporal regions.

4.4.7. Parsing regions identified in case-control studies

By implementing a dimensional model of internalizing psychopathology, we hoped to provide an additional level of specificity to gray matter alterations observed in case-control studies. Across multiple internalizing disorders, case-control studies frequently report altered gray matter in patients within the prefrontal cortex, insula, and subcortex. However, such studies often fail to account for comorbidity and overlapping symptomology between disorders, raising questions as to whether or not these alterations in gray matter are specific to certain aspects of internalizing psychopathology. Our analyses allow us to address this question at two levels of granularity: at a coarse ROI level and a fine grain, vertex-wise level.

First, the ROI-based analyses in young adults largely confirmed our hypotheses regarding the brain systems that may support the distinct internalizing dimensions (see figure 5). Specifically, our results suggest that negative affect is associated with brain regions shown to be altered across multiple psychopathologies, namely the insula and caudal anterior cingulate. In line with our predictions that late-developing lateral prefrontal regions would show age-related differences in our more cognitive internalizing dimensions, we found evidence that the

relationships between right middle frontal gyrus and repetitive negative thought, as well as left inferior frontal gyrus and anxious apprehension-specific differ between adolescents and young adults (see figure 19). We also found evidence supporting our hypotheses that low positive affect-specific would be associated with brain regions implicated in reward processing, though these results were largely confined to medial and ventral prefrontal regions, namely the rostral anterior cingulate and orbitofrontal cortex, and not subcortical regions, at least in young adults. In adolescents, however, we found evidence that low positive affect-specific was associated with the amygdala. While not part of the basal ganglia, the subcortical ROI we predicted to be associated with low positive-affect specific, these findings align with an emerging view of amygdalar function as supporting reward processing. Our results suggest that the relationship of the amygdala to internalizing psychopathology appears to change between adolescence and young adulthood, with young adult females showing a relationship between anxious arousal-specific and the amygdala, not low positive affect-specific, as was observed in adolescents. This potential shift in the role of the amygdala in internalizing psychopathology is an intriguing topic of further inquiry and may speak to the source of inconsistencies in the case-control literature as to the role of the amygdala in internalizing disorders.

In addition to confirming a number of our a priori prediction, we found a number of surprising results within our case-control ROIs. Though we had predicted we would find associations between anxious apprehension-specific and the inferior frontal gyrus ROIs when controlling for sex, we instead found anxious apprehension-specific to be associated with the left insula. The inferior frontal gyrus ROIs, on the other hand, showed associations with the two dimensions we believe to be preferentially associated with depression: low positive affect-specific and rumination-specific. These relationships showed a degree of laterality, with left

inferior frontal ROIs showing associations with low positive affect-specific and right inferior fontal ROIs showing associations with rumination-specific.

The whole brain, vertex-wise analyses provided a more nuanced picture into the neuroanatomical correlates of internalizing psychopathology. One of the most striking takeaways from these analyses is the heterogeneous associations observed within specific regions. That is, within many of the regions implicated by case-control studies, we observed associations between gray matter and multiple dimensions, despite the fact that we had parametrized these dimensions to be orthogonal. These findings suggest that, even in the context of a fine-grained dimensional model, ascribing a given region a specific role in internalizing psychopathology may be misguided, as each region likely has a multifaceted relationship with internalizing psychopathology. Furthermore, these relationships appear to be largely age-specific and, in some cases, differ between the sexes. Despite this heterogeneity, some general trends do emerge.

First, within medial orbitofrontal and the immediately adjacent subgenual anterior cingulate regions, there appears to be a laterality effect, with right homologs of these regions preferential associating with the two depression-specific dimensions, namely low positive affect-specific (i.e., adolescence and across adolescence and young adults) and rumination-specific (i.e., young adults). Similar laterality distinctions have been made regarding depression, with multiple studies suggesting the depression may be preferentially associated with right lateral mechanisms (Bruder et al., 2016; Hecht, 2010; Li et al., 2018; Rotenberg, 2004). Remaining within the anterior cingulate, more dorsal portions of right anterior cingulate appear to show preferential associations with the more cognitive dimensions employed in this study, including anxious apprehension-specific (i.e., adolescent males), and repetitive negative thought (i.e., young adults). Indeed, dorsal portions of the anterior cingulate show strong functional

connectivity to lateral and anterior prefrontal regions supporting cognitive control (Beckmann et al., 2009; Jin et al., 2018), supporting models of that anterior cingulate as being central to cognitive behaviors within psychopathology.

Second, within lateral prefrontal cortex, particularly left inferior frontal regions, there appears to be a posterior to anterior gradient that largely mirrors our characterizations of these dimensions as being preferentially associated with cognitive control as opposed to bottom-up affective mechanisms. Within adolescents, anxious arousal-specific was associated with a cluster within mid left lateral prefrontal cortex, spanning both the inferior and middle frontal gyri. Negative affect, on the other hand, a dimension we believe to be driven by the interaction between bottom-up sensory systems and top-down control systems, was associated with a more anterior portions of both the inferior frontal and middle frontal gyri. A similar yet more robust gradient was observed in young adults, albeit with different dimensions. We found evidence that the most posterior portions of lateral prefrontal cortex, namely the inferior frontal junction, was associated with low positive affect-specific in the left hemisphere and anxious arousal-specific in the right hemisphere, dimensions we believe to be largely grounded in bottom-up subcortical reward and threat processing, respectively. In the left hemisphere, immediately anterior, within posterior portions of pars opercularis, we found evidence of associations between gray matter and both low positive affect-specific and negative affect. In the right hemisphere, immediately anterior to the anxious arousal-specific/inferior frontal junction cluster, we found evidence of overlapping associations between rumination-specific and negative affect. Then, in the most anterior portions of bilateral prefrontal cortex, we found associations with repetitive negative thought, the most purely cognitive dimension under our six-dimension framework. To summarize, we observed the following gradient in adults: in the left hemisphere, as you move

anteriorly from the inferior frontal junction towards the frontal pole, we observed associations with low positive affect-specific, to negative affect, to repetitive negative thought. In the right hemisphere, we observe associations with anxious arousal-specific, to rumination-specific and negative affect, to repetitive negative thought. These findings suggest that, while lateral prefrontal regions may show a complex array of associations with internalizing dimensions, distinct subregions appear to be associated with distinct dimensions, with more cognitive dimensions associating with more anterior subregions. This gradient model is similar to other models noted elsewhere, suggesting that the more anterior portions of the prefrontal cortex support more abstract, cognitive representations than more posterior portions (O'Reilly, 2010).

Third, the bilateral insula may have a particularly heterogeneous association with internalizing psychopathology, showing associations with all six internalizing dimensions. Specifically, in adolescents, we found associations between insula gray matter and repetitive negative thought (i.e., left anterior insula), low positive affect-specific (i.e., right posterior insula), and rumination-specific (i.e., right anterior insula). On the other hand, in young adults, we found associations between the insula and negative affect (i.e., bilateral insula), anxious apprehension-specific (i.e., bilateral insula), rumination-specific (i.e., bilateral insula), and anxious arousal-specific (i.e., left anterior insula). These results stand out in the context of previous research showing alterations in insula gray matter across all major psychopathologies (Goodkind et al., 2015). Though the insula does appear to be altered across all disorders, it is unclear if this commonality reflects behaviors that are shared across all disorders or rather distinct behaviors that are all associated with the insula in one way or another. Our current results suggest that both possibilities may be true. In line with a role of the insula in behaviors that are common across internalizing disorders, we find evidence that negative affect and

repetitive negative thought are associated with insular gray matter. However, also supporting dissociable relationships between the insula and multiple distinct behaviors, we found evidence that insular gray matter was associated with all four of the specific dimensions tested in this study.

Finally, subcortical regions may be preferentially associated with low positive affect-specific during adolescence, but may diversify in their relationships to internalizing psychopathology as individuals age. Despite preexisting literature suggesting a prominent role of subcortical structures in internalizing psychopathology, in adolescents, we only observed significant relationships between subcortical gray matter (i.e., the amygdala) and low positive affect-specific. However, in the young adult sample, we observed a number of associations across most of the subcortex, though many of these were marginal, including the caudate (i.e., rumination-specific, anxious arousal-specific, and negative affect), the amygdala (i.e., anxious arousal-specific and negative affect), and the nucleus accumbens (i.e., anxious apprehension-specific). However, because of the far greater statistical power to detect effects in the young adult sample, it is unclear if this discrepancy between the samples reflects an important biological distinction or is merely a result of the different sample sizes between the groups. With that being said, our results highlight the need for further research targeting the development of subcortical systems and their relationship to specific dimensions of internalizing psychopathology.

4.4.8. Conclusions

One of the ongoing challenges facing research on psychopathology is characterizing psychopathology in such a way that both captures the complex behavioral manifestations of psychopathology while simultaneously providing a framework that is tractable. To date, the dominating characterization has treated psychopathology as multiple discrete disorders, with individuals either meeting criteria for a disorder or instead being treated as healthy controls. In the development of alternative characterizations of psychopathology, it is important to show that such characterizations have explanatory power over and above the case-control standard. In this chapter, we demonstrated that a six factor dimensional characterization of the internalizing psychopathology provides a more nuanced mapping of the brain systems associated with psychopathology than can be obtained from case-control studies alone. Specifically, we showed that brain regions which frequently show alterations in gray matter across patients of all internalizing disorders can be differentiated into associations with specific internalizing behaviors. Furthermore, we provide evidence that individual differences in these internalizing behaviors are associated with brain regions outside of those regions commonly implicated in case-control studies, suggesting that the neural systems associated with internalizing behaviors are multifaceted, and distributed throughout much of the brain. We also find evidence that demographic variables, including age and sex, may have profound effects on the relationship between internalizing psychopathology and the brain, highlighting the need to closely consider development and sex in the etiology of psychopathology. We hope that these findings may inform future research into internalizing psychopathology by promoting the use of both dimensional models of psychopathology and analyses that explicitly test for age and sex related effects

CHAPTER 5

GENETIC AND ENVIRONMENTAL INFLUENCES ON INTERNALIZING DIMENSIONS AND ASSOCIATED GRAY MATTER

5.1. Introduction

Central to understanding the etiology of psychopathology is differentiating the contributions of genes and the environment to pathological behaviors and relevant endophenotypes. Psychopathology runs in families (e.g., Kendler et al., 1997) but determining whether this familial transmission is due to shared genes or shared environment has proven to be a challenge. Looking across decades of twin and family studies, there is strong evidence that risk for most psychopathologies are influenced by genetic and non-shared environmental factors. On the other hand, evidence of shared environmental influences remains comparatively scant (for a review, see section 2.3). Meta-analyses of twin and family studies suggest additive genetic and non-shared environmental influences on diagnostic status for most internalizing disorders, including MDD (Sullivan et al., 2000), GAD (Kendler et al., 1992; Roy et al., 1995), and OCD (Taylor, 2011), with some evidence of shared environmental effects influencing PTSD (Afifi et al., 2010). Yet these findings are not universal. For example, Ehringer and colleagues found evidence that GAD and MDD in adolescents may indeed be influenced by shared environmental factors (Ehringer et al., 2006). Furthermore, heritability estimates of behavioral dimensions fundamental to internalizing disorders suggest that many of the behaviors that are characteristic of internalizing psychopathology including anxiety/depression symptoms (Hansell et al., 2012), somatic anxiety (Gustavsson et al., 1996), and worry (Warren et al., 1999) are indeed influenced by shared environmental factors. As is the case with research into the neural correlates of

psychopathology, research into the genetic and environmental contributions to psychopathology can be bolstered by implementing dimensional models that parse internalizing behaviors into orthogonal behavioral constructs. In doing so, researchers are afforded a degree of specificity that is lacking in genetic studies of diagnostic status.

In addition to understanding the relative contributions of genes and the environment to internalizing psychopathology, it is important to understand the biological endophenotypes that bridge genes to behavior. In the case of psychopathology, functional and structural properties of brain are the most obvious and likely domain for identifying endophenotypes. Because gray matter morphometry is heritable (e.g., Winkler et al., 2010), highly reliable (e.g., Elliot et al., 2020), and associated with a broad array of clinical phenotypes (e.g., diagnoses: e.g. Goodkind et al., 2015; symptom dimensions: e.g. Koutsouleris et al., 2008; treatment response: e.g. Lyoo et al., 2010), it may be a particularly useful methodology to explore the biological basis of psychopathology. To date, of the handful of studies investigating the genetic and environmental contributions to the relationships between psychopathology and gray matter, the vast majority have focused on schizophrenia (e.g., Brans et al., 2008; Rijsdijk et al., 2005; van Haren et al., 2012), generally reporting overlapping genetic influences on diagnostic status and gray matter endophenotypes. However, there is a dearth of studies investigating shared genetic and environmental influences between internalizing psychopathology and gray matter morphometry. Of the studies that have evaluated the genetic and environmental contributions to internalizing psychopathology and gray matter, the majority have employed a discordant monozygotic twin design, in which gray matter volume from a region of interest is compared between monozygotic twin pairs concordant or discordant for a given diagnosis (Alemany et al., 2013; de Gues et al., 2007). These studies report mixed results, with some studies suggesting that genetic risk for

psychopathology underlies properties of gray matter structure (e.g., Alemany et al., 2013) with others suggesting environmental risk underlies these properties (e.g., de Gues et al., 2007). The power of such designs is predominately to identify influences of non-shared environmental factors and, in the absence of dizygotic twins, it is difficult to parse additive genetic, shared environmental, and non-shared environmental influences. To do this, it is best to utilize classic twin methodologies in which researchers collect data on both monozygotic and dizygotic twins and leverage the fact that monozygotic twins are genetically identical whereas dizygotic twins share only half their genes. The lack of classic twin studies on the relationship between internalizing psychopathology and gray matter is likely due to the difficulty in obtaining adequately powered twin samples, compounded with the relatively high costs and technical expertise required for neuroimaging. Despite this challenge, elucidating the degree to which relationships between the brain and behavior can be explained by shared genetic and/or environmental mechanisms is an emerging area of interest. For example, the Adolescent Brain Cognitive Development (ABCD) study, a landmark longitudinal neurodevelopmental project, has prioritized collecting a substantial twin sample to better understand how the influence of genes and the environment on the brain and behavior unfolds across adolescence (Iacono et al., 2018). However, the field of imaging genetics remains in a nascent stage, with many important questions remaining unanswered (for a review, see Nathoo et al., 2019).

To date, much of the imaging genetics literature has focused on understanding the contributions of genes and the environment to basic properties of the brain, particularly gray matter morphometry (for a review, see Blokland et al., 2012; Jansen et al., 2015). Univariate twin studies of gray matter morphometry suggest that the heritability of gray matter structure is dependent on the specific property of gray matter investigated (i.e., volume, surface area or

thickness) and is highly variable across the brain. Though gray matter volume is phenotypically correlated with surface area and cortical thickness, cortical thickness and surface area are largely orthogonal (Winkler et al., 2010) and under distinct genetic control (Panizzon et al., 2009). This underscores the importance of simultaneously considering volume, surface area, and thickness when evaluating the neuroanatomical correlates of psychopathology, as they may not only capture distinct functional properties of the brain (Panizzon et al., 2009; Rakic, 1995), but may also be shaped by distinct genetic and environmental influences. While whole brain measures of gray matter morphometry show high degrees of heritability (i.e., volume: h^2= .696; thickness: h^2= .691; surface area: h^2= .705), distinct brain regions show a wide range of heritability estimates (Winkler et al., 2010). Collapsing across both hemispheres and controlling for whole brain morphometry, heritability of cortical brain regions has been estimated to range for as low as h^2=.07 (i.e., thickness of temporal pole) and to as high as h^2=.73 (i.e., thickness of precentral gyrus) (Winkler et al., 2010), with some but limited evidence of shared environmental influences on gray matter morphometry (Joshi et al., 2011). Interestingly, though the heritability of volume of subcortical brain regions is also largely region-dependent, in general, subcortical structures show a higher degree of heritability than the cortex (den Braber et al., 2013).

Our research group stands out for performing a well powered imaging genetics study decomposing relationships between dimensional characterization of internalizing psychopathology and neuroanatomy into additive genetic, shared environmental, and non-shared environmental components. Specifically, Hatoum and colleague (2019) identified areas in the brain where the genetic influence of cortical thickness was overlapping with dimensional characterizations of depression severity and callousness/unemotionality. In related work, researchers evaluated the degree to which individual differences in negative emotionality, a

proxy for negative affect, and positive emotionality, a proxy for low positive affect, show genetic and environmental correlations with gray matter volume in regions of interest (Lewis et al., 2014). Specifically, Lewis and colleagues (2014) found that positive emotionality and left amygdala volume had partially overlapping genetic influences whereas negative emotionality and medial orbitofrontal cortex volume showed partially overlapping genetic and non-shared environmental influences. This study largely aligns with the current project, though we extend this work by employing a six factor dimensional model of internalizing psychopathology and by evaluating the genetic and environmental influences on gray matter clusters that were selected based on a phenotypic relationship with a given dimension.

In the current study, we apply twin modeling to evaluate the genetic and environmental contributions to the six factor internalizing dimension model discussed in Chapter 3, the gray matter correlates of this model in young adults identified in Chapter 4, and their relationships. To do this, we utilize univariate and bivariate twin modeling techniques. First, employing univariate twin models, we identify the contributions of genetic, shared-, and non-shared environmental influences to factor scores of the six internalizing dimensions. Then, using bivariate twin models, we identify the genetic and environmental correlations between each dimension and all associated gray matter clusters, separately.

5.2. Methods

5.2.1. Participants

Participants consisted of the young adult subsample utilized in Chapters 3 and 4, which included same-sex twin pairs and singletons from the Institute for Behavioral Genetics' Longitudinal Twin Study (LTS) (N= 630; 284 males/346 females; Age= 28.7 (.8)).

5.2.2. Internalizing Dimension Factor Scores

Internalizing dimension factor scores were drawn from the CFA discussed in Chapter 3 and were the same as those employed in the surface-based morphometry analyses discussed in Chapter 4. We elected to perform twin analyses on the factor scores instead of at the latent level because of our desire to run bivariate twin analyses on the relationship between the internalizing dimensions and associated gray matter morphometry. Because the gray matter morphometry analyses discussed in Chapter 4 were conducted on factor scores, we elected to use factor scores in twin models to remain consistent.

5.2.3. Gray Matter Morphometry Regions of Interest

Twin analyses were performed on the properties of gray matter relevant to internalizing psychopathology identified in Chapter 4, including both ROIs and clusters identified in whole brain exploratory analyses. At the ROI level, this included testing for the genetic and

environmental correlations between the following: negative affect and volume and thickness of the left insula, volume of the right insula, and volume of the right caudal anterior cingulate; anxious apprehension-specific and thickness of the left insula, low positive affect-specific and area of left lateral orbitofrontal cortex, area and volume of right lateral orbitofrontal cortex, area and thickness of left rostral anterior cingulate, and volume of left pars triangularis, and rumination-specific and area of right pars opercularis. Repetitive negative thought and anxious arousal-specific showed no significant relationships with ROI gray matter when controlling for sex.

5.2.4 Structural Equation Modeling: ACE Twin Models

All twin analyses were carried out using Mplus. Univariate twin analyses were conducted testing for the relative contribution of additive genetic (A), shared environmental (C), and non-shared environmental (E) influences on individual differences in internalizing factor scores. As is customary, A was set to correlate at 1 within MZ twin pairs and .5 within DZ pairs, reflecting the degree of genetic similarity between twin pairs, C was set to correlate at 1 within both MZ and DZ twin pairs, and E was not set to correlate between twin pairs. To evaluate the degree to which significant relationships between internalizing dimension factor scores and gray matter identified in Chapter 4 were driven by overlapping genetic and/or environmental influences, we carried out bivariate Cholesky decompositions. These analyses allowed us to determine the genetic (rA), shared environmental (rC), and non-shared environmental (rE) correlations between phenotypically associated factor scores and gray matter. To evaluate the best fitting bivariate genetic models, we performed chi-square difference tests comparing a bivariate ACE model to

AE, CE, and E models. Prior to genetic analyses, internalizing factor scores were residualized by gender and age and gray matter clusters were residualized by gender, age, scanner software version and the appropriate whole brain morphometry measure (i.e., total intracranial volume for volume, total surface area for surface area, and mean cortical thickness for cortical thickness).

5.3. Results

5.3.1. Univariate Twin Models

5.3.1.1. Internalizing Dimension

Mz/Dz correlations of internalizing dimension factor scores can be seen in table 14. Mz/Dz correlations were as follows: negative affect: r_{MZ}= .492(.357-.607 95% confidence interval), r_{DZ}= .194(.022-.356 95% confidence interval); repetitive negative thought: r_{MZ}= .204(.041-.356 95% confidence interval), r_{DZ}= .072(-.103-.243 95% confidence interval). Anxious arousal-specific: r_{MZ}= .113(-.052-.272 95% confidence interval), r_{DZ}= .138(-.036-.305 95% confidence interval); anxious apprehension-specific: r_{MZ}= .390(.241-.521 95% confidence interval), r_{DZ}= .333(.169-.479 95% confidence interval); low positive affect-specific: r_{MZ}= .392(.244-.523 95% confidence interval), r_{DZ}= .103(-.073-.271 95% confidence interval); rumination-specific: r_{MZ}= .229(.067-.379 95% confidence interval), r_{DZ}= .013(-.160-.187 95% confidence interval).

	Negative Affect	Repetitive Negative Thinking	Anxious Arousal-specific	Anxious Apprehension-specific	Low Positive Affect-specific	Rumination-specific
Mz	.492 (.357-.607)	.204 (.041-.356)	.113 (-.052-.272)	.390 (.241-.521)	.392 (.244-.523)	.229 (.067-.379)
Dz	.194 (.022-.356)	.072 (-.103-.243)	.138 (-.036-.305)	.333 (.169-.479)	.103 (-.073-.271)	.013 (-.160-.187)

Table 14. Mz/Dz twin correlations of internalizing factor scores. Within twin pair twin correlations split by monozygotic (Mz) and dizygotic (Dz) twin pairs, separately. Parentheses show 95% confidence interval.

For full results of ACE twin models, including heritability estimates, see table 15. For negative affect (a^2 = .47(.36-.59 95% confidence interval) e^2= .53(.43-.65 95% confidence interval)), repetitive negative thought (a^2 = .23(.11-.39 95% confidence interval) e^2= .77(.64-.92 95% confidence interval)), low positive affect-specific (a^2 = .34(.23-.47 95% confidence interval) e^2= .66(.55-.79 95% confidence interval)), and rumination-specific (a^2 = .21(.09-.38 95% confidence interval) e^2= .79(.65-.95 95% confidence interval)), ACE models found no evidence of significant contributions of C, with AE models providing the best fit for all of these dimensions. On the other hand, for anxious arousal-specific (c^2 = .13(.04-.27 95% confidence interval) e^2= .87(.76-.99 95% confidence interval)) and anxious apprehension-specific (c^2 = .42(.32-.54 95% confidence interval) e^2= .58(.49-.69 95% confidence interval)) the best fitting models were CE models. However, for anxious arousal-specific, both the AE and CE models provided better fits than the ACE models and the difference in fit between the two models was negligible.

		Parameters			Model Fit			Comparison to ACE		
Dimension	***Model***	a^2	c^2	e^2	χ^2	*df*	*p*	$\Delta\chi^2$	Δdf	*p*
NA	ACE	.47 (.36-.59)	0 (0-1)	.53 (.43-.65)	5.51	6	0.48	-	-	-
	*AE	.47 (.36-.59)	-	.53 (.43-.65)	5.51	7	0.60	0	1	1
	CE	-	.37 (.28-.48)	.63 (.53-.73)	10.79	7	0.15	5.28	1	.02
	E	-	-	1	50.87	8	<.001	45.35	2	<.001
RNT	ACE	.23 (.11-.39)	0 (0-1)	.77 (.64-.92)	5.80	6	0.45	-	-	-
	*AE	.23 (.11-.39)	-	.77 (.64-.92	5.80	7	0.56	0	1	1
	CE	-	.17 (.08-.31)	.83 (.71-.95)	6.88	7	0.44	1.08	1	.30
	E	-	-	1	14.99	8	0.06	9.19	2	.01
AA	ACE	0 (0-1)	.13 (.04-.27)	.87 (.76-.99)	1.98	6	0.92	-	-	-
	^AE	.16 (.04-.34)	-	.84 (.70-1)	2.55	7	0.92	0.57	1	.45
	*CE	-	.13 (.04-.27)	.87 (.76-.99)	1.98	7	0.96	0	1	1
	E	-	-	1	6.61	8	0.58	4.63	2	.10
AAp	ACE	.04 (0-1)	.39 (.13-.77)	.58 (.46-.70)	6.80	6	0.34	-	-	-
	AE	.46 (.35-.57)	-	.54 (.44-.70)	11.36	7	0.12	4.56	1	.03
	*CE	-	.42 (.32-.54)	.58 (.49-.69)	6.84	7	0.45	0.04	1	.85
	E	-	-	1	56.74	8	<.001	49.94	2	<.001
LPA	ACE	.34 (.23-.47)	0 (0-.38)	.66 (.55-.79)	6.48	6	0.37	-	-	-
	*AE	.34 (.23-.47)	-	.66 (.55-.79)	6.48	7	0.49	0	1	1
	CE	-	.27 (.17-.38)	.73 (.63-.85)	10.40	7	0.17	3.92	1	.048
	E	-	-	1	31.19	8	<.001	24.71	2	<.001
R	ACE	.21 (.09-.38)	0 (0-.26)	.79 (.65-.95)	7.13	6	0.31	-	-	-
	*AE	.21 (.09-.38	-	.79 (.65-.95)	7.13	7	0.42	0	1	1
	CE	-	.12 (.04-.26)	.88 (.77-.99)	10.00	7	0.19	2.88	1	.09
	E	-	-	1	14.45	8	0.07	7.32	2	.03

Table 15. Univariate ACE twin models of internalizing dimension factor scores. Model comparison results from univariate ACE models of internalizing dimension factor scores. "a^2"= variance in internalizing dimensions accounted for by additive genetic effects with 95% confidence interval in parentheses; "c^2"= variance in internalizing dimensions accounted for by shared environmental effects with 95% confidence interval in parentheses; "e^2"= variance in internalizing dimensions accounted for by non-shared environmental effects with 95% confidence interval in parentheses. "χ^2" = chi-square value of model. "df"= degrees of freedom of model. "p"= p-value of chi-square model fit. "$\Delta\chi^2$"= difference in chi-square value between a given model and the ACE model

used in chi-square difference tests; "Δ*df*"= differences in degrees of freedom between a given model and the ACE model used in chi-square differences tests. *= indicates best fitting model for a given internalizing dimension.

5.3.1.2. Gray matter morphometry

Results from univariate ACE models of ROIs and exploratory clusters can be seen in table 16. To summarize ACE models of gray matter from the ROIs, we found that an AE model provided the best fit for all ROIs except for area of the right parietal operculum, which was best described by a CE model. For the exploratory whole brain clusters, we found a number of instances in which AE, CE, or E were the best fitting models. We summarize these results by the internalizing dimension a specific cluster was associated with.

For clusters associated with *negative affect*, an AE model provided the best fit for volume of the left central operculum, volume of the right precentral gyrus, thickness of the left insula, thickness of the left inferior frontal sulcus, thickness of the left medial orbitofrontal cortex, and thickness of the right postcentral gyrus. CE model provided the best fit for thickness of the right insula, thickness of the right precentral gyrus, and thickness of the right inferior frontal gyrus, and an E model provided that best for area of the left temporoparietal junction.

For clusters associated with *repetitive negative thought*, an AE model provided the best fit for area of the right lingual gyrus, volume of the left superior frontal gyrus, volume of the left lingual gyrus, volume of the right lingual gyrus, volume of the right inferior parietal lobe, and thickness of the left medial superior frontal gyrus. CE model provided the best fit for volume of the right posterior cingulate and thickness of the right lingual gyrus, and an E only model provide the best fit for thickness of the right anterior cingulate.

For *anxious arousal-specific*, an AE model provided the best fit volume of the left temporal pole, thickness of the left paracentral lobule, and thickness of the left calcarine fissure,

a CE model provided the best fit for volume of the right lateral occipital cortex, thickness of the left anterior insula, and thickness of the right inferior frontal junction, and an E only model provided the best fit for area and volume of left postcentral gyrus.

For *anxious apprehension-specific*, an AE model provided the best fit for area and volume of the left lingual gyrus, area of the left cuneus, area of the right medial occipital cortex, volume of the left entorhinal cortex, volume of the left posterior cingulate, volume of the right insula, thickness of the left and right entorhinal cortex, thickness of the right temporal pole and a CE model provided the best fit for volume of the left ventral insula.

For *low positive affect-specific*, an AE model provided the best fit for volume of the right superior temporal gyrus and thickness of the left posterior inferior frontal gyrus and a CE model provided the best fit for thickness of the left inferior frontal junction.

For *rumination-specific*, an AE model provided the best fit for volume of the right subgenual cingulate and thickness of the left temporal sulcus.

Dimens-ion	Region	Best Fit Model	a^2	c^2	e^2
NA	lh insula volume	AE	.58 (.50-.67)	-	.42 (.33-.51)
	lh insula thickness	AE	.39 (.29-.52)	-	.61 (.49-.73)
	rh insula volume	AE	.50 (.40-.61)	-	.50 (.40-.61)
	rh cACC volume	AE	.27 (.15-.43)	-	.73 (.59-.88)
AAp	lh insula thickness	AE	.39 (.29-.52)	-	.61 (.49-.73)
LPA	lh lOFC area	AE	.28 (.16-.44)	-	.72 (.59-.87)
	rh lOFC area	AE	.25 (.13-.41)	-	.75 (.61-.90)
	rh lOFC volume	AE	.43 (.31-.56)	-	.57 (.45-.71)
	lh rACC area	AE	.37 (.26-.51)	-	.63 (.51-.76)
	lh rACC thickness	AE	.47 (.35-.60)	-	.53 (.42-.66)
	lh p. triang. volume	AE	.29 (.17-.45)	-	.71 (.58-.85)
R	rh p. operc. area	CE	-	.11 (.02-.26)	.89 (.78-1)
NA	lh temporoparietal junction area	E	-	-	1

	lh central operculum volume	AE	.43 (.32-.57)	-	.57 (.45-.70)
	rh precentral gyrus volume	AE	.32 (.20-.47)	-	.68 (.82-.55)
	lh insula thickness	AE	.39 (.27-.52)	-	.61 (.49-.75)
	lh inferior frontal sulcus thickness	AE	.30 (.18-.45)	-	.70 (.57-.85)
	lh medial orbitofrontal thickness	AE	.20 (.08-.37)	-	.80 (.66-.95)
	rh insula thickness	CE	-	.39 (.30-.50)	.61 (.51-.71)
	rh precentral gyrus thickness	CE	-	.14 (.05-.28)	.86 (.75-98)
	rh postcentral gyrus thickness	AE	.43 (.29-.59)	-	.57 (.46-.70)
	rh inferior frontal gyrus thickness	CE	-	.15 (.05-.29)	.85 (.74-.97)
AA	lh postcentral gyrus area	E	-	-	1
	lh postcentral gyrus volume	E	-	-	1
	lh temporal pole volume	AE	.44 (.34-.57)	-	.56 (.44-.68)
	rh lateral occipital cortex volume	CE	-	.07 (0-.24)	.93 (.81-1)
	lh anterior insula thickness	CE	-	.35 (.25-.46)	.65 (.55-.76)
	lh paracentral lobule thickness	AE	.31 (.20-.45)	-	.69 (.57-.82)
	lh calcarine fissure thickness	AE	.43 (.31-.56)	-	.57 (.45-.70)
	rh inferior frontal junction thickness	CE	-	.13 (.04-.27)	.87 (.76-.99)
LPA	rh superior temporal gyrus volume	AE	.23 (.11-.38)	-	.77 (.65-.91)
	lh po. inferior frontal gyrus thickness	AE	.33 (.20-.50)	-	.67 (.53-.82)
	lh inferior frontal junction thickness	CE	-	.27 (.17-.39)	.73 (.62-.84)
AAp	lh lingual gyrus area	AE	.57 (.47-.67)	-	.44 (.34-.54)
	lh cuneus area	AE	.39 (.26-.55)	-	.61 (.49-.74)
	rh medial occipital cortex area	AE	.60 (.51-.70)	-	.40 (.31-.50)
	lh lingual gyrus volume	AE	.49 (.39-.61)	-	.51 (.40-.63)
	lh entorhinal cortex volume	AE	.26 (.14-.41)	-	.74 (.61-.89)
	lh ventral insula volume	CE	-	.35 (.26-.46)	.65 (.55-.75)
	lh posterior cingulate volume	AE	.35 (.22-.50)	-	.65 (.52-.80)
	rh insula volume	AE	.54 (.45-.65)	-	.45 (.36-.56)
	lh entorhinal cortex thickness	AE	.31 (.19-.46)	-	.69 (.56-.83)
	rh entorhinal cortex thickness	AE	.42 (.31-.54)	-	.58 (.47-.71)
	rh temporal pole thickness	AE	.60 (.51-.70)	-	.40 (.31-.50)
R	rh subgenual cingulate volume	AE	.23 (.10-.41)	-	.77 (.63-.93)
	lh superior temporal sulcus thickness	AE	.18 (.06-.36)	-	.82 (.65-1)
RNT	rh lingual gyrus area	AE	.49 (.39-60)	-	.51 (.41-.62)
	lh superior frontal gyrus volume	AE	.28 (.16-.43)	-	.72 (.59-.87)

	lh lingual gyrus volume	AE	.62 (.52-.71)	-	.38 (.29-.49)
	rh lingual gyrus volume	AE	.59 (.50-69)	-	.41 (.32-.51)
	rh inferior parietal lobe volume	AE	.39 (.26-.54)	-	.61 (.48-.76)
	rh posterior cingulate volume	CE	-	.21 (.11-.34)	.79 (.68-.91)
	lh med. sup. frontal gyrus thickness	AE	.26 (.13-.43)	-	.74 (.60-.89)
	rh lingual gyrus thickness	CE	-	.34 (.21-.51)	.66 (.52-.81)
	rh anterior cingulate thickness	E	-	-	1

Table 16. Univariate ACE twin models of gray matter regions associated with each dimension. Results from best fitting univariate ACE models. "Best Fit Model" indicates the best fitting model as determined by Chi-square difference test. "a_2"= variance in gray matter accounted for by additive genetic effects with 95% confidence interval in parentheses; "c_2"= variance in gray matter accounted for by shared environmental effects with 95% confidence interval in parentheses; "e_2"= variance in gray matter accounted for by non-shared environmental effects with 95% confidence interval in parentheses.NA= negative affect; RNT= repetitive negative thought; AA= anxious arousal-specific; AAp= anxious apprehension-specific; LPA= low positive affect-specific; R= rumination-specific; lh= left hemisphere; rh= right hemisphere; cACC= caudal anterior cingulate; lOFC= lateral orbitofrontal cortex; rACC= rostral anterior cingulate; p. triang.= pars triangularis; p. operc.= pars opercularis; po.= posterior; med. sup.= medial superior.

5.3.2. Bivariate Twin Models of Internalizing Dimensions and Gray Matter

Results from bivariate ACE model evaluating genetic, shared environmental, and non-shared environmental correlations can be seen in table 17.

Dimens-ion	Region	Best Fit Model	rA (SE)	rC (SE)	rE (SE)	rP
Regions of Interest						
NA	lh insula volume	AE	-.22 (.26)	-	.01 (.08)	-.11
	lh insula thickness	AE	-.21 (.12)	-	-.02 (.07)	-.10
	rh insula volume	AE	-.12 (.10)	-	-.07 (.07)	-.10
	rh cACC volume	AE	-.10 (.15)	-	-.08 (.07)	-.10
AAp	lh insula thickness	AE	-.17 (.12)	-	-.08 (.07)	-.12
LPA	lh lOFC area	AE	-.19 (.17)	-	-.07 (.07)	-.10
	rh lOFC area	AE	-.35 (.17)	-	.01 (.07)	-.10
	rh lOFC volume	AE	-.21 (.13)	-	-.02 (.07)	-.10
	lh rACC area	AE	-.09 (.15)	-	.18 (.07)	.08
	lh rACC thickness	AE	-.19 (.13)	-	-.07 (.07)	-.11

	lh p. triang. Volume	AE	-.13 (.16)	-	-.10 (.07)	-.11
R	rh p. operc. Area	AE	-.05 (.37)	-	.13 (.07)	.10
Exploratory Whole Brain Clusters						
NA	lh temporoparietal junction area	AE	-.96 (1.96)	-	-.06 (.07)	-.14
	lh central operculum volume	AE	-.24 (0.11)	-	-.12 (.08)	-.18
	rh precentral gyrus volume	AE	-.35 (.14)	-	-.05 (.07)	-.17
	lh insula thickness	AE	-.36 (.12)	-	-.04 (.08)	-.17
	lh inferior frontal sulcus thickness	AE	-.42 (13)	-	-.05 (.07)	-.19
	lh medial orbitofrontal thickness	AE	-0.32 (0.17)	-	-0.08 (.07)	-.17
	rh insula thickness	AE	-0.22 (.11)	-	-0.12 (.07)	-.18
	rh precentral gyrus thickness	AE	-1 (0)	-	-0.03 (.07)	-.15
	rh postcentral gyrus thickness	AE	-0.21 (.11)	-	-0.12 (.07)	-.17
	rh inferior frontal gyrus thickness	AE	-.34 (.22)	-	-.05 (.07)	-.12
AA	lh postcentral gyrus area	E	-	-	-.15 (.07)	-.15
	lh postcentral gyrus volume	E	-	-	-.17 (.04)	-.17
	lh temporal pole volume	AE	-.37 (.21)	-	-.74 (.07)	-.14
	rh lateral occipital cortex volume	CE		-.26 (.23)	-.10 (.06)	-.16
	lh anterior insula thickness	CE	-	.22 (.20)	-.18 (.06)	-.18
	lh paracentral lobule thickness	AE	-.25 (.23)	-	-.15 (.07)	-.16
	lh calcarine fissure thickness	AE	-.07 (.21)	-	-.18 (.07)	-.15
	rh inferior frontal junction thickness	CE	-	-.04 (.33)	-.17 (.06)	-.15
LPA	rh superior temporal gyrus volume	AE	-.36 (.18)	-	-.06 (.07)	-.14
	lh po. Inferior frontal gyrus thickness	AE	-.29 (.15)	-	-.09 (.07)	-.16
	lh inferior frontal junction thickness	AE	-.28 (.14)	-	-.16 (.07)	-.19
AAp	lh lingual gyrus area	AE	.38 (.10)	-	-.04 (.07)	.16
	lh cuneus area	CE	-	.31 (.13)	.10 (.06)	.17
	rh medial occipital cortex area	AE	.26 (.10)	-	.13 (.07)	.19
	lh lingual gyrus volume	AE	.36 (.11)	-	.04 (.07)	.18
	lh entorhinal cortex volume	CE	-	.35 (.16)	.07 (.06)	.15
	lh ventral insula volume	CE	-	-.30 (.12)	-.13 (.06)	-.19
	lh posterior cingulate volume	AE	-.53 (.13)	-	.08 (.08)	-.15
	rh insula volume	AE	-.19 (.10)	-	-.15 (.07)	-.16
	lh entorhinal cortex thickness	AE	.40 (.14)	-	.01 (.07)	.16
	rh entorhinal cortex thickness	CE	-	.26 (.12)	.13 (.06)	.17
	rh temporal pole thickness	CE	-	-.34	-.09	-.16

				(.15)	(.06)	
R	rh subgenual cingulate volume	AE	-.26 (.26)	-	-.12 (.07)	-.15
	lh superior temporal sulcus thickness	AE	-.19 (.28)	-	-.16 (.07)	-.16
RNT	rh lingual gyrus area	AE	-.31 (.17)	-	-.05 (.07)	-.13
	lh superior frontal gyrus volume	AE	.13 (.23)	-	.14 (.07)	.13
	lh lingual gyrus volume	AE	-.38 (.16)	-	-.09 (.08)	-.18
	rh lingual gyrus volume	AE	-.34 (.16)	-	-.07 (.08)	-.15
	rh inferior parietal lobe volume	AE	.03 (.20)	-	-.22 (.07)	-.15
	rh posterior cingulate volume	CE	-	-.59 (.28)	-.06 (.06)	-.15
	lh med. sup. Frontal gyrus thickness	AE	-.19 (.24)	-	-.15 (.07)	-.16
	rh lingual gyrus thickness	CE	-	.21 (.20)	-.15 (.06)	-.16
	rh anterior cingulate thickness	CE	-	.31 (.22)	-.09 (.06)	-.13

Table 17. Bivariate ACE twin models of internalizing factor scores and associated gray matter. Results from best fitting bivariate Cholesky decomposition model of relationships between internalizing dimension and gray matter ROI or cluster. "Best Fit Model" indicates the best fitting bivariate Cholesky decomposition between the given dimension and gray matter ROI or cluster. "rA" indicates genetic correlation coefficient between a given dimension and gray matter ROI or cluster. "rC" indicates shared environmental correlation coefficient between a given dimension and gray matter ROI or cluster. "rE" indicates the non-shared environmental correlation coefficient between a given dimension and gray matter ROI or cluster. "rP" indicates the phenotypic correlation between a given dimension and gray matter ROI or cluster. Standard error of coefficients shown in parentheses. NA= negative affect; RNT= repetitive negative thought; AA= anxious arousal-specific; AAp= anxious apprehension-specific; LPA= low positive affect-specific; R= rumination-specific; lh= left hemisphere; rh= right hemisphere; cACC= caudal anterior cingulate; lOFC= lateral orbitofrontal cortex; rACC= rostral anterior cingulate; p. triang.= pars triangularis; p. operc.= pars opercularis; po.= posterior; med. sup.= medial superior.

In the following, we summarize the best fitting bivariate models from these analyses. For all bivariate Cholesky decompositions between internalizing dimensions and ROIs, an AE model provided the best fit, with rA estimates ranging from -.35 to -.05. In analyses on the exploratory whole brain clusters, we found that AE bivariate Cholesky decompositions provided the best fit for all clusters associated with *negative affect*, with rA estimates ranging from -1 to -.21.

For *repetitive negative thought*, AE bivariate Cholesky decompositions provided the best fit for all clusters excluding the right posterior cingulate volume cluster and the right lingual gyrus and anterior cingulate thickness clusters. For these three clusters, a CE model provided the best fit. rA estimates ranged from -.38 to .03 whereas rC estimates ranged from -.59 to .31.

For *anxious arousal-specific,* AE bivariate Cholesky decompositions provided the best fit for volume of a cluster in left temporal pole and thickness of clusters in left paracentral lobule and calcarine fissure. CE bivariate models provided the best for volume of a cluster right lateral occipital cortex and thickness of clusters in left anterior insula and right inferior frontal junction. E only bivariate models provided the best fit for area and volume of clusters in the left postcentral gyrus. rA estimates ranged from -.37 to -.07 whereas rC estimates ranged from -.04 to .22.

For *anxious apprehension-specific,* AE bivariate Cholesky decompositions provided the best fit for area of clusters in left lingual gyrus and right medial occipital cortex, volume of clusters in left lingual gyrus, left posterior cingulate, and right insula, as well as thickness of a cluster in left entorhinal cortex. CE bivariate models provided the best fit for volume of clusters in volume of a cluster in left entorhinal cortex, area of a cluster in left cuneus, and thickness of clusters in right entorhinal cortex and temporal pole. rA estimates ranged from -.53 to .40 whereas rC estimates ranged from -.34 to .35.

For *low positive affect-specific,* an AE bivariate Cholesky decomposition provided the best for all three associated whole brain clusters. rA estimates ranged from -.38 to -.26.

For *rumination-specific,* an AE Cholesky decomposition provided the best fit for both relevant clusters, with rA estimates of -.26 and -.19.

5.4. Discussion

In the current chapter, we employed classical twin designs to evaluate the degree to which genetic and environmental influences are driving individual differences in internalizing

psychopathology. Our univariate results suggest that while most of the internalizing dimensions are driven by additive genetic and non-shared environmental factors, two dimensions we believe to be preferentially associated with anxiety showed some evidence of shared environmental influences, particularly anxious apprehension-specific. We also found evidence that the relationships between the internalizing dimensions and cortical gray matter are largely driven by overlapping genetic influences.

5.4.1 Heritability of Internalizing Dimensions

Previous research into the comorbidity between internalizing disorders suggests that the co-occurrence of multiple disorders within a given individual are largely due to additive genetic influences (Alegrini et al., 2020; Selzman et al., 2018). Under this framework, there exist a number of genes that confer a general susceptibility to psychopathology, regardless of the disorder. Our results largely confirm this model, with both negative affect and repetitive negative thought showing significant evidence of additive genetic effects, albeit to a greater degree in negative affect. Importantly, we believe that at least a portion of the variance in negative affect may not necessarily be specific to internalizing psychopathology, but rather captures variance that is attributable to a general p-factor (e.g., Caspi et al., 2014). Converging evidence from family, twin, and molecular genetics research suggest that the p-factor is moderately heritable, with family-based estimates of heritability in adults (Selzam et al., 2018) and adolescents (Alegrini et al., 2020) aligning with our current estimate of about ~50% of the variability in negative affect arising from additive genetic influences and the other ~50% arising for non-shared environmental influences.

To our knowledge, no study has evaluated the heritability of repetitive negative thought, particularly in the context of a bifactor model. Though the difference in model fit between the AE and CE models was only slightly better for the AE model, comparing Mz/Dz correlations suggests that repetitive negative thought is indeed influenced by genes, though potentially in a non-additive fashion. Even still, the genetic contributions to repetitive negative thought appear to be small as compared to the effects of non-shared environmental contributions, with non-shared environmental factors accounting for 77% of the variance in repetitive negative thought. Though not assessing repetitive negative thought per se, previous longitudinal analyses of developmental risk factors for rumination suggest that exposure to negative stressful life events may serve as an environmental factor driving rumination later in life (Johnson, 2015). Because repetitive negative thought is a central process in rumination, it is possible that frequent or particularly impactful negative life events may be one of the environmental mechanisms driving the influence of non-shared environmental factors on repetitive negative thought.

While there has been relatively little evidence of shared environmental influences on internalizing psychopathology, when researchers have found shared environmental effects, they have often been with anxiety-related phenotypes, including PTSD (Afifi et al., 2010) and GAD (Ehringer et al., 2006) diagnoses, as well as on dimensions analogous to anxious arousal (Gustavsson et al., 1996) and anxious apprehension (Warren et al., 1999). Our results provide further insight into this literature. Specifically, we found that anxious arousal-specific and anxious apprehension-specific both show evidence of shared environmental influences, with minimal evidence of additive genetic effects. Our CE model of anxious arousal-specific provided a negligibly better fit than the AE model, but the similar magnitude between Mz and Dz twin-pair correlations suggest an absence of additive genetic effects. Anxious apprehension-specific,

on the other hand, showed robust evidence of shared environmental influences, with over 40% of the variance attributable to shared environment within twin pairs. This begs the question: if anxious apprehension-specific shows robust shared environmental effects and is a key component of internalizing disorders, why do so few case-control studies find evidence of shared environmental effects on diagnostic status? We speculate that this discrepancy may reflect the requirement across internalizing disorders for an individual to experience psychological distress to meet diagnostic criteria. Under the current dimensional model, we propose that this tendency to experience psychological distress is captured by our negative affect factor, which we have shown to be the most heritable of all six dimensions tested. However, beyond this general requirement to experience distress, there is often considerable variability within a given disorder as to the behavioral manifestation of that disorder. This creates a situation in which nearly all individuals meeting diagnostic criteria for a given disorder will be high on negative affect, but may show considerable variability in other behaviors. As such, studies evaluating the heritability of diagnostic status may be predominately capturing additive genetic variance attributable to negative affect, while largely failing to detect subtle variance attributable to more specific behaviors. This further underscores the utility of bifactor dimensional models of psychopathology, in conjunction with multivariate twin analyses, allowing researchers to parse a complex array of interrelated behaviors into discrete constructs with potentially distinct genetic and environmental influences.

Whereas we observed evidence of shared environmental influences on the anxiety-specific dimensions, we found that low positive affect-specific and rumination-specific were both best described under additive genetic and non-shared environment models. These findings align with previous research on related constructs, with anhedonia (Hay et al., 2001; Linney et

al., 2003; MacDonald et al., 2001) and rumination (Chen & Li, 2013; du Pont et al., 2019; Johnson et al., 2014; Johnson et al., 2016; Moore et al., 2013) both showing moderate levels of additive genetic effects with no evidence of shared environmental effects. Importantly, our findings provide further evidence that depression-specific dimensions show additive genetic effects, even when taking into account negative affect. This suggests a multifaceted genetic architecture to internalizing psychopathology, in which dissociable genetic mechanisms uniquely contribute to a general susceptibility to psychopathology (i.e., negative affect), common cognitive behaviors across internalizing disorders (i.e., repetitive negative thought), as well as more specific behavioral dimensions.

5.4.2 Genetic and Environmental Correlations Between Internalizing Dimensions and Gray Matter

In addition to evaluating the contributions of genes and the environment to individual differences in internalizing dimensions, we also evaluated the degree to which the relationships between these dimensions and gray matter were driven by overlapping genetic and environmental factors. These analyses revealed three important points. First, though the effect size of phenotypic relationships between internalizing dimensions and gray matter may be small, the two appear to be supported by largely overlapping genetic mechanisms. Specifically, within the exploratory whole brain analyses, negative affect showed the largest array of genetic correlations with gray matter. As such, a better understanding of the genetic architecture contributing to gray matter morphometry may prove informative in our quest to understand the genetic mechanisms driving psychopathology. That is, by identifying the genetic pathways that

are shared between psychopathology and gray matter morphometry, researchers may be able to identify additional related pathways that may not influence gray matter per se, but may have important implications for psychopathology. While this is true of nearly all endophenotypes, gray matter morphometry has already begun to pay dividends as an endophenotype of pathological behaviors (Cannon et al., 2006), a trend that will likely only get stronger with the ongoing proliferation of large scale imaging genetic studies, such as the UK Biobank (Miller et al., 2016).

Second, the phenotypic and genetic correlations between internalizing dimensions and gray matter morphometry are influenced by the relative granularity of how gray matter morphometry is measured. When comparing ROI and vertex-wise characterizations of gray matter morphometry, we found relatively smaller genetic correlations between internalizing dimensions and the large scale ROIs, but relatively larger genetic correlations with vertex-wise gray matter clusters. This was in part due to the relatively weaker phenotypic relationships observed for the ROIs as compared to the vertex-wise clusters. Despite the prominence of ROI-based imaging studies, the tendency to chunk the brain into relatively large-scale ROIs may mask relationships between brain and behavior that are more focal in nature. Relatedly, fine-scale mapping of the heritability of gray matter morphometry suggests that traditional ROI methodologies may average across subregions that may not only have distinct genetic influences, but may also vary in the relative influence of genetic as compared to environmental factors. We believe vertex-wise analyses, though computationally intensive, may prove to be well worth it given the variable contributions of genes and the environment across the brain, even between immediately adjacent brain regions.

Third, despite limited evidence of shared environmental influences on case-control parameterizations of psychopathology, some of the relationships between internalizing dimensions and gray matter are supported by overlapping shared environmental influences. This was particularly true for anxious apprehension-specific, which not only showed robust evidence of shared environmental effects in univariate analyses, but also showed overlapping shared environmental influences with gray matter properties of regions distributed throughout the brain. Despite considerable focus on understanding the genetic links between brain and behavior, understanding the overlapping environmental contributions to both gray matter and psychopathology is likely just as important. For example, chronic stress is not only an environmental factor that is highly predictive of psychopathology (Juster et al., 2011), but it also appears to drive changes in neural organization (Bremner et al., 2006). Though genetic factors likely influence these relationships, there is some evidence suggesting that the relationship between stress and psychopathology may be mediated by the effects of stress on brain structure (e.g., Frodl et al., 2010). Thus, understanding the environmental contributions to brain organization may provide a window into how environmental experiences play a critical role in shaping behavior, including behaviors at the core of psychopathology.

5.4.3 Conclusions

Looking across over 600 young adult twins, we found evidence of additive genetic and non-shared environmental contributions to individual differences in behavioral dimensions that are shared across disorders, as well as specific to depression. However, for dimensions that are thought to be specific to anxiety, we found evidence of shared environmental influences over and

above additive genetic effects. These results suggest that, while much of the behaviors in internalizing psychopathology are driven by genetic and unique environmental experiences, anxious behaviors may in fact be driven by familial environments that are shared between twins within the same household. Furthermore, relationships between internalizing dimensions and gray matter structure appear to be driven by partially overlapping etiological factors, including additive genetic, shared environmental, and non-shared environmental factors. Taken together, our findings highlight the potential utility of dimensional models of psychopathology in teasing apart the etiological influences on mental illness, while demonstrating that gray matter morphometry is valuable neural endophenotype when trying to identify the pathway from genes to behavior.

CHAPTER 6

CONCLUSIONS AND FUTURE DIRECTIONS

6.1. Conclusions

In this dissertation project, we set out to elucidate a number of important issues regarding internalizing psychopathology. First, we put forth a novel dimensional model of internalizing psychopathology that characterizes it not as distinct discrete disorders, but rather an interaction of multiple behavioral spectra. This dimensional framework aligns with recent calls to expand how researchers and clinicians alike think about mental illness, and builds off of decades of previous research into identifying behavioral dimensions that capture both commonalities across disorders, as well as heterogeneity within specific disorders. Our results suggest that internalizing psychopathology can be described by a six factor dimensional model, with dimensions falling along two distinct gradients: affective to cognitive and threat-related to reward-related. Importantly, we found evidence that these dimensions are predictive of diagnostic status, suggesting that a framework centered around our dimensional model may have clinical utility.

Second, employing structural MRI data on almost 800 participants, we sought out to parse brain regions frequently implicated in case-control diagnoses into specific associations with specific dimensions. This line of research may contribute to our understanding of the neural causes and consequences of mental illness, providing a window into what brain systems appear to be supporting what aspects of internalizing psychopathology. We not only found evidence confirming our theoretical model of the mechanisms supporting all six dimensions, but we

demonstrated a robust assortment of age and sex related effects on the relationship between brain and behavior.

Third, utilizing classical twin designs in over 600 young adult twins, we examined the degree to which specific internalizing behaviors are driven by genetic or environmental influences. A better understanding of the etiological factors driving mental illness will undoubtedly lead to improved diagnostic schemas, prevention, and treatment of mental illness. Our results suggest that while a general risk for psychopathology is largely genetic in nature, we found evidence that specific behaviors associated with anxiety disorders may indeed by driven by shared environmental influences. Furthermore, the relationship between gray matter morphometry and these internalizing dimensions appear to be largely due to overlapping genetic influences, suggesting that gray matter may be a viable endophenotype for understanding the biological basis of internalizing psychopathology.

6.2. Future Directions

We hope that this dissertation project is just the beginning of a research program testing the utility of dimensional models in clinical neuroscience. A number of future avenues of research stand out. First, we would like to test the validity of the current six factor model in a larger, more clinically oriented sample that spans the entire lifespan, not just adolescence and young adulthood. This would allow us to better understand if the factor structure of internalizing psychopathology is the same in the general population as it is in patients. With a larger clinical sample spanning a range of disorders, we may be able to identify disorder-specific dimensional profiles, further elucidating the structure of internalizing psychopathology. We would also like to

expand our investigation of neural systems associated with our internalizing psychopathology model to include properties of white matter structural connectivity and rest-state functional connectivity. This includes integrating across multiple imaging modalities to identify multimodal brain signatures of each dimension. Our understanding of the brain systems driving these dimensions may also be bolstered by utilizing multivariate analysis techniques which allow us to better capture the network-like organization of the brain. While the mass univariate approach employed in Chapter 4 can be informative, further insights can be made by trying to model the interrelationship between networks of brain regions. Finally, we plan to conduct follow up genetic analyses, including multivariate twin analyses on the brain properties associated with each dimension. Of particular interest is determining the degree to which a set of brain properties that are associated with a particular dimension are driven by overlapping genetic and environmental influences.

6.3. Final Remarks

Understanding the incredibly complex and dynamic relationship between genes, the brain, and behavior can be considered a final frontier in science and is a central part of understanding what it is to be human. However, it is not merely a search of knowledge for knowledge's sake. It is of the utmost importance. Despite rapid advancements in our understanding of the biological basis of behavior over the last century, our ability to adequately prevent and treat problematic behaviors throughout our society remains, in many ways, stymied. Both the prevalence and severity of mental illness appear to be on the rise and the stakes couldn't be any higher (Stone et al., 2018). As such, it is vital that we double down on our commitment as a society to prioritize evidence-based practices and to support the sciences in such a way as to

promote the implementation of knowledge for the greater good. As the world begins to grapple with the psychological effects of the unfolding COVID-19 pandemic, effects that will almost assuredly last for a generation if not longer, it is our call as scientists to evaluate what role we can play in making for a better future. It is my goal to pursue a career focused on better understanding the biological basis of psychopathology with the hope that some bit of knowledge I unlock, no matter how small, may, in some way, better the lives of generations to come.

REFERENCES

Abdallah, C. G., Coplan, J. D., Jackowski, A., Sato, J. R., Mao, X., Shungu, D. C., & Mathew, S. J. (2013). A pilot study of hippocampal volume and N-acetylaspartate (NAA) as response biomarkers in riluzole-treated patients with GAD. *European Neuropsychopharmacology*, *23*(4), 276-284.

Addis, D. R., Wong, A. T., & Schacter, D. L. (2007). Remembering the past and imagining the future: common and distinct neural substrates during event construction and elaboration. *Neuropsychologia*, *45*(7), 1363-1377.

Adolphs, R. (2004). Emotional vision. *Nature neuroscience*, *7*(11), 1167-1168.

Afifi, T. O., Asmundson, G. J., Taylor, S., & Jang, K. L. (2010). The role of genes and environment on trauma exposure and posttraumatic stress disorder symptoms: a review of twin studies. *Clinical psychology review*, *30*(1), 101-112.

Aina, Y., & Susman, J. L. (2006). Understanding comorbidity with depression and anxiety disorders. *The Journal of the American Osteopathic Association*, *106*(5 Suppl 2), S9.

Allegrini, A. G., Cheesman, R., Rimfeld, K., Selzam, S., Pingault, J. B., Eley, T. C., & Plomin, R. (2020). The p factor: genetic analyses support a general dimension of psychopathology in childhood and adolescence. *Journal of child psychology and psychiatry*, *61*(1), 30-39.

Alemany, S., Mas, A., Goldberg, X., Falcón, C., Fatjó-Vilas, M., Arias, B., ... & Fañanás, L. (2013). Regional gray matter reductions are associated with genetic liability for anxiety and depression: an MRI twin study. *Journal of affective disorders*, *149*(1-3), 175-181.

Altemus, M., Sarvaiya, N., & Epperson, C. N. (2014). Sex differences in anxiety and depression clinical perspectives. *Frontiers in neuroendocrinology*, *35*(3), 320-330.

American Psychiatric Association. (2013). *Diagnostic and statistical manual of mental disorders (DSM-5®)*. American Psychiatric Pub.

Andreescu, C., Tudorascu, D., Sheu, L. K., Rangarajan, A., Butters, M. A., Walker, S., ... & Aizenstein, H. (2017). Brain structural changes in late-life generalized anxiety disorder. *Psychiatry Research: Neuroimaging*, *268*, 15-21.

Angst, J., Angst, F., & Stassen, H. H. (1999). Suicide risk in patients with major depressive disorder. *The Journal of clinical psychiatry*.

Asami, T., Hayano, F., Nakamura, M., Yamasue, H., Uehara, K., Otsuka, T., ... & Hirayasu, Y. (2008). Anterior cingulate cortex volume reduction in patients with panic disorder. *Psychiatry and clinical neurosciences*, *62*(3), 322-330.

Asami, T., Nakamura, R., Takaishi, M., Yoshida, H., Yoshimi, A., Whitford, T. J., & Hirayasu, Y. (2018a). Smaller volumes in the lateral and basal nuclei of the amygdala in patients with panic disorder. *PloS one*, *13*(11).

Asami, T., Yoshida, H., Takaishi, M., Nakamura, R., Yoshimi, A., Whitford, T. J., & Hirayasu, Y. (2018b). Thalamic shape and volume abnormalities in female patients with panic disorder. *PloS one*, *13*(12).

Asami, T., Yamasue, H., Hayano, F., Nakamura, M., Uehara, K., Otsuka, T., ... & Hirayasu, Y. (2009). Sexually dimorphic gray matter volume reduction in patients with panic disorder. *Psychiatry Research: Neuroimaging*, *173*(2), 128-134.

Ashburner, J., & Friston, K. J. (2000). Voxel-based morphometry—the methods. *Neuroimage*, *11*(6), 805-821.

Asher, M., Asnaani, A., & Aderka, I. M. (2017). Gender differences in social anxiety disorder: A review. *Clinical psychology review*, *56*, 1-12.

Auerbach, R. P., Pisoni, A., Bondy, E., Kumar, P., Stewart, J. G., Yendiki, A., & Pizzagalli, D. A. (2017). Neuroanatomical prediction of anhedonia in adolescents. *Neuropsychopharmacology*, *42*(10), 2087-2095.

Badre, D., Poldrack, R. A., Paré-Blagoev, E. J., Insler, R. Z., & Wagner, A. D. (2005). Dissociable controlled retrieval and generalized selection mechanisms in ventrolateral prefrontal cortex. *Neuron*, *47*(6), 907-918.

Bair, M. J., Robinson, R. L., Katon, W., & Kroenke, K. (2003). Depression and pain comorbidity: a literature review. *Archives of internal medicine*, *163*(20), 2433-2445.

Banich, M. T. (2009). Executive function: The search for an integrated account. *Current directions in psychological science*, *18*(2), 89-94.

Banich, M. T., & Depue, B. E. (2015). Recent advances in understanding neural systems that support inhibitory control. *Current Opinion in Behavioral Sciences*, *1*, 17-22.

Banich, M. T., Smith, L. L., Smolker, H. R., Hankin, B. L., Silton, R. L., Heller, W., & Snyder, H. R. (2020). Common and specific dimensions of internalizing disorders are characterized by unique patterns of brain activity on a task of emotional cognitive control. *International Journal of Psychophysiology*.

Bar, M., & Neta, M. (2007). Visual elements of subjective preference modulate amygdala activation. *Neuropsychologia*, *45*(10), 2191-2200.

Baur, V., Hänggi, J., & Jäncke, L. (2012). Volumetric associations between uncinate fasciculus, amygdala, and trait anxiety. *BMC neuroscience*, *13*(1), 4.

Baur, V., Hänggi, J., Langer, N., & Jäncke, L. (2013). Resting-state functional and structural connectivity within an insula–amygdala route specifically index state and trait anxiety. *Biological psychiatry*, *73*(1), 85-92.

Beckmann, M., Johansen-Berg, H., & Rushworth, M. F. (2009). Connectivity-based parcellation of human cingulate cortex and its relation to functional specialization. *Journal of Neuroscience*, *29*(4), 1175-1190.

Beckwé, M., Deroost, N., Koster, E. H., De Lissnyder, E., & De Raedt, R. (2014). Worrying and rumination are both associated with reduced cognitive control. *Psychological research*, *78*(5), 651-660.

Behar, E., Zuellig, A. R., & Borkovec, T. D. (2005). Thought and imaginal activity during worry and trauma recall. *Behavior Therapy*, *36*(2), 157-168.

Bekker, M. H., & van Mens-Verhulst, J. (2007). Anxiety disorders: sex differences in prevalence, degree, and background, but gender-neutral treatment. *Gender medicine*, *4*, S178-S193.

Bellmund, J. L., Deuker, L., & Doeller, C. F. (2018). Structuring time in human lateral Entorhinal cortex. *BioRxiv*, 458133.

Berenbaum, H., Oltmanns, T. F. & Gottesman, I.I. (1990). Hedonic capacity in schizophrenics and their twins. *Psychological Medicine, 20*, 367-374.

Besteher, B., Gaser, C., Langbein, K., Dietzek, M., Sauer, H., & Nenadić, I. (2017). Effects of subclinical depression, anxiety and somatization on brain structure in healthy subjects. *Journal of affective disorders*, *215*, 111-117.

Bjørnebekk, A., Fjell, A. M., Walhovd, K. B., Grydeland, H., Torgersen, S., & Westlye, L. T. (2013). Neuronal correlates of the five factor model (FFM) of human personality: Multimodal imaging in a large healthy sample. *Neuroimage*, *65*, 194-208.

Blackmon, K., Barr, W. B., Carlson, C., Devinsky, O., DuBois, J., Pogash, D., ... & Thesen, T. (2011). Structural evidence for involvement of a left amygdala-orbitofrontal network in subclinical anxiety. *Psychiatry Research: Neuroimaging*, *194*(3), 296-303.

Blankstein, U., Chen, J. Y., Mincic, A. M., McGrath, P. A., & Davis, K. D. (2009). The complex minds of teenagers: neuroanatomy of personality differs between sexes. *Neuropsychologia*, *47*(2), 599-603.

Blokland, G. A., de Zubicaray, G. I., McMahon, K. L., & Wright, M. J. (2012). Genetic and environmental influences on neuroimaging phenotypes: a meta-analytical perspective on twin imaging studies. *Twin Research and Human Genetics*, *15*(3), 351-371.

Bludau, S., Bzdok, D., Gruber, O., Kohn, N., Riedl, V., Sorg, C., ... & Eickhoff, S. B. (2016). Medial prefrontal aberrations in major depressive disorder revealed by cytoarchitectonically informed voxel-based morphometry. *American Journal of Psychiatry*, *173*(3), 291-298.

Boes, A. D., McCormick, L. M., Coryell, W. H., & Nopoulos, P. (2008). Rostral anterior cingulate cortex volume correlates with depressed mood in normal healthy children. *Biological psychiatry*, *63*(4), 391-397.

Bora, E., Fornito, A., Pantelis, C., & Yücel, M. (2012). Gray matter abnormalities in major depressive disorder: a meta-analysis of voxel based morphometry studies. *Journal of Affective Disorders*, *138*(1), 9-18.

Bracha, H. S. (2004). Freeze, flight, fight, fright, faint: Adaptationist perspectives on the acute stress response spectrum. *CNS spectrums*, *9*(9), 679-685.

Brans, R. G., van Haren, N. E., van Baal, G. C. M., Schnack, H. G., Kahn, R. S., & Pol, H. E. H. (2008). Heritability of changes in brain volume over time in twin pairs discordant for schizophrenia. *Archives of General Psychiatry*, *65*(11), 1259-1268.

Bremner, J. D., Vythilingam, M., Vermetten, E., Nazeer, A., Adil, J., Khan, S., ... & Charney, D. S. (2002). Reduced volume of orbitofrontal cortex in major depression. *Biological psychiatry*, *51*(4), 273-279.

Bremner, J. D. (2006). Traumatic stress: effects on the brain. *Dialogues in clinical neuroscience*, *8*(4), 445.

Breslau, J., Kendler, K. S., Su, M., Gaxiola-Aguilar, S., & Kessler, R. C. (2005). Lifetime risk and persistence of psychiatric disorders across ethnic groups in the United States. *Psychological medicine*, *35*(3), 317-327.

Brown, T. A., Chorpita, B. F., & Barlow, D. H. (1998). Structural relationships among dimensions of the DSM-IV anxiety and mood disorders and dimensions of negative affect, positive affect, and autonomic arousal. *Journal of abnormal psychology*, *107*(2), 179.

Bruder, G. E., Alvarenga, J., Abraham, K., Skipper, J., Warner, V., Voyer, D., ... & Weissman, M. M. (2016). Brain laterality, depression and anxiety disorders: New findings for emotional and verbal dichotic listening in individuals at risk for depression. *Laterality: Asymmetries of Body, Brain and Cognition*, *21*(4-6), 525-548.

Brühl, A. B., Hänggi, J., Baur, V., Rufer, M., Delsignore, A., Weidt, S., ... & Herwig, U. (2014). Increased cortical thickness in a frontoparietal network in social anxiety disorder. *Human brain mapping*, *35*(7), 2966-2977.

Burdwood, E. N., Infantolino, Z. P., Crocker, L. D., Spielberg, J. M., Banich, M. T., Miller, G. A., & Heller, W. (2016). Resting-state functional connectivity differentiates anxious apprehension and anxious arousal. *Psychophysiology*, *53*(10), 1451-1459.

Burgess, P. W., Gilbert, S. J., & Dumontheil, I. (2007). Function and localization within rostral prefrontal cortex (area 10). *Philosophical Transactions of the Royal Society B: Biological Sciences*, *362*(1481), 887-899.

Calmes, C. A., & Roberts, J. E. (2007). Repetitive thought and emotional distress: Rumination and worry as prospective predictors of depressive and anxious symptomatology. *Cognitive Therapy and Research*, *31*(3), 343-356.

Campbell, S., Marriott, M., Nahmias, C., & MacQueen, G. M. (2004). Lower hippocampal volume in patients suffering from depression: a meta-analysis. *American Journal of Psychiatry*, *161*(4), 598-607.

Canbeyli, R. (2010). Sensorimotor modulation of mood and depression: an integrative review. *Behavioural brain research*, *207*(2), 249-264.

Cannon, T. D., Thompson, P. M., van Erp, T. G., Huttunen, M., Lonnqvist, J., Kaprio, J., & Toga, A. W. (2006). Mapping heritability and molecular genetic associations with cortical features using probabilistic brain atlases. *Neuroinformatics*, *4*(1), 5-19.

Canu, E., Kostić, M., Agosta, F., Munjiza, A., Ferraro, P. M., Pesic, D., ... & Filippi, M. (2015). Brain structural abnormalities in patients with major depression with or without generalized anxiety disorder comorbidity. *Journal of neurology*, *262*(5), 1255-1265.

Cardinale, E. M., Kircanski, K., Brooks, J., Gold, A. L., Towbin, K. E., Pine, D. S., ... & Brotman, M. A. (2019). Parsing neurodevelopmental features of irritability and anxiety: Replication and validation of a latent variable approach. *Development and psychopathology*, *31*(3), 917-929.

Carlson, J. M., Depetro, E., Maxwell, J., Harmon-Jones, E., & Hajcak, G. (2015). Gender moderates the association between dorsal medial prefrontal cortex volume and depressive symptoms in a subclinical sample. *Psychiatry Research: Neuroimaging*, *233*(2), 285-288.

Carnevali, L., Mancini, M., Koenig, J., Makovac, E., Watson, D. R., Meeten, F., ... & Ottaviani, C. (2019). Cortical morphometric predictors of autonomic dysfunction in generalized anxiety disorder. *Autonomic Neuroscience*, *217*, 41-48.

Carter, R. M., & Huettel, S. A. (2013). A nexus model of the temporal–parietal junction. *Trends in cognitive sciences*, *17*(7), 328-336.

Caspi, A., Houts, R. M., Belsky, D. W., Goldman-Mellor, S. J., Harrington, H., Israel, S., ... & Moffitt, T. E. (2014). The p factor: one general psychopathology factor in the structure of psychiatric disorders?. *Clinical Psychological Science*, *2*(2), 119-137.

Castagna, P. J., Roye, S., Calamia, M., Owens-French, J., Davis, T. E., & Greening, S. G. (2018). Parsing the neural correlates of anxious apprehension and anxious arousal in the grey-matter of healthy youth. *Brain imaging and behavior*, *12*(4), 1084-1098.

Chantarujikapong, S. I., Scherrer, J. F., Xian, H., Eisen, S. A., Lyons, M. J., Goldberg, J., ... & True, W. R. (2001). A twin study of generalized anxiety disorder symptoms, panic disorder symptoms and post-traumatic stress disorder in men. *Psychiatry research*, *103*(2-3), 133-145.

Chen, L. S., Eaton, W. W., Gallo, J. J., & Nestadt, G. (2000). Understanding the heterogeneity of depression through the triad of symptoms, course and risk factors: a longitudinal, population-based study. *Journal of affective disorders*, *59*(1), 1-11.

Chen, F. F., Hayes, A., Carver, C. S., Laurenceau, J. P., & Zhang, Z. (2012). Modeling general and specific variance in multifaceted constructs: A comparison of the bifactor model to other approaches. *Journal of personality*, *80*(1), 219-251.

Chen, J., & Li, X. (2013). Genetic and environmental influences on adolescent rumination and its association with depressive symptoms. *Journal of abnormal child psychology*, *41*(8), 1289-1298.

Christensen RHB (2019). "ordinal—Regression Models for Ordinal Data ." R package version 2019.12-10. https://CRAN.R-project.org/package=ordinal.

Ciesla, J. A., & Roberts, J. E. (2002). Self-directed thought and response to treatment for depression: A preliminary investigation. *Journal of Cognitive Psychotherapy*, *16*(4), 435-453.

Clark, D. M., & Wells, A. (1995). A cognitive model of social phobia. *Social phobia: Diagnosis, assessment, and treatment*, *41*(68), 00022-3.

Clark LA, & Watson D., (1991a) Tripartite model of anxiety and depression: Psychometric evidence and taxonomic implications. *Journal of Abnormal Psychology, 100 (3)*, 316-336.

Clark, L. A., & Watson, D. (1991b). General affective dispositions in physical and psychological health. *Handbook of social and clinical psychology*, *12*, 221-245.

Cloutman, L. L., Binney, R. J., Drakesmith, M., Parker, G. J., & Ralph, M. A. L. (2012). The variation of function across the human insula mirrors its patterns of structural connectivity: evidence from in vivo probabilistic tractography. *Neuroimage*, *59*(4), 3514-3521.

Cooney, R. E., Joormann, J., Eugène, F., Dennis, E. L., & Gotlib, I. H. (2010). Neural correlates of rumination in depression. *Cognitive, Affective, & Behavioral Neuroscience*, *10*(4), 470-478.

Copeland, W. E., Shanahan, L., Costello, E. J., & Angold, A. (2009). Childhood and adolescent psychiatric disorders as predictors of young adult disorders. *Archives of general psychiatry*, *66*(7), 764-772.

Craig, A. D. (2009). How do you feel--now? The anterior insula and human awareness. *Nature reviews neuroscience*, *10*(1).

Craig, A. D. (2011). Significance of the insula for the evolution of human awareness of feelings from the body. *Annals of the New York Academy of Sciences*, *1225*(1), 72-82.

Critchley, H. D., Lewis, P. A., Orth, M., Josephs, O., Deichmann, R., Trimble, M. R., & Dolan, R. J. (2007). Vagus nerve stimulation for treatment-resistant depression: behavioural and neural effects on encoding negative material. *Psychosomatic medicine*, *69*(1), 17.

Cummings, C. M., Caporino, N. E., & Kendall, P. C. (2014). Comorbidity of anxiety and depression in children and adolescents: 20 years after. *Psychological bulletin*, *140*(3), 816.

Cuthbert, B. N., & Insel, T. R. (2013). Toward the future of psychiatric diagnosis: the seven pillars of RDoC. *BMC medicine*, *11*(1), 126.

Dale, A. M., Fischl, B., & Sereno, M. I. (1999). Cortical surface-based analysis: I. Segmentation and surface reconstruction. *Neuroimage*, *9*(2), 179-194.

de Bellis, M. D., Casey, B. J., Dahl, R. E., Birmaher, B., Williamson, D. E., Thomas, K. M., ... & Ryan, N. D. (2000). A pilot study of amygdala volumes in pediatric generalized anxiety disorder. *Biological psychiatry*, *48*(1), 51-57.

de Geus, E. J., van't Ent, D., Wolfensberger, S. P., Heutink, P., Hoogendijk, W. J., Boomsma, D. I., & Veltman, D. J. (2007). Intrapair differences in hippocampal volume in monozygotic twins discordant for the risk for anxiety and depression. *Biological Psychiatry*, *61*(9), 1062-1071.

De La Vega, A., Chang, L. J., Banich, M. T., Wager, T. D., & Yarkoni, T. (2016). Large-scale meta-analysis of human medial frontal cortex reveals tripartite functional organization. *Journal of Neuroscience*, *36*(24), 6553-6562.

de Lijster, J. M., Dierckx, B., Utens, E. M., Verhulst, F. C., Zieldorff, C., Dieleman, G. C., & Legerstee, J. S. (2017). The age of onset of anxiety disorders: a meta-analysis. *Canadian Journal of Psychiatry. Revue Canadienne de Psychiatrie*, *62*(4), 237.

Delgado, M. R., & Dickerson, K. C. (2012). Reward-related learning via multiple memory systems. *Biological psychiatry*, *72*(2), 134-141.

den Braber, A., Bohlken, M. M., Brouwer, R. M., van't Ent, D., Kanai, R., Kahn, R. S., ... & Boomsma, D. I. (2013). Heritability of subcortical brain measures: a perspective for future genome-wide association studies. *NeuroImage*, *83*, 98-102.

Der-Avakian, A., & Markou, A. (2012). The neurobiology of anhedonia and other reward-related deficits. *Trends in neurosciences*, *35*(1), 68-77.

2017

Desikan, R. S., Ségonne, F., Fischl, B., Quinn, B. T., Dickerson, B. C., Blacker, D., ... & Albert, M. S. (2006). An automated labeling system for subdividing the human cerebral cortex on MRI scans into gyral based regions of interest. *Neuroimage*, *31*(3), 968-980.

DeYoung, C. G., Hirsh, J. B., Shane, M. S., Papademetris, X., Rajeevan, N., & Gray, J. R. (2010). Testing predictions from personality neuroscience: Brain structure and the big five. *Psychological science*, *21*(6), 820-828.

Diamond, A. (2002). Normal development of prefrontal cortex from birth to young adulthood: Cognitive functions, anatomy, and biochemistry. *Principles of frontal lobe function*, 466-503.

Dickie, E. W., & Armony, J. L. (2008). Amygdala responses to unattended fearful faces: interaction between sex and trait anxiety. *Psychiatry Research: Neuroimaging*, *162*(1), 51-57.

Disner, S. G., Beevers, C. G., Haigh, E. A., & Beck, A. T. (2011). Neural mechanisms of the cognitive model of depression. *Nature Reviews Neuroscience*, *12*(8), 467-477.

Donaldson, C., Lam, D., & Mathews, A. (2007). Rumination and attention in major depression. *Behaviour research and therapy*, *45*(11), 2664-2678.

Donzuso, G., Cerasa, A., Gioia, M. C., Caracciolo, M., & Quattrone, A. (2014). The neuroanatomical correlates of anxiety in a healthy population: differences between the State-Trait Anxiety Inventory and the Hamilton Anxiety Rating Scale. *Brain and behavior*, *4*(4), 504-514.

Drevets, W. C., Savitz, J., & Trimble, M. (2008). The subgenual anterior cingulate cortex in mood disorders. *CNS spectrums*, *13*(8), 663.

Du, M. Y., Wu, Q. Z., Yue, Q., Li, J., Liao, Y., Kuang, W. H., ... & Gong, Q. Y. (2012). Voxelwise meta-analysis of gray matter reduction in major depressive disorder. *Progress in Neuro-Psychopharmacology and Biological Psychiatry*, *36*(1), 11-16.

Ducharme, S., Albaugh, M. D., Hudziak, J. J., Botteron, K. N., Nguyen, T. V., Truong, C., ... & Schapiro, M. (2014). Anxious/depressed symptoms are linked to right ventromedial prefrontal cortical thickness maturation in healthy children and young adults. *Cerebral cortex*, *24*(11), 2941-2950.

du Pont, A., Rhee, S. H., Corley, R. P., Hewitt, J. K., & Friedman, N. P. (2019). Are rumination and neuroticism genetically or environmentally distinct risk factors for psychopathology?. *Journal of abnormal psychology*, *128*(5), 385.

Düzel, E., Habib, R., Rotte, M., Guderian, S., Tulving, E., & Heinze, H. J. (2003). Human hippocampal and parahippocampal activity during visual associative recognition memory for spatial and nonspatial stimulus configurations. *Journal of Neuroscience*, *23*(28), 9439-9444.

Ehringer, M. A., Rhee, S. H., Young, S., Corley, R., & Hewitt, J. K. (2006). Genetic and environmental contributions to common psychopathologies of childhood and adolescence: a study of twins and their siblings. *Journal of abnormal child psychology*, *34*(1), 1-17.

Eley, T. C. (1999). Behavioral genetics as a tool for developmental psychology: Anxiety and depression in children and adolescents. *Clinical Child and Family Psychology Review*, *2*, 21–36.

Elliott, M. L., Knodt, A. R., Ireland, D., Morris, M. L., Poulton, R., Ramrakha, S., ... & Hariri, A. R. (2020). What Is the Test-Retest Reliability of Common Task-Functional MRI Measures? New Empirical Evidence and a Meta-Analysis. *Psychological Science*, 0956797620916786.

Elliott, R., Rubinsztein, J. S., Sahakian, B. J., & Dolan, R. J. (2000). Selective attention to emotional stimuli in a verbal go/no-go task: an fMRI study. *Neuroreport*, *11*(8), 1739-1744.

Engels, A. S., Heller, W., Mohanty, A., Herrington, J. D., Banich, M. T., Webb, A. G., et al. (2007). Specificity of regional brain activity in anxiety types during emotion processing. *Psychophysiology, 44*, 352–363.

Enneking, V., Kruessel, P., Zaremba, D., Dohm, K., Grotegerd, D., Förster, K., ... & Böhnlein, J. (2019). Social anhedonia in major depressive disorder: a symptom-specific neuroimaging approach. *Neuropsychopharmacology*, *44*(5), 883-889.

Essau, C. A., Lewinsohn, P. M., Lim, J. X., Moon-ho, R. H., & Rohde, P. (2018). Incidence, recurrence and comorbidity of anxiety disorders in four major developmental stages. *Journal of affective disorders*, *228*, 248-253.

Etkin, A. (2009). Functional neuroanatomy of anxiety: a neural circuit perspective. In *Behavioral neurobiology of anxiety and its treatment* (pp. 251-277). Springer, Berlin, Heidelberg.

Etkin, A., Egner, T., & Kalisch, R. (2011). Emotional processing in anterior cingulate and medial prefrontal cortex. *Trends in cognitive sciences*, *15*(2), 85-93.

Fallucca, E., MacMaster, F. P., Haddad, J., Easter, P., Dick, R., May, G., ... & Rosenberg, D. R. (2011). Distinguishing between major depressive disorder and obsessive-compulsive disorder in children by measuring regional cortical thickness. *Archives of general psychiatry*, *68*(5), 527-533.

Fanous, A., Gardner, C. O., Prescott, C. A., Cancro, R., & Kendler, K. S. (2002). Neuroticism, major depression and gender: a population-based twin study. *Psychological medicine*, *32*(4), 719-728.

Fedorenko, E., & Thompson-Schill, S. L. (2014). Reworking the language network. *Trends in cognitive sciences*, *18*(3), 120-126.

Finan, P. H., & Garland, E. L. (2015). The role of positive affect in pain and its treatment. *The Clinical journal of pain*, *31*(2), 177.

Fischl, B. (2012). FreeSurfer. *Neuroimage*, *62*(2), 774-781.

Fischl, B., & Dale, A. M. (2000). Measuring the thickness of the human cerebral cortex from magnetic resonance images. *Proceedings of the National Academy of Sciences*, *97*(20), 11050-11055.

Fischl, B., Liu, A., & Dale, A. M. (2001). Automated manifold surgery: constructing geometrically accurate and topologically correct models of the human cerebral cortex. *IEEE transactions on medical imaging*, *20*(1), 70-80.

Fischl, B., Sereno, M. I., & Dale, A. M. (1999a). Cortical surface-based analysis: II: inflation, flattening, and a surface-based coordinate system. *Neuroimage*, *9*(2), 195-207.

Fischl, B., Sereno, M. I., Tootell, R. B., & Dale, A. M. (1999b). High-resolution intersubject averaging and a coordinate system for the cortical surface. *Human brain mapping*, *8*(4), 272-284.

Fischl, B., Van Der Kouwe, A., Destrieux, C., Halgren, E., Ségonne, F., Salat, D. H., ... & Caviness, V. (2004). Automatically parcellating the human cerebral cortex. *Cerebral cortex*, *14*(1), 11-22.

Floyd, T. A., Philippi, C. L., & Bruce, S. E. Rumination is Associated with PTSD Severity, Symptom Clusters, & Self-Related Brain Structures. *Trauma*, *8*(6.5), 10-3.

Forbes, E. E., & Dahl, R. E. (2005). Neural systems of positive affect: Relevance to understanding child and adolescent depression?. *Development and psychopathology*, *17*(3), 827.

Fouche, J. P., Du Plessis, S., Hattingh, C., Roos, A., Lochner, C., Soriano-Mas, C., ... & Jung, W. H. (2017). Cortical thickness in obsessive–compulsive disorder: Multisite mega-analysis of 780 brain scans from six centres. *The British Journal of Psychiatry*, *210*(1), 67-74.

Fresco, D. M., Frankel, A. N., Mennin, D. S., Turk, C. L., & Heimberg, R. G. (2002). Distinct and overlapping features of rumination and worry: The relationship of cognitive production to negative affective states. *Cognitive Therapy and Research*, *26*(2), 179-188.

Frick, A., Howner, K., Fischer, H., Eskildsen, S. F., Kristiansson, M., & Furmark, T. (2013). Cortical thickness alterations in social anxiety disorder. *Neuroscience letters*, *536*, 52-55.

Friederici, A. D., & Gierhan, S. M. (2013). The language network. *Current opinion in neurobiology*, *23*(2), 250-254.

Frodl, T., Reinhold, E., Koutsouleris, N., Reiser, M., & Meisenzahl, E. M. (2010). Interaction of childhood stress with hippocampus and prefrontal cortex volume reduction in major depression. *Journal of psychiatric research*, *44*(13), 799-807.

Garber, J., & Weersing, V. R. (2010). Comorbidity of anxiety and depression in youth: Implications for treatment and prevention. *Clinical Psychology: Science and Practice*, *17*(4), 293-306.

Gennatas, E. D., Avants, B. B., Wolf, D. H., Satterthwaite, T. D., Ruparel, K., Ciric, R., ... & Gur, R. C. (2017). Age-related effects and sex differences in gray matter density, volume, mass, and cortical thickness from childhood to young adulthood. *Journal of Neuroscience*, *37*(20), 5065-5073.

Geuze, E., Westenberg, H. G., Heinecke, A., de Kloet, C. S., Goebel, R., & Vermetten, E. (2008). Thinner prefrontal cortex in veterans with posttraumatic stress disorder. *Neuroimage*, *41*(3), 675-681.

Giedd, J. N., Blumenthal, J., Jeffries, N. O., Castellanos, F. X., Liu, H., Zijdenbos, A., ... & Rapoport, J. L. (1999). Brain development during childhood and adolescence: a longitudinal MRI study. *Nature neuroscience*, *2*(10), 861.

Giedd, J. N., Clasen, L. S., Lenroot, R., Greenstein, D., Wallace, G. L., Ordaz, S., ... & Samango-Sprouse, C. A. (2006). Puberty-related influences on brain development. *Molecular and cellular endocrinology*, *254*, 154-162.

Giedd, J. N., Raznahan, A., Mills, K. L., & Lenroot, R. K. (2012). magnetic resonance imaging of male/female differences in human adolescent brain anatomy. *Biology of sex differences*, *3*(1), 19.

Gilbert, A. R., Keshavan, M. S., Diwadkar, V., Nutche, J., MacMaster, F., Easter, P. C., ... & Rosenberg, D. R. (2008). Gray matter differences between pediatric obsessive-compulsive disorder patients and high-risk siblings: a preliminary voxel-based morphometry study. *Neuroscience letters*, *435*(1), 45-50.

Goenjian, A. K., Noble, E. P., Walling, D. P., Goenjian, H. A., Karayan, I. S., Ritchie, T., & Bailey, J. N. (2008). Heritabilities of symptoms of posttraumatic stress disorder, anxiety, and depression in earthquake exposed Armenian families. *Psychiatric Genetics*, *18*(6), 261-266.

Gogtay, N., Giedd, J. N., Lusk, L., Hayashi, K. M., Greenstein, D., Vaituzis, A. C., ... & Rapoport, J. L. (2004). Dynamic mapping of human cortical development during childhood through early adulthood. *Proceedings of the National Academy of Sciences*, *101*(21), 8174-8179.

Gogtay, N., & Thompson, P. M. (2010). Mapping gray matter development: implications for typical development and vulnerability to psychopathology. *Brain and cognition*, *72*(1), 6-15.

Gold, A. L., Steuber, E. R., White, L. K., Pacheco, J., Sachs, J. F., Pagliaccio, D., ... & Pine, D. S. (2017). Cortical thickness and subcortical gray matter volume in pediatric anxiety disorders. *Neuropsychopharmacology*, *42*(12), 2423-2433.

Goodkind, M., Eickhoff, S. B., Oathes, D. J., Jiang, Y., Chang, A., Jones-Hagata, L. B., ... & Grieve, S. M. (2015). Identification of a common neurobiological substrate for mental illness. *JAMA psychiatry*, *72*(4), 305-315.

Goodwin, R. D., & Hamilton, S. P. (2002). The early-onset fearful panic attack as a predictor of severe psychopathology. *Psychiatry research*, *109*(1), 71-79.

Goring, H. J., & Papageorgiou, C. (2008). Rumination and worry: Factor analysis of self-report measures in depressed participants. *Cognitive Therapy and Research*, *32*(4), 554-566.

Gorka, A. X., Hanson, J. L., Radtke, S. R., & Hariri, A. R. (2014). Reduced hippocampal and medial prefrontal gray matter mediate the association between reported childhood maltreatment and trait anxiety in adulthood and predict sensitivity to future life stress. *Biology of mood & anxiety disorders*, *4*(1), 12.

Gorwood, P. (2008). Neurobiological mechanisms of anhedonia. *Dialogues in clinical neuroscience*, *10*(3), 291.

Grill-Spector, K., Henson, R., & Martin, A. (2006). Repetition and the brain: neural models of stimulus-specific effects. *Trends in cognitive sciences*, *10*(1), 14-23.

Gustavson, D. E., du Pont, A., Whisman, M. A., & Miyake, A. (2018). Evidence for transdiagnostic repetitive negative thinking and its association with rumination, worry, and depression and anxiety symptoms: A commonality analysis. *Collabra. Psychology*, *4*(1).

Gustavsson, J. P., Pedersen, N. L., Åsberg, M., & Schalling, D. (1996). Origins of individual differences in anxiety proneness: a twin/adoption study of the anxiety-related scales from the Karolinska Scales of Personality (KSP). *Acta Psychiatrica Scandinavica*, *93*(6), 460-469.

Haldane, M., & Frangou, S. (2006). Functional neuroimaging studies in mood disorders. *Acta Neuropsychiatrica*, *18*(2), 88-99.

Hamilton, J. P., Farmer, M., Fogelman, P., & Gotlib, I. H. (2015). Depressive rumination, the default-mode network, and the dark matter of clinical neuroscience. *Biological psychiatry*, *78*(4), 224-230.

Hamilton, J. P., Siemer, M., & Gotlib, I. H. (2008). Amygdala volume in major depressive disorder: a meta-analysis of magnetic resonance imaging studies. *Molecular psychiatry*, *13*(11), 993.

Hammar, Å., Lund, A., & Hugdahl, K. (2003a). Long-lasting cognitive impairment in unipolar major depression: a 6-month follow-up study. *Psychiatry research*, *118*(2), 189-196.

Hammar, Å., Lund, A., & Hugdahl, K. (2003b). Selective impairment in effortful information processing in major depression. *Journal of the International Neuropsychological society*, *9*(6), 954-959.

Han, K. M., Choi, S., Jung, J., Na, K. S., Yoon, H. K., Lee, M. S., & Ham, B. J. (2014). Cortical thickness, cortical and subcortical volume, and white matter integrity in patients with their first episode of major depression. *Journal of affective disorders*, *155*, 42-48.

Hankin, B. L. (2006). Adolescent depression: Description, causes, and interventions. *Epilepsy & behavior*, *8*(1), 102-114.

Hankin, B. L. (2009). Development of sex differences in depressive and co-occurring anxious symptoms during adolescence: Descriptive trajectories and potential explanations in a multiwave prospective study. *Journal of Clinical Child & Adolescent Psychology*, *38*(4), 460-472.

Hankin, B. L. (2015). Depression from childhood through adolescence: risk mechanisms across multiple systems and levels of analysis. *Current opinion in psychology*, *4*, 13-20.

Hankin, B. L., Mermelstein, R., & Roesch, L. (2007). Sex differences in adolescent depression: Stress exposure and reactivity models. *Child development*, *78*(1), 279-295.

Hankin, B. L., Wetter, E., & Cheely, C. (2008). Sex differences in child and adolescent depression: A developmental psychopathological approach.

Hansell, N. K., Wright, M. J., Medland, S. E., Davenport, T. A., Wray, N. R., Martin, N. G., & Hickie, I. B. (2012). Genetic co-morbidity between neuroticism, anxiety/depression and somatic distress in a population sample of adolescent and young adult twins. *Psychological medicine*, *42*(6), 1249-1260.

Harvey, P. O., Pruessner, J., Czechowska, Y., & Lepage, M. (2007). Individual differences in trait anhedonia: a structural and functional magnetic resonance imaging study in non-clinical subjects. *Molecular psychiatry*, *12*(8), 767-775.

Hatoum, A. S., Reineberg, A. E., Smolker, H. R., Hewitt, J. K., & Friedman, N. P. (2019). Whole-cortex mapping of common genetic influences on depression and a social deficits dimension. *Translational psychiatry*, *9*(1), 1-10.

Hay, D. A., Martin, N. G., Foley, D., Treloar, S. A., Kirk, K. M., & Heath, A. C. (2001). Phenotypic and genetic analyses of a short measure of psychosis-proneness in a large-scale Australian twin study. *Twin Research and Human Genetics*, *4*(1), 30-40.

Hayano, F., Nakamura, M., Asami, T., Uehara, K., Yoshida, T., Roppongi, T., ... & Hirayasu, Y. (2009). Smaller amygdala is associated with anxiety in patients with panic disorder. *Psychiatry and clinical neurosciences*, *63*(3), 266-276.

Hecht, D. (2010). Depression and the hyperactive right-hemisphere. *Neuroscience research*, *68*(2), 77-87.

Henry, J. D., & Crawford, J. R. (2005). The short-form version of the Depression Anxiety Stress Scales (DASS-21): Construct validity and normative data in a large non-clinical sample. *British journal of clinical psychology*, *44*(2), 227-239.

Hilbert, K., Lueken, U., & Beesdo-Baum, K. (2014). Neural structures, functioning and connectivity in Generalized Anxiety Disorder and interaction with neuroendocrine systems: a systematic review. *Journal of affective disorders*, *158*, 114-126.

Hilbert, K., Pine, D. S., Muehlhan, M., Lueken, U., Steudte-Schmiedgen, S., & Beesdo-Baum, K. (2015). Gray and white matter volume abnormalities in generalized anxiety disorder by categorical and dimensional characterization. *Psychiatry Research: Neuroimaging*, *234*(3), 314-320.

Hirsch, C. R., & Holmes, E. A. (2007). Mental imagery in anxiety disorders. *Psychiatry*, *6*(4), 161-165.

Hiser, J., & Koenigs, M. (2018). The multifaceted role of the ventromedial prefrontal cortex in emotion, decision making, social cognition, and psychopathology. *Biological Psychiatry*, *83*(8), 638-647.

Hoexter, M. Q., de Souza Duran, F. L., D'alcante, C. C., Dougherty, D. D., Shavitt, R. G., Lopes, A. C., ... & Miguel, E. C. (2012). Gray matter volumes in obsessive-compulsive disorder before and after fluoxetine or cognitive-behavior therapy: a randomized clinical trial. *Neuropsychopharmacology*, *37*(3), 734-745.

Holland, P. C., & Gallagher, M. (2004). Amygdala–frontal interactions and reward expectancy. *Current opinion in neurobiology*, *14*(2), 148-155.

Holmes, A. J., Lee, P. H., Hollinshead, M. O., Bakst, L., Roffman, J. L., Smoller, J. W., & Buckner, R. L. (2012). Individual differences in amygdala-medial prefrontal anatomy link negative affect, impaired social functioning, and polygenic depression risk. *Journal of Neuroscience*, *32*(50), 18087-18100.

Hong, R. Y. (2007). Worry and rumination: Differential associations with anxious and depressive symptoms and coping behavior. *Behaviour research and therapy*, *45*(2), 277-290.

Hothorn, T., Bretz, F., & Westfall, P. (2008). "Simultaneous Inference in General Parametric Models." *Biometrical Journal*, **50**(3), 346–363.

Hu, L. T., & Bentler, P. M. (1999). Cutoff criteria for fit indexes in covariance structure analysis: Conventional criteria versus new alternatives. *Structural equation modeling: a multidisciplinary journal*, *6*(1), 1-55.

Hu, Y., & Dolcos, S. (2017). Trait anxiety mediates the link between inferior frontal cortex volume and negative affective bias in healthy adults. *Social cognitive and affective neuroscience*, *12*(5), 775-782.

Hughes, M. E., Alloy, L. B., & Cogswell, A. (2008). Repetitive thought in psychopathology: The relation of rumination and worry to depression and anxiety symptoms. *Journal of Cognitive Psychotherapy*, *22*(3), 271-288.

Hur, J., Heller, W., Kern, J. L., & Berenbaum, H. (2017). A bi-factor approach to modeling the structure of worry and rumination. *Journal of Experimental Psychopathology*, *8*(3), 252-264.

Hwang, J. W., Egorova, N., Yang, X. Q., Zhang, W. Y., Chen, J., Yang, X. Y., ... & Kong, J. (2015). Subthreshold depression is associated with impaired resting-state functional connectivity of the cognitive control network. *Translational psychiatry*, *5*(11), e683-e683.

Iacono, W. G., Heath, A. C., Hewitt, J. K., Neale, M. C., Banich, M. T., Luciana, M. M., ... & Bjork, J. M. (2018). The utility of twins in developmental cognitive neuroscience research: How twins strengthen the ABCD research design. *Developmental cognitive neuroscience*, *32*, 30-42.

Inkster, B., Rao, A. W., Ridler, K., Nichols, T. E., Saemann, P. G., Auer, D. P., ... & Matthews, P. M. (2011). Structural brain changes in patients with recurrent major depressive disorder presenting with anxiety symptoms. *Journal of Neuroimaging*, *21*(4), 375-382.

Insel, T. R. (2014). The NIMH research domain criteria (RDoC) project: precision medicine for psychiatry. *American Journal of Psychiatry*, *171*(4), 395-397.

Insel, T., Cuthbert, B., Garvey, M., Heinssen, R., Pine, D. S., Quinn, K., ... & Wang, P. (2010). Research domain criteria (RDoC): toward a new classification framework for research on mental disorders.

Janak, P. H., & Tye, K. M. (2015). From circuits to behaviour in the amygdala. *Nature*, *517*(7534), 284.

Jang, K. L., Livesley, W. J., Taylor, S., Stein, M. B., & Moon, E. C. (2004). Heritability of individual depressive symptoms. *Journal of affective disorders*, *80*(2-3), 125-133.

Jansen, A. G., Mous, S. E., White, T., Posthuma, D., & Polderman, T. J. (2015). What twin studies tell us about the heritability of brain development, morphology, and function: a review. *Neuropsychology review*, *25*(1), 27-46.

Jaworska, N., Yücel, K., Courtright, A., MacMaster, F. P., Sembo, M., & MacQueen, G. (2016). Subgenual anterior cingulate cortex and hippocampal volumes in depressed youth: the role of comorbidity and age. *Journal of affective disorders*, *190*, 726-732.

Jin, F., Zheng, P., Liu, H., Guo, H., & Sun, Z. (2018). Functional and anatomical connectivity-based parcellation of human cingulate cortex. *Brain and behavior*, *8*(8), e01070.

Johansen-Berg, H., Gutman, D. A., Behrens, T. E. J., Matthews, P. M., Rushworth, M. F. S., Katz, E., ... & Mayberg, H. S. (2008). Anatomical connectivity of the subgenual cingulate region targeted with deep brain stimulation for treatment-resistant depression. *Cerebral cortex*, *18*(6), 1374-1383.

Johnson, D. P. (2015). *A twin study examining the development of rumination and its role as a transdiagnostic risk factor for psychopathology* (Doctoral dissertation, Doctoral dissertation). Retrieved from http://scholar. colorado. edu/cgi/viewcontent. cgi).

Johnson, D. P., Rhee, S. H., Friedman, N. P., Corley, R. P., Munn-Chernoff, M. A., Hewitt, J. K., & Whisman, M. A. (2016). A twin study examining rumination as a transdiagnostic correlate of psychopathology. *Clinical Psychological Science*, *4*(6), 971-987.

Johnson, D. P., Whisman, M. A., Corley, R. P., Hewitt, J. K., & Friedman, N. P. (2014). Genetic and environmental influences on rumination and its covariation with depression. *Cognition and Emotion*, *28*(7), 1270-1286.

Joshi, A. A., Lepore, N., Joshi, S. H., Lee, A. D., Barysheva, M., Stein, J. L., ... & Wright, M. J. (2011). The contribution of genes to cortical thickness and volume. *Neuroreport*, *22*(3), 101.

Juster, R. P., Bizik, G., Picard, M., Arsenault-Lapierre, G., Sindi, S., Trepanier, L., ... & Fiocco, A. J. (2011). A transdisciplinary perspective of chronic stress in relation to psychopathology throughout life span development. *Development and psychopathology*, *23*(3), 725-776.

Kaiser, R. H., Kang, M. S., Lew, Y., Van Der Feen, J., Aguirre, B., Clegg, R., ... & Pizzagalli, D. A. (2019a). Abnormal frontoinsular-default network dynamics in adolescent depression and rumination: a preliminary resting-state co-activation pattern analysis. *Neuropsychopharmacology*, *44*(9), 1604-1612.

Kaiser, R. H., Peterson, E., Kang, M. S., Van Der Feen, J., Aguirre, B., Clegg, R., ... & Pizzagalli, D. A. (2019b). Frontoinsular network markers of current and future adolescent mood health. *Biological Psychiatry: Cognitive Neuroscience and Neuroimaging*, *4*(8), 715-725.

Kaiser, R. H., Snyder, H. R., Goer, F., Clegg, R., Ironside, M., & Pizzagalli, D. A. (2018). Attention bias in rumination and depression: Cognitive mechanisms and brain networks. *Clinical Psychological Science*, *6*(6), 765-782.

Kang, E. K., Lee, K. S., & Lee, S. H. (2017). Reduced cortical thickness in the temporal pole, insula, and pars triangularis in patients with panic disorder. *Yonsei medical journal*, *58*(5), 1018-1024.

Kapogiannis, D., Sutin, A., Davatzikos, C., Costa Jr, P., & Resnick, S. (2013). The five factors of personality and regional cortical variability in the Baltimore longitudinal study of aging. *Human brain mapping*, *34*(11), 2829-2840.

Kaufman, J., & Charney, D. (2000). Comorbidity of mood and anxiety disorders. *Depression and anxiety*, *12*(S1), 69-76.

Keedwell, P. A., Andrew, C., Williams, S. C., Brammer, M. J., & Phillips, M. L. (2005). The neural correlates of anhedonia in major depressive disorder. *Biological psychiatry*, *58*(11), 843-853.

Keller, M. C., Coventry, W. L., Heath, A. C., & Martin, N. G. (2005). Widespread evidence for non-additive genetic variation in Cloninger's and Eysenck's personality dimensions using a twin plus sibling design. *Behavior Genetics*, *35*(6), 707.

Kendler, K. S., Davis, C. G., & Kessler, R. C. (1997). The familial aggregation of common psychiatric and substance use disorders in the National Comorbidity Survey: a family history study. *The British Journal of Psychiatry*, *170*, 541.

Kendler, K. S., Gardner, C. O., Gatz, M., & Pedersen, N. L. (2007). The sources of co-morbidity between major depression and generalized anxiety disorder in a Swedish national twin sample. *Psychological medicine*, *37*(3), 453-462.

Kendler, K. S., Hettema, J. M., Butera, F., Gardner, C. O., & Prescott, C. A. (2003). Life event dimensions of loss, humiliation, entrapment, and danger in the prediction of onsets of major depression and generalized anxiety. *Archives of general psychiatry*, *60*(8), 789-796.

Kendler, K. S., Neale, M. C., Kessler, R. C., Heath, A. C., & Eaves, L. J. (1992). Major depression and generalized anxiety disorder: same genes,(partly) different environments?. *Archives of general psychiatry*, *49*(9), 716-722.

Kendler, K. S., Ochs, A. L., Gorman, A. M., Hewitt, J. K., Ross, D. E., & Mirsky, A. F. (1991). The structure of schizotypy: a pilot multitrait twin study. *Psychiatry research*, *36*(1), 19-36.

Kessler, R. C., Berglund, P., Demler, O., Jin, R., Merikangas, K. R., & Walters, E. E. (2005a). Lifetime prevalence and age-of-onset distributions of DSM-IV disorders in the National Comorbidity Survey Replication. *Archives of general psychiatry*, *62*(6), 593-602.

Kessler, R. C., Chiu, W. T., Demler, O., & Walters, E. E. (2005b). Prevalence, severity, and comorbidity of 12-month DSM-IV disorders in the National Comorbidity Survey Replication. *Archives of general psychiatry*, *62*(6), 617-627.

Kessler, R. C., McGonagle, K. A., Zhao, S., Nelson, C. B., Hughes, M., Eshleman, S., ... & Kendler, K. S. (1994). Lifetime and 12-month prevalence of DSM-III-R psychiatric disorders in the United States: results from the National Comorbidity Survey. *Archives of general psychiatry*, *51*(1), 8-19.

Kessler, R. C., Nelson, C. B., McGonagle, K. A., Liu, J., Swartz, M., & Blazer, D. G. (1996). Comorbidity of DSM–III–R major depressive disorder in the general population: results from the US National Comorbidity Survey. *The British journal of psychiatry*, *168*(S30), 17-30.

Kim, H., & Eaton, N. R. (2015). The hierarchical structure of common mental disorders: Connecting multiple levels of comorbidity, bifactor models, and predictive validity. *Journal of abnormal psychology*, *124*(4), 1064.

Kim-Cohen, J., Caspi, A., Moffitt, T. E., Harrington, H., Milne, B. J., & Poulton, R. (2003). Prior juvenile diagnoses in adults with mental disorder: developmental follow-back of a prospective-longitudinal cohort. *Archives of general psychiatry*, *60*(7), 709-717.

Koenen, K. C., Fu, Q. J., Ertel, K., Lyons, M. J., Eisen, S. A., True, W. R., ... & Tsuang, M. T. (2008). Common genetic liability to major depression and posttraumatic stress disorder in men. *Journal of affective disorders*, *105*(1-3), 109-115.

Koenig, J., Westlund Schreiner, M., Klimes-Dougan, B., Ubani, B., Mueller, B., Kaess, M., & Cullen, K. R. (2018). Brain structural thickness and resting state autonomic function in adolescents with major depression. *Social cognitive and affective neuroscience*, *13*(7), 741-753.

Kong, L., Chen, K., Womer, F., Jiang, W., Luo, X., Driesen, N., ... & Wang, F. (2013). Sex differences of gray matter morphology in cortico-limbic-striatal neural system in major depressive disorder. *Journal of psychiatric research*, *47*(6), 733-739.

Koolschijn, P. C. M., van Haren, N. E., Lensvelt-Mulders, G. J., Hulshoff Pol, H. E., & Kahn, R. S. (2009). Brain volume abnormalities in major depressive disorder: A meta-analysis of magnetic resonance imaging studies. *Human brain mapping*, *30*(11), 3719-3735.

Koolschijn, P. C. M., van IJzendoorn, M. H., Bakermans-Kranenburg, M. J., & Crone, E. A. (2013). Hippocampal volume and internalizing behavior problems in adolescence. *European Neuropsychopharmacology*, *23*(7), 622-628.

Kotov, R., Krueger, R. F., & Watson, D. (2018). A paradigm shift in psychiatric classification: the Hierarchical Taxonomy Of Psychopathology (HiTOP). *World Psychiatry*, *17*(1), 24.

Kotov, R., Krueger, R. F., Watson, D., Achenbach, T. M., Althoff, R. R., Bagby, R. M., ... & Eaton, N. R. (2017). The Hierarchical Taxonomy of Psychopathology (HiTOP): a dimensional alternative to traditional nosologies. *Journal of abnormal psychology*, *126*(4), 454.

Kovacs, M., & Devlin, B. (1998). Internalizing disorders in childhood. *Journal of Child Psychology and Psychiatry*, *39*, 47–63.

Koutsouleris, N., Gaser, C., Jäger, M., Bottlender, R., Frodl, T., Holzinger, S., ... & Born, C. (2008). Structural correlates of psychopathological symptom dimensions in schizophrenia: a voxel-based morphometric study. *Neuroimage*, *39*(4), 1600-1612.

Kringelbach, M. L. (2005). The human orbitofrontal cortex: linking reward to hedonic experience. *Nature Reviews Neuroscience*, *6*(9), 691.

Kühn, S., & Gallinat, J. (2013a). Gray matter correlates of posttraumatic stress disorder: a quantitative meta-analysis. *Biological psychiatry*, *73*(1), 70-74.

Kühn, S., Kaufmann, C., Simon, D., Endrass, T., Gallinat, J., & Kathmann, N. (2013b). Reduced thickness of anterior cingulate cortex in obsessive-compulsive disorder. *Cortex*, *49*(8), 2178-2185.

Kühn, S., Schubert, F., & Gallinat, J. (2011). Structural correlates of trait anxiety: reduced thickness in medial orbitofrontal cortex accompanied by volume increase in nucleus accumbens. *Journal of affective disorders*, *134*(1-3), 315-319.

Kühn, S., Vanderhasselt, M. A., De Raedt, R., & Gallinat, J. (2012). Why ruminators won't stop: the structural and resting state correlates of rumination and its relation to depression. *Journal of affective disorders*, *141*(2-3), 352-360.

Lahey, B. B., Krueger, R. F., Rathouz, P. J., Waldman, I. D., & Zald, D. H. (2017). A hierarchical causal taxonomy of psychopathology across the life span. *Psychological bulletin*, *143*(2), 142.

Lai, C. H. (2013). Gray matter volume in major depressive disorder: a meta-analysis of voxel-based morphometry studies. *Psychiatry Research: Neuroimaging*, *211*(1), 37-46.

Lener, M. S., Kundu, P., Wong, E., Dewilde, K. E., Tang, C. Y., Balchandani, P., & Murrough, J. W. (2016). Cortical abnormalities and association with symptom dimensions across the depressive spectrum. *Journal of affective disorders*, *190*, 529-536.

Lewinsohn, P. M., Gotlib, I. H., Lewinsohn, M., Seeley, J. R., & Allen, N. B. (1998). Gender differences in anxiety disorders and anxiety symptoms in adolescents. *Journal of abnormal psychology*, *107*(1), 109.

Lewis, G. J., Panizzon, M. S., Eyler, L., Fennema-Notestine, C., Chen, C. H., Neale, M. C., ... & Franz, C. E. (2014). Heritable influences on amygdala and orbitofrontal cortex contribute to genetic variation in core dimensions of personality. *Neuroimage*, *103*, 309-315.

Lai, C. H. (2011). Gray matter deficits in panic disorder: a pilot study of meta-analysis. *Journal of clinical psychopharmacology*, *31*(3), 287-293.

Li, L., Wu, M., Liao, Y., Ouyang, L., Du, M., Lei, D., ... & Gong, Q. (2014). Grey matter reduction associated with posttraumatic stress disorder and traumatic stress. *Neuroscience & Biobehavioral Reviews*, *43*, 163-172.

Li, M., Xu, H., & Lu, S. (2018). Neural basis of depression related to a dominant right hemisphere: A resting-state fMRI study. *Behavioural neurology*, *2018*.

Liao, M., Yang, F., Zhang, Y., He, Z., Song, M., Jiang, T., ... & Li, L. (2013). Childhood maltreatment is associated with larger left thalamic gray matter volume in adolescents with generalized anxiety disorder. *PLoS One*, *8*(8).

Liao, M., Yang, F., Zhang, Y., He, Z., Su, L., & Li, L. (2014). Lack of gender effects on gray matter volumes in adolescent generalized anxiety disorder. *Journal of affective disorders*, *155*, 278-282.

Liberzon, I., Phan, K. L., Decker, L. R., & Taylor, S. F. (2003). Extended amygdala and emotional salience: a PET activation study of positive and negative affect. *Neuropsychopharmacology*, *28*(4), 726-733.

Lichtenberg, N. T., Pennington, Z. T., Holley, S. M., Greenfield, V. Y., Cepeda, C., Levine, M. S., & Wassum, K. M. (2017). Basolateral amygdala to orbitofrontal cortex projections enable cue-triggered reward expectations. *Journal of Neuroscience*, *37*(35), 8374-8384.

Linney, Y. M., Murray, R. M., Peters, E. R., MacDonald, A. M., Rijsdijk, F., & Sham, P. C. (2003). A quantitative genetic analysis of schizotypal personality traits. *Psychological medicine*, *33*(5), 803.

Liu, X., Kakeda, S., Watanabe, K., Yoshimura, R., Abe, O., Ide, S., ... & Ueda, I. (2015). Relationship between the cortical thickness and serum cortisol levels in drug-naive, first-episode patients with major depressive disorder: a surface-based morphometric study. *Depression and anxiety*, *32*(9), 702-708.

Lutz, A., McFarlin, D. R., Perlman, D. M., Salomons, T. V., & Davidson, R. J. (2013). Altered anterior insula activation during anticipation and experience of painful stimuli in expert meditators. *Neuroimage*, *64*, 538-546.

Lydon-Staley, D. M., Kuehner, C., Zamoscik, V., Huffziger, S., Kirsch, P., & Bassett, D. S. (2019). Repetitive negative thinking in daily life and functional connectivity among default mode, fronto-parietal, and salience networks. *Translational psychiatry*, *9*(1), 1-12.

Lyoo, I. K., Dager, S. R., Kim, J. E., Yoon, S. J., Friedman, S. D., Dunner, D. L., & Renshaw, P. F. (2010). Lithium-induced gray matter volume increase as a neural correlate of treatment response in bipolar disorder: a longitudinal brain imaging study. *Neuropsychopharmacology*, *35*(8), 1743-1750.

MacDonald III, A. W., Pogue-Geile, M. F., Debski, T. T., & Manuck, S. (2001). Genetic and environmental influences on schizotypy: a community-based twin study. *Schizophrenia bulletin*, *27*(1), 47-58.

Machino, A., Kunisato, Y., Matsumoto, T., Yoshimura, S., Ueda, K., Yamawaki, Y., ... & Yamawaki, S. (2014). Possible involvement of rumination in gray matter abnormalities in persistent symptoms of major depression: an exploratory magnetic resonance imaging voxel-based morphometry study. *Journal of affective disorders*, *168*, 229-235.

Mackintosh, M. A., Gatz, M., Wetherell, J. L., & Pedersen, N. L. (2006). A twin study of lifetime generalized anxiety disorder (GAD) in older adults: genetic and environmental

influences shared by neuroticism and GAD. *Twin research and human genetics*, *9*(1), 30-37.

MacMaster, F. P., Carrey, N., Langevin, L. M., Jaworska, N., & Crawford, S. (2014). Disorder-specific volumetric brain difference in adolescent major depressive disorder and bipolar depression. *Brain imaging and behavior*, *8*(1), 119-127.

MacMaster, F. P., Mirza, Y., Szeszko, P. R., Kmiecik, L. E., Easter, P. C., Taormina, S. P., ... & Rosenberg, D. R. (2008). Amygdala and hippocampal volumes in familial early onset major depressive disorder. *Biological psychiatry*, *63*(4), 385-390.

Maeng, L. Y., & Milad, M. R. (2015). Sex differences in anxiety disorders: interactions between fear, stress, and gonadal hormones. *Hormones and behavior*, *76*, 106-117.

Makino, Y., Yokosawa, K., Takeda, Y., & Kumada, T. (2004). Visual search and memory search engage extensive overlapping cerebral cortices: an fMRI study. *Neuroimage*, *23*(2), 525-533.

Manohar, S. G., & Husain, M. (2016). Human ventromedial prefrontal lesions alter incentivisation by reward. *cortex*, *76*, 104-120.

Massana, G., Serra-Grabulosa, J. M., Salgado-Pineda, P., Gastó, C., Junqué, C., Massana, J., ... & Salamero, M. (2003). Amygdalar atrophy in panic disorder patients detected by volumetric magnetic resonance imaging. *Neuroimage*, *19*(1), 80-90.

Mayberg, H. S., Lozano, A. M., Voon, V., McNeely, H. E., Seminowicz, D., Hamani, C., ... & Kennedy, S. H. (2005). Deep brain stimulation for treatment-resistant depression. *Neuron*, *45*(5), 651-660.

McEvoy, P. M., & Brans, S. (2013). Common versus unique variance across measures of worry and rumination: Predictive utility and mediational models for anxiety and depression. *Cognitive therapy and research*, *37*(1), 183-196.

McEvoy, P. M., Watson, H., Watkins, E. R., & Nathan, P. (2013). The relationship between worry, rumination, and comorbidity: Evidence for repetitive negative thinking as a transdiagnostic construct. *Journal of affective disorders*, *151*(1), 313-320.

McGinty, V. B., Hayden, B. Y., Heilbronner, S. R., Dumont, E. C., Graves, S. M., Mirrione, M. M., ... & DiFeliceantonio, A. G. (2011). Emerging, reemerging, and forgotten brain areas of the reward circuit: Notes from the 2010 Motivational Neural Networks conference. *Behavioural brain research*, *225*(1), 348-357.

McLaren, M. E., Szymkowicz, S. M., O'shea, A., Woods, A. J., Anton, S. D., & Dotson, V. M. (2016). Dimensions of depressive symptoms and cingulate volumes in older adults. *Translational psychiatry*, *6*(4), e788-e788.

McLean, C. P., Asnaani, A., Litz, B. T., & Hofmann, S. G. (2011). Gender differences in anxiety disorders: prevalence, course of illness, comorbidity and burden of illness. *Journal of psychiatric research*, *45*(8), 1027-1035.

Meier, T. B., Drevets, W. C., Wurfel, B. E., Ford, B. N., Morris, H. M., Victor, T. A., ... & Savitz, J. (2016). Relationship between neurotoxic kynurenine metabolites and reductions in right medial prefrontal cortical thickness in major depressive disorder. *Brain, behavior, and immunity*, *53*, 39-48.

Meier, B. P., Robinson, M. D., Crawford, L. E., & Ahlvers, W. J. (2007). When" light" and" dark" thoughts become light and dark responses: Affect biases brightness judgments. *Emotion*, *7*(2), 366.

Menon, V. (2011). Large-scale brain networks and psychopathology: a unifying triple network model. *Trends in cognitive sciences*, *15*(10), 483-506.

Merikangas, K. R., He, J. P., Burstein, M., Swanson, S. A., Avenevoli, S., Cui, L., ... & Swendsen, J. (2010). Lifetime prevalence of mental disorders in US adolescents: results from the National Comorbidity Survey Replication–Adolescent Supplement (NCS-A). *Journal of the American Academy of Child & Adolescent Psychiatry*, *49*(10), 980-989.

Merz, E. C., He, X., & Noble, K. G. (2018). Anxiety, depression, impulsivity, and brain structure in children and adolescents. *NeuroImage: Clinical*, *20*, 243-251.

Meyer, T. J., Miller, M. L., Metzger, R. L., & Borkovec, T. D. (1990). Development and validation of the penn state worry questionnaire. *Behaviour research and therapy*, *28*(6), 487-495.

Milad, M. R., & Rauch, S. L. (2007). The role of the orbitofrontal cortex in anxiety disorders. *Annals of the New York Academy of Sciences*, *1121*(1), 546-561.

Milham, M. P., Nugent, A. C., Drevets, W. C., Dickstein, D. S., Leibenluft, E., Ernst, M., ... & Pine, D. S. (2005). Selective reduction in amygdala volume in pediatric anxiety disorders: a voxel-based morphometry investigation. *Biological psychiatry*, *57*(9), 961-966.

Miller, K. L., Alfaro-Almagro, F., Bangerter, N. K., Thomas, D. L., Yacoub, E., Xu, J., ... & Griffanti, L. (2016). Multimodal population brain imaging in the UK Biobank prospective epidemiological study. *Nature neuroscience*, *19*(11), 1523-1536.

Modi, S., Thaploo, D., Kumar, P., & Khushu, S. (2019). Individual differences in trait anxiety are associated with gray matter alterations in hypothalamus: Preliminary neuroanatomical evidence. *Psychiatry Research: Neuroimaging*, *283*, 45-54.

Mohlman, J., Price, R. B., Eldreth, D. A., Chazin, D., Glover, D. M., & Kates, W. R. (2009). The relation of worry to prefrontal cortex volume in older adults with and without generalized anxiety disorder. *Psychiatry Research: Neuroimaging*, *173*(2), 121-127.

Molent, C., Maggioni, E., Cecchetto, F., Garzitto, M., Piccin, S., Bonivento, C., ... & Altamura, A. C. (2018). Reduced cortical thickness and increased gyrification in generalized anxiety disorder: a 3 T MRI study. *Psychological medicine*, *48*(12), 2001-2010.

Montchal, M. E., Reagh, Z. M., & Yassa, M. A. (2019). Precise temporal memories are supported by the lateral entorhinal cortex in humans. *Nature neuroscience*, *22*(2), 284-288.

Moon, C. M., Kim, G. W., & Jeong, G. W. (2014). Whole-brain gray matter volume abnormalities in patients with generalized anxiety disorder: voxel-based morphometry. *Neuroreport*, *25*(3), 184-189.

Moore, M. N., Salk, R. H., Van Hulle, C. A., Abramson, L. Y., Hyde, J. S., Lemery-Chalfant, K., & Goldsmith, H. H. (2013). Genetic and environmental influences on rumination, distraction, and depressed mood in adolescence. *Clinical psychological science*, *1*(3), 316-322.

Moss, H. E., Abdallah, S., Fletcher, P., Bright, P., Pilgrim, L., Acres, K., & Tyler, L. K. (2005). Selecting among competing alternatives: selection and retrieval in the left inferior frontal gyrus. *Cerebral Cortex*, *15*(11), 1723-1735.

Mueller, S. C., Aouidad, A., Gorodetsky, E., Goldman, D., Pine, D. S., & Ernst, M. (2013). Gray matter volume in adolescent anxiety: an impact of the brain-derived neurotrophic factor Val66Met polymorphism?. *Journal of the American Academy of Child & Adolescent Psychiatry*, *52*(2), 184-195.

Murty, V. P., Ritchey, M., Adcock, R. A., & LaBar, K. S. (2010). fMRI studies of successful emotional memory encoding: A quantitative meta-analysis. *Neuropsychologia*, *48*(12), 3459-3469.

Muthen, L. K., & Muthen, B. O. (2012). Mplus user's guide. 7th. *Los Angeles, CA: Muthén & Muthén*, *19982006*.

Na, K. S., Won, E., Kang, J., Chang, H. S., Yoon, H. K., Tae, W. S., ... & Ham, B. J. (2016). Brain-derived neurotrophic factor promoter methylation and cortical thickness in recurrent major depressive disorder. *Scientific reports*, *6*, 21089.

Nakamae, T., Narumoto, J., Sakai, Y., Nishida, S., Yamada, K., Kubota, M., ... & Fukui, K. (2012). Reduced cortical thickness in non-medicated patients with obsessive-compulsive disorder. *Progress in Neuro-Psychopharmacology and Biological Psychiatry*, *37*(1), 90-95.

Nathoo, F. S., Kong, L., Zhu, H., & Alzheimer's Disease Neuroimaging Initiative. (2019). A review of statistical methods in imaging genetics. *Canadian Journal of Statistics*, *47*(1), 108-131.

Neale, M. C., & Kendler, K. S. (1995). Models of comorbidity for multifactorial disorders. *American journal of human genetics*, *57*(4), 935.

Newby, J. M., & Moulds, M. L. (2012). A comparison of the content, themes, and features of intrusive memories and rumination in major depressive disorder. *British Journal of Clinical Psychology*, *51*(2), 197-205.

Newton, J. M., Dong, Y., Hidler, J., Plummer-D'Amato, P., Marehbian, J., Albistegui-DuBois, R. M., ... & Dobkin, B. H. (2008). Reliable assessment of lower limb motor representations with fMRI: use of a novel MR compatible device for real-time monitoring of ankle, knee and hip torques. *Neuroimage*, *43*(1), 136-146.

Nikolova, Y. S., Bogdan, R., Brigidi, B. D., & Hariri, A. R. (2012). Ventral striatum reactivity to reward and recent life stress interact to predict positive affect. *Biological psychiatry*, *72*(2), 157-163.

Nitschke, J. B., Heller, W., Imig, J. C., McDonald, R. P., & Miller, G. A. (2001). Distinguishing dimensions of anxiety and depression. *Cognitive Therapy and Research*, *25*(1), 1-22.

Nolen-Hoeksema, S. (1991). Responses to depression and their effects on the duration of depressive episodes. *Journal of abnormal psychology*, *100*(4), 569.

Nolen-Hoeksema, S. (2000). The role of rumination in depressive disorders and mixed anxiety/depressive symptoms. *Journal of abnormal psychology*, *109*(3), 504.

Oh, S. Y., Boegle, R., Ertl, M., Stephan, T., & Dieterich, M. (2018). Multisensory vestibular, vestibular-auditory, and auditory network effects revealed by parametric sound pressure stimulation. *Neuroimage*, *176*, 354-363.

Öhman, A. (2005). The role of the amygdala in human fear: automatic detection of threat. *Psychoneuroendocrinology*, *30*(10), 953-958.

Olson, I. R., Plotzker, A., & Ezzyat, Y. (2007). The enigmatic temporal pole: a review of findings on social and emotional processing. *Brain*, *130*(7), 1718-1731.

Omura, K., Constable, R. T., & Canli, T. (2005). Amygdala gray matter concentration is associated with extraversion and neuroticism. *Neuroreport*, *16*(17), 1905-1908.

O'Neill, P. K., Gore, F., & Salzman, C. D. (2018). Basolateral amygdala circuitry in positive and negative valence. *Current opinion in neurobiology*, *49*, 175-183.

Öngür, D., & Price, J. L. (2000). The organization of networks within the orbital and medial prefrontal cortex of rats, monkeys and humans. *Cerebral cortex*, *10*(3), 206-219.

Ono, Y., Ando, J., Onoda, N., Yoshimura, K., Momose, T., Hirano, M., & Kanba, S. (2002). Dimensions of temperament as vulnerability factors in depression. *Molecular psychiatry*, *7*(9), 948-953.

O'Reilly, R. C. (2010). The what and how of prefrontal cortical organization. *Trends in neurosciences*, *33*(8), 355-361.

Orr, J. M., Smolker, H. R., & Banich, M. T. (2015). Organization of the human frontal pole revealed by large-scale DTI-based connectivity: implications for control of behavior. *PloS one*, *10*(5).

Østby, Y., Walhovd, K. B., Tamnes, C. K., Grydeland, H., Westlye, L. T., & Fjell, A. M. (2012). Mental time travel and default-mode network functional connectivity in the developing brain. *Proceedings of the National Academy of Sciences*, *109*(42), 16800-16804.

Ozalay, O., Aksoy, B., Tunay, S., Simsek, F., Chandhoki, S., Kitis, O., ... & Gonul, A. S. (2016). Cortical thickness and VBM in young women at risk for familial depression and their depressed mothers with positive family history. *Psychiatry Research: Neuroimaging*, *252*, 1-9.

Panizzon, M. S., Fennema-Notestine, C., Eyler, L. T., Jernigan, T. L., Prom-Wormley, E., Neale, M., ... & Xian, H. (2009). Distinct genetic influences on cortical surface area and cortical thickness. *Cerebral cortex*, *19*(11), 2728-2735.

Pannekoek, J. N., van der Werff, S. J., van den Bulk, B. G., van Lang, N. D., Rombouts, S. A., van Buchem, M. A., ... & van der Wee, N. J. (2014). Reduced anterior cingulate gray matter volume in treatment-naive clinically depressed adolescents. *NeuroImage: Clinical*, *4*, 336-342.

Papageorgiou, C., & Wells, A. (1999). Process and meta-cognitive dimensions of depressive and anxious thoughts and relationships with emotional intensity. *Clinical Psychology & Psychotherapy: An International Journal of Theory & Practice*, *6*(2), 156-162.

Papmeyer, M., Giles, S., Sussmann, J. E., Kielty, S., Stewart, T., Lawrie, S. M., ... & McIntosh, A. M. (2015). Cortical thickness in individuals at high familial risk of mood disorders as they develop major depressive disorder. *Biological psychiatry*, *78*(1), 58-66.

Park, S. C., Kim, J. M., Jun, T. Y., Lee, M. S., Kim, J. B., Yim, H. W., & Park, Y. C. (2017). How many different symptom combinations fulfil the diagnostic criteria for major depressive disorder? Results from the CRESCEND study. *Nordic journal of psychiatry*, *71*(3), 217-222.

Parker, J. G., Zalusky, E. J., & Kirbas, C. (2014). Functional MRI mapping of visual function and selective attention for performance assessment and presurgical planning using conjunctive visual search. *Brain and behavior*, *4*(2), 227-237.

Peng, W., Jia, Z., Huang, X., Lui, S., Kuang, W., Sweeney, J. A., & Gong, Q. (2019). Brain structural abnormalities in emotional regulation and sensory processing regions associated with anxious depression. *Progress in Neuro-Psychopharmacology and Biological Psychiatry*, *94*, 109676.

Peng, D., Shi, F., Li, G., Fralick, D., Shen, T., Qiu, M., ... & Fang, Y. (2015). Surface vulnerability of cerebral cortex to major depressive disorder. *PLoS One*, *10*(3), e0120704.

Peper, J. S., Pol, H. H., Crone, E. A., & Van Honk, J. (2011). Sex steroids and brain structure in pubertal boys and girls: a mini-review of neuroimaging studies. *Neuroscience*, *191*, 28-37.

Perlman, G., Bartlett, E., DeLorenzo, C., Weissman, M., McGrath, P., Ogden, T., ... & Oquendo, M. (2017). Cortical thickness is not associated with current depression in a clinical treatment study. *Human brain mapping*, *38*(9), 4370-4385.

Perry, J. C., Lavori, P. W., Cooper, S. H., Hoke, L., & O'Connell, M. E. (1987). The Diagnostic Interview Schedule and DSM-III antisocial personality disorder. *Journal of Personality Disorders*, *1*(2), 121-131.

Piguet, C., Desseilles, M., Sterpenich, V., Cojan, Y., Bertschy, G., & Vuilleumier, P. (2014). Neural substrates of rumination tendency in non-depressed individuals. *Biological psychology*, *103*, 195-202.

Pillay, S. S., Renshaw, P. F., Bonello, C. M., Lafer, B., Fava, M., & Yurgelun-Todd, D. (1998). A quantitative magnetic resonance imaging study of caudate and lenticular nucleus gray matter volume in primary unipolar major depression: relationship to treatment response and clinical severity. *Psychiatry Research: Neuroimaging*, *84*(2-3), 61-74.

Pinheiro J, Bates D, DebRoy S, Sarkar D, R Core Team (2020). *nlme: Linear and Nonlinear Mixed Effects Models*. R package version 3.1-148

Pizzi, S. D., Chiacchiaretta, P., Mantini, D., Bubbico, G., Ferretti, A., Edden, R. A., ... & Bonanni, L. (2017). Functional and neurochemical interactions within the amygdala–medial prefrontal cortex circuit and their relevance to emotional processing. *Brain Structure and Function*, *222*(3), 1267-1279.

Poeppl, T. B., Müller, V. I., Hoffstaedter, F., Bzdok, D., Laird, A. R., Fox, P. T., ... & Goya-Maldonado, R. (2016). Imbalance in subregional connectivity of the right temporoparietal junction in major depression. *Human brain mapping*, *37*(8), 2931-2942.

Posse, S., Fitzgerald, D., Gao, K., Habel, U., Rosenberg, D., Moore, G. J., & Schneider, F. (2003). Real-time fMRI of temporolimbic regions detects amygdala activation during single-trial self-induced sadness. *Neuroimage*, *18*(3), 760-768.

Posthuma, D., De Geus, E., Baaré, W. *et al.* The association between brain volume and intelligence is of genetic origin. *Nat Neurosci* **5,** 83–84 (2002). https://doi.org/10.1038/nn0202-83

Privado, J., Roman, F. J., Saenz-Urturi, C., Burgaleta, M., & Colom, R. (2017). Gray and white matter correlates of the Big Five personality traits. *Neuroscience*, *349*, 174-184.

Putnick, D. L., & Bornstein, M. H. (2016). Measurement invariance conventions and reporting: The state of the art and future directions for psychological research. *Developmental review*, *41*, 71-90.

Qi, H., Ning, Y., Li, J., Guo, S., Chi, M., Gao, M., ... & Wu, K. (2014). Gray matter volume abnormalities in depressive patients with and without anxiety disorders. *Medicine*, *93*(29).

Qiu, L., Lui, S., Kuang, W., Huang, X., Li, J., Zhang, J., ... & Gong, Q. (2014). Regional increases of cortical thickness in untreated, first-episode major depressive disorder. *Translational psychiatry*, *4*(4), e378-e378.

Radua, J., van den Heuvel, O. A., Surguladze, S., & Mataix-Cols, D. (2010). Meta-analytical comparison of voxel-based morphometry studies in obsessive-compulsive disorder vs other anxiety disorders. *Archives of general psychiatry*, *67*(7), 701-711.

Raes, F. (2010). Rumination and worry as mediators of the relationship between self-compassion and depression and anxiety. *Personality and Individual Differences*, *48*(6), 757-761.

Rakic, P. (1995). A small step for the cell, a giant leap for mankind: a hypothesis of neocortical expansion during evolution. *Trends in neurosciences*, *18*(9), 383-388.

Reise, S. P. (2012). The rediscovery of bifactor measurement models. *Multivariate behavioral research*, *47*(5), 667-696.

Reynolds, S., Carrey, N., Jaworska, N., Langevin, L. M., Yang, X. R., & MacMaster, F. P. (2014). Cortical thickness in youth with major depressive disorder. *BMC psychiatry*, *14*(1), 83.

Riccelli, R., Toschi, N., Nigro, S., Terracciano, A., & Passamonti, L. (2017). Surface-based morphometry reveals the neuroanatomical basis of the five-factor model of personality. *Social cognitive and affective neuroscience*, *12*(4), 671-684.

Rijsdijk, F. V., Van Haren, N. E. M., Picchioni, M. M., McDonald, C., Toulopoulou, T., Pol, H. H., ... & Sham, P. C. (2005). Brain MRI abnormalities in schizophrenia: same genes or same environment?. *Psychological medicine*, *35*(10), 1399-1409.

Robichaud, M., Dugas, M. J., & Conway, M. (2003). Gender differences in worry and associated cognitive-behavioral variables. *Journal of anxiety disorders*, *17*(5), 501-516.

Robins, L. N., Helzer, J. E., Croughan, J., & Ratcliff, K. S. (1981). National Institute of Mental Health diagnostic interview schedule: Its history, characteristics, and validity. *Archives of general psychiatry*, *38*(4), 381-389.

Roehrig, C. (2016). Mental disorders top the list of the most costly conditions in the United States: $201 billion. *Health Affairs*, *35*(6), 1130-1135.

Rosenström, T., Gjerde, L. C., Krueger, R. F., Aggen, S. H., Czajkowski, N. O., Gillespie, N. A., ... & Ystrom, E. (2019). Joint factorial structure of psychopathology and personality. *Psychological medicine*, *49*(13), 2158-2167.

Rosso, I. M., Cintron, C. M., Steingard, R. J., Renshaw, P. F., Young, A. D., & Yurgelun-Todd, D. A. (2005). Amygdala and hippocampus volumes in pediatric major depression. *Biological psychiatry*, *57*(1), 21-26.

Rotenberg, V. S. (2004). The peculiarity of the right-hemisphere function in depression: solving the paradoxes. *Progress in Neuro-Psychopharmacology and Biological Psychiatry*, *28*(1), 1-13.

Rotge, J. Y., Langbour, N., Guehl, D., Bioulac, B., Jaafari, N., Allard, M., ... & Burbaud, P. (2010). Gray matter alterations in obsessive–compulsive disorder: an anatomic likelihood estimation meta-analysis. *Neuropsychopharmacology*, *35*(3), 686-691.

Roy, M. A., Neale, M. C., Pedersen, N. L., Mathe, A. A., & Kendler, K. S. (1995). A twin study of generalized anxiety disorder and major depression. *Psychological Medicine*, *25*(5), 1037-1049.

Rugg, M. D., & Vilberg, K. L. (2013). Brain networks underlying episodic memory retrieval. *Current opinion in neurobiology*, *23*(2), 255-260.

Ruigrok, A. N., Salimi-Khorshidi, G., Lai, M. C., Baron-Cohen, S., Lombardo, M. V., Tait, R. J., & Suckling, J. (2014). A meta-analysis of sex differences in human brain structure. *Neuroscience & Biobehavioral Reviews*, *39*, 34-50.

Rutter, M., Caspi, A., & Moffitt, T. E. (2003). Using sex differences in psychopathology to study causal mechanisms: unifying issues and research strategies. *Journal of child psychology and psychiatry*, *44*(8), 1092-1115.

Sacher, J., Neumann, J., Fünfstück, T., Soliman, A., Villringer, A., & Schroeter, M. L. (2012). Mapping the depressed brain: a meta-analysis of structural and functional alterations in major depressive disorder. *Journal of affective disorders*, *140*(2), 142-148.

Salk, R. H., Hyde, J. S., & Abramson, L. Y. (2017). Gender differences in depression in representative national samples: meta-analyses of diagnoses and symptoms. *Psychological bulletin*, *143*(8), 783.

Salvadore, G., Nugent, A. C., Lemaitre, H., Luckenbaugh, D. A., Tinsley, R., Cannon, D. M., ... & Drevets, W. C. (2011). Prefrontal cortical abnormalities in currently depressed versus currently remitted patients with major depressive disorder. *Neuroimage*, *54*(4), 2643-2651.

Sarinopoulos, I., Grupe, D. W., Mackiewicz, K. L., Herrington, J. D., Lor, M., Steege, E. E., & Nitschke, J. B. (2010). Uncertainty during anticipation modulates neural responses to aversion in human insula and amygdala. *Cerebral Cortex*, *20*(4), 929-940.

Scaini, S., Belotti, R., & Ogliari, A. (2014). Genetic and environmental contributions to social anxiety across different ages: A meta-analytic approach to twin data. *Journal of anxiety disorders*, *28*(7), 650-656.

Schienle, A., Ebner, F., & Schäfer, A. (2011). Localized gray matter volume abnormalities in generalized anxiety disorder. *European archives of psychiatry and clinical neuroscience*, *261*(4), 303-307.

Schienle, A., Schäfer, A., Pignanelli, R., & Vaitl, D. (2009). Worry tendencies predict brain activation during aversive imagery. *Neuroscience letters*, *461*(3), 289-292.

Schmaal, L., Hibar, D. P., Sämann, P. G., Hall, G. B., Baune, B. T., Jahanshad, N., ... & Vernooij, M. W. (2017). Cortical abnormalities in adults and adolescents with major depression based on brain scans from 20 cohorts worldwide in the ENIGMA Major Depressive Disorder Working Group. *Molecular psychiatry*, *22*(6), 900-909.

Schmaal, L., Veltman, D. J., van Erp, T. G., Sämann, P. G., Frodl, T., Jahanshad, N., ... & Vernooij, M. W. (2016). Subcortical brain alterations in major depressive disorder: findings from the ENIGMA Major Depressive Disorder working group. *Molecular psychiatry*, *21*(6), 806-812.

Schultz, W. (2016). Reward functions of the basal ganglia. *Journal of neural transmission*, *123*(7), 679-693.

Ségonne, F., Dale, A. M., Busa, E., Glessner, M., Salat, D., Hahn, H. K., & Fischl, B. (2004). A hybrid approach to the skull stripping problem in MRI. *Neuroimage*, *22*(3), 1060-1075.

Servaas, M. N., Riese, H., Ormel, J., & Aleman, A. (2014). The neural correlates of worry in association with individual differences in neuroticism. *Human brain mapping*, *35*(9), 4303-4315.

Shad, M. U., Muddasani, S., & Rao, U. (2012). Gray matter differences between healthy and depressed adolescents: a voxel-based morphometry study. *Journal of child and adolescent psychopharmacology*, *22*(3), 190-197.

Shang, J., Fu, Y., Ren, Z., Zhang, T., Du, M., Gong, Q., ... & Zhang, W. (2014). The common traits of the ACC and PFC in anxiety disorders in the DSM-5: meta-analysis of voxel-based morphometry studies. *PloS one*, *9*(3), e93432.

Shansky, R. M., Hamo, C., Hof, P. R., Lou, W., McEwen, B. S., & Morrison, J. H. (2010). Estrogen promotes stress sensitivity in a prefrontal cortex–amygdala pathway. *Cerebral Cortex*, *20*(11), 2560-2567.

Sharp, P. B., Miller, G. A., & Heller, W. (2015). Transdiagnostic dimensions of anxiety: neural mechanisms, executive functions, and new directions. *International Journal of Psychophysiology*, *98*(2), 365-377.

Shaw, P., Kabani, N. J., Lerch, J. P., Eckstrand, K., Lenroot, R., Gogtay, N., ... & Giedd, J. N. (2008). Neurodevelopmental trajectories of the human cerebral cortex. *Journal of neuroscience*, *28*(14), 3586-3594.

Sheline, Y. I. (2003). Neuroimaging studies of mood disorder effects on the brain. *Biological psychiatry*, *54*(3), 338-352.

Shura, R. D., Hurley, R. A., & Taber, K. H. (2014). Insular cortex: structural and functional neuroanatomy. *The Journal of neuropsychiatry and clinical neurosciences*, *26*(4), iv-282.

Simmons, A., Matthews, S. C., Stein, M. B., & Paulus, M. P. (2004). Anticipation of emotionally aversive visual stimuli activates right insula. *Neuroreport*, *15*(14), 2261-2265.

Simmons, A., Strigo, I., Matthews, S. C., Paulus, M. P., & Stein, M. B. (2006). Anticipation of aversive visual stimuli is associated with increased insula activation in anxiety-prone subjects. *Biological psychiatry*, *60*(4), 402-409.

Sin, E. L., Shao, R., Geng, X., Cho, V., & Lee, T. (2018). The neuroanatomical basis of two subcomponents of rumination: A VBM study. *Frontiers in human neuroscience*, *12*, 324.

Selzam, S., Coleman, J. R., Caspi, A., Moffitt, T. E., & Plomin, R. (2018). A polygenic p factor for major psychiatric disorders. *Translational psychiatry*, *8*(1), 1-9.

Slavich, G. M., O'Donovan, A., Epel, E. S., & Kemeny, M. E. (2010). Black sheep get the blues: A psychobiological model of social rejection and depression. *Neuroscience & Biobehavioral Reviews*, *35*(1), 39-45.

Sled, J. G., Zijdenbos, A. P., & Evans, A. C. (1998). A nonparametric method for automatic correction of intensity nonuniformity in MRI data. *IEEE transactions on medical imaging*, *17*(1), 87-97.

Snyder, H. R., Banich, M. T., & Munakata, Y. (2011). Choosing our words: retrieval and selection processes recruit shared neural substrates in left ventrolateral prefrontal cortex. *Journal of cognitive neuroscience*, *23*(11), 3470-3482.

Snyder, H. R., Banich, M. T., & Munakata, Y. (2014). All competition is not alike: Neural mechanisms for resolving underdetermined and prepotent competition. *Journal of Cognitive Neuroscience*, *26*(11), 2608-2623.

Snyder, H. R., Hankin, B. L., Sandman, C. A., Head, K., & Davis, E. P. (2017). Distinct patterns of reduced prefrontal and limbic gray matter volume in childhood general and internalizing psychopathology. *Clinical Psychological Science*, *5*(6), 1001-1013.

Spampinato, M. V., Wood, J. N., De Simone, V., & Grafman, J. (2009). Neural correlates of anxiety in healthy volunteers: a voxel-based morphometry study. *The Journal of neuropsychiatry and clinical neurosciences*, *21*(2), 199-205.

Spear, L. P. (2000). Neurobehavioral changes in adolescence. *Current directions in psychological science*, *9*(4), 111-114.

Spinhoven, P., van Balkom, A., & Nolen, W. A. (2011). Comorbidity patterns of anxiety and depressive disorders in a large cohort study: the Netherlands Study of Depression and Anxiety (NESDA). *J Clin Psychiatry*, *72*(3), 341-348.

Steinberg, L. (2010). A dual systems model of adolescent risk-taking. *Developmental Psychobiology: The Journal of the International Society for Developmental Psychobiology*, *52*(3), 216-224.

Stokes, C., & Hirsch, C. R. (2010). Engaging in imagery versus verbal processing of worry: Impact on negative intrusions in high worriers. *Behaviour Research and Therapy*, *48*(5), 418-423.

Stone, D. M., Simon, T. R., Fowler, K. A., Kegler, S. R., Yuan, K., Holland, K. M., ... & Crosby, A. E. (2018). Vital signs: trends in state suicide rates—United States, 1999–2016 and circumstances contributing to suicide—27 states, 2015. *Morbidity and Mortality Weekly Report*, *67*(22), 617.

Stratmann, M., Konrad, C., Kugel, H., Krug, A., Schöning, S., Ohrmann, P., ... & Arolt, V. (2014). Insular and hippocampal gray matter volume reductions in patients with major depressive disorder. *PloS one*, *9*(7).

Strawn, J. R., Wehry, A. M., Chu, W. J., Adler, C. M., Eliassen, J. C., Cerullo, M. A., ... & DelBello, M. P. (2013). Neuroanatomic abnormalities in adolescents with generalized

anxiety disorder: A voxel-based morphometry study. *Depression and anxiety*, *30*(9), 842-848.

Strawn, J. R., Wegman, C. J., Dominick, K. C., Swartz, M. S., Wehry, A. M., Patino, L. R., ... & DelBello, M. P. (2014). Cortical surface anatomy in pediatric patients with generalized anxiety disorder. *Journal of anxiety disorders*, *28*(7), 717-723.

Strawn, J. R., Hamm, L., Fitzgerald, D. A., Fitzgerald, K. D., Monk, C. S., & Phan, K. L. (2015). Neurostructural abnormalities in pediatric anxiety disorders. *Journal of anxiety disorders*, *32*, 81-88.

Stroud, L. R., Salovey, P., & Epel, E. S. (2002). Sex differences in stress responses: social rejection versus achievement stress. *Biological psychiatry*, *52*(4), 318-327.

Stuhrmann, A., Dohm, K., Kugel, H., Zwanzger, P., Redlich, R., Grotegerd, D., ... & Zwitserlood, P. (2013). Mood-congruent amygdala responses to subliminally presented facial expressions in major depression: associations with anhedonia. *Journal of psychiatry & neuroscience: JPN*, *38*(4), 249.

Suffren, S., Chauret, M., Nassim, M., Lepore, F., & Maheu, F. S. (2019). On a continuum to anxiety disorders: Adolescents at parental risk for anxiety show smaller rostral anterior cingulate cortex and insula thickness. *Journal of affective disorders*, *248*, 34-41.

Suh, J. S., Schneider, M. A., Minuzzi, L., MacQueen, G. M., Strother, S. C., Kennedy, S. H., & Frey, B. N. (2019). Cortical thickness in major depressive disorder: a systematic review and meta-analysis. *Progress in Neuro-Psychopharmacology and Biological Psychiatry*, *88*, 287-302.

Sullivan P.F., Neale M.C., & Kendler K.S. (2000). Genetic epidemiology of major depression: review and meta-analysis. Am J Psychiatry, 157:1552–1562.

Sussman, D., Leung, R. C., Chakravarty, M. M., Lerch, J. P., & Taylor, M. J. (2016a). The developing human brain: age-related changes in cortical, subcortical, and cerebellar anatomy. *Brain and behavior*, *6*(4), e00457.

Sussman, D., Pang, E. W., Jetly, R., Dunkley, B. T., & Taylor, M. J. (2016b). Neuroanatomical features in soldiers with post-traumatic stress disorder. *BMC neuroscience*, *17*(1), 13.

Svoboda, E., McKinnon, M. C., & Levine, B. (2006). The functional neuroanatomy of autobiographical memory: a meta-analysis. *Neuropsychologia*, *44*(12), 2189-2208.

Syal, S., Hattingh, C. J., Fouché, J. P., Spottiswoode, B., Carey, P. D., Lochner, C., & Stein, D. J. (2012). Grey matter abnormalities in social anxiety disorder: a pilot study. *Metabolic Brain Disease*, *27*(3), 299-309.

Szeszko, P. R., MacMillan, S., McMeniman, M., Chen, S., Baribault, K., Lim, K. O., ... & Moore, G. J. (2004). Brain structural abnormalities in psychotropic drug-naive pediatric patients with obsessive-compulsive disorder. *American Journal of Psychiatry*, *161*(6), 1049-1056.

Taki, Y., Thyreau, B., Kinomura, S., Sato, K., Goto, R., Kawashima, R., & Fukuda, H. (2011). Correlations among brain gray matter volumes, age, gender, and hemisphere in healthy individuals. *PloS one*, *6*(7), e22734.

Tamnes, C. K., Herting, M. M., Goddings, A. L., Meuwese, R., Blakemore, S. J., Dahl, R. E., ... & Mills, K. L. (2017). Development of the cerebral cortex across adolescence: a multisample study of inter-related longitudinal changes in cortical volume, surface area, and thickness. *Journal of Neuroscience*, *37*(12), 3402-3412.

Taylor, S. (2011). Etiology of obsessions and compulsions: a meta-analysis and narrative review of twin studies. *Clinical psychology review*, *31*(8), 1361-1372.

Thomason, M. E., Hamilton, J. P., & Gotlib, I. H. (2011). Stress-induced activation of the HPA axis predicts connectivity between subgenual cingulate and salience network during rest in adolescents. *Journal of Child Psychology and Psychiatry*, *52*(10), 1026-1034.

Thompson, P. M., Cannon, T. D., Narr, K. L., Van Erp, T., Poutanen, V. P., Huttunen, M., ... & Dail, R. (2001). Genetic influences on brain structure. *Nature neuroscience*, *4*(12), 1253-1258.

Thompson, W. L., & Kosslyn, S. M. (2000). Neural systems activated during visual mental imagery: A review and meta-analyses. In *Brain mapping: The systems* (pp. 535-560). Academic Press.

Thompson-Schill, S. L., D'Esposito, M., Aguirre, G. K., & Farah, M. J. (1997). Role of left inferior prefrontal cortex in retrieval of semantic knowledge: a reevaluation. *Proceedings of the National Academy of Sciences*, *94*(26), 14792-14797.

Treynor, W., Gonzalez, R., & Nolen-Hoeksema, S. (2003). Rumination reconsidered: A psychometric analysis. *Cognitive therapy and research*, *27*(3), 247-259.

Tsao, A., Sugar, J., Lu, L., Wang, C., Knierim, J. J., Moser, M. B., & Moser, E. I. (2018). Integrating time from experience in the lateral entorhinal cortex. *Nature*, *561*(7721), 57-62.

Tu, P. C., Chen, L. F., Hsieh, J. C., Bai, Y. M., Li, C. T., & Su, T. P. (2012). Regional cortical thinning in patients with major depressive disorder: a surface-based morphometry study. *Psychiatry Research: Neuroimaging*, *202*(3), 206-213.

Twenge, J. M., & Nolen-Hoeksema, S. (2002). Age, gender, race, socioeconomic status, and birth cohort difference on the children's depression inventory: A meta-analysis. *Journal of abnormal psychology*, *111*(4), 578.

Uchida, R. R., Del-Ben, C. M., Busatto, G. F., Duran, F. L., Guimarães, F. S., Crippa, J. A., ... & Graeff, F. G. (2008). Regional gray matter abnormalities in panic disorder: a voxel-based morphometry study. *Psychiatry Research: Neuroimaging*, *163*(1), 21-29.

Uddin, L. Q., Nomi, J. S., Hébert-Seropian, B., Ghaziri, J., & Boucher, O. (2017). Structure and function of the human insula. *Journal of clinical neurophysiology: official publication of the American Electroencephalographic Society*, *34*(4), 300.

Ullman, J. B., & Bentler, P. M. (2003). Structural equation modeling. *Handbook of psychology*, 607-634.

Underwood, A. G., Guynn, M. J., & Cohen, A. L. (2015). The future orientation of past memory: The role of BA 10 in prospective and retrospective retrieval modes. *Frontiers in human neuroscience*, *9*, 668.

Vanderhasselt, M. A., Kühn, S., & De Raedt, R. (2011). Healthy brooders employ more attentional resources when disengaging from the negative: an event-related fMRI study. *Cognitive, Affective, & Behavioral Neuroscience*, *11*(2), 207-216.

van Eijndhoven, P., van Wingen, G., Katzenbauer, M., Groen, W., Tepest, R., Fernández, G., ... & Tendolkar, I. (2013). Paralimbic cortical thickness in first-episode depression: evidence for trait-related differences in mood regulation. *American Journal of Psychiatry*, *170*(12), 1477-1486.

van Essen, D. C., Ugurbil, K., Auerbach, E., Barch, D., Behrens, T. E. J., Bucholz, R., ... & Della Penna, S. (2012). The Human Connectome Project: a data acquisition perspective. *Neuroimage*, *62*(4), 2222-2231.

van Haren, N. E., Rijsdijk, F., Schnack, H. G., Picchioni, M. M., Toulopoulou, T., Weisbrod, M., ... & Boomsma, D. I. (2012). The genetic and environmental determinants of the association between brain abnormalities and schizophrenia: the schizophrenia twins and relatives consortium. *Biological psychiatry*, *71*(10), 915-921.

van Tol, M. J., van der Wee, N. J., van den Heuvel, O. A., Nielen, M. M., Demenescu, L. R., Aleman, A., ... & Veltman, D. J. (2010). Regional brain volume in depression and anxiety disorders. *Archives of general psychiatry*, *67*(10), 1002-1011.

Vasic, N., Walter, H., Höse, A., & Wolf, R. C. (2008). Gray matter reduction associated with psychopathology and cognitive dysfunction in unipolar depression: a voxel-based morphometry study. *Journal of affective disorders*, *109*(1-2), 107-116.

Veronese, E., Ragogna, M., Meduri, M., Del Fabro, L., Canalaz, F., Zamboli, R., ... & Serretti, A. (2015). Reduced frontal cortical thickness in generalized anxiety disorder. *European Psychiatry*, *30*(S1), 1-1.

Vesga-López, O., Schneier, F., Wang, S., Heimberg, R., Liu, S. M., Hasin, D. S., & Blanco, C. (2008). Gender differences in generalized anxiety disorder: results from the National Epidemiologic Survey on Alcohol and Related Conditions (NESARC). *The Journal of clinical psychiatry*, *69*(10), 1606.

Videbech, P. & Ravnkilde, B. Hippocampal volume and depression: a meta-analysis of MRI studies. *Am. J. Psychiatry* **161**, 1957–1966 (2004).

Vijayakumar, N., Allen, N. B., Youssef, G., Dennison, M., Yücel, M., Simmons, J. G., & Whittle, S. (2016). Brain development during adolescence: A mixed-longitudinal investigation of cortical thickness, surface area, and volume. *Human brain mapping*, *37*(6), 2027-2038.

Wacker, J., Dillon, D. G., & Pizzagalli, D. A. (2009). The role of the nucleus accumbens and rostral anterior cingulate cortex in anhedonia: integration of resting EEG, fMRI, and volumetric techniques. *Neuroimage*, *46*(1), 327-337.

Wager, T. D., Atlas, L. Y., Lindquist, M. A., Roy, M., Woo, C. W., & Kross, E. (2013). An fMRI-based neurologic signature of physical pain. *New England Journal of Medicine*, *368*(15), 1388-1397.

Wagner, A. D., Paré-Blagoev, E. J., Clark, J., & Poldrack, R. A. (2001). Recovering meaning: left prefrontal cortex guides controlled semantic retrieval. *Neuron*, *31*(2), 329-338.

Wagner, G., Schultz, C. C., Koch, K., Schachtzabel, C., Sauer, H., & Schlösser, R. G. (2012). Prefrontal cortical thickness in depressed patients with high-risk for suicidal behavior. *Journal of psychiatric research*, *46*(11), 1449-1455.

Wang, K., Wei, D., Yang, J., Xie, P., Hao, X., & Qiu, J. (2015). Individual differences in rumination in healthy and depressive samples: association with brain structure, functional connectivity and depression. *Psychological medicine*, *45*(14), 2999-3008.

Wang, X., Cheng, B., Luo, Q., Qiu, L., & Wang, S. (2018). Gray matter structural alterations in social anxiety disorder: a voxel-based meta-analysis. *Frontiers in psychiatry*, *9*, 449.

Wang, Y., Deng, Y., Fung, G., Liu, W. H., Wei, X. H., Jiang, X. Q., ... & Chan, R. C. (2014). Distinct structural neural patterns of trait physical and social anhedonia: Evidence from cortical thickness, subcortical volumes and inter-regional correlations. *Psychiatry Research: Neuroimaging*, *224*(3), 184-191.

Warnell, K. R., Pecukonis, M., & Redcay, E. (2018). Developmental relations between amygdala volume and anxiety traits: Effects of informant, sex, and age. *Development and psychopathology*, *30*(4), 1503-1515.

Warren, S. L., Schmitz, S., & Emde, R. N. (1999). Behavioral genetic analyses of self-reported anxiety at 7 years of age. *Journal of the American Academy of Child & Adolescent Psychiatry*, *38*(11), 1403-1408.

Watkins, E. D., Moulds, M., & Mackintosh, B. (2005). Comparisons between rumination and worry in a non-clinical population. *Behaviour research and therapy*, *43*(12), 1577-1585.

Watson, D., & Clark, L. A. (1991). The mood and anxiety symptom questionnaire. *Unpublished manuscript, University of Iowa, department of psychology, Iowa City*.

Watson, D., Clark, L. A., Weber, K., Assenheimer, J. S., Strauss, M. E., & McCormick, R. A. (1995a). Testing a tripartite model: II. Exploring the symptom structure of anxiety and depression in student, adult, and patient samples. *Journal of abnormal Psychology*, *104*(1), 15.

Watson, D., Weber, K., Assenheimer, J. S., Clark, L. A., Strauss, M. E., & McCormick, R. A. (1995b). Testing a tripartite model: I. Evaluating the convergent and discriminant validity of anxiety and depression symptom scales. *Journal of abnormal psychology*, *104*(1), 3.

Webb, C. A., Weber, M., Mundy, E. A., & Killgore, W. D. (2014). Reduced gray matter volume in the anterior cingulate, orbitofrontal cortex and thalamus as a function of mild depressive symptoms: a voxel-based morphometric analysis. *Psychological medicine*, *44*(13), 2833-2843.

Wehry, A. M., McNamara, R. K., Adler, C. M., Eliassen, J. C., Croarkin, P., Cerullo, M. A., ... & Strawn, J. R. (2015). Neurostructural impact of co-occurring anxiety in pediatric patients with major depressive disorder: a voxel-based morphometry study. *Journal of affective disorders*, *171*, 54-59.

Wei, D., Du, X., Li, W., Chen, Q., Li, H., Hao, X., ... & Qiu, J. (2015). Regional gray matter volume and anxiety-related traits interact to predict somatic complaints in a non-clinical sample. *Social cognitive and affective neuroscience*, *10*(1), 122-128.

Werner, K. B., Few, L. R., & Bucholz, K. K. (2015). Epidemiology, comorbidity, and behavioral genetics of antisocial personality disorder and psychopathy. *Psychiatric annals*, *45*(4), 195-199.

Wessel, J. R., & Aron, A. R. (2017). On the globality of motor suppression: unexpected events and their influence on behavior and cognition. *Neuron*, *93*(2), 259-280.

Whitfield-Gabrieli, S., & Ford, J. M. (2012). Default mode network activity and connectivity in psychopathology. *Annual review of clinical psychology*, *8*, 49-76.

Whitmer, A., & Gotlib, I. H. (2011). Brooding and reflection reconsidered: A factor analytic examination of rumination in currently depressed, formerly depressed, and never depressed individuals. *Cognitive Therapy and Research*, *35*(2), 99-107.

Wieser, M. J., Hambach, A., & Weymar, M. (2018). Neurophysiological correlates of attentional bias for emotional faces in socially anxious individuals–Evidence from a visual search task and N2pc. *Biological psychology*, *132*, 192-201.

Winkler, A. M., Kochunov, P., Blangero, J., Almasy, L., Zilles, K., Fox, P. T., ... & Glahn, D. C. (2010). Cortical thickness or grey matter volume? The importance of selecting the phenotype for imaging genetics studies. *Neuroimage*, *53*(3), 1135-1146.

Winkler, A. M., Ridgway, G. R., Webster, M. A., Smith, S. M., & Nichols, T. E. (2014). Permutation inference for the general linear model. *Neuroimage*, *92*, 381-397.

Won, E., Choi, S., Kang, J., Lee, M. S., & Ham, B. J. (2016). Regional cortical thinning of the orbitofrontal cortex in medication-naïve female patients with major depressive disorder is not associated with MAOA-uVNTR polymorphism. *Annals of general psychiatry*, *15*(1), 26.

Wong, J. J., O'Daly, O., Mehta, M. A., Young, A. H., & Stone, J. M. (2016). Ketamine modulates subgenual cingulate connectivity with the memory-related neural circuit—a mechanism of relevance to resistant depression?. *PeerJ*, *4*, e1710.

Woo, C. W., Koban, L., Kross, E., Lindquist, M. A., Banich, M. T., Ruzic, L., ... & Wager, T. D. (2014). Separate neural representations for physical pain and social rejection. *Nature communications*, *5*(1), 1-12.

Wood, A. C., & Neale, M. C. (2010). Twin studies and their implications for molecular genetic studies: endophenotypes integrate quantitative and molecular genetics in ADHD research. *Journal of the American Academy of Child & Adolescent Psychiatry*, *49*(9), 874-883.

Wright, C. I., Feczko, E., Dickerson, B., & Williams, D. (2007). Neuroanatomical correlates of personality in the elderly. *Neuroimage*, *35*(1), 263-272.

Yang, X. H., Wang, Y., Huang, J., Zhu, C. Y., Liu, X. Q., Cheung, E. F., ... & Chan, R. C. (2015). Increased prefrontal and parietal cortical thickness does not correlate with anhedonia in patients with untreated first-episode major depressive disorders. *Psychiatry Research: Neuroimaging*, *234*(1), 144-151.

Yeo, B. T., Krienen, F. M., Sepulcre, J., Sabuncu, M. R., Lashkari, D., Hollinshead, M., ... & Fischl, B. (2011). The organization of the human cerebral cortex estimated by intrinsic functional connectivity. *Journal of neurophysiology*.

Yoon, H. J., Seo, E. H., Kim, J. J., & Choo, I. H. (2019). Neural correlates of self-referential processing and their clinical implications in social anxiety disorder. *Clinical Psychopharmacology and Neuroscience*, *17*(1), 12.

Zahn-Waxler, C., Crick, N. R., Shirtcliff, E. A., & Woods, K. E. (2006). The origins and development of psychopathology in females and males.

Zalta, A. K., & Chambless, D. L. (2008). Exploring sex differences in worry with a cognitive vulnerability model. *Psychology of Women Quarterly*, *32*(4), 469-482.

Zarei, M., Mataix-Cols, D., Heyman, I., Hough, M., Doherty, J., Burge, L., ... & James, A. (2011). Changes in gray matter volume and white matter microstructure in adolescents with obsessive-compulsive disorder. *Biological psychiatry*, *70*(11), 1083-1090.

Zbozinek, T. D., Rose, R. D., Wolitzky-Taylor, K. B., Sherbourne, C., Sullivan, G., Stein, M. B., ... & Craske, M. G. (2012). Diagnostic overlap of generalized anxiety disorder and major depressive disorder in a primary care sample. *Depression and anxiety*, *29*(12), 1065-1071.

Zetsche, U., Bürkner, P. C., & Schulze, L. (2018). Shedding light on the association between repetitive negative thinking and deficits in cognitive control–A meta-analysis. *Clinical Psychology Review*, *63*, 56-65.

Zhao, K., Liu, H., Yan, R., Hua, L., Chen, Y., Shi, J., ... & Yao, Z. (2017). Cortical thickness and subcortical structure volume abnormalities in patients with major depression with and without anxious symptoms. *Brain and behavior*, *7*(8), e00754.

Zinbarg, R. E., & Barlow, D. H. (1996). Structure of anxiety and the anxiety disorders: a hierarchical model. *Journal of Abnormal Psychology*, *105*(2), 181.

Zisook, S., Lesser, I., Stewart, J. W., Wisniewski, S. R., Balasubramani, G. K., Fava, M., ... & Trivedi, M. H. (2007). Effect of age at onset on the course of major depressive disorder. *American Journal of Psychiatry*, *164*(10), 1539-1546.

Zuo, Z., Ran, S., Wang, Y., Li, C., Han, Q., Tang, Q., ... & Li, H. (2018). Altered structural covariance among the dorsolateral prefrontal cortex and amygdala in treatment-naïve patients with major depressive disorder. *Frontiers in psychiatry*, *9*, 323.

APPENDICES

Appendix 1: Factor loadings from CFA of six-factor bifactor dimensional model

Quest.	Item Text	NA Est. (SE)	AA Est. (SE)	LPA Est. (SE)	AAp Est. (SE)	R Est. (SE)	RNT Est. (SE)
MASQ-AA	Startled easily	.487(.035)	.207(.044)	-	-	-	-
	Hands were shaky	.483(.038)	.491(.039)	-	-	-	-
	Was short of breath	.467(.035)	.522(.040)	-	-	-	-
	Felt faint	.529(.046)	.625(.041)	-	-	-	-
	Had hot or cold spells	.449(.033)	.301(.040)	-	-	-	-
	Hands were cold or sweaty	.493(.047)	.468(.042)	-	-	-	-
	Was trembling or shaking	.650(.043)	.589(.037)	-	-	-	-
	Had trouble swallowing	.508(.065)	.544(.054)	-	-	-	-
	Felt dizzy or lightheaded	.516(.041)	.640(.032)	-	-	-	-
	Had a pain in my chest	.476(.050)	.545(.050)	-	-	-	-
	Felt like I was choking	.567(.062)	.593(.058)	-	-	-	-
	Muscles twitched or trembled	.445(.041)	.535(.039)	-	-	-	-
	Had a very dry mouth	.472(.038)	.443(.044)	-	-	-	-
	Was afraid I was going to die	.515(.048)	.309(.062)	-	-	-	-
	Heart was racing or pounding	.540(.038)	.518(.036)	-	-	-	-
	Felt numbness or tingling in my body	.447(.045)	.568(.040)	-	-	-	-
	Had to urinate frequently	.274(.044)	.337(.050)	-	-	-	-
MASQ-GDA	Felt afraid	.572(.030)	-	-	-	-	-
	Had diarrhea	.372(.037)	-	-	-	-	-
	Felt nervous	.594(.024)	-	-	-	-	-
	Felt uneasy	.731(.022)	-	-	-	-	-
	Had a lump in my throat	.482(.042)	-	-	-	-	-
	Had an upset stomach	.479(.033)	-	-	-	-	-
	Felt keyed up, "on edge"	.638(.025)	-	-	-	-	-
	Was unable to relax	.718(.021)	-	-	-	-	-
	Felt nauseous	.611(.031)	-	-	-	-	-
	Felt tense or "high-strung"	.649(.027)	-	-	-	-	-
	Muscles were tense or sore	.395(.034)	-	-	-	-	-
MASQ-GDD	Felt sad	.711(.02)	-	-	-	-	-
	Felt discouraged	.647(.023)	-	-	-	-	-
	Felt worthless	.831(.02)	-	-	-	-	-
	Felt depressed	.825(.016)	-	-	-	-	-
	Felt like a failure	.893(.013)	-	-	-	-	-
	Blamed myself for a lot of things	.777(.017)	-	-	-	-	-
	Felt inferior to others	.770(.021)	-	-	-	-	-
	Felt like crying	.665(.025)	-	-	-	-	-
	Was disappointed in myself	.839(.014)	-	-	-	-	-
	Felt hopeless	.876(.016)	-	-	-	-	-
	Felt sluggish or tired	.612(.023)	-	-	-	-	-
	Felt pessimistic about the future	.690(.025)	-	-	-	-	-
MASQ-LPA	Felt cheerful	.407(.034)	-	.646(.021)	-	-	-
	Felt optimistic	.432(.033)	-	.601(.023)	-	-	-
	Felt really happy$_R$	.443(.031)	-	.682(.02)	-	-	-
	Was proud of myself$_R$	.387(.031)	-	.672(.02)	-	-	-
	Felt like I was having a lot of fun$_R$	.327(.035)	-	.740(.017)	-	-	-
	Felt like I had a lot of energy$_R$	.314(.036)	-	.683(.02)	-	-	-
	Felt really "up" or lively$_R$	.236(.037)	-	.721(.018)	-	-	-
	Looked forward to things with enjoyment$_R$	.277(.035)	-	.703(.02)	-	-	-
	Felt like I had a lot of interesting things to do$_R$	.298(.033)	-	.645(.022)	-	-	-
	Felt like had accomplished a lot$_R$	.264(.036)	-	.610(.022)	-	-	-
	Felt like I had a lot to look forward to$_R$	.316(.034)	-	.705(.019)	-	-	-
	Felt hopeful about the future$_R$	.378(.032)	-	.663(.019)	-	-	-
	Seemed to move quickly and easily$_R$	.313(.034)	-	.559(.024)	-	-	-
	Felt really good about myself$_R$	.508(.030)	-	.652(.020)	-	-	-
MASQ-LI	Felt unattractive	.632(.027)	-	-	-	-	-
	Felt withdrawn from other people	.727(.022)	-	-	-	-	-
	Felt really slowed down	.690(.024)	-	-	-	-	-
	Felt really bored	.431(.032)	-	-	-	-	-
	Felt like it took an extra effort to get started	.654(.023)	-	-	-	-	-
	Felt like nothing was very enjoyable	.791(.027)	-	-	-	-	-
	Felt like there wasn't anything interesting or fun to do	.597(.030)	-	-	-	-	-
	Thought about death or suicide	.508(.033)	-	-	-	-	-
PSWQ	If I do not have enough time to do everything, I do not worry about it$_R$	.167(.037)	-	-	.298(.039)	-	.393(.036)
	My worries overwhelm me.	.516(.028)	-	-	.592(.024)	-	.186(.046)
	I do not tend to worry about things$_R$	.291(.035)	-	-	.419(.041)	-	.530(.036)
	Many situations make me worry.	.518(.027)	-	-	.699(.021)	-	.143(.050)
	I know I should not worry about things, but I just cannot help it.	.507(.028)	-	-	.699(.021)	-	.217(.048)
	When I am under pressure I worry a lot.	.475(.029)	-	-	.643(.023)	-	.157(.048)
	I am always worrying about something.	.525(.029)	-	-	.736(.023)	-	.221(.050)
	I find it easy to dismiss worrisome thoughts$_R$	.341(.032)	-	-	.300(.038)	-	.524(.033)

	As soon as I finish one task, I start to worry about everything else I have to do.	.434(.03)	-	-	.613(.022)	-	.146(.048)
	I never worry about anything$_R$	.330(.036)	-	-	.541(.037)	-	.495(.040)
	When there is nothing more I can do about a concern, I do not worry about it anymore$_R$	.301(.032)	-	-	.311(.042)	-	.577(.030)
	I have been a worrier all my life.	.380(.034)	-	-	.714(.025)	-	.295(.049)
	I notice that I have been worrying about things.	.472(.029)	-	-	.677(.022)	-	.219(.048)
	Once I start worrying, I cannot stop.	.543(.026)	-	-	.640(.023)	-	.255(.044)
	I worry all the time.	.543(.027)	-	-	.703(.024)	-	.279(.048)
	I worry about projects until they are all done.	.410(.030)	-	-	.679(.022)	-	.132(.053)
RRS-B	Think “What am I doing to deserve this?”	.446(.034)	-	-	-	.403(.035)	.251(.042)
	Think “Why do I always react this way?”	.456(.033)	-	-	-	.526(.028)	.314(.045)
	Think about a recent situation, wishing it had gone better.	.484(.033)	-	-	-	.479(.033)	.359(.043)
	Think “Why do I have problems other people don’t have?”	.508(.032)	-	-	-	.417(.036)	.349(.038)
	Think “Why can’t I handle things better?”	.566(.029)	-	-	-	.468(.034)	.441(.041)
RRS-R	Analyze recent events to try to understand why you are depressed.	.386(.035)	-	-	-	.626(.025)	.125(.053)
	Go away by yourself and think about why you feel this way.	.380(.036)	-	-	-	.831(.021)	.127(.058)
	Write down what you are thinking and analyze it.	.253(.039)	-	-	-	.481(.035)	.052(.060)
	Analyze your personality to try to understand why you are depressed.	.474(.032)	-	-	-	.651(.024)	.168(.050)
	Go someplace alone to think about your feelings.	.351(.038)	-	-	-	.781(.022)	.100(.056)

Appendix 1. Factor loadings of questionnaire items from sex invariant confirmatory factor analysis. Factor loadings from confirmatory factor analyses across adolescents, young adult, and middle adult samples. “Quest.” column indicates the questionnaire and manifest subscale the items are drawn from. “Item text” column indicates the prompt participants were responding to for every item. “NA Est. (SE)” column indicates the standardize loading of that item on the negative affect (NA) factor with the standard error in parentheses. “AA Est. (SE)” column indicates the standardize loading of that item on the anxious arousal-specific (AA) factor with the standard error in parentheses. “LPA Est. (SE)” column indicates the standardize loading of that item on the low positive affect-specific (LPA) factor with the standard error in parentheses. “AAp Est. (SE)” column indicates the standardize loading of that item on the anxious apprehension-specific (AAp) factor with the standard error in parentheses. “R Est. (SE)” column indicates the standardize loading of that item on the rumination-specific (R) factor with the standard error in parentheses. “RNT Est. (SE)” column indicates the standardize loading of that item on the repetitive negative thought (RNT) factor with the standard error in parentheses.

Appendix 2: Adolescent ROI analyses – controlling for sex

		Volume				Area				Thickness			
ROI	**Dimension**	**Est.**	**SE**	**t-value**	**p-value**	**Est.**	**SE**	**t-value**	**p-value**	**Est.**	**SE**	**t-value**	**p-value**
lh insula	NA*	0.083	0.073	1.135	0.28	-0.043	0.067	-0.64	0.535	0.132	0.078	1.691	0.119
	RNT	-0.004	0.072	-0.049	0.962	-0.034	0.066	-0.517	0.615	-0.006	0.066	-0.094	0.927
	AA	0.052	0.074	0.708	0.494	0.089	0.067	1.327	0.211	0.021	0.077	0.278	0.786
	LPA	0.053	0.076	0.693	0.503	0.065	0.069	0.936	0.37	-0.015	0.079	-0.185	0.857
	AAp	-0.037	0.076	-0.492	0.633	-0.01	0.069	-0.145	0.888	-0.018	0.08	-0.225	0.826
	R	-0.082	0.071	-1.154	0.273	-0.142	0.065	-2.185	0.051	0.06	0.073	0.83	0.424
rh insula	NA*	0.04	0.077	0.515	0.617	-0.038	0.078	-0.485	0.637	0.077	0.086	0.898	0.389
	RNT	0.067	0.074	0.909	0.383	0.008	0.071	0.113	0.912	0.118	0.078	1.511	0.159
	AA	0.039	0.078	0.504	0.624	0.085	0.077	1.092	0.298	-0.001	0.086	-0.01	0.992
	LPA	0.03	0.08	0.379	0.712	0.086	0.079	1.085	0.301	-0.024	0.088	-0.268	0.794
	AAp	-0.017	0.08	-0.214	0.835	0.039	0.08	0.49	0.634	-0.014	0.089	-0.153	0.881
	R	-0.051	0.074	-0.688	0.506	-0.082	0.074	-1.114	0.289	-0.039	0.082	-0.477	0.643
lh cMFG	NA	0.086	0.085	1.013	0.333	0.098	0.078	1.256	0.235	0.035	0.076	0.465	0.651
	RNT*	0.027	0.073	0.379	0.712	-0.04	0.069	-0.588	0.569	0.125	0.073	1.722	0.113
	AA	-0.09	0.084	-1.075	0.305	-0.086	0.078	-1.107	0.292	0.01	0.076	0.137	0.894
	LPA	-0.093	0.086	-1.084	0.301	-0.116	0.08	-1.458	0.173	-0.056	0.078	-0.717	0.488
	AAp	0.036	0.086	0.411	0.689	0.066	0.08	0.829	0.425	-0.01	0.078	-0.13	0.899
	R	0.054	0.079	0.688	0.506	0.007	0.073	0.09	0.93	-0.007	0.073	-0.1	0.922
rh cMFG	NA	0.093	0.08	1.168	0.268	0.059	0.081	0.731	0.48	0.097	0.08	1.224	0.247
	RNT*	-0.077	0.071	-1.083	0.302	-0.081	0.073	-1.108	0.291	-0.042	0.068	-0.612	0.553
	AA	-0.137	0.079	-1.718	0.114	-0.112	0.081	-1.38	0.195	-0.104	0.079	-1.317	0.215
	LPA	0.033	0.081	0.402	0.695	0.025	0.083	0.3	0.77	-0.048	0.081	-0.6	0.561
	AAp	0.042	0.082	0.511	0.619	0.061	0.083	0.729	0.481	-0.117	0.082	-1.431	0.18
	R	0.073	0.075	0.975	0.35	0.051	0.077	0.66	0.523	0.088	0.074	1.177	0.264
lh rMFG	NA	-0.048	0.075	-0.646	0.532	-0.029	0.056	-0.513	0.618	-0.082	0.059	-1.386	0.193
	RNT*	0.022	0.065	0.337	0.742	0.009	0.051	0.183	0.859	0.038	0.058	0.663	0.521
	AA	-0.03	0.074	-0.402	0.696	-0.016	0.056	-0.278	0.786	0.058	0.059	0.974	0.351
	LPA	0.093	0.076	1.219	0.248	0.042	0.058	0.725	0.484	0.022	0.061	0.358	0.727
	AAp	***0.16***	***0.076***	***2.093***	***0.06***	**0.157**	**0.058**	**2.729**	**0.02**	0.011	0.061	0.18	0.86
	R	0.034	0.07	0.489	0.634	-0.003	0.053	-0.051	0.96	-0.044	0.057	-0.777	0.454
rh rMFG	NA	0.028	0.076	0.368	0.72	0.058	0.061	0.958	0.359	-0.121	0.063	-1.927	0.08
	RNT*	0.125	0.075	1.667	0.124	0.022	0.059	0.369	0.719	0.067	0.061	1.102	0.294
	AA	-0.036	0.077	-0.47	0.647	-0.066	0.061	-1.082	0.302	***0.151***	***0.063***	***2.39***	***0.036***
	LPA	-0.002	0.079	-0.024	0.981	-0.017	0.063	-0.274	0.789	0.023	0.065	0.35	0.733
	AAp	0.057	0.079	0.729	0.481	0.051	0.063	0.808	0.436	0.044	0.065	0.678	0.512
	R	0.068	0.074	0.915	0.38	0.056	0.059	0.94	0.368	-0.078	0.061	-1.292	0.223
lh pars triangularis	***NA***	0.085	0.094	0.894	0.39	-0.015	0.089	-0.174	0.865	***0.194***	***0.077***	***2.537***	***0.028***
	RNT	***-0.202***	***0.092***	***-2.186***	***0.050***	-0.187	0.086	-2.171	0.053	-0.082	0.075	-1.097	0.296
	AA	0.112	0.095	1.173	0.265	0.146	0.089	1.64	0.129	0.024	0.077	0.305	0.766
	LPA	0.077	0.098	0.791	0.446	0.051	0.092	0.56	0.587	0.076	0.079	0.961	0.357
	AAp*	0.048	0.098	0.49	0.634	0.022	0.092	0.24	0.815	0.091	0.079	1.156	0.272
	R	-0.069	0.092	-0.755	0.466	-0.088	0.086	-1.017	0.331	-0.069	0.074	-0.925	0.375
rh pars triangularis	NA	-0.035	0.092	-0.383	0.709	0.002	0.086	0.023	0.982	-0.08	0.069	-1.156	0.272
	RNT	-0.017	0.083	-0.2	0.845	-0.085	0.081	-1.042	0.32	0.044	0.063	0.697	0.501
	AA	***0.227***	***0.092***	***2.463***	***0.032***	***0.227***	***0.087***	***2.616***	***0.024***	0.052	0.07	0.745	0.472
	LPA	-0.076	0.094	-0.803	0.439	-0.113	0.089	-1.267	0.231	0.061	0.071	0.857	0.41
	AAp*	-0.157	0.095	-1.664	0.124	-0.157	0.089	-1.764	0.105	0.074	0.071	1.042	0.32
	R	-0.144	0.087	-1.653	0.127	***-0.204***	***0.083***	***-2.462***	***0.032***	-0.004	0.066	-0.057	0.956
lh pars opercularis	NA	-0.007	0.09	-0.077	0.94	0.026	0.086	0.306	0.765	-0.121	0.073	-1.659	0.125
	RNT	-0.049	0.083	-0.599	0.561	-0.08	0.081	-0.995	0.341	-0.053	0.066	-0.802	0.44
	AA	0.077	0.09	0.853	0.412	0.087	0.086	1.009	0.335	0.06	0.073	0.824	0.428
	LPA	-0.04	0.092	-0.436	0.671	-0.089	0.088	-1.006	0.336	0.132	0.075	1.767	0.105
	AAp*	-0.15	0.093	-1.623	0.133	-0.164	0.088	-1.859	0.09	0.078	0.075	1.031	0.325
	R	0.031	0.086	0.356	0.729	-0.048	0.082	-0.578	0.575	0.082	0.069	1.185	0.261
rh pars opercularis	NA	0.071	0.089	0.789	0.447	0.038	0.09	0.421	0.682	0.068	0.084	0.812	0.434
	RNT	-0.032	0.087	-0.37	0.718	-0.032	0.088	-0.36	0.726	0.006	0.078	0.081	0.937
	AA	-0.054	0.09	-0.6	0.561	-0.016	0.09	-0.177	0.863	-0.145	0.084	-1.726	0.112
	LPA	0.026	0.092	0.285	0.781	0.078	0.093	0.842	0.418	***-0.226***	***0.086***	***-2.632***	***0.023***
	AAp*	-0.005	0.092	-0.058	0.955	0.002	0.093	0.019	0.985	-0.036	0.086	-0.418	0.684
	R	-0.034	0.087	-0.395	0.701	-0.064	0.087	-0.735	0.478	-0.001	0.08	-0.01	0.992
lh pars orbitalis	***NA***	-0.042	0.087	-0.481	0.64	0.044	0.079	0.556	0.589	***-0.208***	***0.079***	***-2.637***	***0.023***
	RNT	***0.239***	***0.082***	***2.923***	***0.014***	0.125	0.072	1.735	0.111	0.144	0.077	1.861	0.09
	AA	0.115	0.087	1.318	0.214	0.087	0.079	1.105	0.293	0.132	0.08	1.649	0.127
	LPA	0.051	0.089	0.576	0.576	0.027	0.081	0.339	0.741	0.037	0.082	0.451	0.661
	AAp*	-0.075	0.089	-0.845	0.416	-0.001	0.081	-0.013	0.99	-0.05	0.082	-0.609	0.555
	R	0.065	0.083	0.78	0.452	-0.021	0.075	-0.281	0.784	0.066	0.077	0.856	0.41

rh pars orbitalis	NA	0.06	0.089	0.676	0.513	0.061	0.078	0.775	0.455	-0.038	0.084	-0.451	0.661
	RNT	0.01	0.087	0.119	0.908	-0.065	0.077	-0.837	0.42	0.063	0.082	0.773	0.456
	AA	0.154	0.089	1.733	0.111	0.136	0.079	1.727	0.112	0.04	0.084	0.473	0.646
	LPA	0.069	0.092	0.751	0.468	-0.013	0.082	-0.163	0.873	0.033	0.087	0.378	0.713
	AAp*	-0.074	0.091	-0.811	0.434	-0.127	0.081	-1.561	0.147	0.09	0.086	1.041	0.32
	R	0.125	0.086	1.45	0.175	0.049	0.076	0.646	0.531	0.02	0.081	0.246	0.811
lh cACC	NA*	0.006	0.094	0.065	0.949	-0.047	0.086	-0.546	0.596	0.125	0.095	1.317	0.215
	RNT	0.105	0.092	1.138	0.279	0.03	0.085	0.359	0.727	***0.196***	***0.088***	***2.219***	***0.048***
	AA	-0.157	0.095	-1.651	0.127	-0.12	0.086	-1.395	0.191	0.023	0.096	0.242	0.813
	LPA	0.033	0.098	0.339	0.741	0.057	0.089	0.642	0.534	-0.08	0.097	-0.819	0.43
	AAp	0.016	0.097	0.162	0.874	0.008	0.089	0.087	0.932	0.053	0.098	0.543	0.598
	R	0.037	0.091	0.408	0.691	0.03	0.084	0.359	0.726	-0.152	0.091	-1.673	0.122
rh cACC	NA*	-0.094	0.093	-1.014	0.333	-0.105	0.084	-1.242	0.24	-0.063	0.091	-0.69	0.505
	RNT	-0.092	0.091	-1.014	0.333	-0.116	0.083	-1.393	0.191	-0.073	0.089	-0.826	0.426
	AA	0.099	0.093	1.058	0.313	0.124	0.085	1.461	0.172	***0.205***	***0.092***	***2.241***	***0.047***
	LPA	0.132	0.096	1.369	0.198	0.111	0.088	1.261	0.234	0.118	0.094	1.251	0.237
	AAp	0.085	0.096	0.883	0.396	0.081	0.087	0.934	0.37	0.126	0.094	1.337	0.208
	R	0.189	0.09	2.097	0.06	0.158	0.082	1.925	0.081	0.04	0.088	0.457	0.657
lh rACC	NA	-0.067	0.088	-0.766	0.46	0.016	0.073	0.22	0.83	-0.128	0.087	-1.476	0.168
	RNT	-0.007	0.075	-0.087	0.932	-0.147	0.071	-2.088	0.061	0.089	0.082	1.084	0.301
	AA	-0.157	0.087	-1.805	0.099	-0.111	0.073	-1.522	0.156	-0.013	0.087	-0.153	0.881
	LPA*	-0.029	0.089	-0.328	0.749	-0.038	0.075	-0.5	0.627	-0.015	0.089	-0.169	0.869
	AAp	0.081	0.09	0.901	0.387	0.05	0.075	0.67	0.517	-0.001	0.09	-0.009	0.993
	R	0.105	0.082	1.286	0.225	0.055	0.07	0.786	0.449	-0.007	0.083	-0.084	0.934
rh rACC	NA	-0.127	0.093	-1.37	0.198	-0.083	0.084	-0.982	0.347	-0.145	0.093	-1.55	0.149
	RNT	0.021	0.091	0.23	0.822	0.028	0.083	0.338	0.742	-0.106	0.087	-1.224	0.246
	AA	0.159	0.093	1.7	0.117	0.145	0.085	1.712	0.115	0.094	0.094	0.998	0.34
	LPA*	-0.032	0.096	-0.329	0.749	-0.031	0.088	-0.358	0.727	0.096	0.095	1.006	0.336
	AAp	-0.059	0.096	-0.612	0.553	-0.062	0.087	-0.709	0.493	0.006	0.096	0.062	0.952
	R	0.007	0.09	0.083	0.935	-0.043	0.082	-0.52	0.613	-0.03	0.089	-0.332	0.746
lh lateral OFC	NA	0.019	0.081	0.231	0.821	-0.038	0.071	-0.53	0.607	-0.044	0.075	-0.585	0.571
	RNT	-0.048	0.078	-0.623	0.546	-0.07	0.062	-1.13	0.283	0.012	0.069	0.176	0.863
	AA	0.002	0.082	0.026	0.98	0	0.07	0.006	0.996	0.081	0.075	1.085	0.301
	LPA*	0.061	0.084	0.735	0.478	0.084	0.072	1.156	0.272	-0.05	0.076	-0.661	0.522
	AAp	-0.134	0.084	-1.601	0.138	-0.136	0.073	-1.875	0.088	0.099	0.077	1.287	0.225
	R	0.016	0.078	0.198	0.846	0.06	0.067	0.905	0.385	-0.049	0.071	-0.695	0.502
rh lateral OFC	NA	-0.014	0.083	-0.174	0.865	-0.025	0.069	-0.359	0.726	-0.103	0.074	-1.389	0.192
	RNT	-0.066	0.079	-0.836	0.421	-0.078	0.062	-1.273	0.229	-0.024	0.071	-0.335	0.744
	AA	-0.058	0.083	-0.692	0.503	-0.019	0.069	-0.278	0.786	-0.006	0.074	-0.085	0.934
	LPA*	0.093	0.085	1.084	0.302	0.038	0.07	0.534	0.604	0.07	0.076	0.912	0.381
	AAp	-0.085	0.085	-0.993	0.342	-0.131	0.071	-1.847	0.092	0.109	0.076	1.429	0.181
	R	0.111	0.08	1.392	0.192	0.092	0.065	1.406	0.187	-0.033	0.071	-0.465	0.651
lh medial OFC	NA	-0.066	0.09	-0.737	0.477	-0.005	0.083	-0.064	0.95	-0.068	0.096	-0.715	0.49
	RNT	0.091	0.078	1.169	0.267	0.069	0.073	0.947	0.364	0.034	0.088	0.388	0.705
	AA	-0.063	0.089	-0.708	0.493	-0.071	0.082	-0.865	0.406	0.131	0.096	1.367	0.199
	LPA	0.061	0.091	0.666	0.519	0.014	0.085	0.166	0.871	0.057	0.098	0.589	0.568
	AAp	-0.061	0.092	-0.664	0.521	-0.114	0.085	-1.346	0.205	0.026	0.098	0.262	0.798
	R	0.051	0.084	0.61	0.554	0.012	0.078	0.15	0.884	0.048	0.091	0.532	0.605
rh medial OFC	NA	0.064	0.088	0.728	0.482	0.092	0.072	1.269	0.231	-0.084	0.088	-0.944	0.366
	RNT	-0.03	0.085	-0.351	0.732	0.01	0.068	0.146	0.887	-0.138	0.075	-1.827	0.095
	AA	-0.058	0.088	-0.66	0.523	-0.075	0.073	-1.035	0.323	0.102	0.088	1.171	0.266
	LPA	0.062	0.091	0.683	0.509	-0.016	0.074	-0.208	0.839	0.073	0.09	0.81	0.435
	AAp	-0.051	0.091	-0.561	0.586	-0.062	0.074	-0.83	0.424	-0.02	0.091	-0.223	0.828
	R	-0.019	0.085	-0.227	0.824	-0.066	0.069	-0.949	0.363	0.041	0.083	0.492	0.633
lh amygdala	***NA***	***0.153***	***0.07***	***2.187***	***0.050***	-	-	-	-	-	-	-	-
	RNT	0.01	0.068	0.144	0.888	-	-	-	-	-	-	-	-
	AA*	-0.133	0.07	-1.883	0.086	-	-	-	-	-	-	-	-
	LPA	**-0.258**	**0.072**	**-3.565**	**0.004**	-	-	-	-	-	-	-	-
	AAp	-0.055	0.072	-0.766	0.46	-	-	-	-	-	-	-	-
	R	0.052	0.068	0.759	0.464	-	-	-	-	-	-	-	-
rh amygdala	NA	0.091	0.072	1.268	0.231	-	-	-	-	-	-	-	-
	RNT	0.027	0.067	0.402	0.696	-	-	-	-	-	-	-	-
	AA*	-0.1	0.072	-1.385	0.194	-	-	-	-	-	-	-	-
	LPA	-0.12	0.074	-1.634	0.131	-	-	-	-	-	-	-	-
	AAp	-0.016	0.074	-0.214	0.834	-	-	-	-	-	-	-	-
	R	0.018	0.069	0.26	0.8	-	-	-	-	-	-	-	-
lh hippocampus	NA	0.141	0.084	1.674	0.122	-	-	-	-	-	-	-	-
	RNT	0.022	0.078	0.289	0.778	-	-	-	-	-	-	-	-
	AA	-0.119	0.084	-1.418	0.184	-	-	-	-	-	-	-	-
	LPA	-0.076	0.086	-0.885	0.395	-	-	-	-	-	-	-	-
	AAp	0.074	0.086	0.858	0.409	-	-	-	-	-	-	-	-

	R*	0.008	0.08	0.101	0.922	-	-	-	-	-	-	-	-
rh hippocampus	NA	0.126	0.072	1.753	0.108	-	-	-	-	-	-	-	-
	RNT	-0.001	0.07	-0.019	0.985	-	-	-	-	-	-	-	-
	AA	-0.08	0.072	-1.104	0.293	-	-	-	-	-	-	-	-
	LPA	-0.026	0.074	-0.347	0.735	-	-	-	-	-	-	-	-
	AAp	0.044	0.074	0.59	0.567	-	-	-	-	-	-	-	-
	R*	-0.013	0.07	-0.19	0.853	-	-	-	-	-	-	-	-
lh caudate	NA	0.132	0.082	1.612	0.135	-	-	-	-	-	-	-	-
	RNT	0.075	0.071	1.06	0.312	-	-	-	-	-	-	-	-
	AA	0.078	0.081	0.967	0.354	-	-	-	-	-	-	-	-
	LPA*	0.038	0.083	0.457	0.656	-	-	-	-	-	-	-	-
	AAp	-0.02	0.084	-0.241	0.814	-	-	-	-	-	-	-	-
	R	-0.018	0.077	-0.239	0.815	-	-	-	-	-	-	-	-
rh caudate	NA	0.159	0.083	1.924	0.081	-	-	-	-	-	-	-	-
	RNT	0.072	0.072	1.001	0.339	-	-	-	-	-	-	-	-
	AA	0.049	0.082	0.596	0.563	-	-	-	-	-	-	-	-
	LPA*	0.011	0.084	0.126	0.902	-	-	-	-	-	-	-	-
	AAp	0.004	0.084	0.052	0.959	-	-	-	-	-	-	-	-
	R	0.01	0.077	0.134	0.896	-	-	-	-	-	-	-	-
lh putamen	NA	0.142	0.078	1.803	0.099	-	-	-	-	-	-	-	-
	RNT	-0.051	0.071	-0.717	0.488	-	-	-	-	-	-	-	-
	AA	-0.02	0.078	-0.257	0.802	-	-	-	-	-	-	-	-
	LPA*	-0.026	0.08	-0.328	0.749	-	-	-	-	-	-	-	-
	AAp	0.019	0.08	0.231	0.822	-	-	-	-	-	-	-	-
	R	-0.047	0.075	-0.625	0.545	-	-	-	-	-	-	-	-
rh putamen	NA	0.174	0.081	2.148	0.055	-	-	-	-	-	-	-	-
	RNT	-0.07	0.068	-1.024	0.328	-	-	-	-	-	-	-	-
	AA	0.067	0.08	0.837	0.421	-	-	-	-	-	-	-	-
	LPA*	0.009	0.082	0.107	0.917	-	-	-	-	-	-	-	-
	AAp	-0.023	0.083	-0.28	0.785	-	-	-	-	-	-	-	-
	R	-0.007	0.075	-0.095	0.926	-	-	-	-	-	-	-	-
lh pallidum	NA	0.015	0.091	0.161	0.875	-	-	-	-	-	-	-	-
	RNT	0.007	0.089	0.078	0.939	-	-	-	-	-	-	-	-
	AA	0.004	0.092	0.043	0.967	-	-	-	-	-	-	-	-
	LPA*	-0.173	0.095	-1.83	0.094	-	-	-	-	-	-	-	-
	AAp	-0.073	0.094	-0.776	0.454	-	-	-	-	-	-	-	-
	R	-0.076	0.089	-0.856	0.41	-	-	-	-	-	-	-	-
rh pallidum	NA	0.093	0.085	1.1	0.295	-	-	-	-	-	-	-	-
	RNT	-0.023	0.083	-0.272	0.791	-	-	-	-	-	-	-	-
	AA	-0.071	0.085	-0.83	0.424	-	-	-	-	-	-	-	-
	LPA*	-0.077	0.088	-0.877	0.4	-	-	-	-	-	-	-	-
	AAp	0.025	0.088	0.281	0.784	-	-	-	-	-	-	-	-
	R	0.008	0.082	0.096	0.925	-	-	-	-	-	-	-	-
lh accumbens	NA	-0.061	0.085	-0.725	0.484	-	-	-	-	-	-	-	-
	RNT	0.005	0.081	0.056	0.956	-	-	-	-	-	-	-	-
	AA	-0.022	0.085	-0.263	0.798	-	-	-	-	-	-	-	-
	LPA*	-0.109	0.087	-1.249	0.238	-	-	-	-	-	-	-	-
	AAp	-0.079	0.087	-0.902	0.386	-	-	-	-	-	-	-	-
	R	-0.108	0.082	-1.322	0.213	-	-	-	-	-	-	-	-
rh accumbens	NA	0.056	0.092	0.613	0.552	-	-	-	-	-	-	-	-
	RNT	0.029	0.083	0.355	0.73	-	-	-	-	-	-	-	-
	AA	0.017	0.092	0.191	0.852	-	-	-	-	-	-	-	-
	LPA*	-0.16	0.094	-1.707	0.116	-	-	-	-	-	-	-	-
	AAp	-0.03	0.094	-0.315	0.759	-	-	-	-	-	-	-	-
	R	-0.082	0.087	-0.941	0.367	-	-	-	-	-	-	-	-
lh thalamus	NA	0.07	0.069	1.018	0.331	-	-	-	-	-	-	-	-
	RNT	0.002	0.067	0.037	0.971	-	-	-	-	-	-	-	-
	AA*	-0.006	0.069	-0.093	0.928	-	-	-	-	-	-	-	-
	LPA	0.028	0.071	0.399	0.697	-	-	-	-	-	-	-	-
	AAp	-0.027	0.071	-0.38	0.711	-	-	-	-	-	-	-	-
	R	0.013	0.066	0.194	0.85	-	-	-	-	-	-	-	-
rh thalamus	NA	0.145	0.07	2.057	0.064	-	-	-	-	-	-	-	-
	RNT	0.069	0.069	1.001	0.338	-	-	-	-	-	-	-	-
	AA*	-0.033	0.071	-0.47	0.648	-	-	-	-	-	-	-	-
	LPA	0.003	0.073	0.038	0.97	-	-	-	-	-	-	-	-
	AAp	-0.051	0.073	-0.703	0.497	-	-	-	-	-	-	-	-
	R	-0.01	0.068	-0.141	0.89	-	-	-	-	-	-	-	-

Appendix 2. Adolescent ROI analyses – controlling for sex. Results from multiple regression models predicting volume, surface area, and cortical thickness of a priori regions of interest. For each ROI, factor scores from all six internalizing dimensions were simultaneously included as predictors, while controlling for age, sex, MRI scanner platform, and a whole brain morphometry measure, treating family as a random effect. Bold and italicized statistics

indicate marginally significant effect ($p<.05$); Bold only statistics indicated significant effect after correction for multiple comparisons ($p<.008$); Est.= beta estimate; SE= standard error of beta estimate; NA= negative affect; RNT= repetitive negative thought; AA= anxious arousal-specific; LPA= low positive affect-specific; AAp= anxious apprehension-specific; R= rumination-specific; lh= left hemisphere; rh= right hemisphere; cMFG= caudal middle frontal gyrus; rMFG= rostral middle frontal gyrus; cACC= caudal anterior cingulate cortex; rACC= rostral anterior cingulate cortex; lOFC= lateral orbitofrontal cortex; mOFC= medial orbitofrontal cortex.

Appendix 3: Young adult ROI analyses – controlling for sex.

		Volume				Surface Area				Thickness			
ROI	**Dime-nsion**	**Est.**	**SE**	**t-value**	**p-value**	**Est.**	**SE**	**t-value**	**p-value**	**Est.**	**SE**	**t-value**	**p-value**
lh insula	**NA***	***-0.06***	***0.028***	***-2.11***	***0.036***	0.005	0.025	0.192	0.848	***-0.074***	***0.032***	***-2.293***	***0.023***
	RNT	0.004	0.028	0.127	0.899	0.016	0.025	0.67	0.503	0.015	0.033	0.448	0.655
	AA	-0.022	0.027	-0.805	0.422	0.038	0.024	1.605	0.11	-0.044	0.032	-1.389	0.166
	LPA	-0.025	0.029	-0.87	0.385	0	0.025	-0.018	0.985	-0.024	0.032	-0.728	0.467
	AAp	-0.039	0.03	-1.282	0.201	0.014	0.026	0.528	0.598	**-0.1**	**0.034**	**-2.936**	**0.004**
	R	-0.013	0.027	-0.49	0.625	-0.023	0.024	-0.949	0.344	0.026	0.032	0.817	0.415
rh insula	**NA***	**-0.066**	**0.028**	**-2.341**	**0.02**	-0.019	0.026	-0.732	0.465	-0.053	0.033	-1.599	0.111
	RNT	0.015	0.028	0.538	0.591	0.025	0.026	0.941	0.348	-0.002	0.033	-0.069	0.945
	AA	-0.01	0.027	-0.354	0.724	0.027	0.025	1.078	0.282	-0.002	0.032	-0.072	0.943
	LPA	-0.014	0.028	-0.51	0.61	-0.003	0.026	-0.102	0.919	-0.025	0.033	-0.754	0.452
	AAp	***-0.078***	***0.03***	***-2.597***	***0.01***	-0.024	0.028	-0.861	0.39	***-0.081***	***0.035***	***-2.302***	***0.022***
	R	0.031	0.027	1.138	0.256	0.037	0.025	1.443	0.15	0.02	0.032	0.62	0.536
lh cMFG	NA	0.022	0.035	0.65	0.516	0.02	0.031	0.664	0.507	0.036	0.029	1.232	0.219
	RNT*	-0.042	0.035	-1.19	0.235	-0.009	0.032	-0.294	0.769	-0.035	0.029	-1.192	0.234
	AA	-0.02	0.034	-0.589	0.557	0.011	0.03	0.347	0.729	-0.017	0.028	-0.581	0.562
	LPA	-0.012	0.035	-0.343	0.732	0.017	0.031	0.56	0.576	***-0.07***	***0.029***	***-2.384***	***0.018***
	AAp	-0.042	0.037	-1.134	0.258	-0.018	0.033	-0.543	0.588	-0.019	0.031	-0.617	0.538
	R	0.004	0.034	0.115	0.909	0.024	0.03	0.774	0.44	-0.021	0.028	-0.744	0.458
rh cMFG	NA	-0.009	0.035	-0.257	0.797	0.019	0.032	0.603	0.547	-0.032	0.031	-1.028	0.305
	RNT*	-0.052	0.036	-1.448	0.149	-0.024	0.033	-0.721	0.472	-0.018	0.032	-0.576	0.565
	AA	0.026	0.035	0.754	0.451	0.061	0.032	1.916	0.056	-0.025	0.031	-0.83	0.407
	LPA	0	0.036	0.007	0.994	0.02	0.033	0.6	0.549	-0.025	0.031	-0.807	0.421
	AAp	-0.035	0.038	-0.932	0.352	-0.012	0.034	-0.357	0.721	-0.009	0.033	-0.281	0.779
	R	0.066	0.035	1.894	0.059	***0.069***	***0.032***	***2.168***	***0.031***	0.002	0.031	0.064	0.949
lh rMFG	NA	-0.024	0.031	-0.771	0.441	-0.006	0.026	-0.217	0.828	0.029	0.028	1.029	0.304
	RNT*	-0.01	0.031	-0.312	0.756	0.011	0.026	0.42	0.675	0.016	0.029	0.554	0.58
	AA	-0.004	0.03	-0.135	0.893	0.032	0.025	1.279	0.202	-0.027	0.028	-0.948	0.344
	LPA	0.016	0.031	0.52	0.604	0.037	0.026	1.446	0.149	-0.031	0.029	-1.09	0.277
	AAp	-0.017	0.033	-0.501	0.617	0.033	0.027	1.211	0.227	***-0.068***	***0.03***	***-2.252***	***0.025***
	R	-0.011	0.03	-0.376	0.707	-0.022	0.025	-0.85	0.396	0.011	0.028	0.384	0.701
rh rMFG	***NA***	***-0.064***	***0.031***	***-2.043***	***0.042***	-0.026	0.026	-1.015	0.311	-0.021	0.028	-0.73	0.466
	RNT*	-0.023	0.032	-0.733	0.464	-0.006	0.026	-0.224	0.823	0.008	0.029	0.261	0.794
	AA	-0.051	0.031	-1.653	0.100	-0.01	0.025	-0.402	0.688	-0.021	0.028	-0.746	0.456
	LPA	0.003	0.032	0.098	0.922	0.036	0.026	1.376	0.17	-0.042	0.029	-1.467	0.144
	AAp	-0.01	0.033	-0.308	0.758	0.011	0.027	0.384	0.702	0.033	0.03	1.098	0.273
	R	-0.017	0.031	-0.555	0.580	-0.001	0.025	-0.04	0.968	-0.015	0.028	-0.537	0.592
lh pars triangularis	NA	-0.026	0.037	-0.701	0.484	-0.02	0.035	-0.579	0.563	0.021	0.032	0.643	0.521
	RNT	0.034	0.039	0.883	0.378	0.044	0.036	1.24	0.216	0.025	0.033	0.755	0.451
	AA	-0.02	0.037	-0.528	0.598	-0.011	0.034	-0.317	0.751	0.022	0.032	0.682	0.496
	LPA	**-0.104**	**0.038**	**-2.737**	**0.007**	***-0.091***	***0.035***	***-2.597***	***0.01***	-0.03	0.032	-0.922	0.358
	AAp*	-0.013	0.04	-0.327	0.744	0.012	0.037	0.328	0.743	-0.032	0.034	-0.947	0.344
	R	-0.005	0.037	-0.138	0.891	-0.005	0.034	-0.138	0.89	0.025	0.032	0.771	0.441
rh pars triangularis	NA	-0.006	0.038	-0.169	0.866	0	0.035	0.008	0.994	0	0.032	-0.003	0.998
	RNT	0.027	0.039	0.7	0.484	0.032	0.037	0.889	0.375	0.023	0.033	0.678	0.498
	AA	-0.059	0.038	-1.555	0.121	-0.028	0.035	-0.8	0.424	-0.027	0.032	-0.85	0.396
	LPA	***-0.079***	***0.038***	***-2.066***	***0.04***	-0.065	0.036	-1.813	0.071	-0.049	0.033	-1.487	0.138
	AAp*	0.001	0.04	0.035	0.972	0.019	0.038	0.508	0.612	0.028	0.034	0.813	0.417
	R	-0.043	0.038	-1.133	0.258	-0.018	0.035	-0.52	0.604	-0.06	0.032	-1.851	0.065
lh pars opercularis	***NA***	***-0.087***	***0.036***	***-2.407***	***0.017***	-0.062	0.034	-1.81	0.072	**-0.063**	**0.03**	**-2.126**	**0.035**
	RNT	***-0.089***	***0.036***	***-2.436***	***0.016***	-0.067	0.035	-1.924	0.055	-0.019	0.031	-0.608	0.544
	AA	-0.048	0.035	-1.354	0.177	-0.017	0.034	-0.492	0.623	-0.035	0.03	-1.188	0.236
	LPA	-0.006	0.036	-0.158	0.875	0.004	0.034	0.108	0.914	-0.048	0.03	-1.574	0.117
	AAp*	-0.053	0.038	-1.383	0.168	-0.037	0.036	-1.026	0.306	-0.015	0.032	-0.48	0.632
	R	-0.02	0.035	-0.567	0.571	-0.002	0.034	-0.074	0.941	-0.038	0.03	-1.267	0.206
rh pars opercularis	NA	-0.032	0.037	-0.861	0.39	-0.014	0.035	-0.408	0.683	-0.004	0.032	-0.116	0.908
	RNT	0.019	0.039	0.485	0.628	0.02	0.036	0.55	0.583	0.04	0.034	1.181	0.239
	AA	-0.022	0.037	-0.591	0.555	0.018	0.035	0.504	0.615	-0.049	0.032	-1.521	0.13
	LPA	-0.01	0.038	-0.276	0.783	0.004	0.035	0.114	0.909	-0.003	0.033	-0.086	0.932

	AAp*	-0.05	0.04	-1.268	0.206	-0.03	0.037	-0.815	0.416	-0.005	0.035	-0.135	0.893
	R	***0.082***	***0.037***	***2.193***	***0.029***	**0.094**	**0.035**	**2.669**	**0.008**	-0.028	0.032	-0.865	0.388
lh pars orbitalis	NA	-0.052	0.036	-1.467	0.144	-0.018	0.031	-0.582	0.561	-0.034	0.036	-0.931	0.353
	RNT	0.001	0.036	0.036	0.971	-0.018	0.031	-0.575	0.566	0.073	0.038	1.946	0.053
	AA	-0.06	0.035	-1.698	0.091	-0.009	0.03	-0.297	0.767	-0.042	0.036	-1.155	0.249
	LPA	-0.014	0.036	-0.388	0.698	-0.019	0.031	-0.619	0.537	0.004	0.037	0.098	0.922
	AAp*	0.012	0.038	0.323	0.747	0.029	0.033	0.88	0.38	0.024	0.038	0.621	0.536
	R	-0.011	0.035	-0.305	0.761	-0.001	0.03	-0.018	0.986	-0.017	0.036	-0.459	0.647
rh pars orbitalis	NA	-0.022	0.037	-0.608	0.544	0.041	0.032	1.295	0.197	-0.013	0.036	-0.364	0.716
	RNT	-0.049	0.038	-1.297	0.196	-0.04	0.033	-1.228	0.221	0.014	0.037	0.387	0.699
	AA	-0.039	0.036	-1.078	0.282	-0.025	0.032	-0.774	0.44	0.027	0.036	0.742	0.459
	LPA	0.019	0.037	0.516	0.606	0.038	0.032	1.177	0.24	-0.011	0.037	-0.299	0.765
	AAp*	0.036	0.039	0.923	0.357	0.04	0.034	1.168	0.244	0.038	0.038	0.99	0.323
	R	-0.013	0.036	-0.349	0.727	-0.008	0.032	-0.25	0.802	0.01	0.036	0.275	0.784
lh cACC	NA*	-0.002	0.038	-0.05	0.96	-0.004	0.033	-0.122	0.903	0.008	0.04	0.208	0.835
	RNT	0.01	0.039	0.251	0.802	0.043	0.034	1.245	0.214	-0.034	0.04	-0.84	0.402
	AA	-0.011	0.038	-0.287	0.774	0.02	0.033	0.6	0.549	-0.002	0.039	-0.045	0.964
	LPA	0.031	0.038	0.794	0.428	0.029	0.034	0.863	0.389	0.03	0.04	0.751	0.453
	AAp	-0.046	0.04	-1.147	0.252	-0.003	0.035	-0.094	0.925	-0.033	0.042	-0.793	0.428
	R	-0.022	0.038	-0.577	0.564	-0.014	0.033	-0.411	0.682	-0.033	0.039	-0.843	0.4
rh cACC	**NA***	***-0.079***	***0.039***	***-2.039***	***0.042***	-0.035	0.035	-0.982	0.327	-0.042	0.039	-1.064	0.288
	RNT	0.012	0.04	0.292	0.77	0.026	0.037	0.709	0.479	0.018	0.04	0.439	0.661
	AA	-0.064	0.039	-1.664	0.097	-0.039	0.036	-1.094	0.275	-0.015	0.039	-0.383	0.702
	LPA	-0.038	0.039	-0.974	0.331	-0.014	0.036	-0.387	0.699	-0.074	0.04	-1.878	0.061
	AAp	0.008	0.041	0.184	0.855	0.025	0.038	0.659	0.511	0.007	0.042	0.167	0.868
	R	-0.037	0.039	-0.965	0.336	-0.031	0.036	-0.867	0.387	-0.037	0.039	-0.949	0.344
lh rACC	***NA***	***-0.069***	***0.034***	***-2.018***	***0.045***	-0.044	0.029	-1.527	0.128	-0.037	0.037	-1.003	0.317
	RNT	0.019	0.035	0.554	0.58	0.039	0.029	1.329	0.185	-0.018	0.038	-0.467	0.641
	AA	-0.006	0.033	-0.185	0.854	0.025	0.028	0.894	0.372	-0.038	0.037	-1.049	0.295
	LPA*	0.031	0.035	0.894	0.372	***0.065***	***0.029***	***2.236***	***0.026***	**-0.1**	**0.038**	**-2.649**	**0.008**
	AAp	-0.047	0.037	-1.29	0.198	-0.011	0.031	-0.37	0.712	-0.039	0.04	-0.983	0.327
	R	-0.037	0.033	-1.12	0.264	-0.027	0.028	-0.945	0.345	-0.018	0.037	-0.482	0.631
rh rACC	NA	-0.003	0.038	-0.072	0.943	0.014	0.034	0.415	0.679	0.031	0.039	0.798	0.426
	RNT	0.022	0.039	0.559	0.577	0.04	0.035	1.148	0.252	-0.017	0.04	-0.43	0.668
	AA	-0.031	0.037	-0.831	0.407	0.013	0.034	0.377	0.706	-0.037	0.038	-0.962	0.337
	LPA*	-0.026	0.038	-0.676	0.5	-0.014	0.034	-0.405	0.686	-0.043	0.039	-1.094	0.275
	AAp	-0.004	0.04	-0.091	0.928	0.03	0.036	0.848	0.398	-0.024	0.041	-0.577	0.565
	R	-0.012	0.038	-0.328	0.743	-0.027	0.034	-0.81	0.419	0.012	0.038	0.313	0.755
lh lateral OFC	NA	-0.049	0.031	-1.598	0.111	0.002	0.026	0.098	0.922	-0.049	0.034	-1.436	0.152
	RNT	-0.01	0.032	-0.305	0.761	-0.014	0.027	-0.512	0.609	***0.07***	***0.035***	***1.995***	***0.047***
	AA	-0.058	0.031	-1.905	0.058	-0.014	0.026	-0.543	0.588	0.002	0.034	0.065	0.948
	LPA*	-0.057	0.031	-1.828	0.069	***-0.063***	***0.026***	***-2.429***	***0.016***	0.028	0.035	0.807	0.42
	AAp	-0.035	0.033	-1.058	0.291	0.006	0.027	0.217	0.828	-0.062	0.036	-1.695	0.091
	R	-0.02	0.031	-0.637	0.525	-0.037	0.026	-1.454	0.147	0.056	0.034	1.652	0.1
rh lateral OFC	***NA***	***-0.064***	***0.032***	***-2.04***	***0.042***	-0.022	0.028	-0.799	0.425	-0.027	0.034	-0.787	0.432
	RNT	-0.037	0.032	-1.153	0.25	-0.004	0.029	-0.125	0.901	-0.013	0.035	-0.379	0.705
	AA	-0.04	0.031	-1.296	0.196	-0.015	0.028	-0.527	0.598	0.017	0.034	0.507	0.613
	LPA*	***-0.066***	***0.032***	***-2.069***	***0.04***	***-0.064***	***0.028***	***-2.254***	***0.025***	0.057	0.034	1.655	0.099
	AAp	0.006	0.034	0.184	0.854	0.022	0.03	0.732	0.465	0.014	0.036	0.38	0.705
	R	-0.019	0.031	-0.601	0.548	-0.025	0.028	-0.908	0.365	0.019	0.033	0.561	0.576
lh medial OFC	NA	-0.048	0.033	-1.458	0.146	-0.011	0.029	-0.375	0.708	-0.025	0.037	-0.666	0.506
	RNT	0.032	0.033	0.963	0.336	0.041	0.029	1.405	0.161	0.026	0.038	0.679	0.498
	AA	0.016	0.032	0.506	0.613	0.03	0.028	1.074	0.284	0.028	0.037	0.77	0.442
	LPA*	-0.045	0.033	-1.335	0.183	-0.039	0.029	-1.359	0.175	0.004	0.038	0.109	0.913
	AAp	-0.048	0.035	-1.363	0.174	-0.019	0.03	-0.619	0.536	-0.022	0.04	-0.546	0.586
	R	0.011	0.032	0.348	0.728	0.009	0.028	0.309	0.757	0.004	0.037	0.096	0.923
rh medial OFC	NA	-0.014	0.034	-0.417	0.677	0.016	0.027	0.585	0.559	0.025	0.037	0.669	0.504
	RNT	-0.017	0.035	-0.496	0.62	0.014	0.028	0.514	0.608	-0.017	0.038	-0.458	0.647
	AA	-0.06	0.034	-1.791	0.074	-0.01	0.027	-0.374	0.709	-0.018	0.036	-0.496	0.621
	LPA*	-0.016	0.035	-0.475	0.635	-0.009	0.028	-0.338	0.735	0.006	0.037	0.157	0.876
	AAp	***-0.072***	***0.036***	***-1.991***	***0.048***	-0.033	0.029	-1.132	0.259	0.006	0.039	0.166	0.868
	R	-0.031	0.034	-0.932	0.352	-0.042	0.027	-1.55	0.122	0.034	0.036	0.939	0.348

lh amygdala	NA	-0.052	0.033	-1.569	0.118	-	-	-	-	-	-	-	-
	RNT	-0.054	0.034	-1.626	0.105	-	-	-	-	-	-	-	-
	AA*	-0.04	0.032	-1.22	0.224	-	-	-	-	-	-	-	-
	LPA	-0.009	0.034	-0.273	0.785	-	-	-	-	-	-	-	-
	AAp	-0.021	0.035	-0.597	0.551	-	-	-	-	-	-	-	-
	R	0.004	0.032	0.121	0.904	-	-	-	-	-	-	-	-
rh amygdala	NA	-0.014	0.034	-0.404	0.687	-	-	-	-	-	-	-	-
	RNT	0.009	0.034	0.26	0.795	-	-	-	-	-	-	-	-
	AA*	-0.041	0.033	-1.246	0.214	-	-	-	-	-	-	-	-
	LPA	-0.034	0.034	-1.018	0.31	-	-	-	-	-	-	-	-
	AAp	-0.013	0.036	-0.359	0.72	-	-	-	-	-	-	-	-
	R	0.01	0.033	0.309	0.757	-	-	-	-	-	-	-	-
lh hippocampus	NA	-0.004	0.032	-0.133	0.894	-	-	-	-	-	-	-	-
	RNT	-0.041	0.032	-1.275	0.203	-	-	-	-	-	-	-	-
	AA	-0.026	0.031	-0.846	0.398	-	-	-	-	-	-	-	-
	LPA	-0.004	0.032	-0.14	0.889	-	-	-	-	-	-	-	-
	AAp	-0.026	0.034	-0.778	0.437	-	-	-	-	-	-	-	-
	R*	-0.004	0.031	-0.141	0.888	-	-	-	-	-	-	-	-
rh hippocampus	NA	-0.04	0.031	-1.312	0.191	-	-	-	-	-	-	-	-
	RNT	-0.025	0.031	-0.828	0.409	-	-	-	-	-	-	-	-
	AA	0.004	0.03	0.15	0.881	-	-	-	-	-	-	-	-
	LPA	-0.014	0.031	-0.461	0.645	-	-	-	-	-	-	-	-
	AAp	0.013	0.033	0.384	0.701	-	-	-	-	-	-	-	-
	R*	0.011	0.03	0.382	0.703	-	-	-	-	-	-	-	-
lh caudate	NA	0.013	0.031	0.437	0.663	-	-	-	-	-	-	-	-
	RNT	0.001	0.03	0.024	0.981	-	-	-	-	-	-	-	-
	AA	-0.037	0.029	-1.255	0.211	-	-	-	-	-	-	-	-
	LPA*	0.017	0.031	0.561	0.575	-	-	-	-	-	-	-	-
	AAp	0.027	0.033	0.827	0.409	-	-	-	-	-	-	-	-
	R	-0.016	0.029	-0.542	0.588	-	-	-	-	-	-	-	-
rh caudate	NA	-0.011	0.032	-0.348	0.728	-	-	-	-	-	-	-	-
	RNT	0.001	0.031	0.047	0.963	-	-	-	-	-	-	-	-
	AA	***-0.06***	***0.03***	***-2.009***	***0.046***	-	-	-	-	-	-	-	-
	LPA*	0.003	0.031	0.087	0.931	-	-	-	-	-	-	-	-
	AAp	0.01	0.033	0.292	0.77	-	-	-	-	-	-	-	-
	R	0.001	0.03	0.024	0.981	-	-	-	-	-	-	-	-
lh putamen	NA	-0.037	0.034	-1.118	0.265	-	-	-	-	-	-	-	-
	RNT	-0.021	0.033	-0.641	0.522	-	-	-	-	-	-	-	-
	AA	-0.022	0.032	-0.691	0.49	-	-	-	-	-	-	-	-
	LPA*	-0.003	0.034	-0.095	0.925	-	-	-	-	-	-	-	-
	AAp	0.028	0.036	0.775	0.439	-	-	-	-	-	-	-	-
	R	-0.037	0.032	-1.152	0.25	-	-	-	-	-	-	-	-
rh putamen	NA	-0.056	0.031	-1.776	0.077	-	-	-	-	-	-	-	-
	RNT	-0.011	0.031	-0.361	0.718	-	-	-	-	-	-	-	-
	AA	-0.017	0.03	-0.564	0.574	-	-	-	-	-	-	-	-
	LPA*	-0.022	0.031	-0.718	0.474	-	-	-	-	-	-	-	-
	AAp	0.021	0.033	0.621	0.535	-	-	-	-	-	-	-	-
	R	-0.024	0.03	-0.824	0.411	-	-	-	-	-	-	-	-
lh pallidum	NA	-0.035	0.037	-0.942	0.347	-	-	-	-	-	-	-	-
	RNT	-0.067	0.037	-1.806	0.072	-	-	-	-	-	-	-	-
	AA	-0.004	0.036	-0.111	0.912	-	-	-	-	-	-	-	-
	LPA*	0.025	0.037	0.681	0.496	-	-	-	-	-	-	-	-
	AAp	0.062	0.039	1.566	0.119	-	-	-	-	-	-	-	-
	R	-0.046	0.036	-1.269	0.206	-	-	-	-	-	-	-	-
rh pallidum	NA	-0.037	0.032	-1.157	0.248	-	-	-	-	-	-	-	-
	RNT	-0.029	0.032	-0.895	0.372	-	-	-	-	-	-	-	-
	AA	-0.026	0.031	-0.85	0.396	-	-	-	-	-	-	-	-
	LPA*	0.035	0.032	1.08	0.281	-	-	-	-	-	-	-	-
	AAp	***0.074***	***0.034***	***2.17***	***0.031***	-	-	-	-	-	-	-	-
	R	-0.011	0.031	-0.35	0.727	-	-	-	-	-	-	-	-
lh accumbens	NA	-0.034	0.035	-0.975	0.331	-	-	-	-	-	-	-	-
	RNT	0.022	0.035	0.615	0.539	-	-	-	-	-	-	-	-
	AA	0.014	0.034	0.402	0.688	-	-	-	-	-	-	-	-
	LPA*	0.032	0.035	0.892	0.373	-	-	-	-	-	-	-	-

	AAp	***-0.083***	***0.037***	***-2.216***	***0.028***	-	-	-	-	-	-	-	-
	R	-0.035	0.034	-1.026	0.306	-	-	-	-	-	-	-	-
rh accumbens	NA	-0.032	0.034	-0.935	0.351	-	-	-	-	-	-	-	-
	RNT	0.028	0.033	0.849	0.396	-	-	-	-	-	-	-	-
	AA	-0.029	0.032	-0.909	0.364	-	-	-	-	-	-	-	-
	LPA*	-0.003	0.034	-0.099	0.922	-	-	-	-	-	-	-	-
	AAp	-0.051	0.036	-1.441	0.151	-	-	-	-	-	-	-	-
	R	-0.023	0.032	-0.727	0.468	-	-	-	-	-	-	-	-
lh thalamus	NA	-0.003	0.029	-0.09	0.928	-	-	-	-	-	-	-	-
	RNT	0.012	0.029	0.415	0.678	-	-	-	-	-	-	-	-
	AA*	-0.002	0.028	-0.061	0.952	-	-	-	-	-	-	-	-
	LPA	0.039	0.029	1.332	0.184	-	-	-	-	-	-	-	-
	AAp	-0.041	0.031	-1.323	0.187	-	-	-	-	-	-	-	-
	R	0.016	0.028	0.565	0.573	-	-	-	-	-	-	-	-
rh thalamus	NA	-0.053	0.028	-1.899	0.059	-	-	-	-	-	-	-	-
	RNT	0.027	0.028	0.982	0.327	-	-	-	-	-	-	-	-
	AA*	0.007	0.027	0.247	0.805	-	-	-	-	-	-	-	-
	LPA	0.022	0.028	0.803	0.423	-	-	-	-	-	-	-	-
	AAp	-0.024	0.03	-0.811	0.418	-	-	-	-	-	-	-	-
	R	0.006	0.027	0.233	0.816	-	-	-	-	-	-	-	-

Appendix 3. Young adult ROI analyses – controlling for sex. Results from multiple regression models predicting volume, surface area, and cortical thickness of a priori regions of interest. For each ROI, factor scores from all six internalizing dimensions were simultaneously included as predictors, while controlling for age, sex, MRI scanner platform, and a whole brain morphometry measure, treating family as a random effect. Bold and italicized statistics indicate marginally significant effect ($p<.05$); Bold only statistics indicated significant effect after correction for multiple comparisons ($p<.008$); Est.= beta estimate; SE= standard error of beta estimate; NA= negative affect; RNT= repetitive negative thought; AA= anxious arousal-specific; LPA= low positive affect-specific; AAp= anxious apprehension-specific; R= rumination-specific; lh= left hemisphere; rh= right hemisphere; cMFG= caudal middle frontal gyrus; rMFG= rostral middle frontal gyrus; cACC= caudal anterior cingulate cortex; rACC= rostral anterior cingulate cortex; lOFC= lateral orbitofrontal cortex; mOFC= medial orbitofrontal cortex.

Appendix 4: Sex differences in underlying gray matter in young adults.

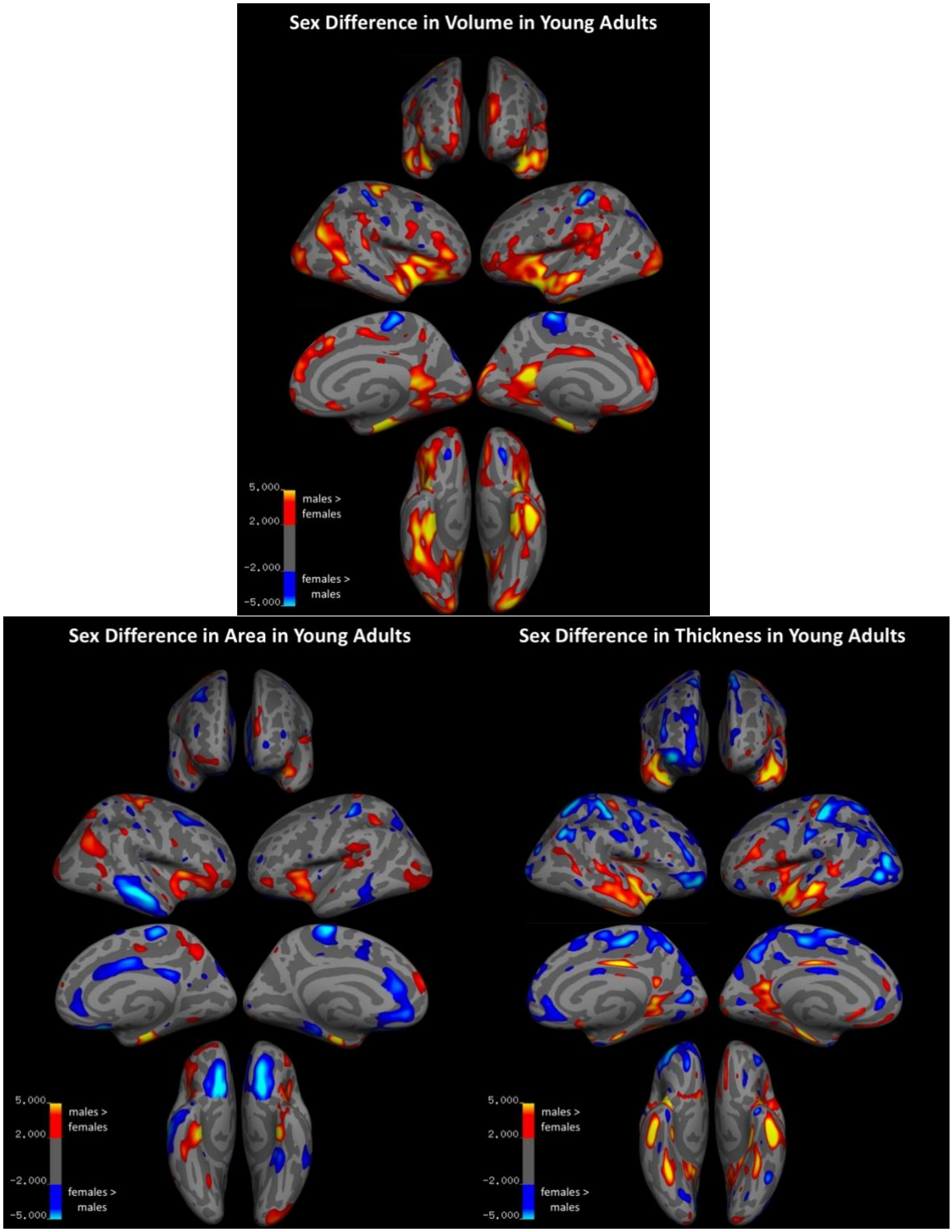

Appendix 4. Young adult sex differences in gray matter. *Top panel:* vertex-wise difference between males and females in cortical volume. *Left panel:* vertex-wise difference between males and females in cortical surface area. *Right panel:* vertex-wise difference between males and females in cortical thickness. Hot colors indicate greater gray matter morphometry in males than females. Cool colors indicate less gray matter morphometry in males than females.

Appendix 5: Sex differences in underlying gray matter in adolescents.

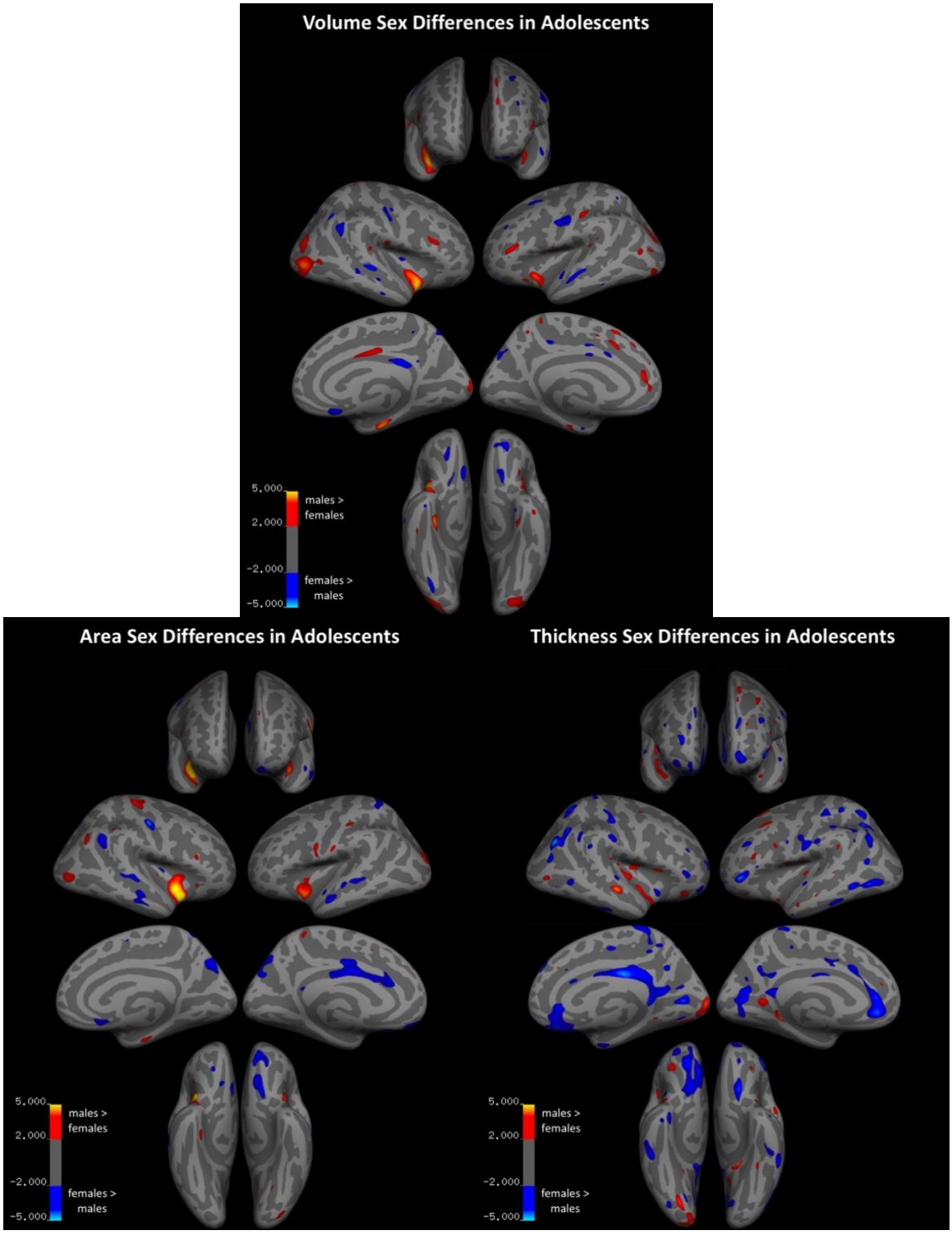

Appendix 5. Adolescent sex differences in gray matter. *Top panel:* vertex-wise difference between males and females in cortical volume. *Left panel:* vertex-wise difference between males and females in cortical surface area. *Right panel:* vertex-wise difference between males and females in cortical thickness. Hot colors indicate greater gray matter morphometry in males than females. Cool colors indicate less gray matter morphometry in males than females.

Appendix 6: Age group differences in underlying gray matter.

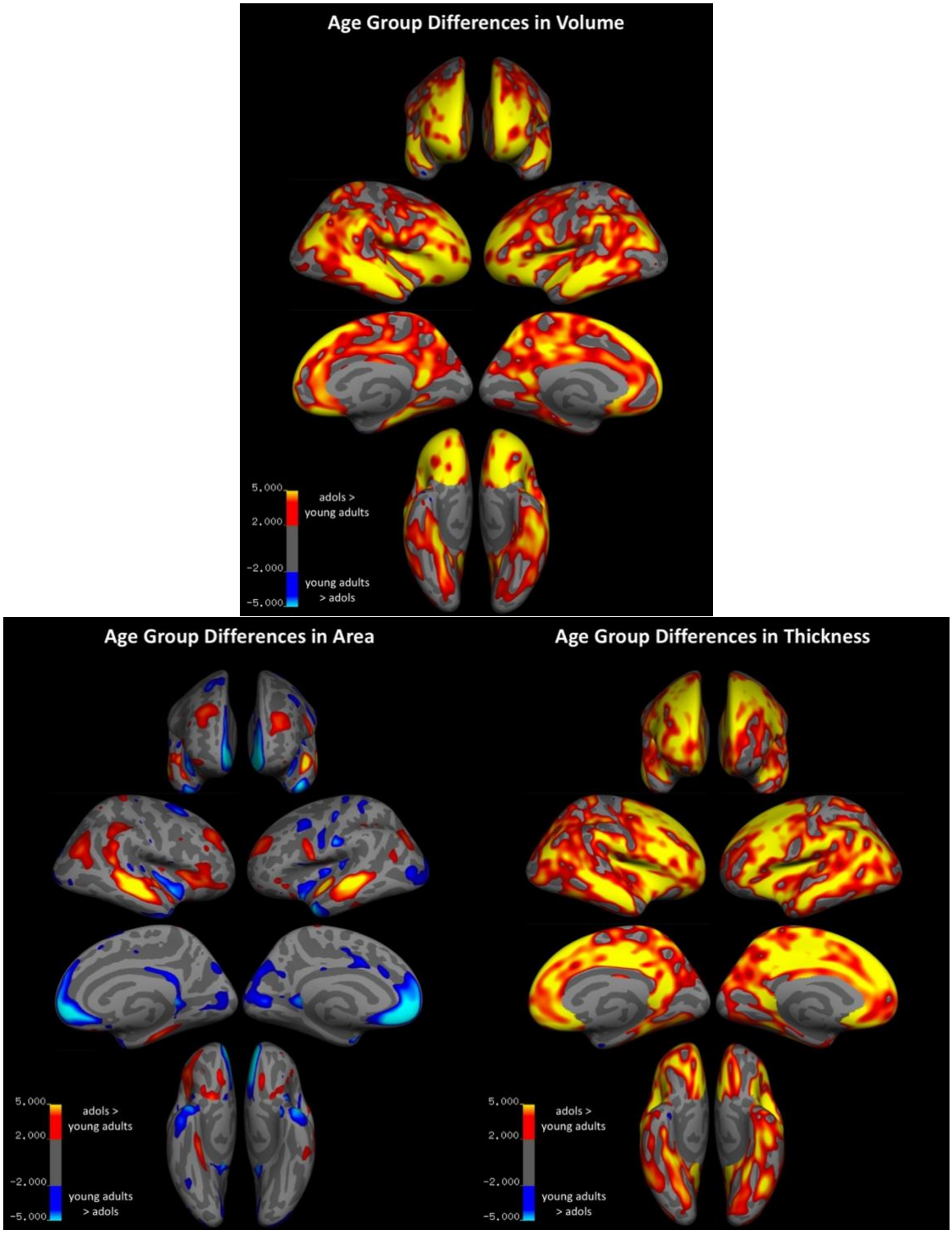

Appendix 6 Age group differences in gray matter. *Top panel:* vertex-wise difference between adolescents and young adults in cortical volume. *Left panel:* vertex-wise difference between adolescents and young adults in cortical surface area. *Right panel:* vertex-wise difference between adolescents and young adults in cortical thickness. Hot colors indicate greater gray matter morphometry in adolescents than young adults. Cool colors indicate less gray matter morphometry in adolescents than young adults.